OBJECTIVE METHODS FOR ANTERIOR OCULAR GRADING

RACHAEL CLAIRE PETERSON

Doctor of Philosophy

ASTON UNIVERSITY

Submitted May 2006

ASTON UNIVERSITY

OBJECTIVE METHODS FOR ANTERIOR OCULAR GRADING

RACHAEL CLAIRE PETERSON

DOCTOR OF PHILOSOPHY

SUBMITTED MAY 2006

Grading scales provide a consistent and universally recognised technique for evaluation of anterior ocular surfaces. Despite their popularity however these subjective scales have been shown to be unreliable, insensitive and non-linear in their display of pathological severity. This thesis set out to develop an objective analysis program that correlates with subjective grades but has improved sensitivity and reliability in its measures so that the possibility of early detection and reliable monitoring of changes in anterior ocular surfaces (bulbar hyperaemia, palpebral redness, palpebral roughness and corneal staining) could be increased.

The sensitivity of the program was 20x greater than subjective grading by optometrists. The reliability was found to be optimal ($r=1.0$) with subjective grading up to 144x more variable ($r=0.08$). Objective measures were used to create formulae for an overall 'objective-grade' (per surface) equivalent to those displayed by the CCLRU or Efron scales. The correlation between the formulated objective verses subjective grades was high, with adjusted r^2 up to 0.96

Determination of baseline levels of objective grade were investigated over four age groups (5-85years $n = 120$) so that in practice a comparison against the 'normal limits' could be made. Differences for bulbar hyperaemia were found between the age groups ($p< 0.001$), and also for palpebral redness and roughness ($p<0.001$). The objective formulae were then applied to the investigation of diurnal variation in order to account for any change that may affect the baseline. Increases in bulbar hyperaemia and palpebral redness were found between examinations in the morning and evening. Correction factors were recommended.

The program was then applied to clinical situations in the form of a contact lens trial and an investigation into iritis and keratoconus where it successfully recognised various surface changes. This programme could become a valuable tool, greatly improving the chances of early detection of anterior ocular abnormalities, and facilitating reliable monitoring of disease progression in clinical as well as research environments.

Key words: Objective grading; Subjective grading; Bulbar hyperaemia; Palpebral conjunctiva; Corneal staining, Digital imaging.

DEDICATED TO MY INCREDIBLE FAMILY

FOR THEIR STRENGTH, AND THEIR BELIEF IN ME

It's no use saying, "We are doing our best." You have got to succeed in doing what is necessary. Never, never, never give up.

~ Winston Churchill

ACKNOWLEDGEMENTS

Firstly and most importantly warmest thanks must go to Dr James Wolffsohn, my supervisor. The objective program described in this thesis is his creation and I am privileged that he would turn such an important work over to me. His generosity of spirit, insight and guidance has made it possible for me to achieve this work.

Dr Richard Armstrong and Dr Mark Dunne provided invaluable help with statistics. I have the deepest respect and affection for their endless patience and sense of humour

Thanks must go to all of the subjects who kindly gave up their time to sit for me. Many of the subjects were recruited at the Queens' Medical Centre - University Hospital NHS Trust in Nottingham. Without the kindness and support of the staff there particularly the optometry department, certain aspects of this thesis would not have been possible and I will always be grateful for their friendship.

A last note and thanks must go to all of my family and friends with a special mention to Hannah Bartlett for sharing a home, and some stormy seas.

CONTENTS

LIST OF TABLES

LIST OF FIGURES

CHAPTER 1

DIGITAL PHOTOGRAPHY AND THE EYE

1.1 INTRODUCTION

The purpose of this thesis is to examine digital imaging with relation to anterior grading and aims to validate and develop objective grading techniques for use in examination of the surfaces of the anterior eye. In order to examine the sensitivity and reliability of objective image analysis programmes many images of the ocular surfaces must be taken. It is therefore expedient to evaluate the digital technology available at this time and to determine the best equipment and best-practice methods with which to perform the intended studies. The initial part of the introduction will concentrate on digital technology, its evolution and variety. This will be followed by a review of the literature related to grading scales for the anterior eye.

1.2 SILVER TO SILICONE

Digital imaging of the anterior eye is an invaluable tool in an ophthalmological clinic and is attracting increased interest in optometric practice. Literature on this area is scarce and academic studies involving this technology are even more so, therefore much of what is known regarding digital imaging is taken only from technical manuals and manufacturer's information. In order to use digital technology to its best advantage in the pursuit of imaging the anterior eye it is appropriate to examine the processes involved so that suitable equipment will be used, and methods will be consistent throughout the investigations in this thesis.

For many years medical and allied professions emphasised the need for recording observations of the human body but the time needed to sketch interesting features and the accuracy of the finished result was not ideal. The advent of photography in 1826 created the opportunity for immediate improvement in the calibre of description of anatomical features, and allowed clinicians to observe an accurate and permanent representation of their object of interest. [1]

In 1886 Jackman and Webster achieved the first photograph of the human retina. [2] This was a great achievement, which along with the development of indirect ophthalmoscopy and subsequent reflex-free photography by Gullstrand in the early 1900s, led to the routine use of retinal photography in ophthalmology and the publication of images of ocular pathology into an ophthalmic atlas. [3, 4]

Invention of artificial light sources allowed Gullstrand to apply a slit-beam during ocular examinations in order to improve observations of anterior eye structures and the lens. [3] This and other major discoveries in the early 20th century led to the creation of the slit-lamp biomicroscope which was a catalyst for developments in ocular photography, as the equipment allowed images of both the anterior and posterior eye to be recorded.

The use of photography in optometric documentation was encouraged, but the expense and the delay between taking the photographs and observing the results made poor images difficult to replace, and rapid monitoring awkward to achieve. [5] Technology evolved further still, bringing with it the capability to capture and process images digitally, and by the end of the 1900s digital cameras were available not just for the professional photographer, but also for the general public and medical practitioner. Digital photography quickly proved

invaluable in the study of ophthalmology when applied to tasks such as Fluorescein angiograms and diabetic retinopathy screening. [6-8]

In the 21st century digital imaging is no longer considered a luxury, but a requirement. To be involved in diabetic screening the National Screening Committee (NSC) in the UK requires digital fundus imaging [9] and to be involved in the imaging of anterior eye conditions and contact lenses it is also of great benefit to be able to utilise instant review and cheap repetition of images while the patient remains present. This allows the photograph to be an educational tool as well as the best method of monitoring changes. Aside from this, digital imaging can offer increased flexibility, improved storage, comparison facilities, image enhancement and even image analysis at the touch of a button.

Photographic technology has come a long way since its advent in the 1800s and can greatly enhance our learning and diagnostic abilities. The applications of digital imagery are exciting and the advantages are broad, however there are perceived weaknesses in the technology, particularly regarding image quality relative to that of traditional film. In order to understand the areas of weakness or rather 'difference' between digital and analogue, the fundamental processes involved should be thoroughly examined.

1.3 DIGITAL FUNDAMENTALS

1.3.1 The capture process

Image capture for preservation of a required object is the aim of photography, yet it is merely the start of the process required to obtain the finished photograph. Both digital and traditional methods of photography begin in a similar fashion, as light passes through a lens and is registered by the medium within.

For analogue cameras this medium is the film, a plastic strip coated in layers of chemicals including silver halide crystals which form the light sensitive component. For digital image capture, this medium is the 'chip' which contains photosites of light-sensitive diodes known as 'pixels'. Pixels have the ability to absorb light photons and convert them into an electrical current. [10] Figure 1.1 portrays the analogy of a CCD pixel array converting light into an electrical current. The rain represents the photons of light falling onto the sensor. Buckets represent capacitors in which the charge from the pixels accumulates, and is transferred into a shift register (measuring cylinder in the diagram) which effectively registers the 'amount' of electrical current. In this way the light registered by pixels can be quantified, and the charge collected is converted into a level of volts on the digital chip.

FIGURE 1.1 Analogy of buckets capturing water as pixels capturing and transferring light [11]

The conversion of this current into a level of volts is the second part of the capture process. The amount of volts is then assigned a numeric code, each piece of which contributes to the pattern of units that is used to recreate the image optically. This system allows information to be transferred and copied indefinitely without causing image degradation, as numeric code is not affected by electronic interference or radiation. [12]

The code assigned can range from short and simple to long and complicated. It is measured in Bits (binary digits) which are 0's (off) or 1's (on). The levels of bits increase with the complexity of the image. 8 bits represents an image with enough code for 256 levels of greyscale, or 256 colours. 16 bits codes for up to 65,536 colours and 24 bits codes for 16.7 million colour images. 24 bits is the most common code in general consumer digital photography as it provides a high quality image. 30 bits or more are possible, coding for over a billion colours. [12]

Image processing occurs to include colour information (pre-determined by the chosen 'bit' level) into the code. The code now represents both the light intensity and colour of the area. Colour processing with regard to digital chip options will be discussed further in section 1.2.3. Reducing the number of colours has a significant effect on file size. An uncompressed 800 by 600 pixel 24-bit image takes up 1.44Mb of storage space (the size of the image can be

calculated from multiplying the number of pixels by the number of colour components; red, green and blue). Therefore when taking optometric images, it is important to consider whether they are to be used for objective or subjective grading (monitoring of physiology/pathology), presentations (where enlargement is likely) or for showing to the patient (where a lower resolution could be adequate).

The digital code is stored on the camera memory card until downloaded onto a computer and displayed, or printed. Care must be taken at this point that the image is stored or printed in the minimum format required in future, to optimise the efficiency of the computer storage, and allow for no reduction in quality upon the chosen reproduction format or size. [8]

1.3.2 Digital chips

The photographic process varies depending on the type of chip which the camera utilises. Digital cameras typically have one of three types of pixelated light detection chip:

1) **CCD** (charged couple device - a description of the technology used to move and store electron charge). CCDs consist of etched pixelated metal oxide semiconductor made from silicone, sensitive in the visible and near infrared spectrum. They convert light that falls onto them into electrons, sensing the level/amount of light rather than colour. Only the photon-to-electron conversion is conducted on the pixel, allowing the maximum amount of space to remain within each pixel for capturing light information. They therefore have a low signal-to-noise ratio ('noise' is the inconstancy of an image e.g. light specs in dark areas caused by electrical interference in the CCD sensor and associated circuitry). [13] The electron-to-voltage conversion is done on the chip, leaving the supporting camera circuitry (3-8 additional chips) to digitise this analogue data. See Figure 1.2.

FIGURE 1.2: CCD chip and image capture pathway. [13] *Reproduced with kind permission from TASi*

2) **CMOS** (complementary metal-oxide semi-conductor - technology used to make a transistor on a silicon wafer). CMOS chips are similar to CCDs, but both the photon-to-electron and electron-to-voltage conversion is conducted within the pixel together with digitisation of the signal, leaving less room for the light sensitive part of the sensor. Normally a microlens is used to capture more light within the pixel area and bend it towards the light sensitive part (the fill factor) of the pixel. CMOS have the advantage of being cheaper and less power hungry than CCDs, due to having fewer components, which also makes them more reliable. See Figure 1.3

FIGURE 1.3: CMOS chip and image capture pathway. [13] *Reproduced with kind permission from TASi*

3) **Foveon** (a chip of transparent quartz containing 3 layers of CMOS) This sensor uses 3 layers of CMOS imagers embedded in silicon, positioned to take advantage of the fact that silicon absorbs different wavelengths (and hence colour) of light at different depths. This should enable each pixel to be able to record individual and independent values of green, red and blue, providing full and accurate colour data from each pixel. However, this new technology is presently held back by technical problems. See Figure 1.4.

FIGURE 1.4: Foveon X3 chip [14] *Reproduced with kind permission from TASi*

As well as stating the type of light receptor chip used (e.g. CCD or CMOS), the *size* of chip should also be recorded (normally ¼ to ¾ inch). Each pixel receptor will obviously be larger on a larger chip of the same resolution as a smaller chip. This is important as the bigger the pixel receptor target, the more chance the photon of light has of hitting it. The latest digital cameras boasting resolutions of around 6 million pixels on a ½ inch chip have pixel receptors of <1 micron in diameter and therefore are limited by the size of a photon. The image will still appear to be of high quality and will take up a large amount of disk space, but will appear blurred upon zooming. [13]

1.3.3 Colour and capture options

To create a complete colour image, the colours must be built from individual colour readings, or by amalgamating readings created by separate filter elements. [15] Most optometric imaging requires the versatility of capturing both dynamic and static objects and therefore uses a matrix or grid of CCD or CMOS elements (area array). Progressive scanning cameras (such as those used in flatbed scanners) do exist, with a sensor consisting of 3 parallel lines of pixels (coated with red, green or blue filters) that are gradually moved across an image by a stepper motor and lead screw building up a complete colour image with accurate colour data at every pixel position, however exposure times are long requiring continuous light and a very stable image. Area array imaging only allows each pixel to capture one colour in a single exposure (shot). To create full colour information the camera can be:

(i) **Single matrix, one shot** - each pixel coated in a different colour, spatially arranged in a mosaic pattern (providing twice as many green as red or blue pixels, based upon the Bayer pattern). The image is then processed (interpolation of colour data from the surrounding pixels) to include the full resolution. Colour fringing can occur around sharp edges, although more modern interpolation algorithms have reduced this effect. Interpolation requires a significant amount of processing, which takes both time and power to accomplish. See Figure 1.7

(ii) **Single matrix, three shot** - instead of individually coating pixels, three shots are taken through a red, then green and blue filter in succession, allowing each pixel to collect full data for that individual pixel position. (See Figure 1.7) Although there are three separate exposures, capture time is fast due to no processor intensive interpolation. See figure 5 and 6. Notice that the 3 shot image is much darker in Figure 1.8.

(iii) **Single matrix, one/three shot** - this works as a single matrix, one shot camera for action shots, but for static imagery can be switched so that the pixel matrix is shifted by one pixel between shots to allow the same pixel position to take consecutive readings in red, green and blue.

(iv) **Single matrix, macroshift** - the limitation for all area array cameras in the physical pixel dimensions of currently available CCD and CMOS sensors, so these cameras take multiple exposures, moving the sensor between shots and use 'stitching' software to create the final image. They work best for stationary, constantly lit targets and have a relatively slow capture process.

(v) **Triple matrix, one shot (often called three-chip cameras)** - each of the 3 chips captures an image of the scene at its full resolution, but through a different filter (red, green or blue). Prisms behind the lens aperture allow green filtered light to pass undiverted to their chip, whereas red and blue light is diverted to their respective chips on either side of the 'green' chip. The processing converts the image to resolution of one chip (not the resolution of one chip times three as is sometimes suggested) with absolute data for red, green and blue light allowing 100% spatial and spectral fidelity. These cameras are more expensive, delicate, heavy and bulky than single matrix cameras and due to the light loss from the two beam splitters, require a higher light output from the slit-lamp for equivalent performance. See Figure 1.5. [13]

FIGURE 1.5: Single matrix 1 shot and single matrix 3 shot comparison [13]

FIGURE 1.6: Comparison of a resolution matched image from a 1-chip (JAI CV-53200, 767 x 569; Yokohama, Japan) and a 3-chip (JVC KYF58, 767 x 569; Yokohama, Japan) camera taken through the same slit lamp optics.

Image taken with 1-CCD chip **Image taken with 3-CCD chip**

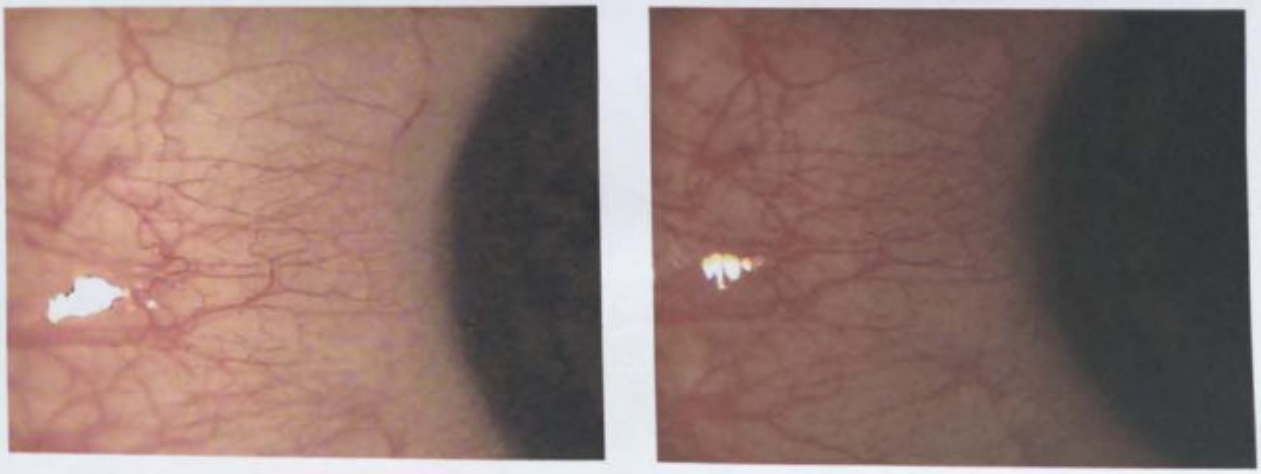

1.3.4 Lighting Considerations

Analogue cameras use mechanical shutters that physically expose the film to light for a predetermined period of time. Digital cameras have the advantage of being able to 'turn-on' the light receptor for a set period of time (which is effectively an electronic shutter). This action is helpful as it involves no moving parts and therefore uses less energy and is less likely to break. Additional lighting is essential for anterior optometric imaging due to the loss of light from intervening beam splitters and lenses, incomplete fill factor of the sensor pixels and a reduced light sensitivity compared to the human eye. This is particularly the case for blue/ultraviolet illumination which will be examined fully in Chapter 3. CCD and CMOS photoreceptors are more responsive to the red end of the spectrum. Therefore they often have an infrared filter and compensate for the low blue sensitivity by amplifying blue signals within the image processing. This compensation creates the opportunity for the blue channel to exhibit more noise than the red or green channels and can be a good way to examine the quality of a digital camera. [13]

International Standards Organisation (ISO) define the capture speed of the film / chip. The rating for speed was developed initially to describe how quickly a film's chemicals reacted to light. A film rated 200 is twice as fast as a film rated 100 ISO. Slower shutter speeds allows the chip to be exposed to the light for a longer duration making the image lighter, but more susceptible to blur with camera or object movement than faster shutter speeds. On current slit-lamp cameras it is not often simple or time effective to be constantly changing shutter speed. Carefully controlled illumination can help to reduce the reflections, or shadow found with sub-optimal shutter speeds.

1.3.5 Interfaces

Analogue interfaces involve sending a composite stream of voltage values (relating to image intensity) and a timed pulse created by the imager, through a Bayonet Neill Concelman connector, (sometimes called a British Naval Connector abbreviated to BNC) or phono connector on the rear of the camera. This system suffers from 'noise' (detrimental effects to the signal) interpreted as a change in intensity and timing errors which are in turn interpreted as a change in localisation. S-video is a two wire system and as such is a more robust format, with chroma (colour) and luminance (greyscale intensity) information transmitted separately. High-end analogue systems transmit red, green and blue signals on separate data lines and a synchronising pulse on the fourth wire. Therefore the signal to noise ratio is lower, but the computer board needed to input the data and reassemble it into an image is more expensive than simpler analogue formats. It is important to note than although many cameras are stated as "digital" as they use a CCD/CMOS for capturing the photons of light, for simplicity and cost-effectiveness they use a composite analogue output (such as a BNC) connector to transmit the image and analogue image capture cards, thereby losing some of the benefits of the digital image capture.[8]

Digital interfaces send a signal in bytes (binary digits) and so noise to the system is unlikely to affect the image. For example, signal noise of +0.05V would convert an intensity of 0.52V on a 0.00-1.00V range to 0.57V, indicating a different intensity to that measured, reducing colour and luminance fidelity, whereas this would not be enough to alter the byte value over the same voltage range (as 0.05V would still be translated as 0.00V by the image processing). Obviously a great deal more data is processed than this example, and so the connector to the computer has multiple pins. This type of interface can cope with 'Mega-Pixel' (MP) images approximately 2 times the resolution of the typical 768x568 PAL image). However, transfer speed is often limited to approximately 12Hz, rather than the 25Hz (PAL) to 30Hz (NTSC) interlaced images transfer speed of analogue.

There are a number of interfaces that are currently used to connect digital cameras or card readers direct to a computer:

a) Small computer system interface (SCSI) - used more often with high-end scanners than digital cameras, offers reasonable transfer speed (Ultra 2 SCSI 40MBps), but limited to a short cable length and difficult to set up (needing to be turned on before the host computer and with each device needing a unique number).

b) Firewire - a high speed serial bus defined by Institute of Electrical and Electronics Engineers (IEEE) standard 1394b which provides auto-configuration and plug-and-play technology. It is robust and easy to use, now with Firewire 800 allowing transfer speeds of up to 100MB/s over long distances with a connector allowing connections up to 1005m away.

c) Universal serial bus (USB) - allows auto-configuration and plug-and-play technology, also providing a small external power source (500mA). The slow transfer speed of USB1 (1.5MBps) has been improved with USB2 (up to 60MBps). [13]

1.3.6 Overview

The assessment of the different methods of image capture determined that a digital single-CCD camera with a single-shot bayer filter matrix would offer the best image for slit-lamp based photography, as the light sensitivity and the time required for completed image capture is critical. The beam-splitter incorporated into the slit-lamp removes some of the light when the image is observed and can cause the image to be at a slightly different point to that viewed down the slit-lamp optics. Therefore a video output with still image capture capabilities is the most appropriate as the image can be viewed on the monitor in real time so that the photographer knows exactly what image will be captured and can focus accordingly.

1.4 GRADING SCALES

1.4.1 Subjective grading scales

Accurate and repeatable records of ocular condition and progression are essential to the appropriate management of all patients, especially in the current climate of ophthalmic care in which a patient may not always be seen by the same examiner. A practitioner must be confident in the previous records and make judgements on the current condition of the patient accordingly. In order to facilitate universal comprehension with evaluation by another practitioner, grading scales were introduced.

A grading scale is a tool with which a specific ocular feature of interest is compared to pre-determined standards of severity of that feature, which range from normal to severe degrees. Grading scales are employed with the aim of adding a degree of objectivity to clinical assessments, to increase reliability and the reproducibility of ocular analysis among practitioners. They also provide a method of standardised quantification of the extent of severity of a physical condition. Grading scales can be verbal, pictorial or computer generated. [16]

Subjective grading has been extensively used to quantify and monitor ocular conditions such as bulbar redness, palpebral roughness, corneal clarity, corneal staining with fluorescein and other related changes. [17-22] It is widely accepted that in anterior ocular physiology there are a large range of 'normal' presentations of the eye, the appearance of which depends on many factors such as age, race, environment, contact-lens wear and time of day. Due to this, a comparison between two subjects with different levels of baseline hyperaemia could result in cause for suspicion as to the health of one or both parties. It is obvious therefore that the *change* in the ocular condition of an individual is a more reliable indication of their ocular health than an inter-subject comparison.

1.4.1.1 Types of scale

Initial attempts at describing ocular conditions relied on various adjectives whose meaning was often relative only to the perspective of the examiners. Descriptions such as 'slightly red' or 'moderate palpebral roughness' were highly subjective, creating opportunity for substantial inaccuracy and misinterpretation.[23, 24]

In order to improve accuracy of description between practitioners, illustrated scales were suggested and were first developed in the 1990's. A small number of scales were eventually introduced and accepted into practice, an example of which is displayed in Figure 1.9. A review of the scales which have been developed for subjective anterior ocular assessment is set out in Table 1.1.

FIGURE 1.7: Example of a row from the Efron grading scale.

TABLE 1.1: Clinical anterior eye grading scales review

Name	First Available	Description
Annunziato	1992	Computer based wide selection of artistically rendered frontal ocular images. Range of conditions displayed. Not widely available. [25]
Vistakon	1996	Student handbook displaying a varying number of artist rendered images for a wide range of conditions. Accompanied with Photographs and description / management options. [26]
CCLRU	1997	4 point scale. Photographic. Range of conditions displayed. [27]
Efron	1998	5 options on scale of severity. Pictorial/artist rendered. Range of conditions displayed. [18]
Efron Millennium	2000	5 options on scale of severity. Pictorial/artist rendered. Range of conditions displayed. [28]

TABLE 1.2: Investigations into subjective grading scales

Author	Title	Scale and subjects used	Training involved	Outcome
Chong et al 2000 [29]	The repeatability of discrete and continuous anterior segment grading scales	Verbal descriptions. Computer morph. Photographs. **5 subjects**	Experienced (>2 years)	Each of the clinical grading scales was reliable ($p < 0.001$ for all)
Dundas et al 2000 [30]	Clinical grading of corneal staining of non-contact lens wearers	CCLRU **2 subjects**	Student Optometrists	Low inter-observer variability suggests that the corneal staining grading scale can be used successfully with decimal rather than integer scale increments.
Papas 2000 [31]	Key factors in the subjective and objective assessment of conjunctival erythema	CCLRU **7 subjects**	Experienced	Subjective erythema judgment can be closely modeled using a linear, univariate, morphometric approach and that, under the conditions of the study, clinical grading displays at least interval level measurement characteristics
Twelker and Bailey 2000 [32]	Grading conjunctival hyperaemia using a photography-based method	Efron **2 subjects**	Experienced	The photography based method used was found to be reliable when decimalised scoring is used. However, different fixation may result in different grades.

TABLE 1.2 continued: Subjective grading scale publications

Author	Title	Scale and subjects used	Training involved	Outcome
Efron et al 2001 [33]	Validation of grading scales for contact lens complications	Annunziato CCLRU, Efron Vistakon **13 subjects**	Minimal experience	The artist rendered systems generally afforded lower grading estimates and better grading reliability than the photographic systems all four grading systems are validated for clinical use.
MacKinven et al 2001. [16]	Clinical grading of the palpebral conjunctiva of non-CL wearers	CCLRU **2 subjects**	Student Optometrists	The grading scale can be used successfully with decimal rather than integer scale increments.
Efron 2002 [34]	Validation of computer morphs for grading contact lens complications	Efron Computer morph **9 subjects**	Experienced	There was no difference in median reliability between the printed scales (±0.41) and the computer morphs (±0.43) ($Z=0.1$, $p=0.95$). Computer morphs are thus considered to have been validated in view of their accuracy and reliability.
Wolffsohn and Purslow 2003 [35]	Clinical monitoring of ocular physiology using digital image analysis	CCLRU **1 PC**	NA	Digital image analysis correlates well with the CCLRU scale images. Repeatability variability was <0.5%.
Wolffsohn 2004 [36]	Incremental nature of anterior eye grading scales determined by objective image analysis	Annunziato CCLRU, Efron Vistakon **1 PC**	NA	Printed grading scales are more sensitive for grading features of low sensitivity. Image analysis techniques are 6-35x more repeatable than subjective grading.

Computer morphs are another form of grading scale which use advanced computer software to create images of intermediate grades between the most and least severe reference images of the condition. The advent of such scales has encouraged discussion in the literature as to which is the more appropriate representation of the varying conditions of the eye; photographic or artistically rendered. [26, 37-39]

Photographic scales have the advantage of being more true to life, but the main photographic grading scale developed by the Cornea and Contact Lens Research Unit (CCLRU) uses very different looking eyes and inconsistent stages of development of severity thereby offering a less linear progression than other scales. [36]. Illustrated scales such as the one developed by Efron in 1998 are able to offer a more linear progression of severity as the outcome is entirely under the control of the artist. [36] However, the diagrams of the ocular surfaces are inevitably dissimilar to the true view of the eye by a practitioner, and although in most of the conditions (for example the bulbar hyperaemia) the scale is easy to use, it is also true that in the case of the corneal section for example, an amount of interpretation is certainly required.

Despite their differences, the CCLRU and Efron scales have both succeeded in popularity where others have failed. They offer clear representations along familiar generic scales and are easy to use, cheap and portable. However, the accuracy of any scale is only as reliable as the practitioner using it.

1.4.1.2 Training and reliability

Grading scales are used in the attempt to remove an element of subjectivity from clinical observations, yet during their research into grading of bulbar redness, Fieguth and Simpson (2002) related that "wildly inconsistent grading is observed, even with clinicians who use grading scales". [19] They captured 30 images of frontal bulbar redness and displayed them on a website which was accessed by 72 optometrists who graded the redness of each eye subjectively (with a purpose designed scale). The average range of grades for a single image was 55% of the entire scale range which is an incredible variety of subjective grades given to each image. [19] There are limitations to this study however such as the differences in environment and screen resolution where the images were reviewed due to the web-based nature of the study. An attempt to compensate for this limitation by offering the clinicians a previously determined median image was made. The clinicians were requested to consider this image as a match the 50% grade on the scale. However, this direction was often ignored which produced even a wide range of grades for this median image. [19]

It has been suggested that high levels of inter observer variability are due to a lack of training. [30] Efron et al investigated the influence of experience and training on grading reliability. They took 23 second year optometry students who had not previously had experience of grading ocular surfaces and used a computer programme to offer all of them initial basic training in the grading task. They then gave half of the group an additional tutorial-based training session, and compared the results of the two different groups grading reliability. Grading reliability was superior for the combined subject cohort at the final session (mean ± standard deviation (S.D) 0.33 ± 0.12) compared with the initial session (0.46 ± 0.25) ($p = 0.004$). However, there was no significant difference in the improvement in grading reliability between the two groups ($F= 0.4$, $p= 0.52$). They concluded by stating that "Grading reliability improves statistically with some experience, although perhaps not to a clinically meaningful extent. No added benefit can be derived from supplemental training". [40]

MacKinven et al also investigated the effect of experience on grading using the palpebral conjunctiva. They found an inter-observer grading distribution (S.D.) of 0.12-0.19 units (2.4-3.8% of the 5 point grading scale). [16] Dundas et al performed similar experiments and also found a similar inter observer variability of 0.18 (S.D. units) between clinicians grading fluorescein staining on the cornea. They stated that to distinguish normal from pathological corneal staining *does* require knowledge of the level of background staining that may be

found in normal/healthy subjects. [30] However, a separate study by Efron et al which compared 9 qualified optometrists to 9 laymen found that the overall grade given by the groups was the same, the only effect of training is an improved reliability score (±0.41 verses ±0.67 units). [37]

1.4.1.3 Discrimination

It has been suggested that accuracy of grading scales could be improved by interpolating between grades. [41] Lofstrom et al showed that an 8 level scale was effective and allowed discrimination which was not previously possible. [39] MacKinven et al applied a decimalised version of the CCLRU scale to evaluate palpebral conjunctival appearance and found that it was a successful method, allowing experienced clinicians to assume significance with a change of greater or equal to 0.5 S.D. units. [16]

Another method of increasing the sensitivity through a broader scale is by video-based 'computer-morphing' which digitally creates interpolated steps between traditional scale grade images. This allows a video-sequence to be created to represent an almost continuous progressive scale of the severity of pathology. [29, 34] The section on the video which most closely matches the captured image is taken to be the grade of severity and the numerical value corresponding to that point of the video is noted with regard to the image captured.

However, Efron warned that decimalisation and increased choice of grade may lead to increased inter observer variation and may limit the usefulness of such scales in clinical practice. [18] Also, interpolation between stages is only accurate when the scale used follows a linear progression. Wolffsohn examined the incremental nature of available grading scales (Efron, CCLRU and Vistakon). It was found that the scales could best be described quadratic functions. [36] This implies that rather than a linear progression of scale increments from one stage of severity to the next, the scales are potentially more sensitive at the lower end of scale severity, which would affect the validity of interpolating between grades to increase the discrimination.

Due to the discrepancies caused by inter-observer variability, even with extensive training, it may be considered that the only accurate and fully repeatable grading system must be objective.

1.4.2 Objective grading

The development of computer-based objective grading systems has increased the sophistication and possibilities associated with clinical grading. They can provide more rapid and up to 35x more accurate results than subjective analysis and allow repeatable comparisons between images taken over time. [35]

Automated grading systems rely on direct image analysis from digital images (directly captured or digitised). Software programmes are applied to the images, and techniques such as edge detection, contrast matching and thresholding are used to quantify the areas of interest. [22, 35]

Automated ocular analysis systems have been applied most often to retinal conditions. Initially simple systems were developed which were capable of detecting blood vessels and determining changes in their width and patterns over time. [7] As technology improved, other features of the retina that had been unable to be automatically analysed are now detectable. Microaneurysms which previously had been individually counted can now be plotted automatically and their positions and numbers monitored to indicate the progression of diabetic retinopathy in the vital early stages of the disease. [6, 42]

Current research into automated retinal image analysis covers a wide range of aspects such as distribution of drusen, optic disc analysis, nerve fibre plotting and blood vessel mapping. These methods are capable of detecting and monitoring changes in tortuosity and blood vessel calibre in retinopathy and progression of glaucoma and macular degeneration. [43-50]

Objective anterior eye analysis is less thoroughly researched, with only a handful of research software programmes having been used to objectively analyse anterior structures. This is possibly due to the relative ease of capturing a consistent image of the retina where focus is often automatic, magnification and field-of-view options limited, the angle of observation fixed and a flash which allows consistent levels of illumination. This is in stark contrast to the many factors that must be continuously modified and controlled when photographing the anterior ocular surfaces. A summery of the reports which relate objective analysis to the anterior eye is displayed in Table 1.3.

TABLE 1.3: Anterior ocular objective analysis publications

Reference	Date	Title	Technique and results
Chen, Kovlacheck and Zweifach. [51]	1987	Analysis of microvascular network in bulbar conjunctival by image processing	Semi automated approach using **thresholding** methods to detect vessels and examine network.
Villumsen, Ringquis and Alm. [52]	1991	Image analysis of **conjunctival hyperemia**	Automated system successful in grading hyperemia. Used **smoothing and edge detection.**
Willingham et al. [53]	1995	Automatic quantitative measurement of ocular **hyperemia**	Validated method of **colour extraction** to measure changes in hyperemia
Horak et al. [54]	1996	Quantification of **conjunctival vascular** reaction by digital imaging	**Morphometry** used to calculate the red density of the conjunctiva during provocation with pollen
Guillon and Shah. [55]	1996	Objective measurement of contact lens induced conjunctival redness	Number of vessels crossing **sampling lines** analysed and vessel width estimated.
Owen et al. [56]	1996	A new computer assisted objective method for quantifying vascular changes of the bulbar **conjunctiva**	**Smoothing and thresholding** techniques used to assess vascular changes on the conjunctiva. It was found to be sufficiently sensitive to detecting hyperemia and changes.

TABLE 1.3 continued: Anterior ocular objective analysis publications

Reference	Date	Title	Technique and results
Maldonado et al. [57]	1997	Reproducibility of digital image analysis for measuring **corneal haze** after myopic photorefractive keratectomy	Evaluation of corneal haze with **edge detection** techniques was found to have good repeatability for quantification of corneal haze
Simpson, Chan and Fonn. [58]	1998	Measuring **ocular redness**: first order (luminance and chromaticity) measurements provide more information than second order (spatial structure) measurements	**Colour extraction** techniques used to monitor hyperemia. Spatial structure measurements add no significant detail to the results
Papas. [31]	2000	Key factors in the subjective and objective assessment of **conjunctival erythema**	Human judgement of grade is not purely based on colour but this can be used as a good approximation to a grade. Therefore **colour extraction** techniques were applied
Chong et al. [29]	2000	Repeatability of discrete and anterior segment grading scales	**Continuous matching** graded with higher precision than descriptive or photographic scales

TABLE 1.3 continued: Anterior ocular objective analysis publications

Reference	Date	Title	Technique and results
Fieguth and Simpson. [19]	2002	Automated measurement of **bulbar redness**	**Canny edge detection and colour extraction** used to examine reliability of grading bulbar redness in comparison to clinicians
Chan et al. [59]	2003	Objective method to measure **corneal clarity** before and after laser in situ keratomileusis	Detection of changes in corneal transparencies that were undetectable clinically. Clarity was determined by averaging 8-bit greyscale pixel intensity over an area
Pritchard. [22]	2003	Subjective and objective measures of **corneal staining** related to multipurpose care systems	Significant staining responses were detected using **video morphing** methods. Total area of staining was calculated
Wolffsohn and Purslow. [35]	2003	Clinical monitoring of ocular physiology using digital image analysis	**Thresholding, colour extraction and edge detection** used to investigate bulbar redness, tarsel roughness and corneal staining. Methods were repeatable and accurate.
Owen. [60]	2004	A comparison of manual and automated methods of measuring conjunctival vessel widths from photographic and digital images	Vessel widths were measured manually and compared to the readings from an automated system. The system used thresholding and Gaussian functions, and was validated

Recent interest into developing automated anterior eye analysis is possibly due to the improvements in digital technology. Equipment such as slit-lamp mounted cameras have greatly improved over recent years, in both their ease of use and also in the quality of the image produced. Technology may enable high image quality, but only if the conditions under which the image is taken are correct. External factors such as lighting and photographer competency can have a greater effect on the outcome of anterior eye photography.

The automated systems that objectively analyse digital images need to be robust in order to compensate for changes in external factors. Several of the methods that have been developed (in order to objectively grade anterior ocular physiology) were examined in detail by Wolffsohn and Purslow to compare their relative robustness to changes in image luminance. [35]

The methods that were examined were thresholding, colour extraction, edge detection and canny edge detection.

- Thresholding – features were identified by difference in pixel grey level from a chosen or calculated level. Fixed and image dependant thresholds were investigated.
- Relative Colour Extraction (RCE) – red green and blue colour planes were extracted from the image
- Edge Detection (ED) – extraction of edges by pixel to pixel comparisons was used to produce a sharpening effect on a feature boundary. A number of filters were used.
- Canny Edge Detection – 'smoothing' filters were used followed by edge detection techniques as above. This method alters the overall shape of a feature of interest and reduces specific detail.

Out of these methods it was found that all but the 'thresholding' analysis were robust to changes in luminance. [35]

A computer programme was designed (in LabView™ and Vision Software, National Instruments USA).

LabView software is a programming language which is built up of graphical components and icons instead of lines of text. A user attaches the icons together to build a face-plate (the measurements access panel shown in Figure 1.10) which allows links to measurement tools that have also been attached by strings of code or graphical functions in a flow-diagram type pattern known as the 'block diagram'. The block diagram contains the code which controls the measurements taken and also directs the data into storage or evaluation if designed to do so.

For example a video feed from a slit-lamp sent into a computer to be displayed via the monitor can be diverted through the LabView program. Or images stored on the computer can be opened in a LabView window ready to analyse. The user then can access tools available on the face plate to measure the width of a blood vessel for example, and the program will store the information in an Excel worksheet.

The LabView program designed for objective analysis of the anterior eye initially applied 4 analysis methods (described on the previous page) to a selection of ocular images, in order to compare the methods of objective quantification of changes in anterior ocular pathology. It was determined that the 3x3 edge detection (ED) method and the relative colour extraction (RCE) were the most robust techniques available with respect to environmental (luminance) changes as the grading of ocular conditions was less affected by the use of these methods. [35] Image analysis with these techniques was found to be approximately 7x more reliable than that reported in the literature for subjective grading, however no direct comparisons have been established. [35] Figure 1.10 demonstrates how the LabView programme is used.

FIGURE 1.8: Diagrammatical representation of the process of image analysis by the purpose designed anterior eye analysis LabView programme.

A. Programme face plate and image opened

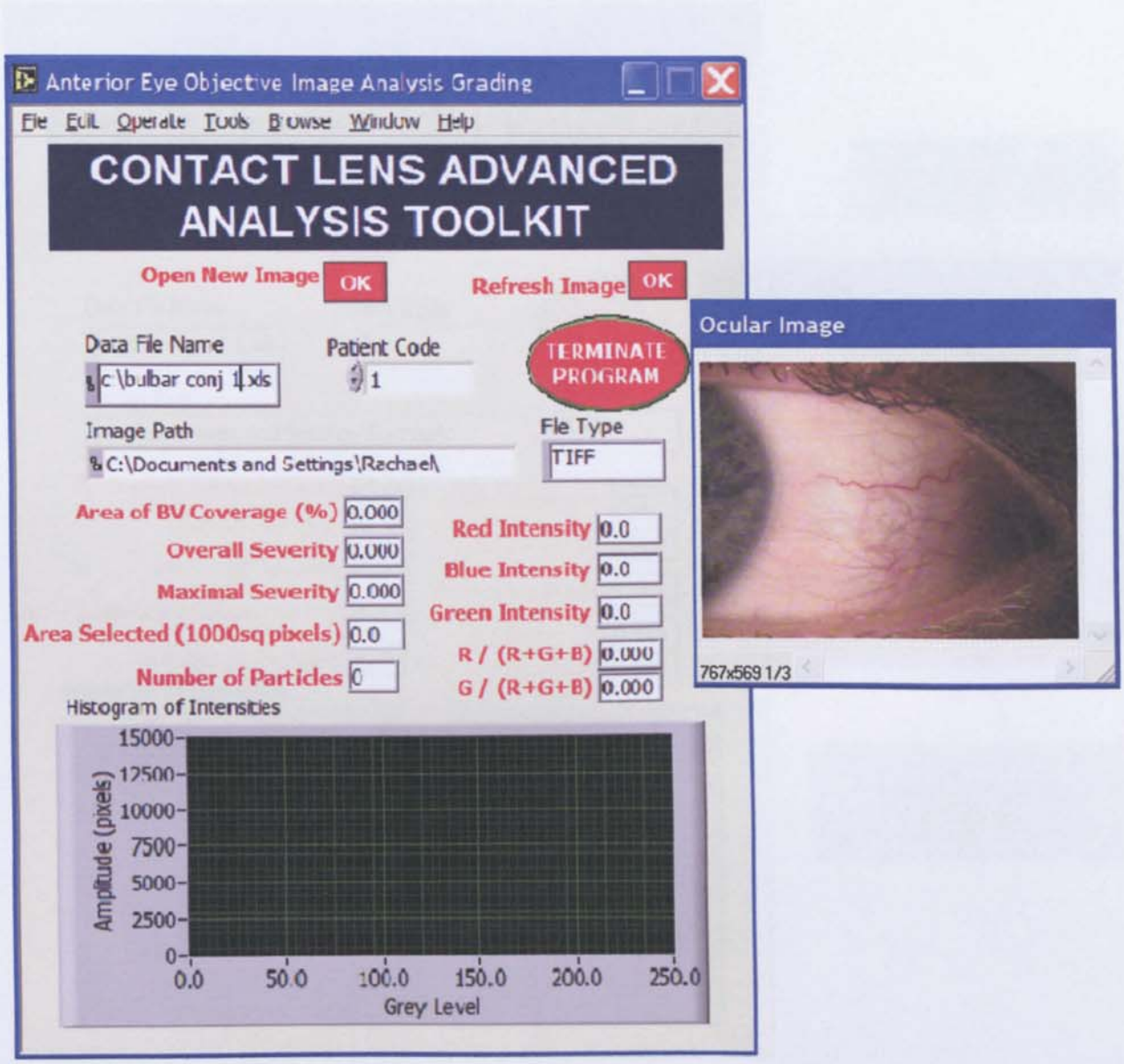

FIGURE 1.8 cont

B. Area selected on image (300x300pixels) and analysis displayed

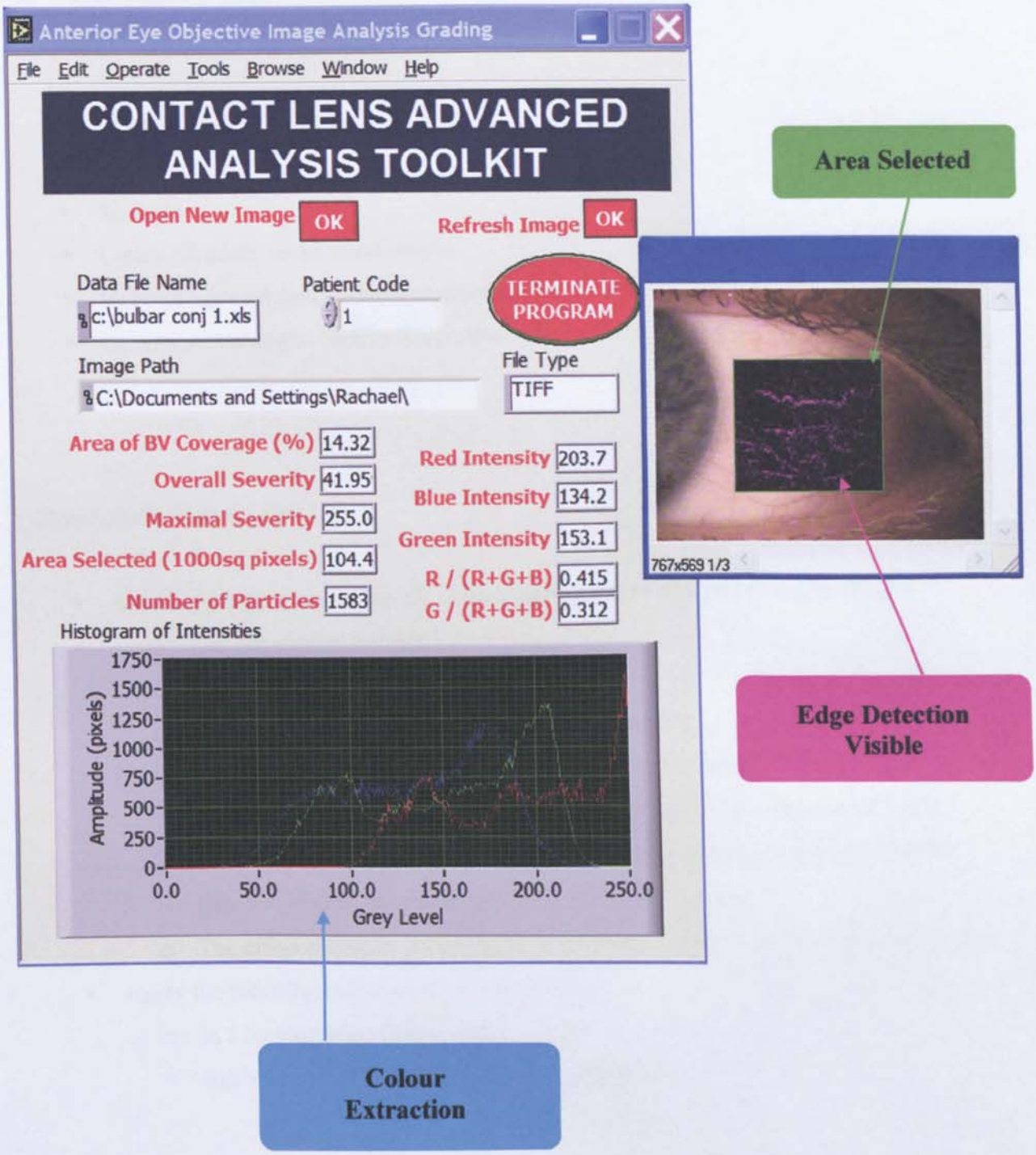

No automated anterior eye analysis program is currently available for use in clinical practice. Part of the reason for this could be that previous techniques have been developed with only one object of analysis in mind and to assess a specific research purpose. A useful automated system must be able to analyse each of the important aspect of anterior eye examination, such as bulbar redness, palpebral redness or roughness and corneal staining. An ideal image grading program would be:

- Objective
- Sensitive
- Reliable
- Create clinically understood results
- Have an age-matched baseline comparison for results
- Be robust to changes such as image luminance and the time of day of image capture

Therefore this thesis intends to:

- Assesses image optimisation for clinical and objective analysis of digital images
    - The optimum resolution
    - The optimum compression
    - Fluorescein dye imaging, lighting and observation
- Determine appropriate baselines and clinically applicable results
    - The sensitivity and reliability of the results compared to subjective grading
    - The relationship of objective image analysis compared to subjective grades
    - Baseline healthy ocular surface values with patient age
    - The effect on ocular surfaces and subsequent objective grades with time of day
- Apply the resulting programme to test its efficacy
    - In a contact lens clinical trial
    - Against the differentiation of ocular pathology

CHAPTER 2

THE EFFECT OF DIGITAL IMAGE RESOLUTION AND COMPRESSION ON ANTERIOR OCULAR IMAGING

2.1 INTRODUCTION

Digital image quality is defined by two components; the resolution of the image (in pixels) needed to image the object of interest and the compression of the file in megabytes (MB) that can be utilised to minimise the space needed to store the image. [3]

Resolution is the ability to distinguish the difference between two sequential points. In digital imagery, this depends on the number of pixels that the image is composed of. [61]
If photographs are to be used to detect pathology, monitor progression and to protect against litigation it is essential that the resolution is sufficient to allow all clinical features of interest to be detected and that this is not compromised by the image storage. Improvements in digital technology have resulted in a sensitivity and specificity to detect retinal pathology comparable with analogue images and direct observation of patients by ophthalmologists, although this has not been assessed for anterior eye images. [62-65] The National Screening Committee (for diabetic retinopathy in the UK) concluded that fundus photography with 1000x1000 pixels is adequate to match the resolving power of the human eye, but adjusted the requirement to 1365x1000 pixels to allow for the rectangular shape of digital camera image sensors. [66]

Image compression is a technique used to reduce file size, by removing redundant information. In some compression methods the full information can be retrieved (termed 'lossless' formats such as Tagged Information File Format or TIFF), but in others the information is permanently deleted ('lossy' formats such as Joint Photographic Experts Group or JPEG). [67] There are two main types of graphic formats used to display graphics, vectors and raster (bitmap) files. Vector files (such as Window Meta Files [*.wmf] and the Pict format used by Macintosh computers) store images as a series of mathematical descriptions representing simple shapes. The image content is divided into its constituent shapes (such as lines and rectangles), with the file storing their position within the image, shape and colour. The image is then reconstructed from these details when opened. As a result, the image size can be changed without any effect on image quality, but they are not suited to complex images such as real images of the eye. The whole image of a bitmap graphic file is divided into tiny squares (pixels) and the colour of each pixel recorded. The result is a relatively large file size which cannot be reduced without loss of information. Common Bitmap file formats include:

- TIFF (Tagged Information File Format) - a lossless format, storing all the data from the camera once its internal processing (such as colour interpolation) has taken place. It uses algorithms to make the file size smaller for storage, but all the compression is reversed on opening.
- JPEG (Joint Photographic Experts Group) - attempts to eliminate redundant or unnecessary information (lossy compression). Red, green and blue (RGB) pixel information is converted into luminance and chrominance components, merging pixels and utilising compression algorithms (Discrete Cosine Transforms) on 8x8 pixel blocks to remove frequencies not utilised by the human eye (dividing the frequencies by individual quantisation coefficient), followed by rounding to integer values. Different compression levels can usually be selected.
- BMP – Microsoft Windows native bitmap format. Rather than storing each of the necessary RGB values for each pixel, Microsoft added a customisable palette so that the colour of each pixel could then be defined by storing its associated index number rather than the much longer RGB value. This look-up table approach was more efficient for handling images with up to 256 colours as each pixel could be stored in 8-bits of information rather than 24-bits. However, to display 24-bit images, the palette would require over 16 million colours, so each indexed entry would be no smaller than the original RGB value. Therefore the BMP format now stores information as rows or scan lines (i.e. RGBRBGRGB...), and the information is compressed by Run Length Encoding (taking repeated sequences and expressing them as number x colour in two bytes). [13]

If all images are taken at maximum quality, storage and archiving can slow a system down considerably due to the large files as there is more processing needed. If this occurs then one of the major advantages of digital technology is compromised. Previous studies have investigated the appropriateness of compression with retinal images. Basu et al suggested that up to a JPEG compression ratio of 1:20 (between 100-75% JPG) was appropriate based on objective analysis with lesion counts. [8] Others have identified 75% JPEG as an appropriate limit from subjective analysis of digital images. [68, 69]

2.2 PURPOSE

For ease of use and efficiency, the images of the anterior eye that will be captured over the course of the investigations in this thesis and in clinical practice could be captured at a lower resolution or compressed. However it is imperative that the quality of the images (resolution and compression) must be of high enough value to ensure that there will be no detrimental effect to the results of any subjective observation or objective images analysis by the techniques described in Chapter 1 (Section 1.3.2). Therefore this study aimed to determine the most appropriate resolution and compression for anterior eye imaging, by evaluating calculated, subjective, and objective results of image compression and reductions in resolution.

2.3 METHODS

Evaluation of the most appropriate resolution and compression for anterior eye imaging was investigated in three ways: theoretical determination of the resolution needed to resolve the smallest clinically important anterior eye features; clinical subjective ranking of a range of images varying in resolution and compression; and clinical objective grading of the same images.

Theoretical: The smallest objects of clinical relevance observed by slit lamp microscopy on the anterior eye were considered to be microcysts and punctate staining. [70] Microcysts have been reported as 15-50μm in diameter. [71, 72] Therefore it seems reasonable that digital imaging should be able to detect an object of 30μm in diameter. The light from an object could fall across the diameter of two pixels, therefore a pixel size equivalent to 15μm is necessary for reliable image capture. A typical slit lamp imaging database (ARC, Carleton, Chesham, UK) was used to measure the extent of the horizontal field of the image obtained at the 5 available magnifications of the slit-lamp (Takagi. Nagano-Ken, Japan). The number of pixels required across the horizontal field was calculated by dividing the horizontal field of the image by the size of the pixels required.

Subjective and objective: Four cameras were utilised to take the images: Nikon CoolPix 990 (2048 x 1360; Tokyo, Japan), DVC 1312 C model (1280 x 811; Austin Texas, USA) and JAI CV-S3200 (767 x 569; CV-53200, Yokohama, Japan) single-chip cameras covered the range of maximum pixel resolutions (noted in brackets) available at the time of the study. The JVC KYF58 (767 x 569; Yokohama, Japan) camera had the same resolution as the JAI CV-S3200, but consists of three chips of this resolution, with light split by prisms to each of the red, green and blue filtered chips. The cameras were attached to the same Takagi slit-lamp (Nagano-Ken, Japan) in turn for images of the anterior eye to be captured.

Identical images of the bulbar conjunctiva, palpebral conjunctiva and central corneal staining of the same subject were taken with each camera and stored as TIFF files (non-compressed format). Copies of the images in TIFF format with reduced resolutions were created using Adobe Photoshop version 5.0 (by bicubic resampling; San Jose, California, USA). The range of resolutions for each camera started at the maximum resolution of that camera and was reduced in the following sequence (horizontal x vertical pixels): 2048x1360, 1600x1063, 1280x811, 1024x680, 767x569, 640x425, 320x213 and 160x107 (see Figure 2.1).

FIGURE 2.1: An example of the range of image resolutions assessed (from the Nikon CoolPix 990 camera) in TIFF format.

2048 x 1360

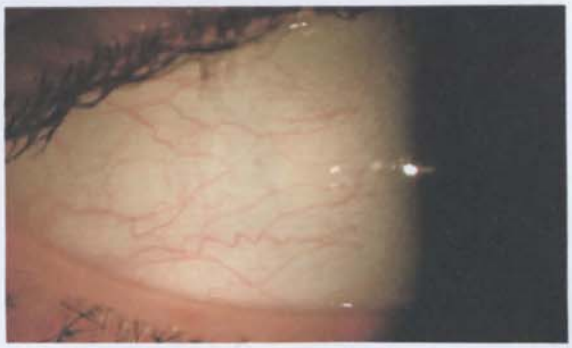

1600 x 1063

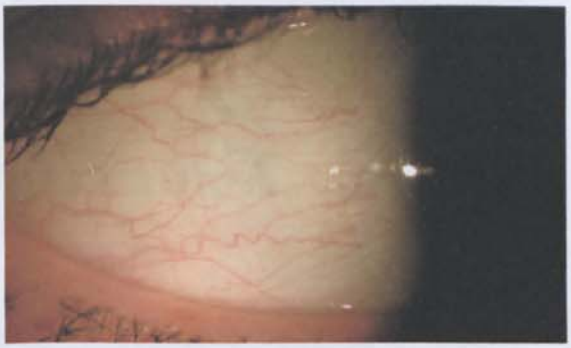

1280 x 811

1024 x 680

767 x 569

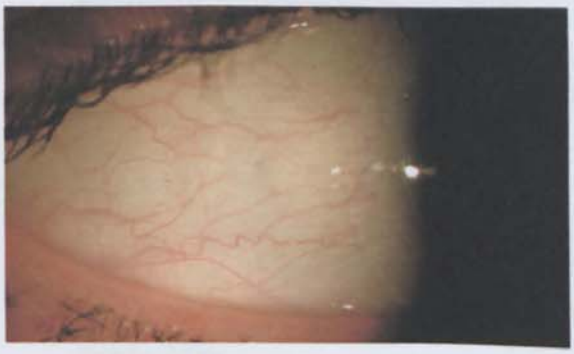

640 x 425

320 x 213

160 x 107

To assess the effect of compression, the original highest resolution TIFF images from each camera were compressed using the international standard devised by the Joint Photographic Experts Group (JPEG 100%, 75%, 50%, 25% and 0% quality settings) and in bitmap (BMP) format using Adobe Photoshop version 5.0. Examples are displayed below in Figure 2.2

FIGURE 2.2: An example of the range of compressed images assessed (from the JVC KYF58)

JPEG 100%

JPEG 75%

JPEG 50%

JPEG 25%

JPEG 0%

BMP

The altered resolution and compression images from each of the digital cameras were inserted into two Microsoft PowerPoint presentations (2002 version; Redmond, WA, USA) the transfer of which did not affect the image quality. The original TIFF image was set in slide one. The other images were entered in random order into the programme and the page with the slide-sorter was displayed. Twenty optometrists were directed to reorder the randomised images in order of image quality compared to the original maximum resolution TIFF image. They were able to do so by inserting a chosen slide into position underneath one which they determined was of a subjectively higher image quality using the slide sorter on the left hand side. The images were displayed to the optometrists on a 15" (LGV 77T5) cathode ray-tube monitor with a resolution of 1280x1024 pixels. A thin film transistor (TFT) screen was not used due to the reported adverse effect on image quality. [68]

The images were then each objectively analysed by edge-detection (ED) and relative colour extraction (RCE) techniques, performed by purpose-written computer grading software which has been previously described in Section 1.3.2. [35]

Due to the non-parametric nature of this data the analysis was performed using Friedman procedures to determine the differences between the 4 cameras. Wilcoxon signed rank tests were then used to determine the order that the images were placed in by the subjective reordering of the images using the PowerPoint package.

As objective grading results in a continuous scale the results of ED and RCE were analysed by analysis of variance (ANOVA) and then the positions of difference within the data determined by Tukey post-hoc analysis.

2.4 RESULTS

2.4.1 Theoretical Calculation

The horizontal resolution of an image needed to allow detection of a 30μm microcyst or other small feature of the anterior eye was calculated by determining the horizontal field of view displayed by an image, over 5 available magnifications. These values were then divided by the size of the pixels required to detect the 30 μm object. E.g. 5590 / 15 = 373. The values calculated are displayed in Table 2.1.

TABLE 2.1: Horizontal resolutions necessary to detect an object of interest of size 30μm with varying typical slit lamp magnifications.

Slit lamp magnification	**Horizontal field of view μm**	**Resolution needed to detect a 30 μm object**
40	5590	373
25	8950	597
16	13,980	932
10	22,365	1491
6.3	35,500	2367

2.4.2 Clinical Subjective Ranking

There was no significant difference in resolution ranking between the results of each camera model (Friedman non-parametric test, $p=0.26$). Analysis of mean ranks for changes in resolution indicated that the ranked order of images was random and the mean rank did not differ from each other until the number of pixels had dropped to 640x425 for each camera (Wilcoxon signed rank comparison test, $p<0.005$) (see Figure 2.3). From this resolution the reduction in image quality was recognised and further degraded images were ranked consecutively. Interestingly, the relative rank of the highest resolution image, 1600x1063 pixels from the Coolpix 990 camera, was ranked as significantly worse than the 1280x1024 image ($p<0.001$).

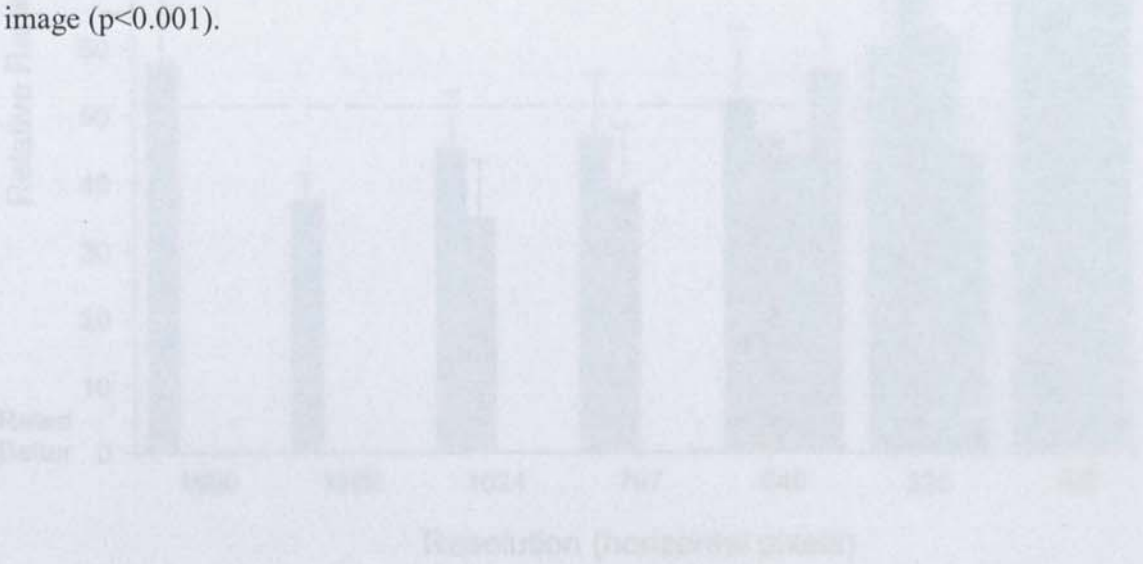

FIGURE 2.3: Mean subjective ranking for the resolution range of each camera model. Error bars = 1 S.D. n=20.

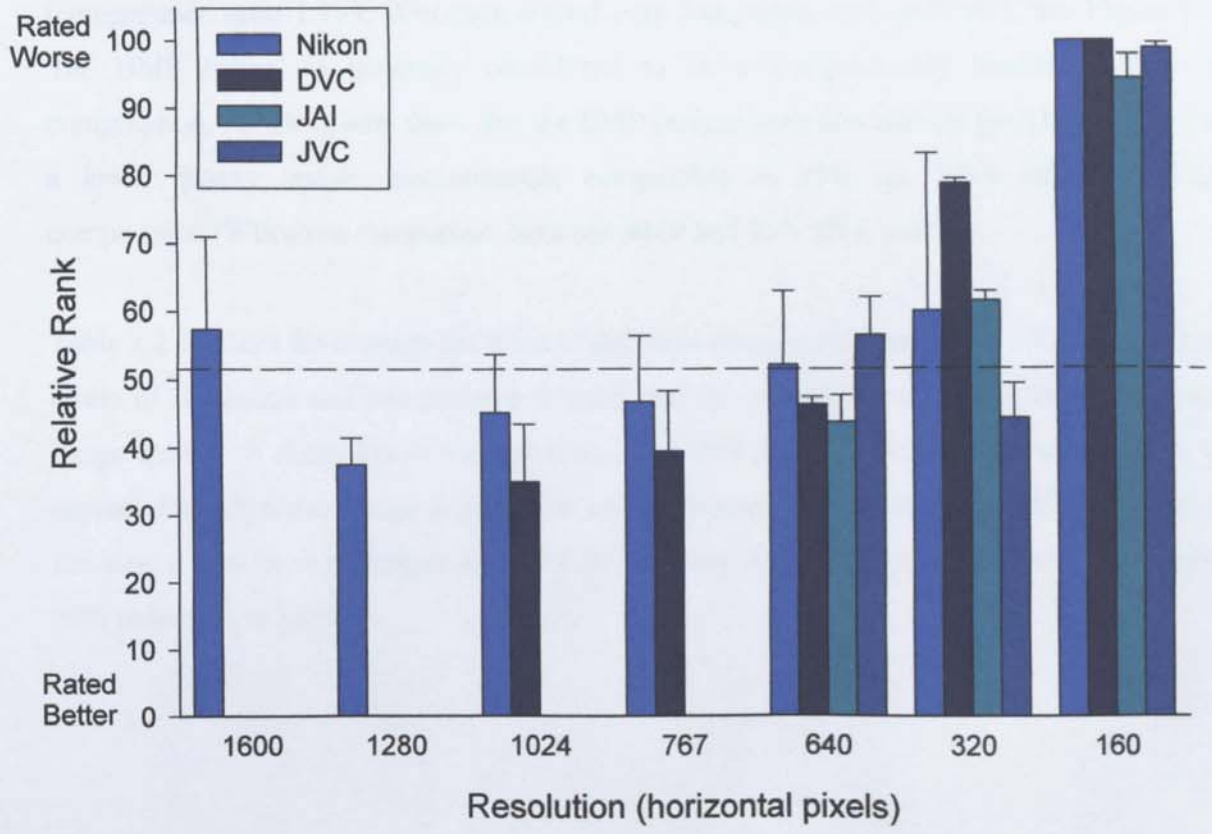

There was no significant difference in compression ranking between the results of each camera model (Friedman non-parametric test, $p>0.05$). Analysis of mean ranks for changes in compression indicated that the ranked order of images was random and the mean rank did not differ from each other until the compression had decreased to 25% JPEG compression (compression ratio 1:109; Wilcoxon signed rank comparison test, $p<0.005$). See Figure 2.4. The BMP format is generally considered to be a comparatively lossless method of compression, yet the results show that the BMP images were consistently ($p<0.005$) ranked as a lower quality image, approximately comparable to 25% (or 1:109 ratio) of JPEG compression (Wilcoxon comparison between BMP and 25% JPG, $p=0.15$).

Table 2.2 displays the average file sizes of the three images and four cameras for the different levels of resolution and compression utilised and the percentage difference from maximum image quality. A reduction in resolution to 767 x 569 pixels, which was shown to cause no appreciable subjective image degradation on a computer screen, caused an 88% reduction in file size. An increase in compression to a 50% quality JPEG (1:70 ratio) resulted in an almost 99% reduction in file size.

FIGURE 2.4: Mean subjective ranking for the compression range of each camera model. Error bars = 1 S.D. n=20.

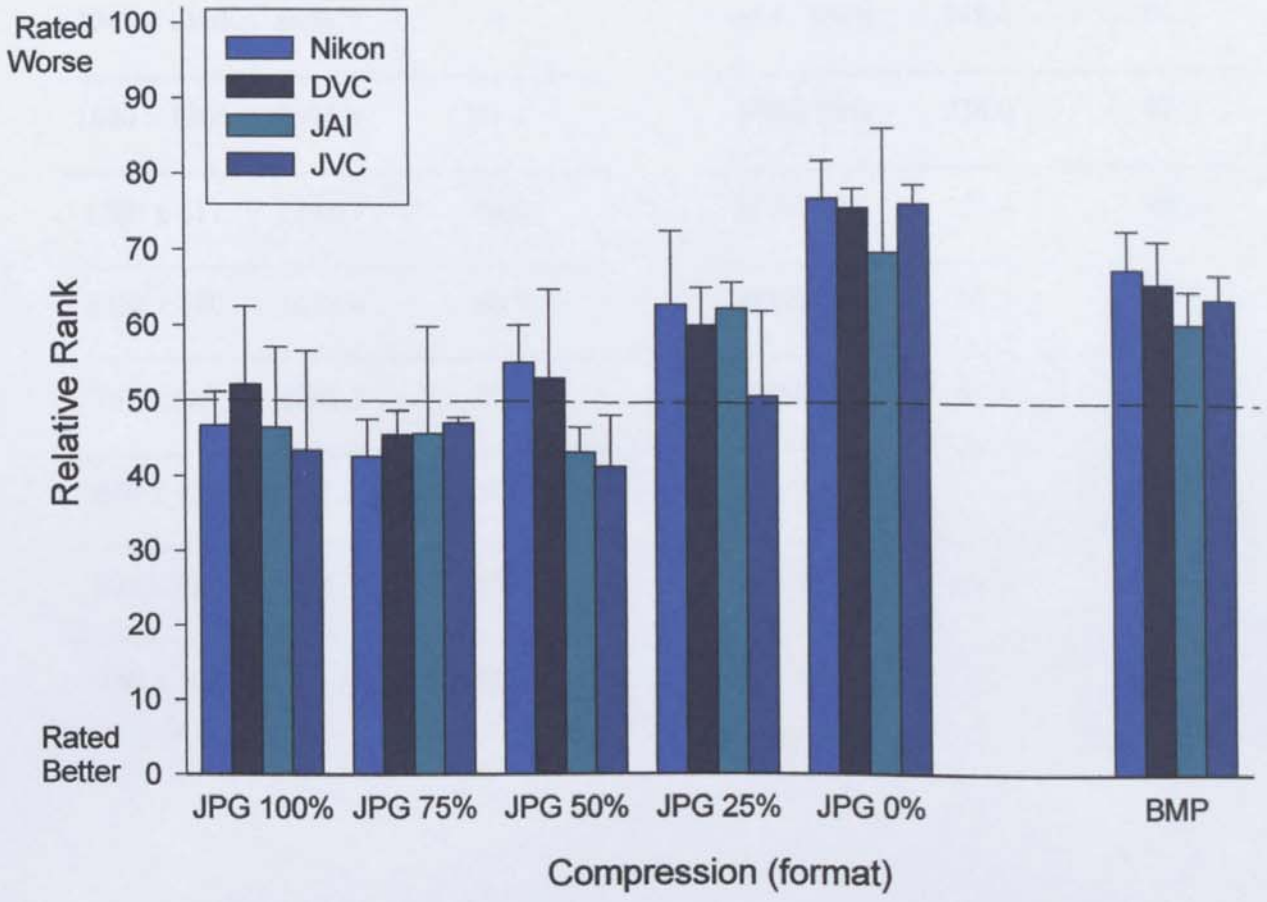

TABLE 2.2: Average file size with changes in resolution and image compression and reduction in file size from full resolution TIFF image.

TIFF pixel resolution	File size MB	Reduction (%)
2048 x 1360	8656.7	0
1600 x 1063	4393.3	49.3
1280 x 811	2198.3	74.6
1024 x 680	1670.0	80.7
767 x 569	1041.3	88.0
640 x 425	621.3	92.8
320 x 213	231.1	97.3
160 x 107	75.5	99.1

Compression Quality	File size MB	Reduction (%)
JPEG 100%	848.4	90.2
JPEG 75%	236.0	97.3
JPEG 50%	123.4	98.6
JPEG 25%	79.3	99.1
JPEG 0%	51.9	99.4
BMP	3211.9	62.9

2.4.3 Clinical Objective Grading

Changes in resolution showed a statistically significant difference with edge detection ($F=2.77$, $p<0.05$), but not with colour extraction ($F=0.01$, $p=1.00$; Figure 2.5). Tukey post-hoc analysis showed that the image analysis results were significantly ($p<0.05$) different from the top resolution images when the image size was reduced to 320 x 213 pixel resolution or less. Compression of images did not significantly affect ED ($F=0.26$, $p=0.93$) or RCE ($F=0.50$, $p=0.99$) image analysis. However, Figure 2.6 indicates that the colour extraction technique to be relatively more affected by changes in compression then resolution.

The camera type significantly affected the image analysis results. ED showed a significant difference between images taken with the Nikon Coolpix and the other three cameras for both resolution ($F=8.14$, $p<0.001$) and compression ($F=11.06$, $p<0.001$). RCE showed a difference between images taken with the Nikon Coolpix and DVC 1312C for both resolution ($F=4.01$, $p<0.01$) and compression ($F=5.10$, $p<0.01$). In comparison with the difference between grades of the commonly used Efron grading scale (of approximately 9.54% additional ED and a 2.04% change in RCE; [35]), the difference between camera types (on average $1.82 \pm 4.27\%$ for ED and $-0.20 \pm 0.72\%$ for RCE) was 0.22 ± 0.40 Efron scale units for ED and 0.14 ± 0.35 Efron scale units for RCE. [36]

FIGURE 2.5: Mean objective edge detection and colouration grading for the resolution range of each camera model. Error bars = 1 S.D.

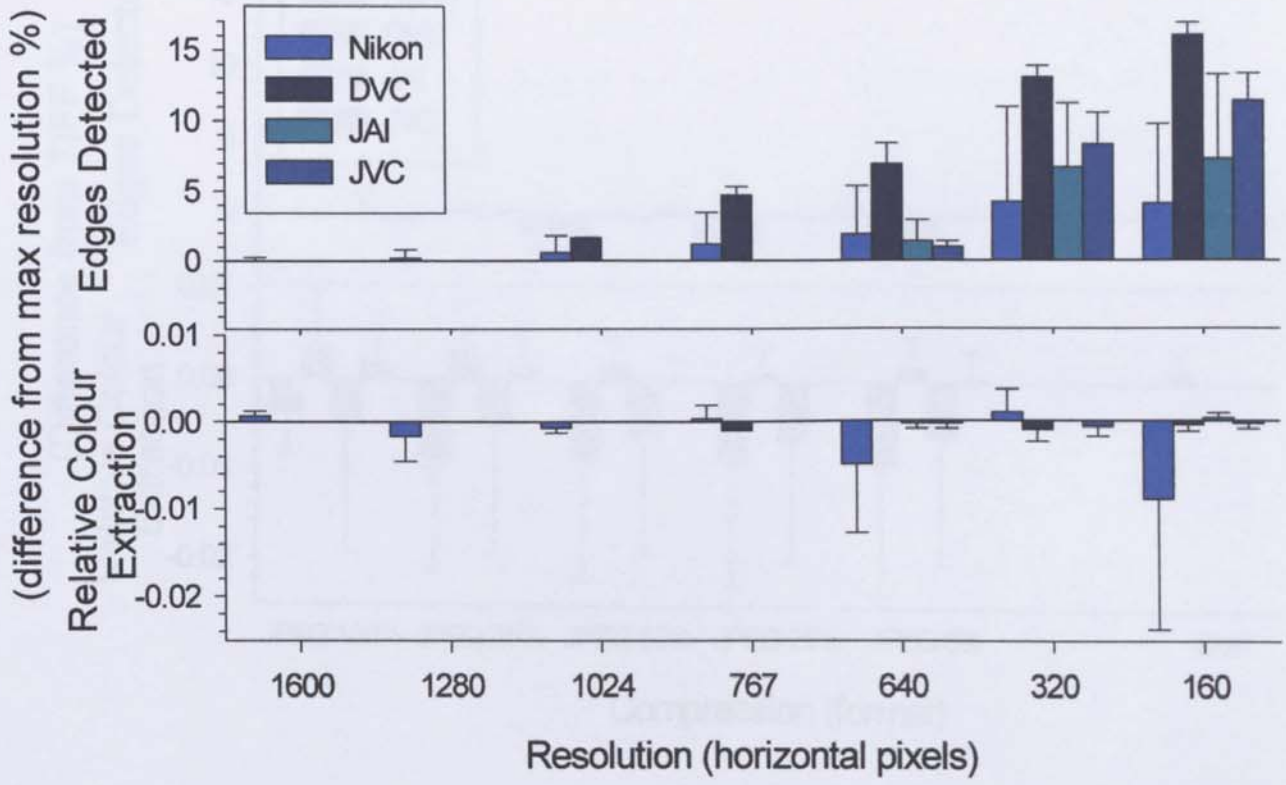

FIGURE 2.6: Mean objective edge detection and colouration grading for the compression range of each camera model. Error bars = 1 S.D.

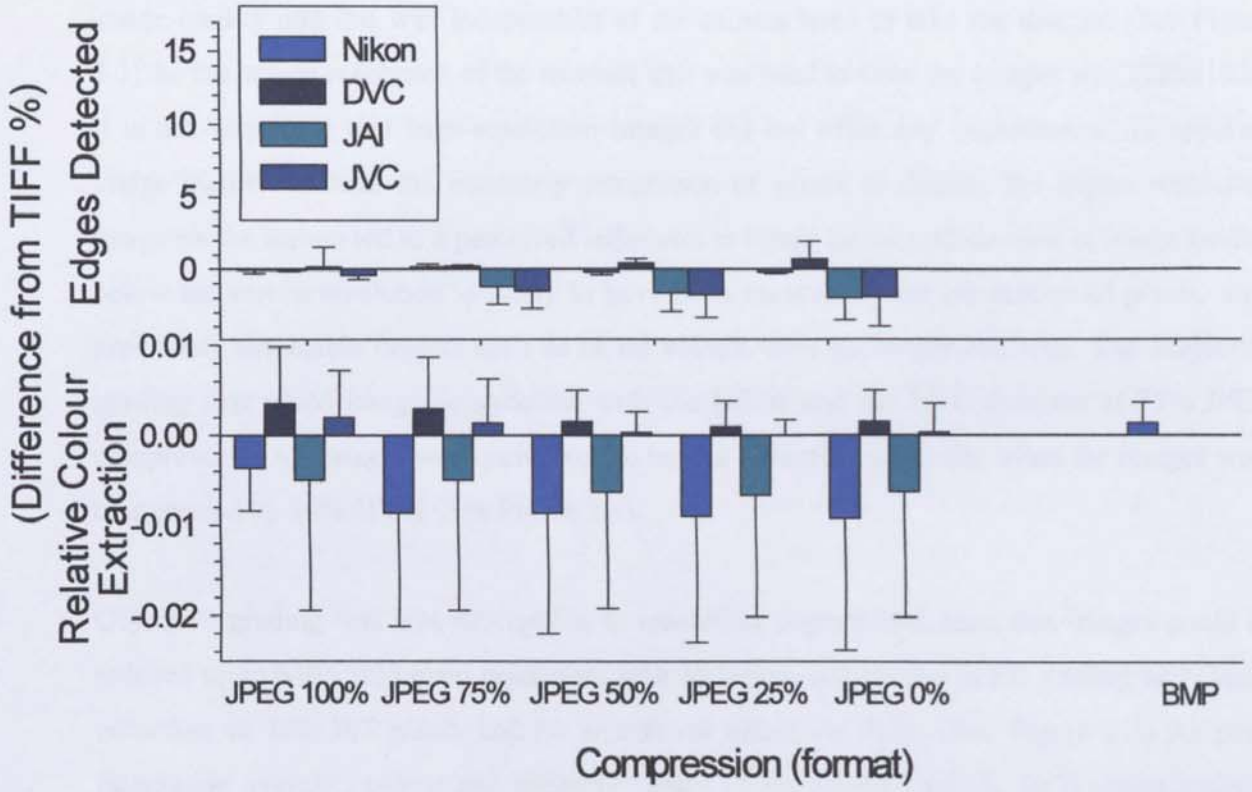

2.5 DISCUSSION

This study aimed to determine the most appropriate resolution and compression for anterior eye imaging. The theoretical resolution required to observe the smallest anterior eye pathological features varies with the magnification level of the slit lamp observation system. At a typical medium to high level of magnification (25x), 567 pixels across the horizontal field of view is required to detect an object 30μm in diameter.

Subjective grading identified that an image could be reduced to 767x569 pixel resolution (an 88% reduction in file size compared to a 2048x1360 pixel image) with no perceivable loss in image quality and this was independent of the camera used to take the images. (See Figure 2.3) As the screen resolution of the monitor that was used to view the images was 1280x1024, it is not surprising that high-resolution images did not offer any improvement in apparent image quality. Instead the necessary integration of pixels to display the higher resolution image on the screen led to a perceived reduction in image quality. Reduction in image quality below the screen resolution is likely to have been masked by the integration of pixels, until previously detectable objects such as blood vessels were no longer resolved. The subjective grading first noted image degradation with the Nikon and the DVC cameras at 75% JPEG compression. All images were perceived to have a reduction in quality when the images were compressed by 50% JPEG (See Figure 2.4).

Objective grading was less susceptible to resolution degradation, such that images could be reduced up to 640 x 425 pixel resolution with no significant change in ED grading and even a reduction to 160x107 pixels had no significant effect on RCE. (See Figure 2.5) As pixel integration averages colour and intensity values of surrounding pixels, RCE image analysis was not expected to change with image resolution. ED examines pixels surrounding a kernel to determine an edge dependent on a threshold value and therefore the sensitivity to changes in resolution will depend on the kernel (size and elements) and threshold used. [35]

The minimal appropriate level of resolution identified by; theoretical calculations, subjective ranking, and objective image analysis grading was lower than the level recommended by the 1999 government statement, that digital images should be of minimum resolution 1365 horizontal pixels. [66] It should be noted that the recommended government resolution is greater than SVGA resolution monitor resolution and therefore if the images are viewed on a

current standard monitor, the images will potentially be reduced in image quality compared to an image captured at a lower resolution.

Up to a 1:70 (50%) JPEG compression could be applied to an image, (regardless of the camera with which the image was taken on or its pixel resolution) without any apparent loss in subjective image quality. JPEG compression is designed to remove frequencies not utilised by the human eye (by using Discrete Cosine Transforms) and therefore the ability to compress an image by 98.6% (compared to a 2048x1360 TIFF) without a loss in subjective image quality confirms this strategy is successful. The limit of compression determined here is slightly greater than the levels that are suggested as being appropriate for retinal images. [68, 69] BMP compression allows an image to be read and displayed more quickly than a TIFF, but as the compression is essentially loss-less it is limited in reducing the image size of real images that continuously change in colour tone. BMP compressed images were subjectively rated as of lower image quality than the same resolution TIFF although it is not clear why this was the case. Objective grading of photographs with image analysis (both ED and RCE) was unaffected even by 0% JPEG compression. It would therefore appear that the frequencies removed by compression do not affect the image parameters examined.

No difference was found between the resolution-matched (767 x 569 pixels) 3-chip JVC KYF58 and the JAI CV-S3200 camera. The study examined the differences with changes in resolution and compression, so the finding does not indicate that there was no apparent difference in spectral fidelity compared to the photographed object between a 1-chip and 3-chip camera. However, once an image has been captured, there is no difference in the degradation caused by resolution and compression regardless of the maximum resolution of or number of chips contained within a camera.

It is reassuring that objective grading was not affected by compression and only significantly affected when the resolution was reduced to 320 x 213 pixels. However, there were differences between cameras, with the highest resolution camera examined (2048x1360 Nikon Coolpix) affected by resolution and compression less when analysed by edge detection and more when analysed by colouration compared to the other cameras. Therefore, ED rather than RCE image analysis may be more appropriate for objective grading with high-resolution cameras.

In conclusion, image sizes between 1280x811 and 767x569 or 1:70 JPEG compression appear to result in no loss in subjective or objective image quality. A higher pixel resolution image results in a larger file size and potential loss of image quality if viewed on a standard monitor. Use of compression has a greater effect on decreasing image size than reducing resolution, before subjective or objective loss of image quality occurs. Smaller image size increases storage capacity of a database, allows faster data transfer speeds and enables a high temporal frequency, real-time image to be displayed.

It is therefore appropriate to use a high-quality JPEG (low compression) to reduce file sizes during the following investigations as the objective analysis is not compromised by compression. The resolution need not be changed as the reduction in file size by compression alone is adequate. The camera used must remain consistent throughout.

Having examined the digital issues which could affect the objective grading, it is now appropriate to examine other factors which could alter the images captured. These include aspects such as filters and fluorescent techniques which will be used regularly in the following investigations when images of the palpebral roughness and corneal staining are taken.

CHAPTER 3

OPTIMISATION OF ANTERIOR EYE FLUORESCEIN VIEWING

3.1 INTRODUCTION

Fluorescein is a vital part of the examination of the anterior ocular surfaces. Sodium fluorescein is an orange/yellow substance that was first used in 1882 by Paul Ehrlich as an antibody labelling agent. [73] Ocular examination followed soon after this event and Pflüger instilled a quantity of fluorescein into the eyes and noted the areas of 'staining' on the cornea. [74] Due to its lack of toxicity fluorescein can be safely used within the body and hence is known as a 'vital dye'. It does not sting on insertion into the eye and does not cause adverse reactions upon single topical instillation; however some side effects have been noted for its use intravenously (in angiography) the most common of which is nausea affecting 8% of patients. [75] Some will argue that as the fluorescein does not penetrate or stain intact tissue [76]it is not strictly a 'dye', rather it is an 'indicator' of damaged areas or fluid dynamics, however for the purposes of this article the term 'staining' which is the adjective of choice in anterior ocular examination will be used throughout.

In order to determine the best-practice method of fluorescein instillation and viewing so that the image capture and objective analysis be more effective, it is necessary to investigate the factors which affect fluorescence. These factors include the wavelength of light used and the concentration of the instillation that would improve the eventual image captured, and allow a optimised method of fluorescein imaging to be used throughout the investigations that follow.

Fluorescein absorbs blue light and fluoresces green, this fluorescence is well established for studying ocular fluid dynamics and structural irregularities of the cornea and conjunctiva. [30, 77, 78] The precise mode of action of fluorescein when it stains the areas of compromised tissue is not fully understood. [30] Topical application into the tear film is generally recommended in a small quantity onto the lower conjunctival fornix as this enables the fast diffusion through the tears and coverage of the eye on blink without leaving a mark on the conjunctiva. Fluorescein mixes with the surrounding fluid highlighting the dynamics and volume. The concentration of fluorescein remaining in a sample of the tear film is correlated to ocular irritation symptoms and eyelid or corneal disease. [78] Fluorescein diffuses into intercellular spaces, such as defects in the tight-junctions of basal epithelial cells or cell drop-out (resulting in punctate staining). It cannot penetrate intact cell membranes, but once it gains entry it diffuses freely to the interior of surrounding cells by passing through junctional surfaces. [79]

Viewing or imaging the fluorescence involves an excitatory light source of sufficient power at the wavelengths absorbed by the fluorophore (485-495nm), [80] minimal power at wavelengths emitted by fluorescence of the fluorophore (510-520nm) or near the peak of the blue light hazard. This is represented in Figure 3.1. A short-wavelength barrier filter to reduce overlap between the excitation and emission spectra is also of benefit.

FIGURE 3.1: Blue light excitation and emission spectra of fluorescein (pH = 7.3) and the blue light hazard spectrum. The ideal source for ocular fluorescein excitation has the majority of its energy focused at the fluorescein emission peak (approximately 485-495nm), with minimal overlap with the fluorescein excitation peak or blue light hazard spectra. Adapted from McLaren and Brubaker. [80]

Blue light can damage the eye if of high enough intensity and long enough duration. [81] Slit-lamps used clinically for macular imaging can produce enough light to exceed the maximum permissible exposure in less than 15s. [82] McLaren and Brubaker examined a range of light sources in combination with barrier filters for their fluorescein excitation and blue light hazard, identifying an argon laser to be the most suitable for fluorescein excitation although tungsten filaments used in slit-lamp biomicroscopes were ranked second, with a safe retinal exposure time (for a 3.00 x 0.20mm slit) of approximately 70 minutes. [80]

A higher tear film pH results in higher fluorescent output, although the peak absorption wavelength remains relatively unaffected (between pH 6-9). [83] The pH in the conjunctival sac is typically 6.93±0.27, (range 5.90 to 7.60), independent of age and gender. [84] The conjunctival fluid is significantly more acid in contact lens wearers (by approximately 0.2 on average), but becomes normalised after lens removal. The conjunctival fluid pH is relatively unaffected by more anterior conditions, but is significantly more alkaline in patients with fungal keratitis (7.40 ± 0.23), 1 day post corneal graft (7.21 ± 0.22) and dry eyes (7.13 ± 0.31). [84]

The intensity of fluorescence of fluorescein in aqueous solution increases with increasing concentration up to a maximum (approximately 0.001-0.04%) and then falls off at higher concentrations (a process termed quenching). [79] At higher concentrations, the maximum emission spectrum is shifted towards longer wavelengths (more yellow than green). [79]

3.2 PURPOSE

This study aimed to examine the spectral radiance output of slit-lamp blue illumination and the spectral transmission of yellow barrier enhancement filters. It also investigated quenching and fluorescein efficiency in the clinical environment in order to assess the optimisation of fluorescein image viewing and digital capture.

3.3 METHODS

Spectral Radiance: The spectral radiance of slit-lamp biomicroscope blue luminance was measured with a Spectrascan PR-650 photometer (Photo Research Inc. California, USA). Nine different models of slit-lamp biomicroscopes were evaluated to examine the range of blue luminance currently employed: Haag-Streit (Koeniz/Bern, Germany) BM900, BQ900 and BC900; Takagi (Nagano, Japan) Mk1 and SM-70; Nikon (Tokyo, Japan) SF-3V; Topcon (Tokyo, Japan) SL.D7 and SL.3F; and CSO SL990 (Scandicci Firenze, Italy). In addition, the illumination outputs from three slit-lamps of the same model (Nikon SF-3V) each 3 years old and having had similar usage were measured to investigate the repeatability of the findings. The Topcon SL.D7 has a filter that can be inserted into the luminance path to adapt the spectral radiance to be more appropriate for fluorescein viewing. Therefore the spectral radiance of a Topcon SL.D7 slit-lamp biomicroscope with this filter in place was also measured. Analysis of the distributions of the radiance were performed using Pearson correlation statistics

Spectral Transmission: The spectral transmission of three manufacturers yellow barrier filters were measured with a Cary-2300 Spectrophotometer (Varian Inc. California, USA). Two filters (from Haag-Streit and Takagi) are integrated into the slit-lamp optics and the third (Bausch and Lomb, Rochester USA, version 2005) is cardboard mounted (held in front of the observation system).

Quenching: To examine the clinical performance of different forms of ocular fluorescein installation, the intensity of green light emitted from the eye was measured with a JAI CV-S3200 (Yokohama, Japan) video camera at 25Hz for 8 minutes attached by beam-splitter to a Takagi SM-70 slit-lamp (Nagano-Ken, Japan) with maximal intensity blue illumination and in-built yellow observation filter applied. The ten subjects (aged 27±3 years, 6 female) had fluorescein instilled into the right lower fornix using a 1% minim, 2% minim, a single drop of saline on a fluoret (Chauvin England UK) and a floret moistened with saline with the excess shaken off, in random order, each instillation separated by 2 days. The study was approved by the institutional ethics committee and conformed to the Declaration of Helsinki. Patient consent was given after a full written explanation of the study methods and intensions. Subjects were directed to blink every ten seconds, metered by metronome (for accuracy, and so that the subjects could count the seconds until their next blink which helped them to maintain an open eye). The 4 videos were analysed in real-time by purpose-designed

LabView™ software (National Instruments, Austin, Texas, USA) which had been modified from the original design (described in section 1.3.2) to measure the intensity of the wavelengths emitted fluorescence in 8-bit greyscale over 20mm of the interpalpebral aperture. The modifications are displayed in Figure 3.2 which shows the analysis of 5 defined areas over the cornea, instead of just one area which is manually selected by the user. The 5 areas were designed to sit in the 4 quadrants and one centrally on the cornea in order to obtain an average of the fluorescence over the whole pre-corneal tear film.

FIGURE 3.2: View of the adapted LabView program with 5 squares of analysis over the video of the cornea to detect the intensity of fluorescence in the pre-corneal tear film over time and with different concentrations of fluorescein.

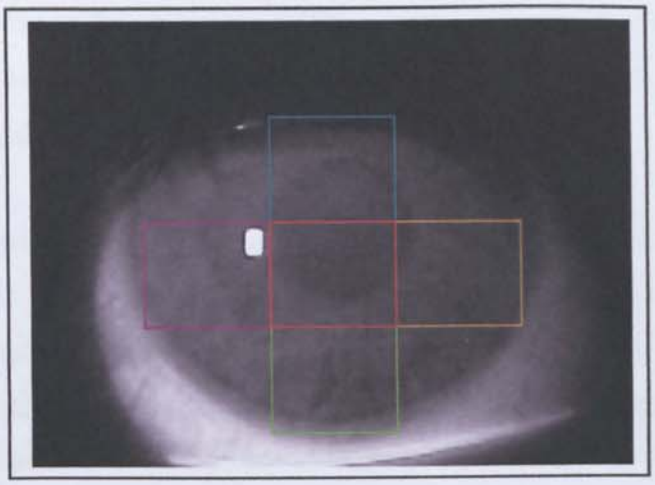

Subjective evaluation was then performed by 10 optometrists who were shown a video of the 1% minim insertion (as this had a shorter duration of useful fluorescence than some of the others). The optometrists examined the video (which was shown using Windows Media Player software using a 15"CRT monitor (CTX Ultrascreen CA, USA) at 40cm distance) and using the cursor chose a point where the fluorescence intensity of the fluorescein in the tear film was first adequate for a clinical assessment. They then moved the video on and stopped the cursor when they determined that the level of fluorescence had dropped below that which would allow for adequate assessment. This process was repeated 3 times on 3 separate occasions.

The intensity of fluorescence which was present at the points where the optometrists deemed the fluorescence to be first adequate and then inadequate for clinical assessment was found. T-tests were utilised here to make the comparisons between the different concentrations.

3.4 RESULTS

Spectral Radiance: The radiance of the blue filters of the slit-lamps showed similar light distributions (Pearsons r=0.80-0.99; p<0.001) close to that of 'Cobalt blue' (Pearsons r=0.91-0.99; p<0.001), except for the Topcon enhancing filter (r=0.09-0.59) and Takagi SM-70 (r=0.70-0.91; Figure 3.2). There was good repeatability between the spectral profile of the three slit-lamps of the same model (Nikon SF-3V; r=0.99, p<0.001), but the intensity of light emitted varied over 438-634cd/m^2 (F=39.3 p<0.001).

Most of the blue light sources have peak intensity at approximately 460nm and have a spectral profile which covered only 8.3-12.2% of the ideal spectral profile for greater than 80% fluorescein absorption. Of the slit-lamps examined, the Takagi SM-70 filter had the best match for fluorescein absorption with a peak at approximately 480nm (30.2% of the profile within the optimal range for absorption). The spectral radiance profile of the Topcon blue enhancement-filter has its peak at approximately 504nm, with 50.6% of the light within the optimal fluorescein absorbance range. (See Figure 3.4)

Hazardous blue light hazard is optimal (i.e. greater than or equal to 80% relative strength) between 420-465nm. A low amount - 6.9% of the Topcon SL.D7 light with the enhancement filter fell in this range, compared to 38.6-60.9% with the other slit lamps examined. A spectral radiance greater than 500nm will interfere with the observation of the fluorescence emission. This was much greater with the Topcon enhancing-filter (23.5% of light output fell in this range), compared with all the other slit lamps examined having an output between 1.2-8.0%, with the Takagi SM-70 having the lowest value.

FIGURE 3.3: Spectral radiance of slit-lamp biomicroscope blue luminance and barrier filter transmittance.

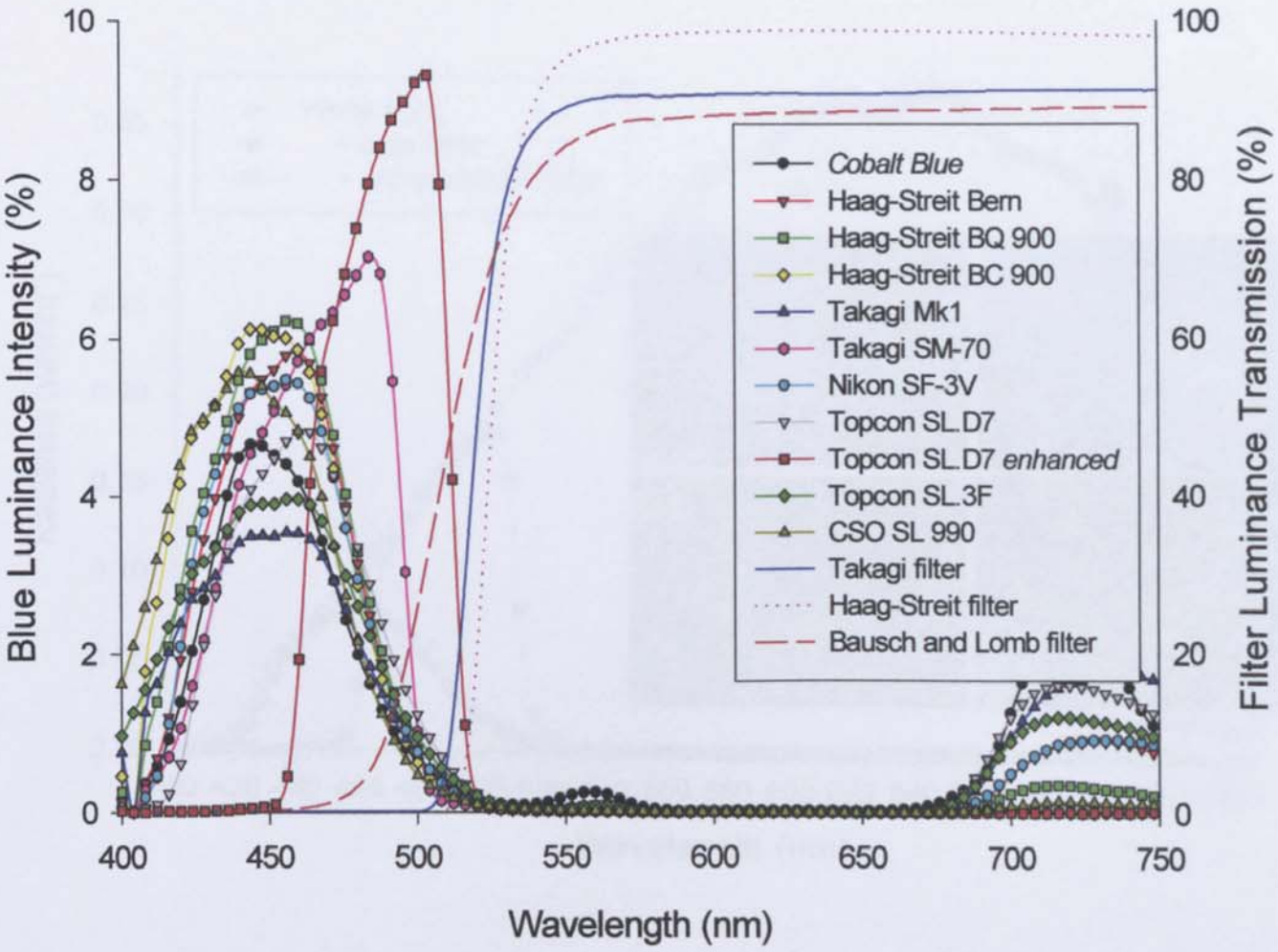

FIGURE 3.4: A comparison of the radiance difference and subsequent fluorescence effect of the original Topcon blue filter (labelled A) with the new enhancement filter (labelled B). Images captured using the Topcon SL-D7 slit-lamp camera system.

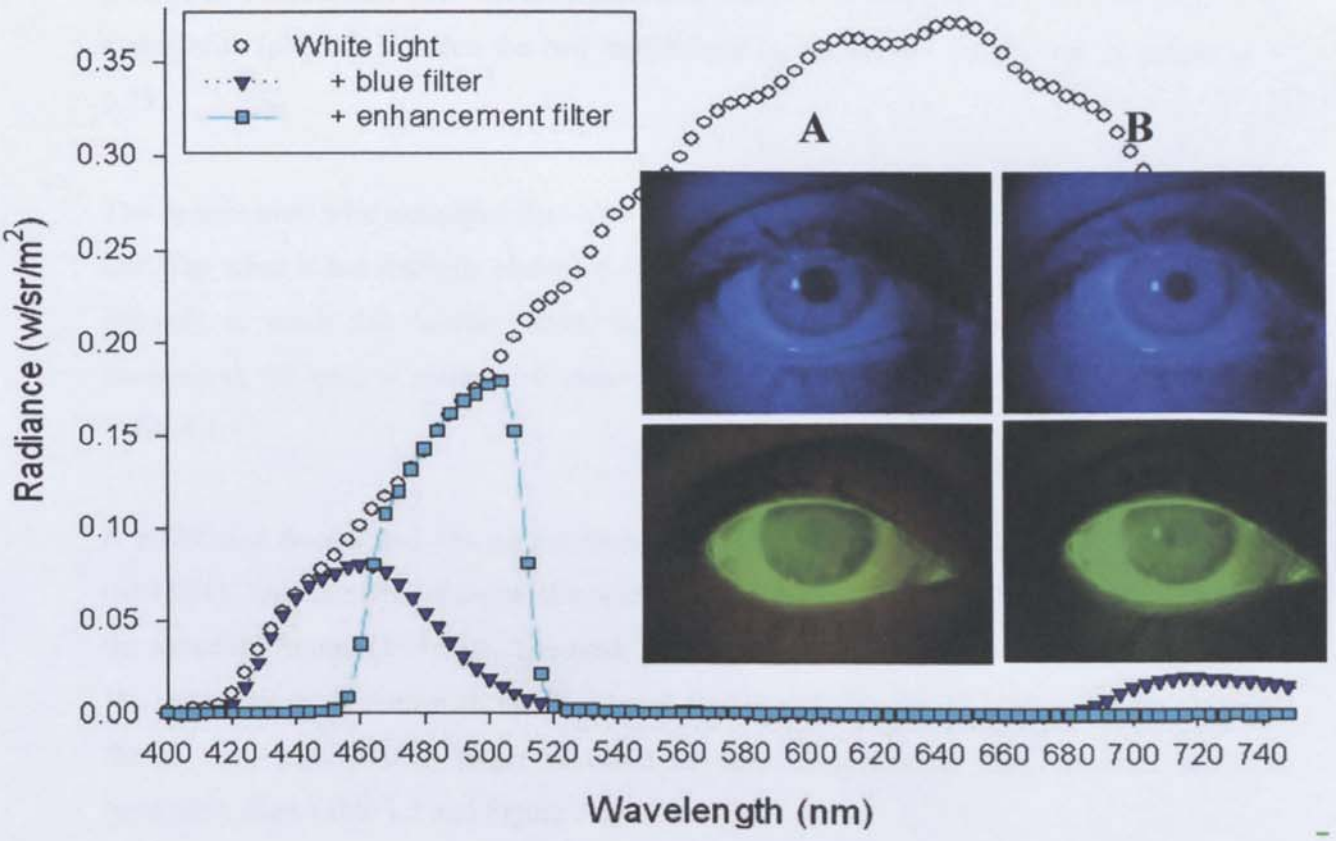

Spectral Transmission: The two internal yellow barrier filters examined had a cut off at approximately 510-520nm, with less than 32% of the wavelengths for greater than 80% optimal fluorescein fluorescence transmitted (See Figure 3.2). The hand-held filter excluded less light less than 500nm (1.7% compared to less than 0.1%), but transmitted 52.6% of optimal fluorescence wavelengths.

Quenching: A comparison of the 4 fluorescein instillation methods showed different intensity profiles of fluorescence between the fluoret and minim methods ($p<0.05$), although there was a similarity ($p>0.05$) between the two instillations by fluoret ($r = -0.15$) and by minim ($r = 0.29$).

The optometrists who examined the video determined that fluorescence is useful to assess the tear film when it has intensity above $16.43 \pm 6.43 cd/m^2$. The time taken for the fluorescence intensity to reach this 'useful' level, the duration over which 'useful' fluorescence was maintained, the time to reach peak intensity, and the peak intensity reached are recorded in Table 3.1.

A moistened fluoret and 1% minim took less time to reach a useful level of fluorescence ($p<0.001$). The duration of useful fluorescence from the 2% instillation differed from all but the saturated fluoret ($p<0.001$). The peak intensity was higher with the saturated fluoret and 1% minim methods than with the moistened fluoret and 2% minim ($p<0.05$). The saturated fluoret took significantly longer to reach its peak fluorescence than the other methods ($p<0.005$). (See Table 1.3 and Figure 3.5)

TABLE 3.1: Comparison of the times taken for the 4 different methods of fluorescein instillation; to reach, and maintain useful fluorescence, the time to peak intensity, and the level of that peak.

Method of instillation	Time to achieve 'useful level' (s)	Duration of 'useful' level (s)	Time to peak intensity (s)	Intensity at peak (cd/m2)
Moistened fluoret	25.80 ± 6.49	158.60 ± 56.14	44.00 ± 39.50	19.17 ± 3.22
Saturated fluoret	59.00 ± 25.58	339.52± 25.14	230.00 ± 29.06	33.26 ± 7.44
1% minim	21.60 ± 4.45	162.02 ± 20.13	74.50 ± 15.89	31.85 ± 10.74
2% minim	57.60 ± 21.59	225.20 ± 31.81	137.00 ± 91.78	22.89 ± 8.65
ANOVA	**F=15.68 p<0.001**	**F=11.27 p<0.001**	**F=23.56 p<0.001**	**F=6.57 p<0.005**

FIGURE 3.5: Average fluorescence intensity profiles for moistened fluoret, saturated fluoret, 1% minim and 2% minim methods of fluorescein instillation over time. n=10

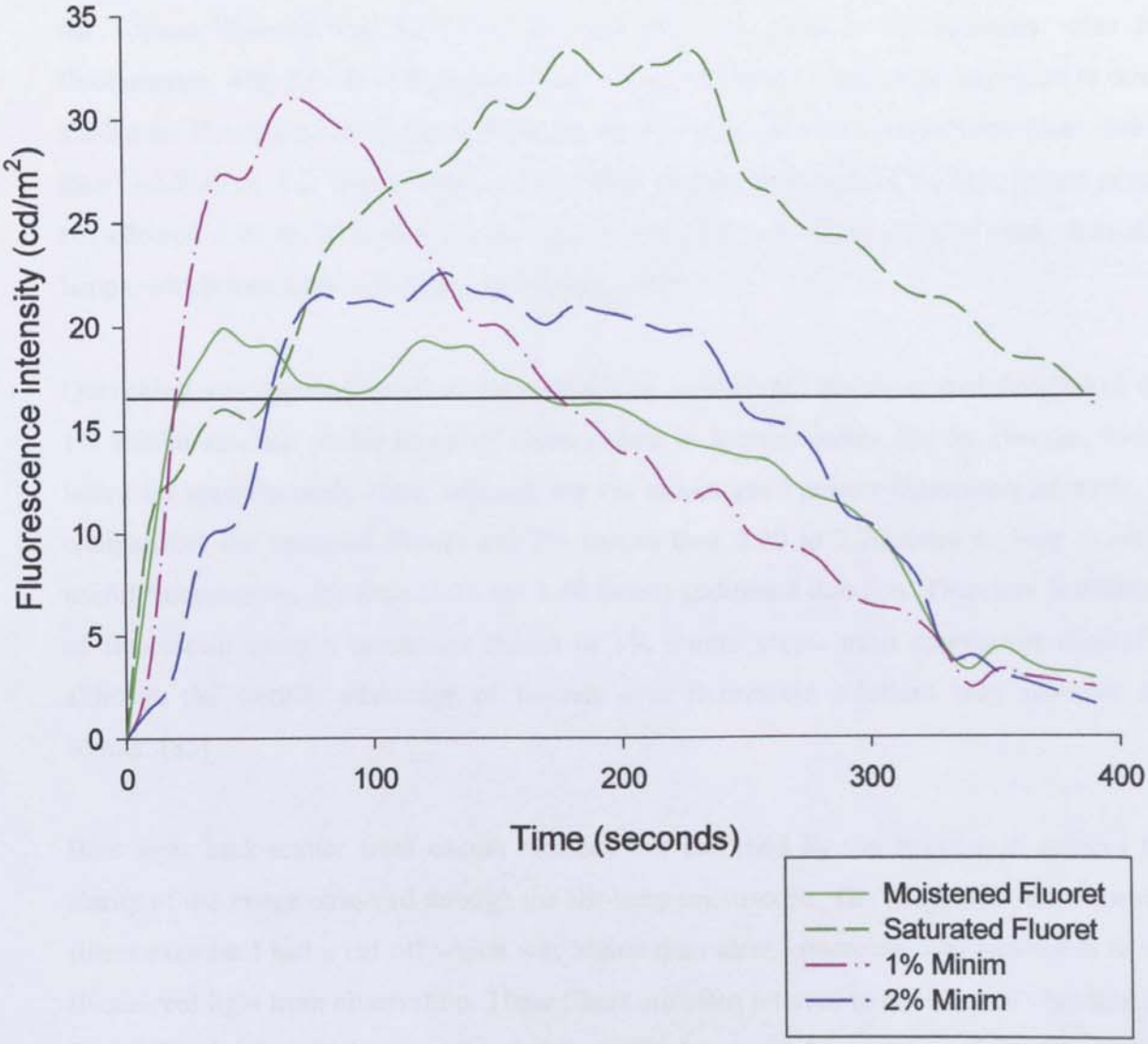

3.5 DISCUSSION

The slit lamp blue illumination should have maximum power at the wavelengths absorbed (approximately 485-495nm) and little at the wavelengths emitted by the fluorophore (approximately 510-520nm). Most of the slit lamps currently on the market had a blue light peak at approximately 460nm (similar to that of cobalt-blue) and only the Takagi SM-70 and the Topcon Enhancement filters emitted light that was close to the optimum value for fluorescence, with 2.50 to 5.70 times as much light within the ideal range compared to other slit-lamps. Hence the blue slit-lamp light setting should be called 'fluoro-enhance blue', rather than Cobalt-blue. The Topcon enhancement filter emitted little light in the blue hazard range, but allowed 2.90 to 19.60 times more light above 500nm to be transmitted than other slit-lamps, which interferes with fluorescein image clarity.

Quenching was apparent in all of the methods of instillation. The moistened fluoret and the 1% minim reached useful levels of fluorescence in approximately 20s on average, which lasted for approximately 160s, although the 1% minim gave greater fluorescent intensity. In comparison, the saturated fluoret and 2% minim took 2.20 to 2.70 times as long to reach useful fluorescence, for little (1.20 ton 1.40 times) additional duration. Therefore instillation of fluorescein using a moistened fluoret or 1% minim seems most appropriate clinically, although the sterility advantage of fluorets over fluorescein solutions may advocate the former. [85]

Blue light back-scatter from excess radiance not absorbed by the fluorescein reduces the clarity of the image observed through the slit-lamp microscope. The integrated yellow barrier filters examined had a cut off which was higher than ideal, obscuring over two-thirds of the fluorescent light from observation. These filters are often referred to as 'Wratten', but this is a Kodak filter make which covers a wide range of colours and does not accurately describe the ideal yellow barrier slit-lamp filter. As a consequence of this study the Bausch and Lomb hand-held filter (for which a new batch was intended to be ordered) incorporated a different filter with a lower wavelength cut-off. The difference in Transmittance is displayed in Figure 3.5

The new filter removes more of the blue light scatter, and allows a better view of the fluorescence on the ocular surfaces (by 8%). This is demonstrated by Figure 3.6 which compares images of the same eye taken after instillation of fluorescein (moistened fluoret)

with the original and the new filter over the observation optics at 10, 20 and then 30 seconds after instillation. The new filter clearly gives a better image of the fluorescence.

FIGURE 3.6: Transmittance of four yellow barrier filters including the new filter.

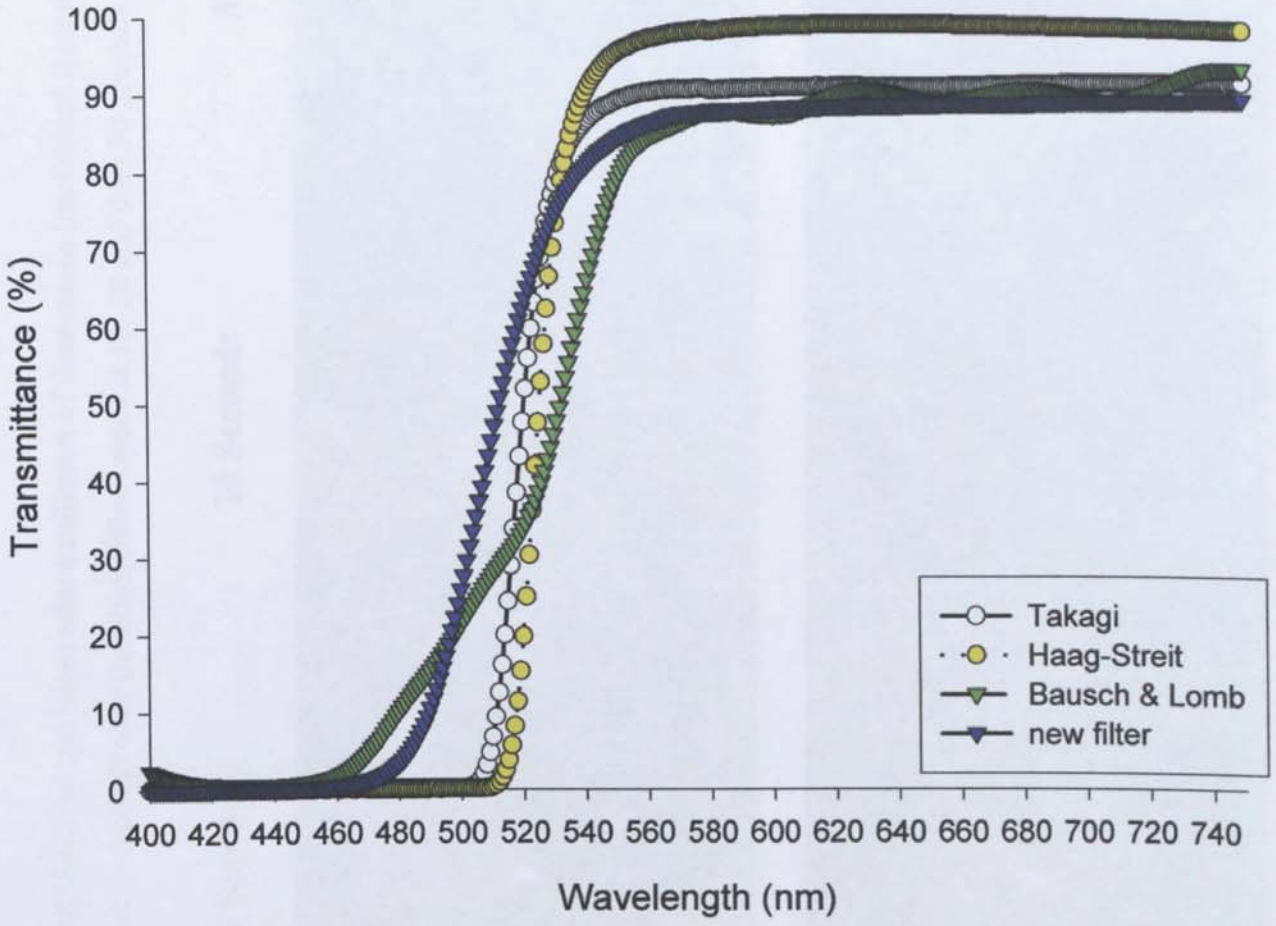

FIGURE 3.6: Comparison of images of the same eye taken after instillation of fluorescein (moistened fluoret) with the original (blue surround) and the new filter (white surround) over the observation optics at 10, 20 and then 30 seconds after instillation.

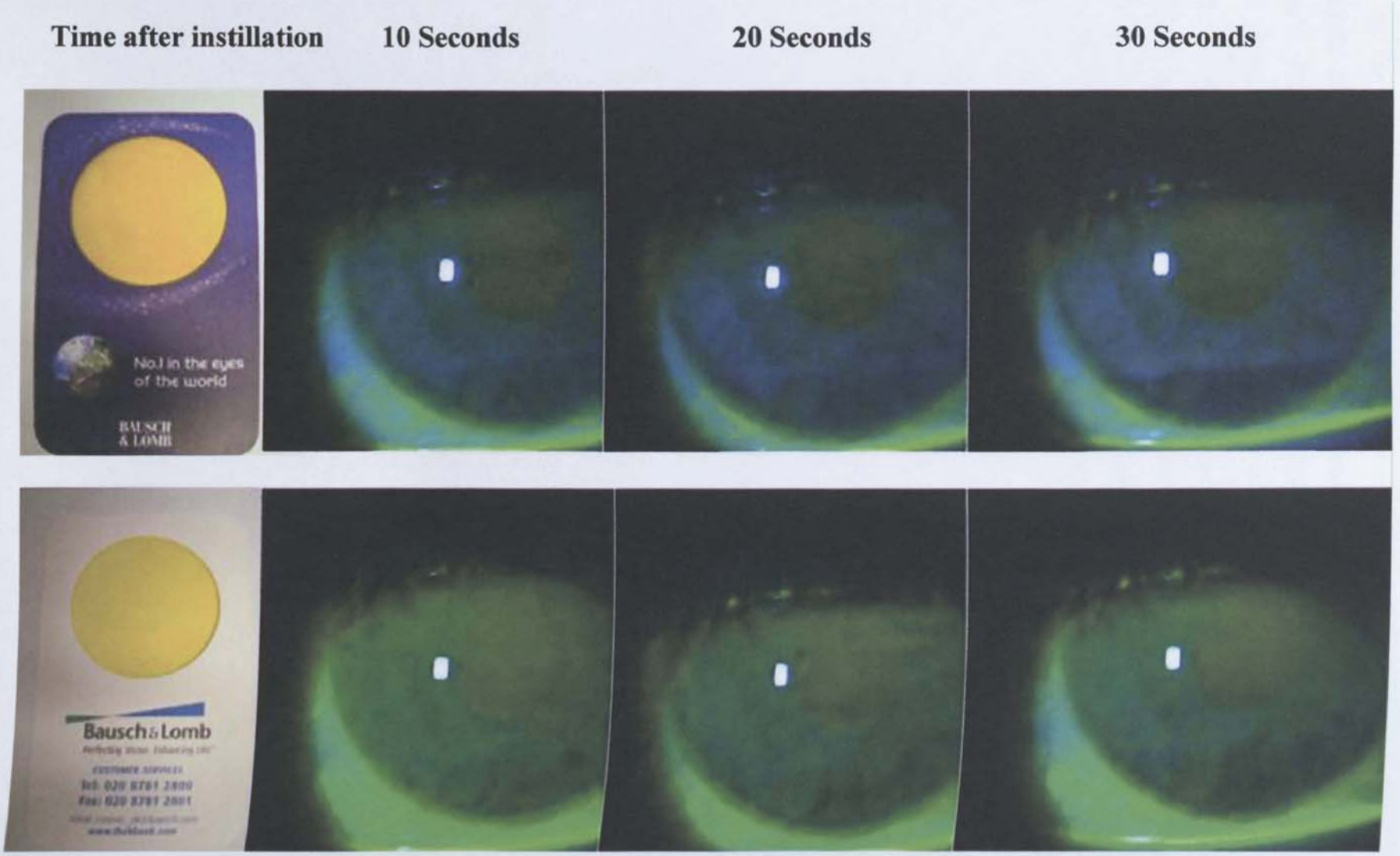

The factors which would affect digital image capture and objective anterior ocular grading are; the equipment used to capture the images (camera and slit-lamp), the digital quality options, and the lighting considerations. Chapter 1 described the factors involved in digital image capture and identified the most appropriate camera options for mass-anterior ocular photography. Chapter 2 evaluated the effect of resolution and image compression on the results of subjective and objective image analysis and determined that the objective analysis was only affected after the image resolution was reduced to 640 x 425 pixel resolution with no significant change in ED grading and even a reduction to 160x107 pixels had no significant effect on RCE. The investigation in Chapter 3 has established the best-practice method for fluorescein instillation and fluorescence viewing / image capture.

CHAPTER 4

SENSITIVITY AND RELIABILITY OF OBJECTIVE IMAGE ANALYSIS COMPARED TO SUBJECTIVE GRADING OF BULBAR HYPERAEMIA

4.1 INTRODUCTION

Redness or hyperaemia of the anterior eye is an important indicator of ocular health. [31] The area has been extensively researched especially with regard to measuring the changes in vasculature, as these have been shown to indicate not only ocular pathology, but also certain systemic conditions. [56, 86, 87] Due to the importance of this area, it is vital that subtle changes in appearance are able to be detected reliably by optometrists and other eye-care practitioners (ECPs)

This chapter aims to evaluate the sensitivity and reliability of the objective image analysis program in order to validate the method for use in clinical evaluations of the anterior surfaces.

To this end it is helpful to define the terms used in this study:
Reliability: In experimental sciences, reliability is the extent to which the measurements of a test remain consistent over repeated tests of the same subject under identical conditions. [88] An experiment is reliable if it yields consistent results of the same measure. Regarding statistical analysis Bland and Altman define reliability as the 'correlation coefficient between repeated measurements. [89]

Sensitivity: The smallest concentration of a substance that can be reliably measured by a particular analytical method. [90] Or in statistics, the proportion of true positives that are correctly identified by the test. [91]

Monitoring of ocular disease and the effect of treatment strategies requires the ability to reliably detect subtle changes in the appearance of the ocular surface. Subjective assessment by optometrists, ophthalmologists and contact-lens practitioners (who are collectively known as eye-care practitioners or ECPs) is however inherently variable and so led to the introduction of grading scales, which aimed to reduce variability and to encourage uniform grading of the anterior eye. [18, 19, 33] (as previously discussed in Section 1.3) In the most commonly utilised scales, the eye under observation is compared subjectively to a scale of four or five predetermined images that ideally represents the full range of severity of a specific condition. The level on the scale that best matches the characteristic of the eye being graded is recorded, ideally interpolated to one decimal place in order to improve discrimination. [41] However, intra and inter-observer variability remains high - even with the use of these scales, as a wide range of the scale is used by different practitioners to represent

the same eye / image. [19, 36] Other factors affecting the reliability and sensitivity of subjective grading are the ECPs reluctance to interpolate between the scale's images, (even if training has been undertaken) [37] and the fact that the scales are not incrementally linear in nature, instead having increased sensitivity at the lower end of the scale and other inconsistencies. [36]

The sensitivity and reliability of grading affects an ECPs ability to monitor and diagnose pathology efficiently and accurately. To improve this situation several studies have investigated computer-based objective grading of ocular surfaces. With respect to vascular changes, a variety of parameters have been the focus of objective analysis software, including the area of blood vessel coverage, the calibre, the redness colouration and the length of visible vessels. [31, 35] Edge detection (ED) and relative colour extraction (RCE) have been shown to be the most repeatable and discriminatory of those techniques used for automated grading of ocular images. [35]

4.2 PURPOSE

Image analysis with LabView ED and RCE techniques were found to be approximately 7 times more reliable than that reported in the literature for subjective grading, however no direct comparisons have previously been established. [35]

Building on the work of Willingham and colleagues who objectively assessed bulbar hyperaemia pre- and post-instillation of a vasodilator, [53] it was hypothesised that capturing digital video of pharmaceutically induced vasodilation would allow a series of images of successively changing bulbar conjunctival hyperaemia to be created, and that this would offer a quantifiable method to assess whether changes in bulbar hyperaemia are more precisely and reliably differentiated by objective image analysis than by subjective grading. The result of this study will indicate whether objective image analysis could be used to enhance the clinical quantification and monitoring of the signs of anterior eye disease.

4.3 METHODS

In order to obtain images of the same eye with a range of severity of hyperaemia, it was necessary to induce hyperaemia by controlled ocular vasodilation. Two drops of 0.5 % Dapiprazole hydrochloride (Rev Eyes, Bausch and Lomb, Rochester USA) were instilled onto the bulbar conjunctiva of the temporal side of the right eye. Informed consent was received after explanation of the study. The study was approved by the institutional ethics committee and conformed to the Declaration of Helsinki.

The subject's right nasal bulbar conjunctiva was imaged at an angle of 35° through a Takagi SM-70 slit-lamp biomicroscope (Nagano-Ken, Japan) set on 10 times magnification providing diffuse white illumination. The instillation and the subsequent vasodilation was captured by a JAI camera (CV-53200, Yokohama, Japan) on DV media tape (resolution 800,000 pixels at 25Hz). Blink rate was regulated every 10 seconds using a metronome. 45 high quality JPEG images were extracted at 2 second intervals after instillation of the vasodilator (avoiding frames with blinks) to cover the main period of vasodilation. This was repeated for 3 eyes (3 subjects; average age 28 ± 4.93 years, 2 female) leaving the total number of images at 135. The effect of the vasodilator can be seen in Figure 4.1

Objective analysis: The 45 images from each of the 3 eyes were analysed by purpose designed and previously validated software [35] (LabView™, National Instruments, Austin, Texas, USA) which used edge detection (ED) with a 3 x 3 kernal, and relative colour extraction of the red plane (Red RCE) [35] in a rectangular area covering the visible temporal bulbar conjunctiva (300x250 pixels at 10x magnification which is equivalent to an area of 6.82x5.68mm. This area was chosen as the largest sample of the conjunctival area possible to measure within the limits of the palpebral apertures.) The measurements were repeated 6 times for each of the 135 images to allow an evaluation of objective reliability.

Subjective analysis: The 135 images from the videos of the 3 individuals were taken and each was placed (in a random order determined by a random number generator from Microsoft Excel - Microsoft Corporation, Redmond, Washington, USA) onto a PowerPoint presentation slide (Microsoft Corporation, Redmond, Washington, USA) which provided the perfect vehicle for efficient access of so many images during the study, and did not reduce the image quality. A 15 inch cathode ray tube monitor (CTX Ultra screen, California, USA) was used to display the presentation. One of the images was duplicated within the PowerPoint

slides to allow the reliability of grading the same image within a single session to be assessed. Six optometrists and 6 non-clinicians were recruited (28±4.93 years). The task of allocating a grade to an image using the grading scale was explained and demonstrated to the non-clinicians and they graded a single trial slide to confirm that they had full comprehension of the task. All subjects were instructed to start at slide 1 and using the cursor keys move through the slides giving each image a grade in comparison to the Efron scale (Millennium edition) [28] to 1/10th of a scale grade. They were not allowed to return to a previous slide in order to make a comparison. The optometrists were required to repeat the grading on a further two occasions, each separated by 2 days, in order to evaluate their reliability.

Statistical methods: Due to the repeated evaluations of the images a 'repeated measures' ANOVA is appropriate, to determine any differences between the subjective groups, and then the objective evaluations of each of the images. A post-hoc assessment must then be made which will show the number of significantly different grades given over the 45 images for each of the 3 thymoxamine instillations. This value indicates the sensitivity of the subjective and objective evaluations. Reliability will be calculated by using the Bland and Altman coefficient of reliability REF, which is similar to the correlation coefficient but takes into account that the order of the measurements is important. It is defined as the following:

$$r_I = mSSB - SST/(m - 1)\ SST$$

Where m is the number of observations per subject. SST is the total sum of squares and SSB the sum of squares between subjects. [89]

4.4 RESULTS

FIGURE 4.1: Images of one eye prior to, and 2 minutes post vasodilator instillation

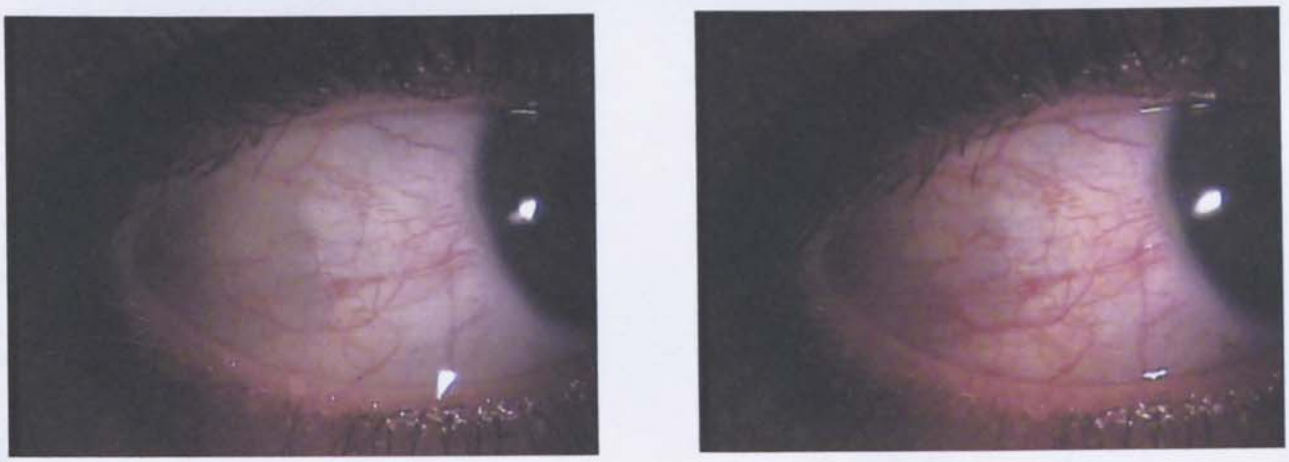

4.4.1 Sensitivity

There was a significant increase in the area of blood vessel coverage measured by ED ($F = 9027.0$, $p < 0.001$) and Red RCE ($F = 2872.6$, $p < 0.001$) following instillation of the vasodilator (Figure 4.2). Tukey post-hoc analysis identified that the average time interval between each significant increase in blood vessel coverage was (3.92 ± 1.90 s) and in red colouration was (4.26 ± 10.65 s). As the average change in ECP grading between the first and last images was (0.40 units), this equates to a sensitivity of 0.014 of an Efron grade for edge detection and 0.015 for colour extraction.

FIGURE 4.2: Mean grades given by ED image analysis, to each of the 45 successive images of increasing hyperaemia averaged for 3 eyes. Error bars = 1 S.D.

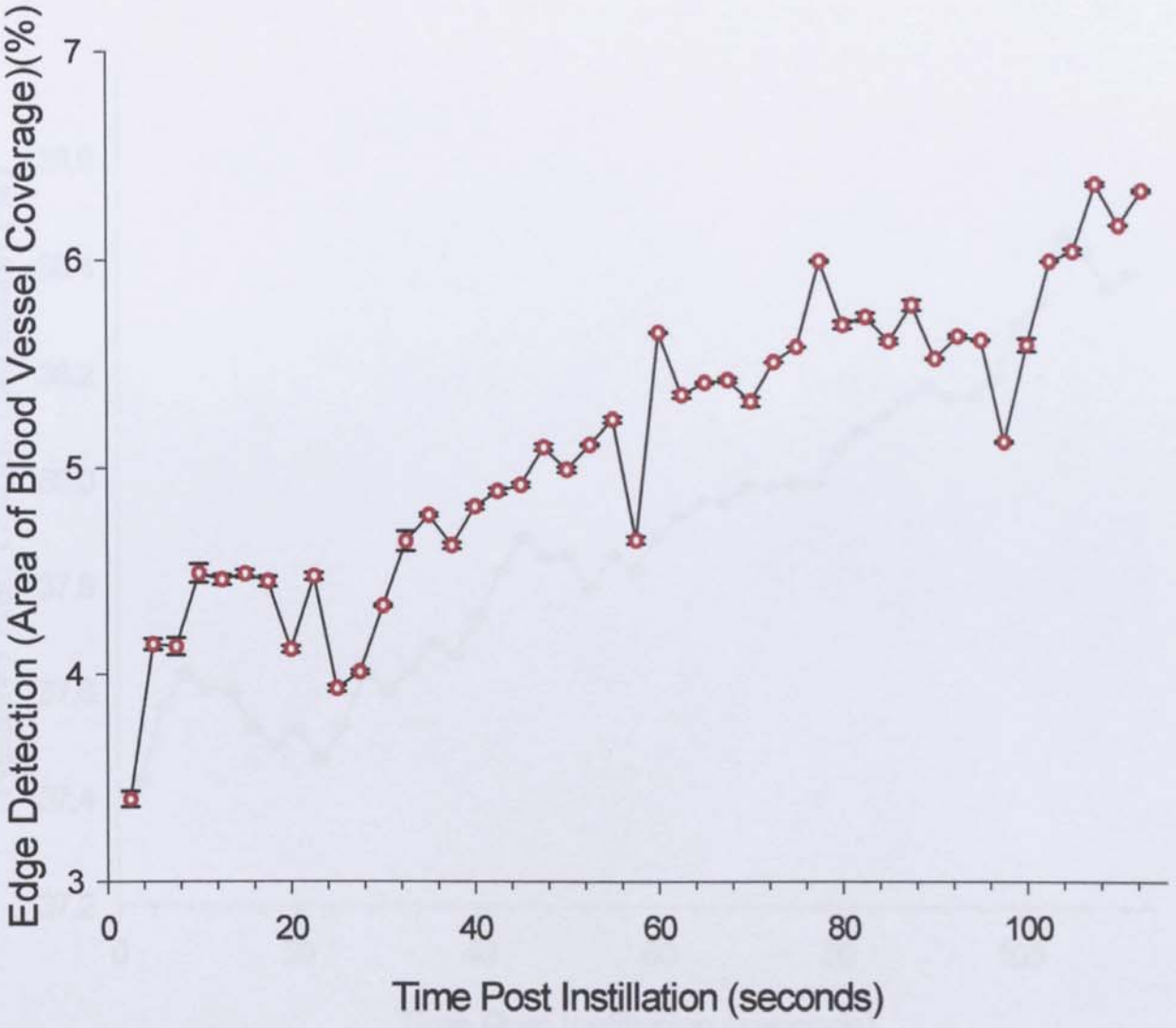

FIGURE 4.3: Mean grades given by RCE image analysis, to each of the 45 successive images of increasing hyperaemia averaged for 3 eyes. Error bars = 1 S.D.

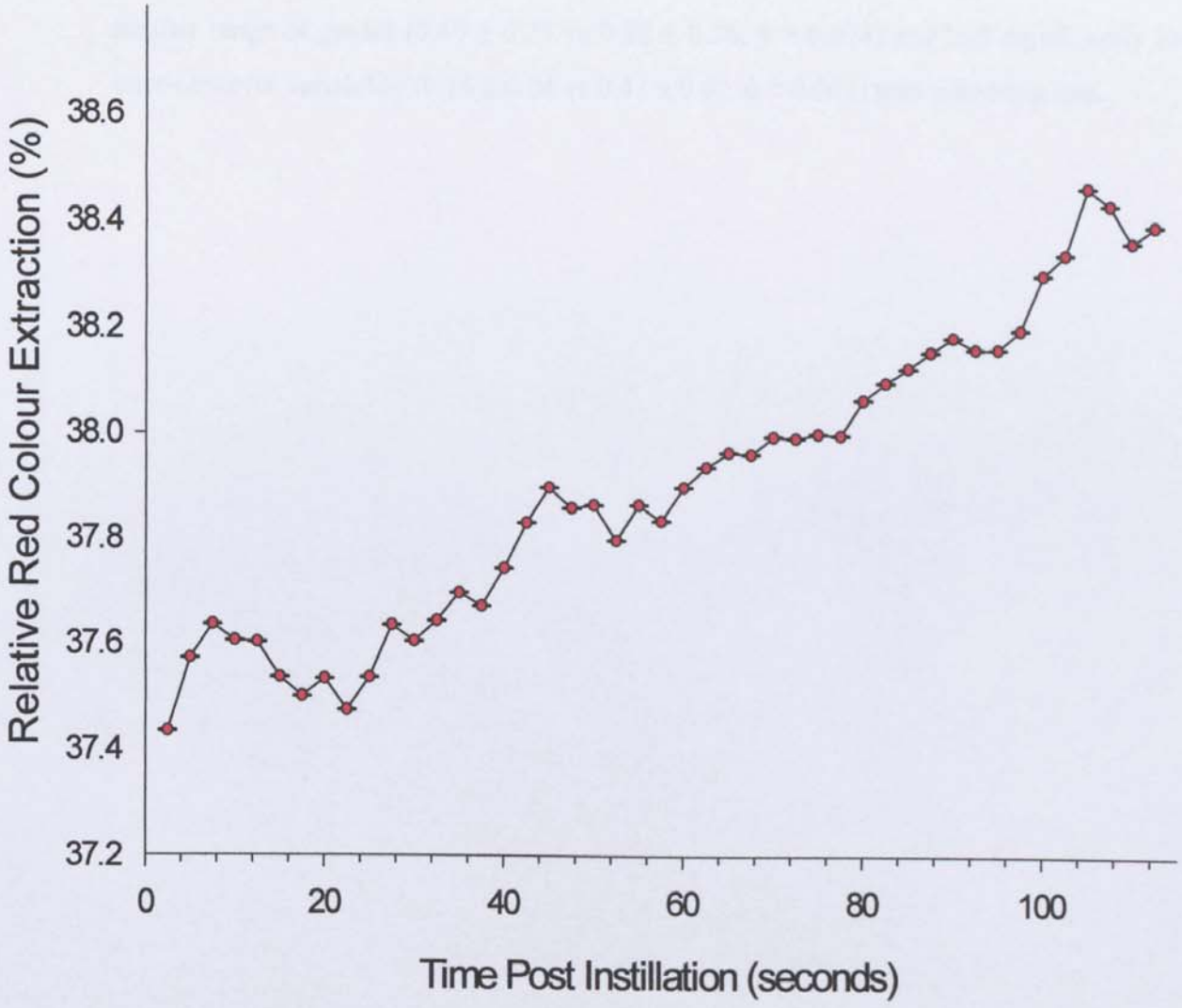

There was a significant increase in the subjectively rated Efron grade for both optometrists ($F = 2.40$, $p < 0.001$) and non-clinicians ($F = 7.30$, $p < 0.001$) following instillation of the vasodilator (Figure 4.43 and 4.5). However, post-hoc analysis showed that the average time interval between each significant increase determined by optometrist grading was (81.88 ± 20.65 s) and for non-clinicians was (59.21 ± 10.41 s). As the average change in optometrist grading between the first and last images was 0.40 units, this equates to a sensitivity of 0.291 Efron units for optometrists and 0.21 Efron units for non-clinicians. Optometrists utilised a smaller range of grades (0.40 ± 0.25 vs 0.88 ± 0.36, $p = 0.074$) and had significantly lower inter-observer variability (0.14 ± 0.04 vs 0.43 ± 0.07, $p < 0.001$) than non-clinicians.

FIGURE 4.4: Mean grades given by optometrists to each of the 45 successive images of increasing hyperaemia averaged for 3 eyes. Error bars = 1 S.D.

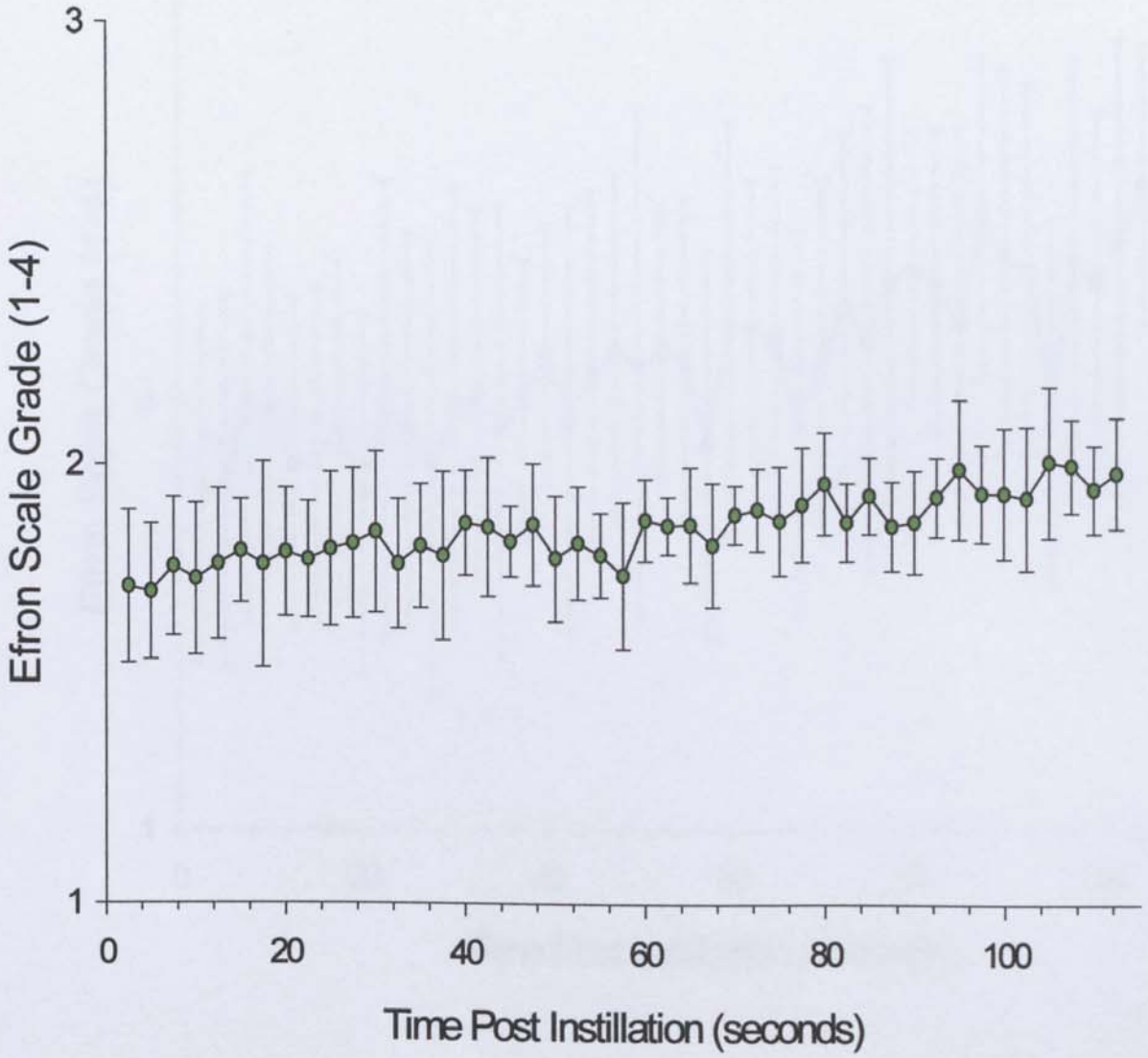

FIGURE 4.5: Mean grades given by non-clinicians, to each of the 45 successive images of increasing hyperaemia averaged for 3 eyes. Error bars = 1 S.D.

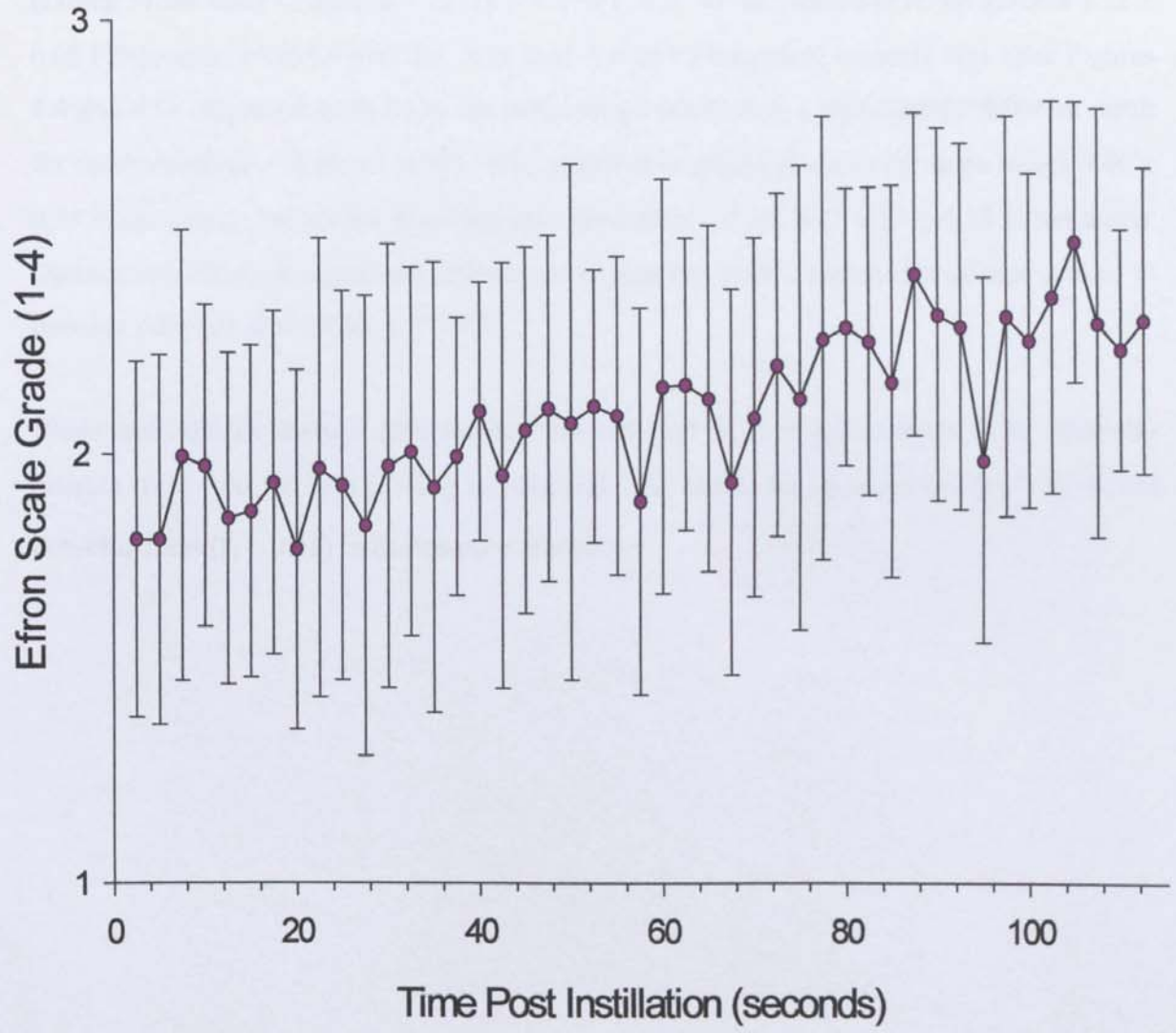

4.3.2 Reliability

There was no significant difference between the 6 repeats of objective image analysis by ED or Red RCE (S.D. = 0.013 %, F = 0.7, p = 0.99; S.D = 0.00007 %, F = 1.2, p = 0.33 respectively).

Eye-care practitioners and non-clinicians showed significant differences between individual's grading of the same images ($F = 28.00$ $p < 0.001$, S.D. of differences between graders 0.12 ± 0.08 Efron units; $F=258.9$ $p<0.001$, S.D. 0.23 ± 0.069 Efron units, respectively). (See Figures 4.4 and 4.5). Repeated analysis of the same image resulted in a significantly different result for optometrists ($F = 6.40$ $p < 0.001$, S.D. of different grades given to the same image 0.46 ± 0.08 Efron units), but not for non-clinicians ($F=1.80$ $p = 0.19$, S.D. 0.57 ± 0.19 Efron units). Optometrists showed significant differences in grading over 3 repeated measures spaced at two day intervals ($F = 20.30$, $p < 0.001$).

Bland and Altman analysis [89] showed ED and Red RCE image analysis to be optimally reliable ($r_I = 1.00$ for both grading techniques). The results for optometrists ($r_I = 0.08$) and non-clinicians ($r_I = 0.01$) indicated poor reliability.

4.5 DISCUSSION

The purpose of this study was to determine if objective image analysis was more sensitive and reliable than trained eye-care practitioners with respect to the grading of bulbar conjunctival hyperaemia.

Dapiprazole Hydrochloride was utilised to cause vasodilation of the conjunctival vessels to obtain high resolution digital images of the same eye with successively increasing hyperaemia. Some deviation from the presumed linear nature of the induced conjunctival vessel dilation is implied from the objective results (Figure 4.2 and 4.3). It is possible that the pulse cycle may have caused small variations in the hyperaemia characteristics detected. In support of this theory, fast Fourier transform analysis of a non-vasodilated eye was conducted and revealed a peak at the temporal frequency of the pulse (62±0.24 beats per minute measured over 10 minutes during the study) for both ED and Red RCE techniques (Figures 4.6 and 4.7). Another contributing factor which could offer an explanation for the deviation in vessel dilation is the physical effect of the blink on the conjunctival vasculature. As the eyelids twitch or close, their attachment to the conjunctiva compresses the conjunctival vessels in the area of interest, whilst the scleral vessels that are imaged remain relatively constant.

FIGURE 4.6: Fast Fourier transform analysis of frequency of ED changes with time in order to examine the possible vessel constriction / dilation of a non-vasodilated eye. (Heart rate of the subject measured at 62 beats per minute)

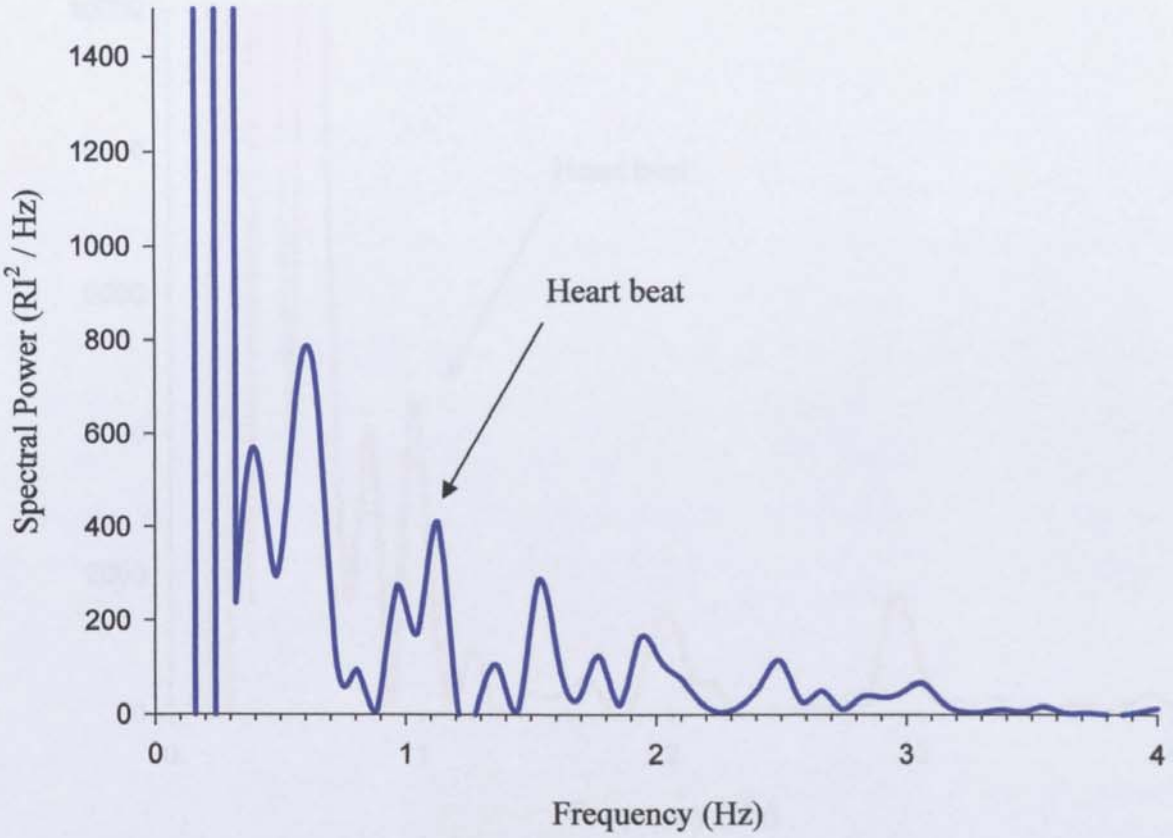

FIGURE 4.7: Fast Fourier transform analysis of frequency of Red RCE changes with time in order to examine the possible vessel constriction / dilation of a non-vasodilated eye. (Heart rate of the subject measured at 62 beats per minute)

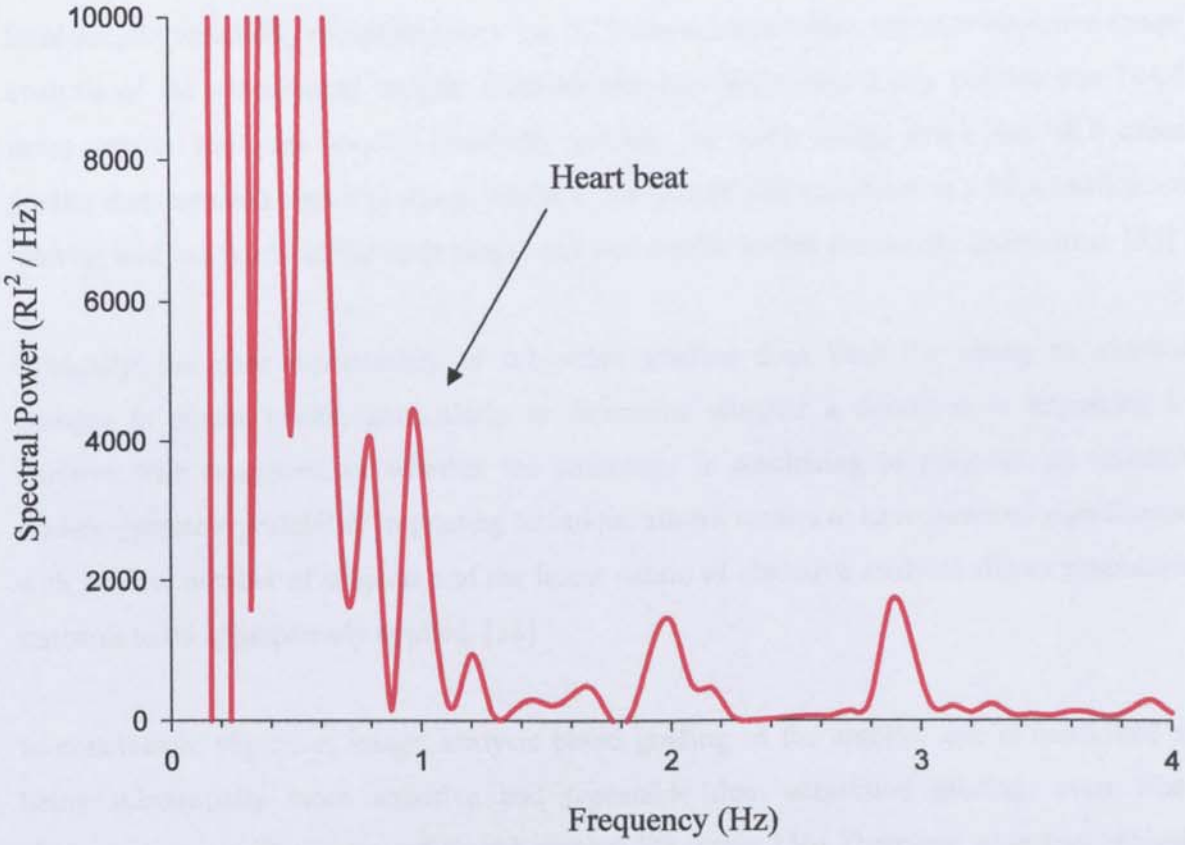

The average change in hyperaemia detected by subjective grading over the 2 minutes after instillation of the vasodilator was only 0.4 units on average. Interestingly the non-clinicians used a wider range of the scale, but were more variable than the optometrists, suggesting that experience and or teaching *does* have an effect on grading, which is contrary to some previous studies. [37] Subjective grading was only able to reliably differentiate between images taken over at least half of the total period of vasodilation, equating to 0.20 to 0.30 of an Efron scale grade. However, image analysis techniques were able to differentiate images separated by 1/26th to 1/29th of this range, equating to 0.01 to 0.02 of an Efron scale grade.

Inter-subject variability of optometrists was 22.0 times greater than repeated objective image analysis of the vasodilating images. Inter-session variability over 2 day periods was 144.0 times greater and intra session variability grading the same image twice was 38.0 times greater than repeated objective image analysis. Image analysis variability at a 95% confidence interval was just 0.4 % of the scale range, and was similar to that previously determined. [35]

Clinically, the poor repeatability of subjective grading does limit the ability to monitor changes in ocular health, particularly to determine whether a condition is beginning to improve with treatment, or whether the pathology is continuing to progress. In research studies, greater repeatability in grading technique allows studies to have powered significance with smaller number of subjects and the linear nature of objective analysis allows parametric statistics to be appropriately applied. [36]

In conclusion, objective, image analysis based grading of the anterior eye is confirmed as being substantially more sensitive and repeatable than subjective grading, even when clinicians use a well constructed most linear grading scale. [36] Therefore, objective analysis may offer a new gold-standard in anterior ocular examination, and should be developed as a clinical tool for use in research and to enhance the clinical monitoring of anterior eye disease.

If the objective analysis programme is to be used regularly by optometrists and researchers to improve their assessment and monitoring of anterior ocular surface conditions, it must be simple, quick to use, and preferably as universally recognised as the Efron and CCLRU scales. The next chapter will assess a method of achieving this goal and is the next step in the development of the LabView program towards commercial / clinical viability.

CHAPTER 5

GRADING

5.1 INTRODUCTION

Despite the evidence supporting the appropriate clinical use of objective grading scales, none have as yet been marketed commercially for analysis of the anterior ocular surfaces. In Chapter 1 the review demonstrated that the need for grading ocular conditions was not met by the variable and insensitive subjective methods currently utilised. [19, 20, 36] Due to this weakness in the clinical assessment of the anterior surfaces, objective analysis methods were suggested and evaluated, but none were developed past the point of an interesting research tool into a clinically viable method of assessment. [16, 60] Chapters 2 and 3 determined the best practice methods for anterior ocular imaging and proved that even with image degradation the edge detection (ED) and relative colour extraction (RCE) objective methods are both robust and can be applied to a variety of different measures. [35, 92] The ED and RCE methods were then further validated by the study in Chapter 4 which investigated the sensitivity and reliability of the measures in comparison with subjective grading. Previous work had been done in comparing subjective to objective grading of bulbar hyperaemia by Fieguth and Simpson who found a high correlation between the objective grading of 30 images, and the subjective grading by 72 clinicians ($r = 0.976$), suggesting that objective analysis can be used to predict clinician's grades. This finding has not been further evaluated with respect to the other ocular surfaces, and no evolution of the objective systems validated has been reported.

5.2 PURPOSE

It is now appropriate to develop the programme further into a user-friendly grading system that will produce results that will be universally recognised by eye-care practitioners (ECPs). This system could replace subjective grading in clinics as a more reliable and accurate substitute, without compromising the interpretation by ECPs and subsequent action when assessing or monitoring pathology.

In the current form, the software outputs are in terms of the percentage of pixels detected as edges or the relative percentage of the average colour of interest intensity compared to the combined red, green and blue image intensities. In order for clinicians to be able to relate these figures to their understanding of the levels of severity of conditions of the ocular surfaces, it would be judicious to express the objective result in the form of a currently recognised and accepted anterior ocular grading scale. This would also help to bridge the gap between clinicians embracing objective grading programmes and those still using subjective grading scales. It would offer an effective way for clinicians to be able to interpret the results of the analysis 'within normal' or 'outside normal limits' in a convenient manner, while gaining the benefit of reliability and sensitivity, which, as it has been previously discussed, is lacking in subjective grading.

5.3 METHODS

Evaluation of the entire range of severity of conditions of the bulbar conjunctiva, palpebral conjunctiva (for redness and roughness) and corneal surface staining required both normal and pathological ocular conditions to be photographed. Over 100 subjects were recruited from a University and a Hospital eye-department in order to obtain the images with which to display the complete range of severity of ocular conditions from normal healthy eyes to pathology. The subjects ranged from 5 to 85 years old. Images of the bulbar and palpebral conjunctiva, palpebral roughness and corneal staining (with fluorescein inserted and optimally imaged as determined in Chapter 3) were captured using a standardised protocol (See Table 5.1). The patients were taken from all clinics in the ophthalmology department but especially the eye-casualty. All images were captured by the same optometrist, as are all of the images used in this thesis. 10x magnification was used with a JAI camera (CV-53200, Yokohama, Japan) at a resolution of 767x569 pixels through a Takagi SM-70 slit-lamp biomicroscope (Nagano-Ken, Japan). The images were stored as TIFF files (non-compressed format). Ethical approval for these measures was previously given by the institutional ethical committee. The subjects gave written consent to the study after a full explanation of the methods to be used

10 images were chosen for each of the bulbar and palpebral conjunctiva, palpebral roughness and corneal staining from those captured which were representative of the most complete range of severity of the anterior ocular surfaces of interest. The images were placed at full resolution onto PowerPoint (Microsoft Corporation, Redmond, Washington, USA) slides in order for them to be displayed efficiently. The slides were then mixed so that the images appeared in random order of severity. See Figure 5.1 to 5.4.

50 optometrists with a full working knowledge of grading scales were recruited to evaluate the images. They were presented with the slides displayed on a 17 inch 1280x1024 resolution monitor (DELL E771p, Texas, USA) and asked to grade the condition of the 4 different ocular surfaces using either the CCLRU or Efron grading scales in random order. Grading was required to a sensitivity of 1 decimal place.

FIGURE 5.1: Images used in the PowerPoint presentations to portray the range of severity of bulbar hyperemia for subjective grading and objective analysis

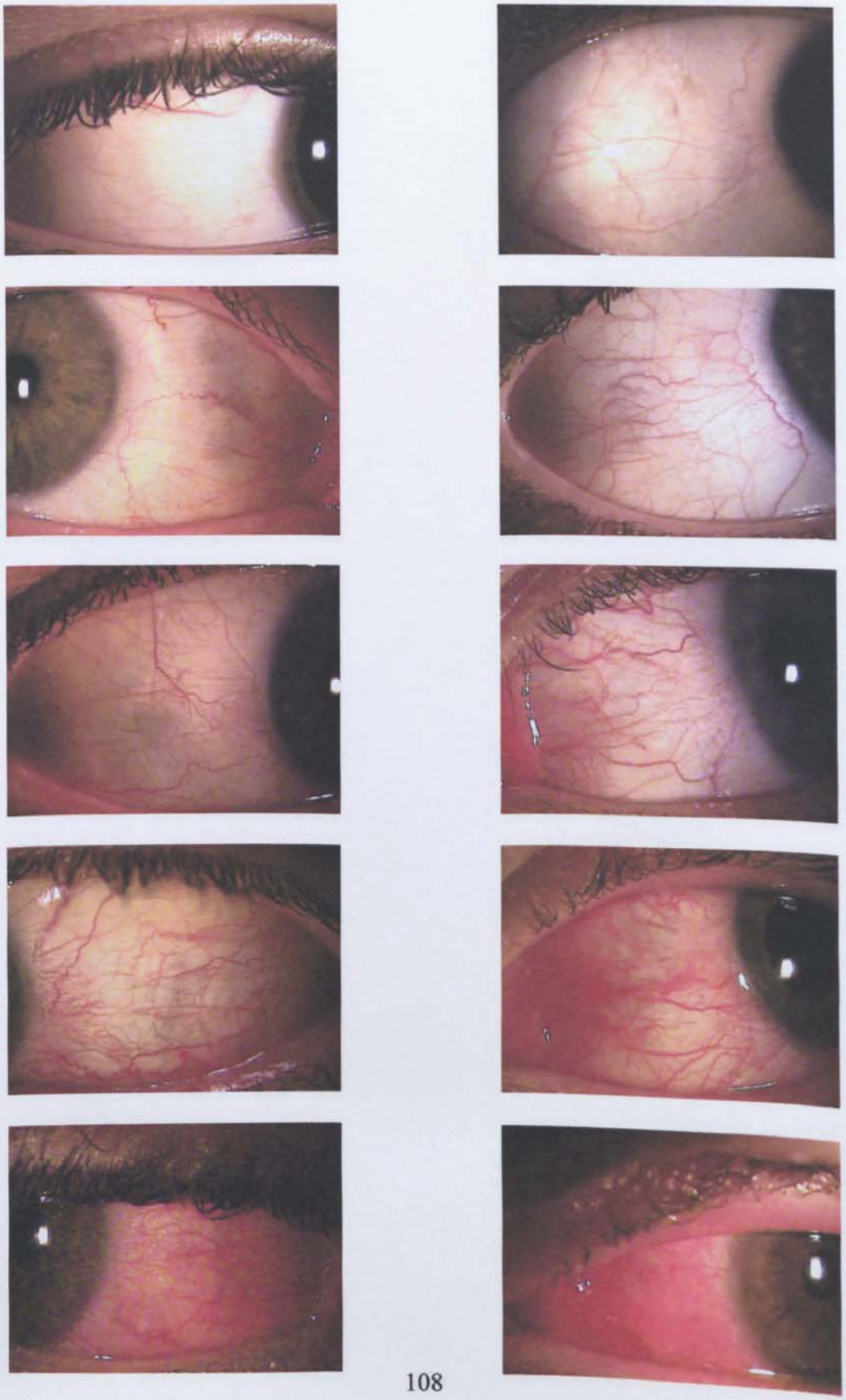

FIGURE 5.2: Images used in the PowerPoint presentations to portray the range of severity of palpebral redness for subjective grading and objective analysis

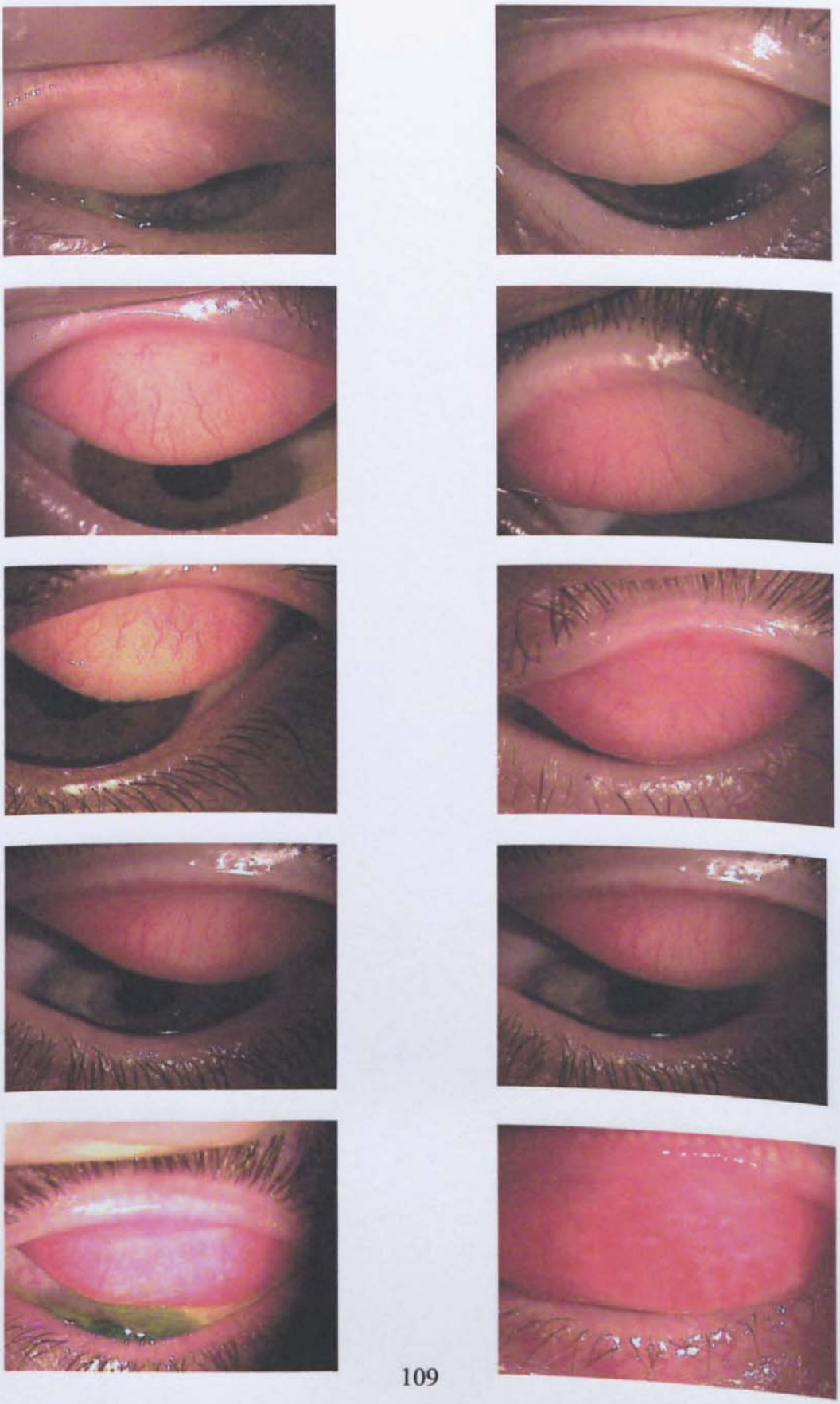

FIGURE 5.3: Images used in the PowerPoint presentations to portray the range of severity of palpebral roughness for subjective grading and objective analysis

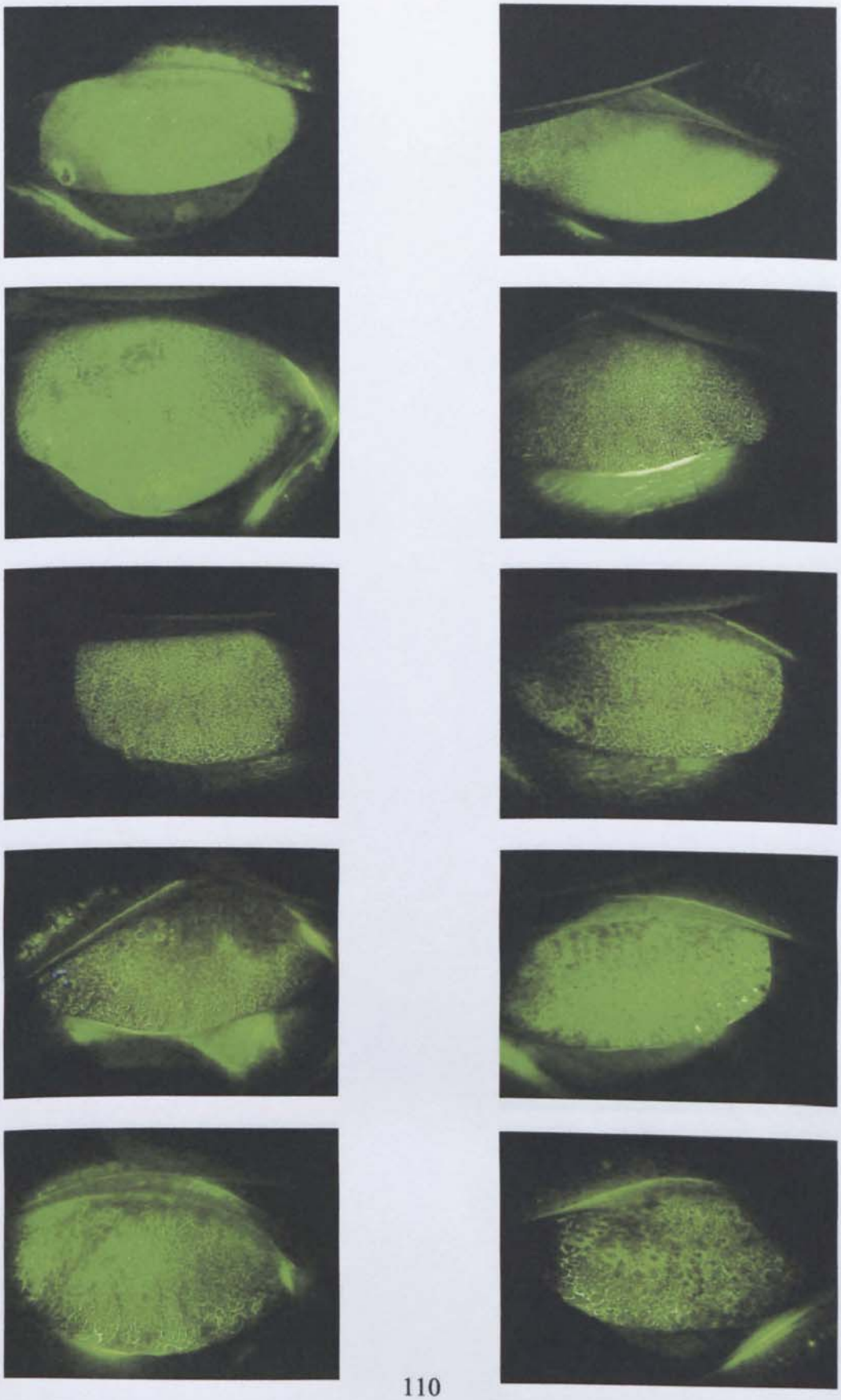

FIGURE 5.4: Images used in the PowerPoint presentations to portray the range of severity of corneal staining for subjective grading and objective analysis

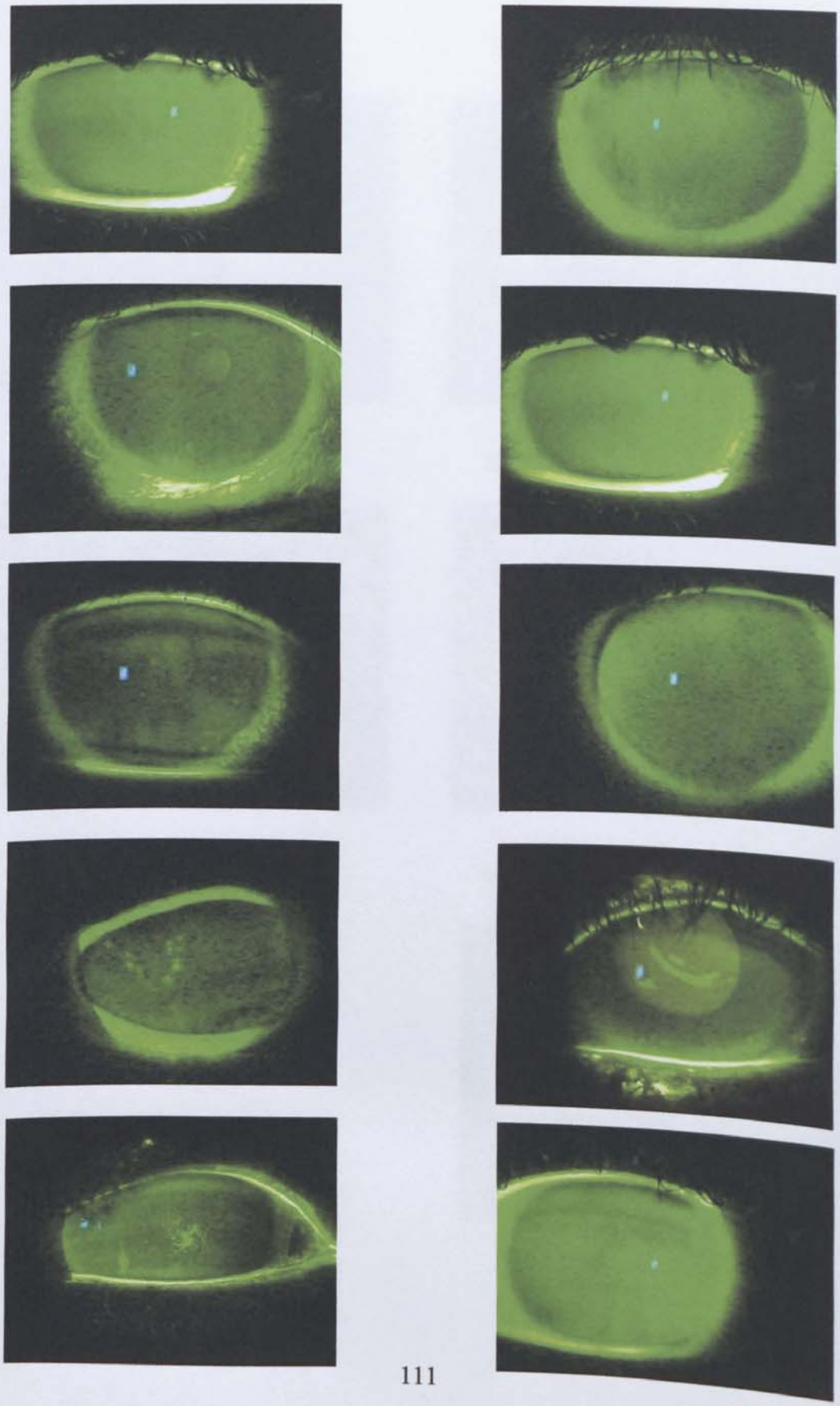

FIGURE 5.5: Images of A) bulbar hyperaemia, B) palpebral redness and C) roughness, and D&E) corneal staining with objective analysis performed in order to indicate the areas selected.

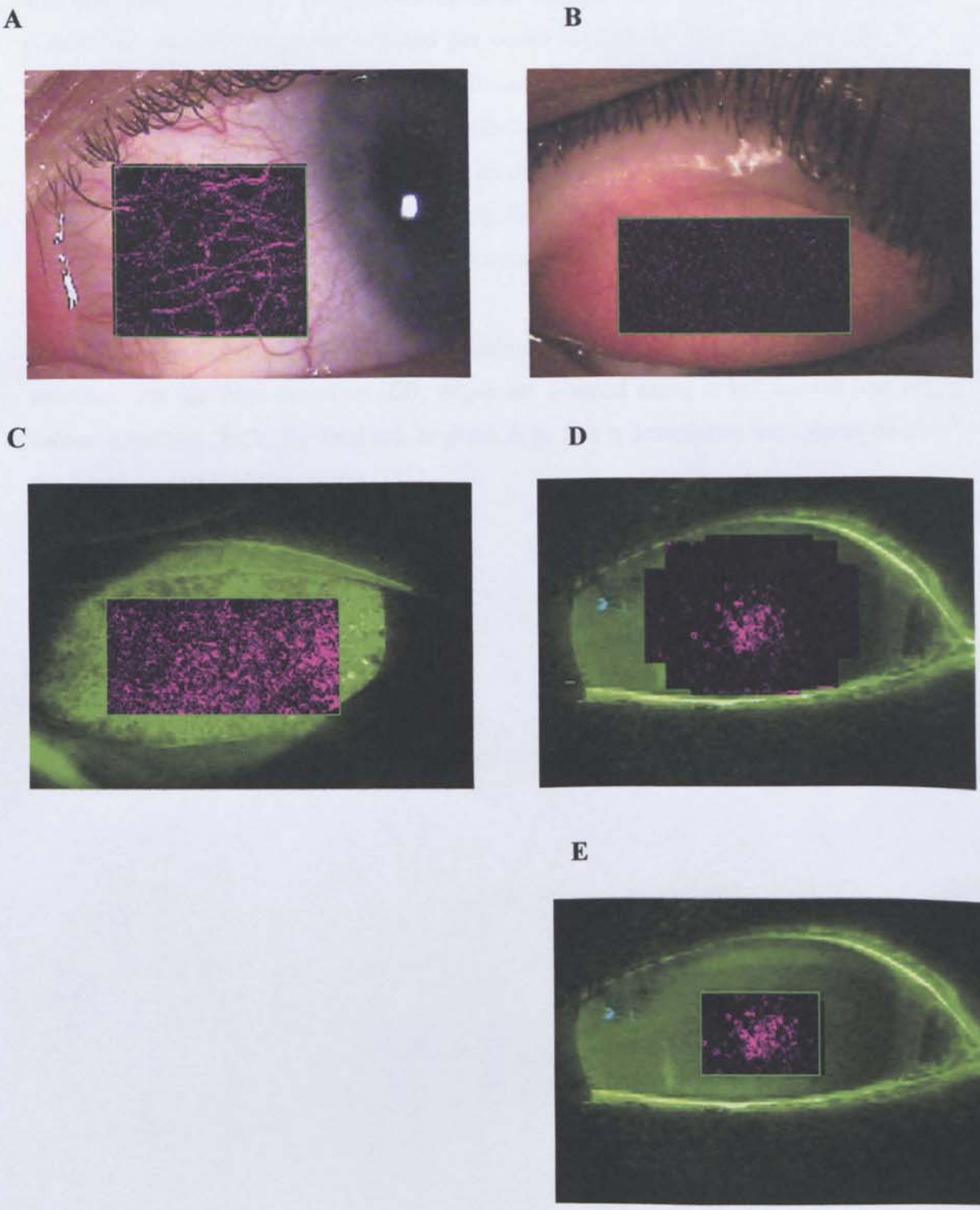

Analysis of the images was conducted with purpose designed and previously validated software (LabView™, National Instruments, Austin, Texas, USA). [35] 3 rectangular areas of the same size (per ocular surface) were selected on each image in order to obtain average values and to cover the majority of the surface area of interest. The size of the area selected was dependant on the physiological deviation of the specific anterior feature over the study population. The different areas selected per ocular surface are displayed in Table 5.1 and Figure 5.5. Two methods of area selection for corneal staining analysis were utilised in order to determine the best possible method for predictive grading. In the first method, the total area of the cornea was selected by means of a series of 5 analysis boxes (Figure 5.5D). The second method involved selecting the area of staining visible only and dividing it by the total area of the cornea (Figure 5.5E). Each image was analysed 3 times with both of these methods.

As discussed in Chapters 1 to 4, the most salient, repeatable and sensitive objective grading measures are the edge detection (ED; edges are mapped using a 3x3 kernal) and relative colour extraction (RCE; the total red, or green light that is detected by the camera divided by the total luminance of the image). [35]

TABLE 5.1: Methods of image capture and analysis

	Images captured	Slit lamp set-up	Size of area analysed by the LabView™ program
Bulbar Hyperemia 4 Images	▪ Right ▪ Left ▪ Nasal ▪ Temporal	Diffuse white light 35° angle	300x250 pixels 6.81x5.68cm
Palpebral Redness 2 Images	▪ Right ▪ Left	Diffuse white light 10° angle	400x200 pixels 9.08x4.54cm
Palpebral Roughness 2 Images	▪ Right ▪ Left	Diffuse blue light Yellow filter 10° angle	400x200 pixels 9.08x4.54cm
Corneal Staining 2 Images	▪ Right ▪ Left	Diffuse blue light Yellow filter 30° angle	1. Whole corneal area, ED and Green RCE assessed 2. Area of actual staining only selected / total corneal area

5.4 RESULTS

In order to determine the most suitable conversion equation for converting objective image values to clinically recognisable Efron or CCLRU scale grades, a multiple regression analysis was performed. Backwards stepwise regression was most appropriate, as with this method the emphasis is on the regression equation itself, which allows the maximum number of variables to be included, thereby improving the predictive worth of the result. Table 5.2 and Figures 5.6 to 5.13 display the results of these analyses.

Figures 5.6 to 5.13 show the relationship between subjective grading of the 10 images for each ocular surface and the 2 methods of objective grading (ED and RCE). Error bars for both the subjective and objective results are included in the figures, and indicate the value of 1 standard deviation (S.D). Values of adjusted r^2 (to signify the fit of the data to the equation but also taking into account the degrees of freedom) are also included with the figures to allow an easier reference to the strength of the relationship shown.

Out of the two methods of corneal staining analysis (see Table 5.1) only one was successful in producing a significant correlation between the subjective results. Neither ED nor Green RCE values were able to predict the extent or depth of staining. Significant results were found however for the second method of corneal analysis. See Table 5.2

TABLE 5.2: Results of multiple regression analyses.

SURFACE ANALYSED	SCALE UTILISED	OBJECTIVE BETA VALUE		INTERCEPT	Rsq	Rsq ADJUSTED	F	p
		ED	RCE					
BULBAR HYPEREMIA	CCLRU	**0.66**	**0.97**	**-2.32**	**0.97**	**0.96**	**111.56**	**0.00**
	EFRON	**0.51**	**1.02**	**-6.74**	**0.98**	**0.98**	**19419**	**0.00**
PALPEBRAL REDNESS	CCLRU	**-0.78**	**1.01**	**-7.16**	**0.7**	**0.61**	**8.03**	**0.03**
	EFRON	**-0.74**	**1.02**	**16.84**	**0.69**	**0.60**	**7.85**	**0.01**
PALPEBRAL ROUGHNESS	CCLRU	**0.52**	**-0.5**	**1.7**	**0.77**	**0.71**	**11.92**	**0.04**
CORNEAL STAINING EXTENT	CCLRU	0.33	0.21	1.78	0.11	-0.14	0.44	0.66
	EFRON	0.56	0.15	1.61	0.09	-0.16	0.36	0.71
DEPTH	CCLRU	0.34	-0.09	1.79	0.12	-0.13	0.48	0.64

SURFACE ANALYSED	SCALE UTILISED	OBJECTIVE BETA VALUE. **Average area of staining/corneal area**	INTERCEPT	Rsq	Rsq ADJUSTED	F	p
CORNEAL STAINING EXTENT	CCLRU	**0.93**	**1.2**	**0.86**	**0.84**	**47.45**	**0.00**
	EFRON	**0.94**	**0.86**	**0.88**	**0.87**	**61.07**	**0.00**
DEPTH	CCLRU	**0.85**	**1.26**	**0.72**	**0.69**	**21.05**	**0.00**

FIGURE 5.6: Regression plots of CCLRU subjective grading verses objective analysis for bulbar hyperaemia. Adjusted r^2 shows a high level of agreement at 0.96.

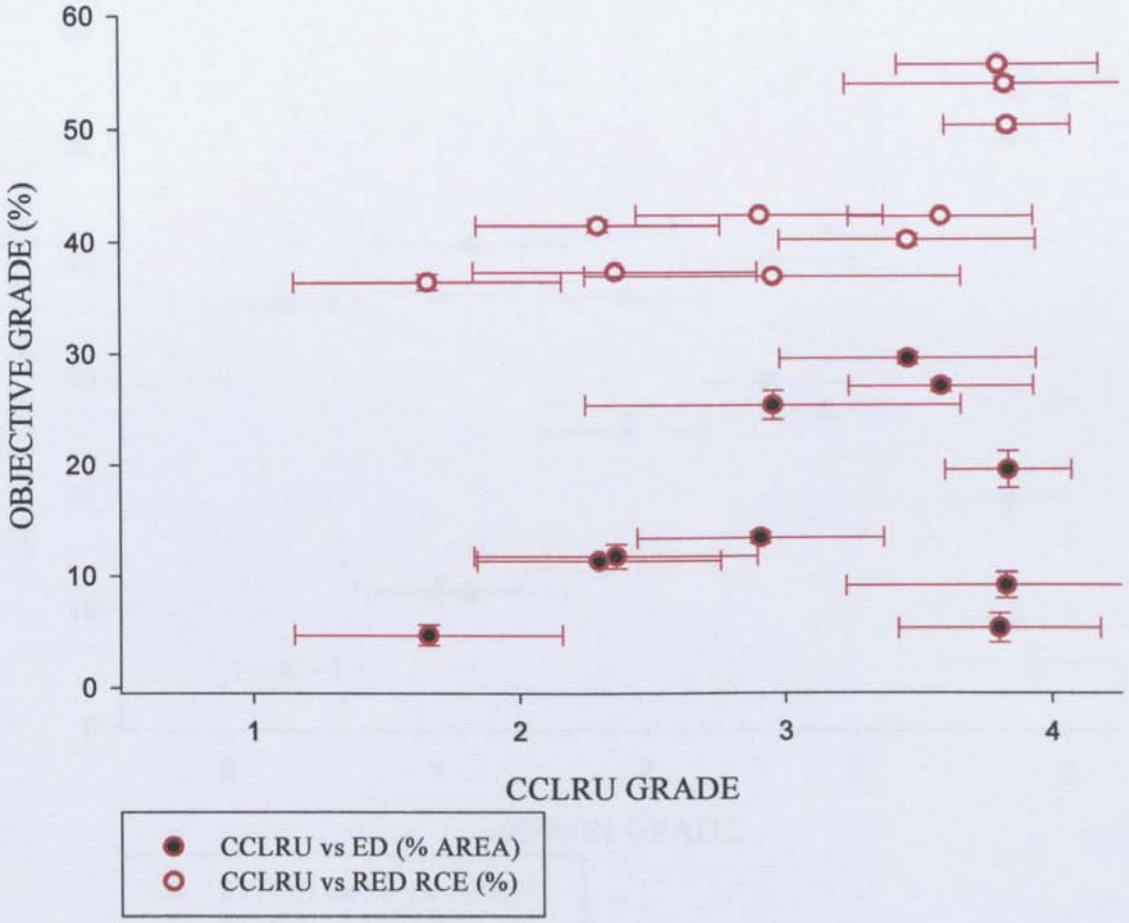

FIGURE 5.7: Regression plots of Efron subjective grading verses objective analysis of bulbar hyperaemia. Adjusted r^2 shows a high level of agreement at 0.98.

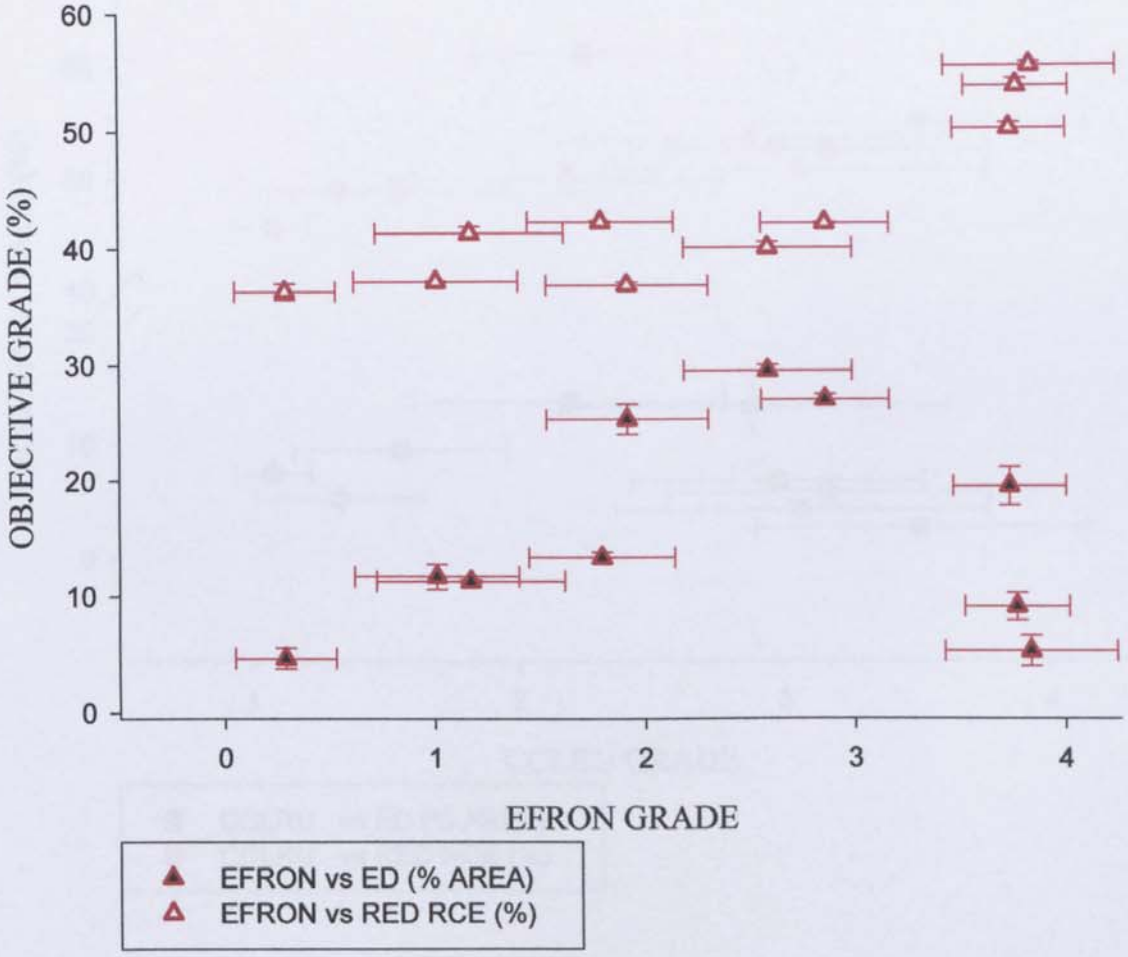

FIGURE 5.8 Regression plots of CCLRU subjective grading verses objective analysis of palpebral redness. Adjusted r^2 shows a significant agreement at 0.61.

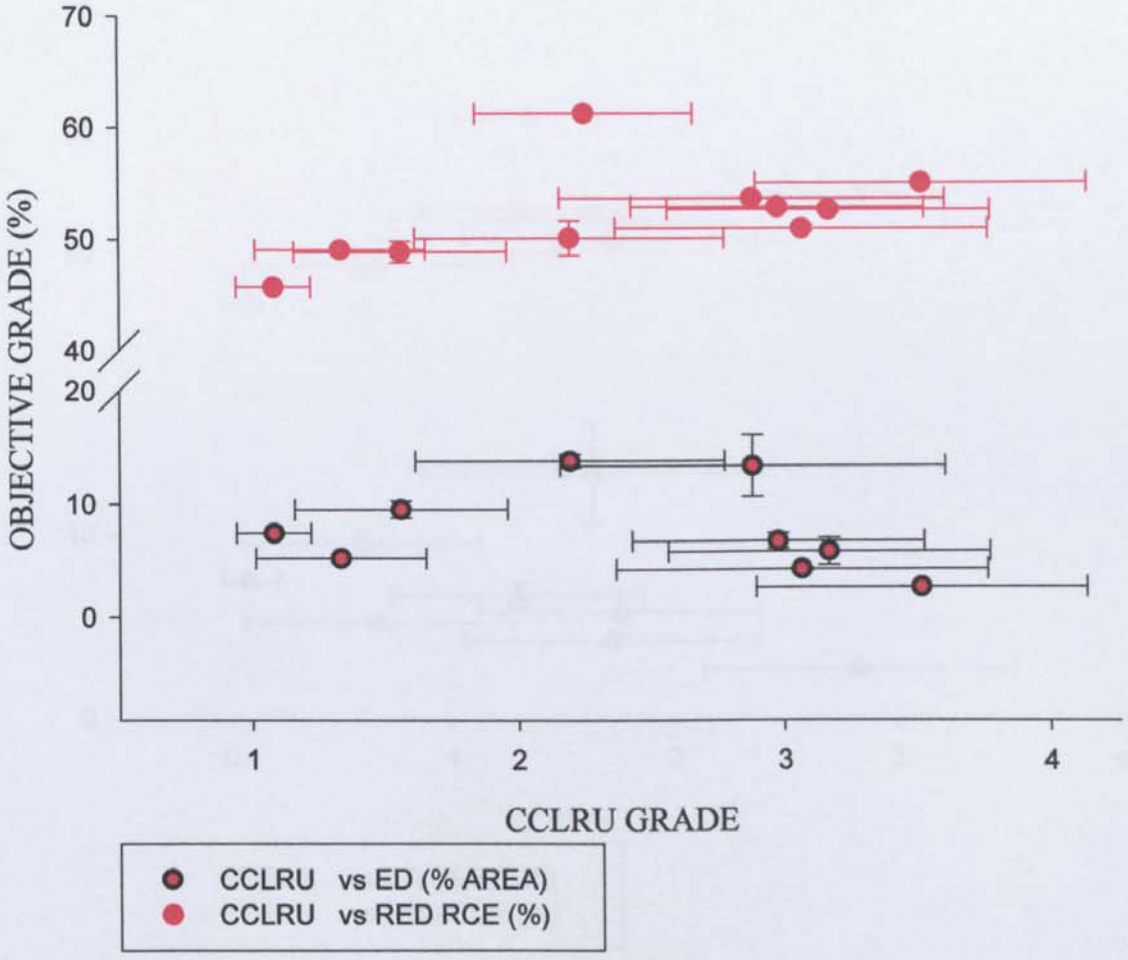

FIGURE 5.9: Regression plots of Efron subjective grading verses objective analysis of palpebral redness. Adjusted r^2 shows a significant agreement at 0.60.

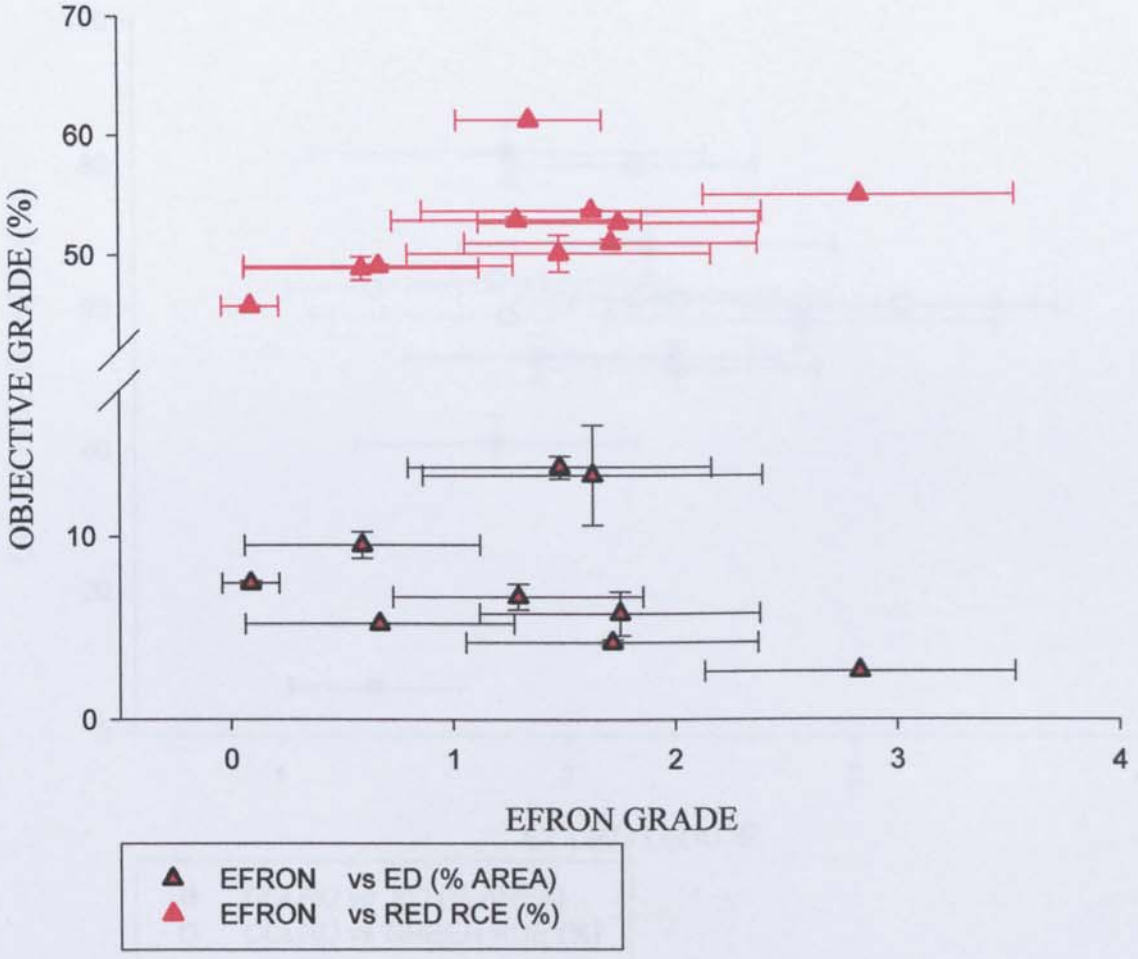

FIGURE 5.10: Regression plots of CCLRU subjective grading verses objective analysis of palpebral roughness. Adjusted r^2 shows a significant level of agreement at 0.71.

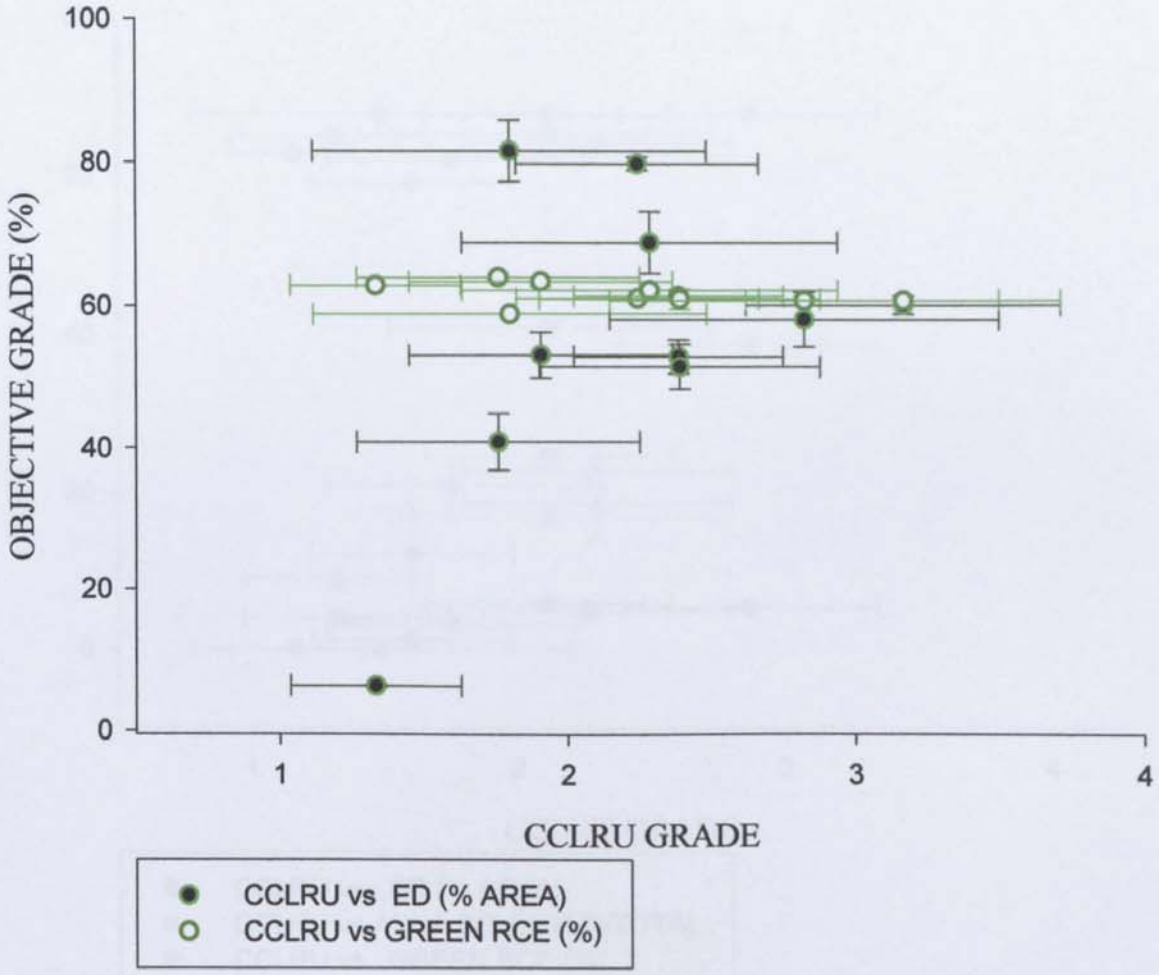

FIGURE 5.11: Regression plots of CCLRU subjective grading verses objective analysis of the extent of corneal staining. Adjusted r^2 shows a high level of agreement for the area of staining elected only at 0.84.

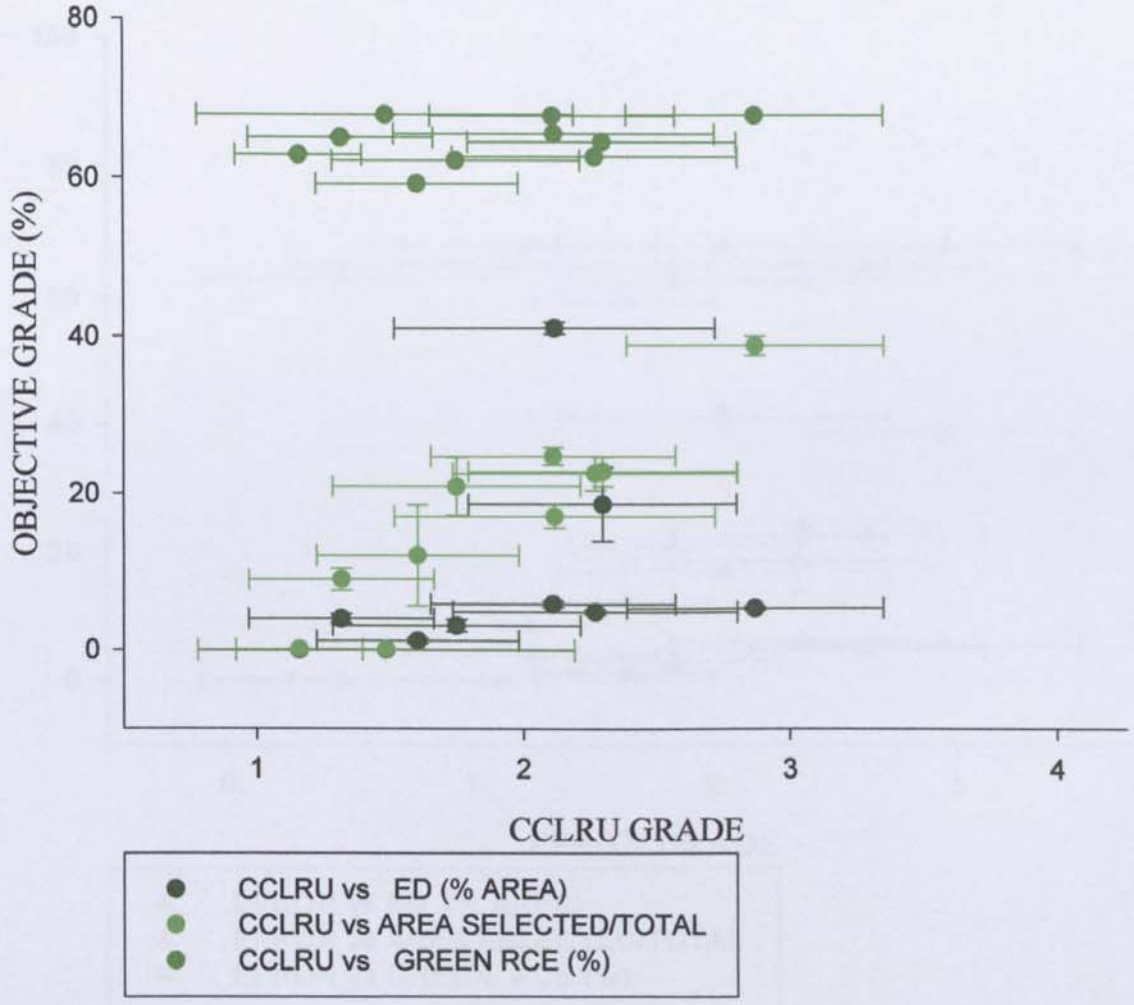

FIGURE 5.12: Regression plots of Efron subjective grading verses objective analysis of the extent of corneal staining. Adjusted r^2 shows a high level of agreement for the area of staining only at 0.87.

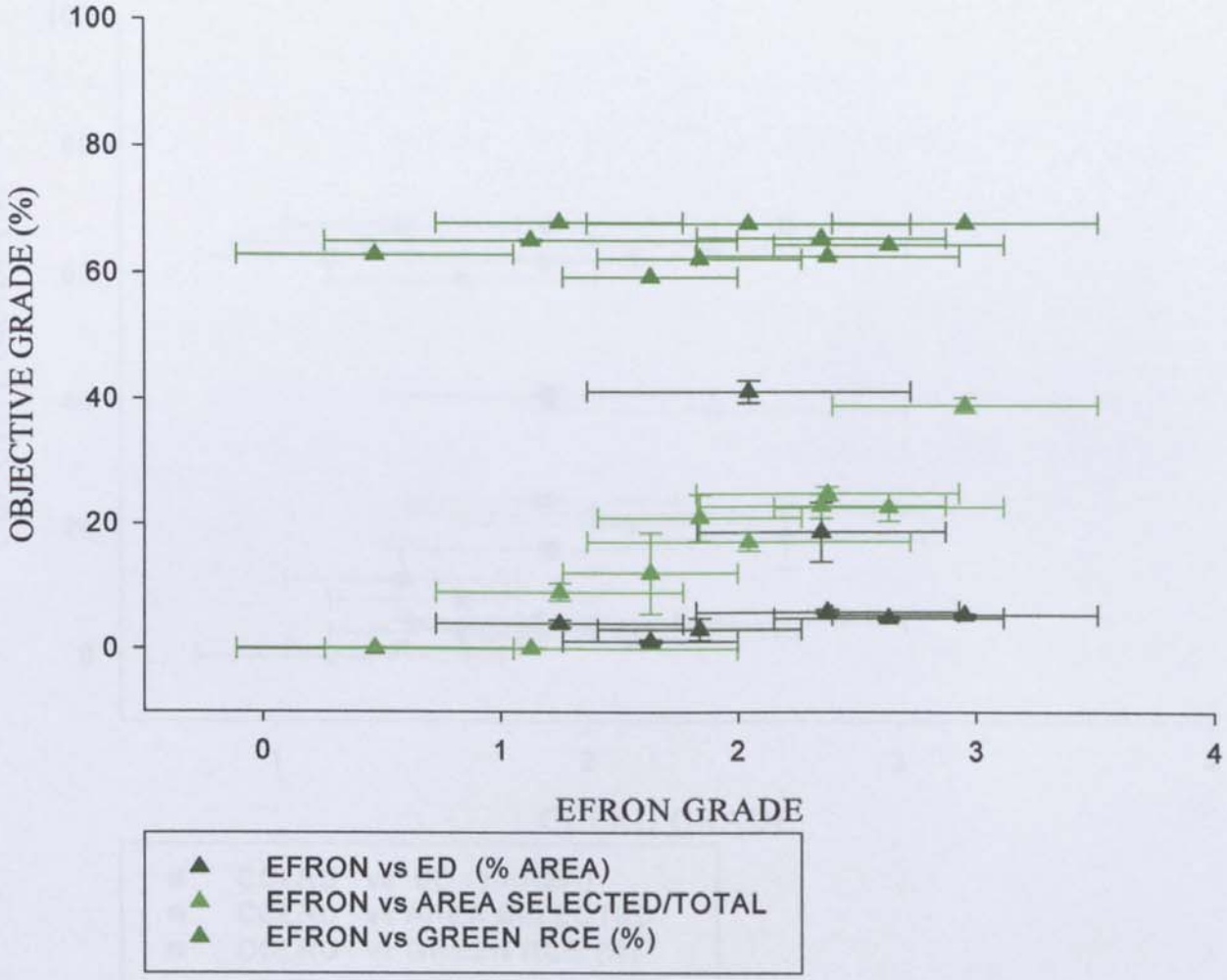

FIGURE 5.13: Regression plots of CCLRU subjective grading verses objective analysis of the **depth** of corneal staining. Adjusted r^2 shows a significant level of agreement at 0.69

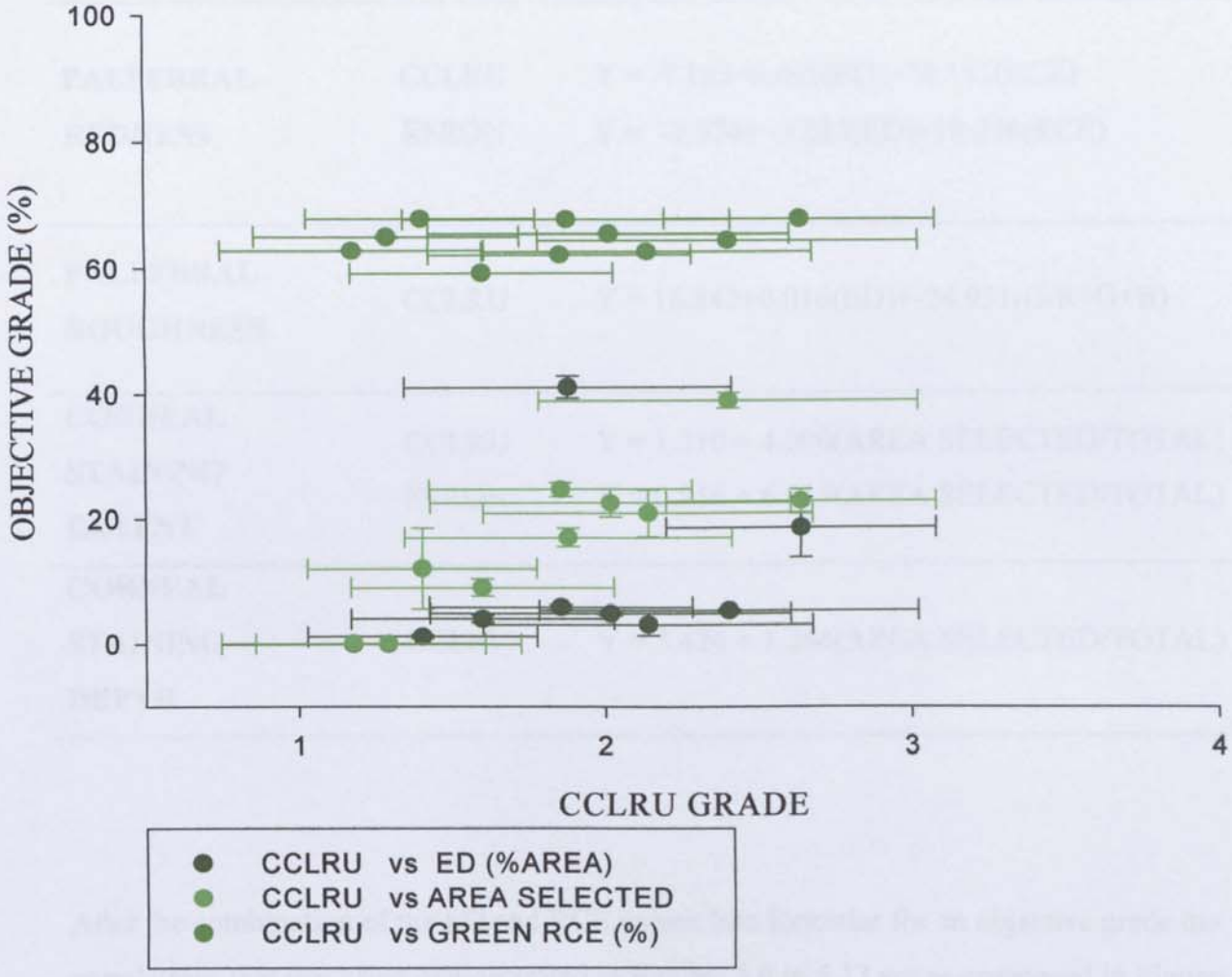

The final regression equations predicting the subjective equivalent of ocular surface grades from objective analysis are displayed below in Table 5.3.

TABLE 5.3: Regression equations for prediction of subjective grades by objective analysis

BULBAR HYPEREMIA	CCLRU	Y = -2.323+0.056(ED)+10.352(RCE)
	EFRON	Y = -6.743+0.071(ED)+18.159(RCE)
PALPEBRAL REDNESS	CCLRU	Y = -7.163+0.098(ED)+20.151(RCE)
	EFRON	Y = -7.374+ -0.083(ED)+18.238(RCE)
PALPEBRAL ROUGHNESS	CCLRU	Y = 16.842+0.016(ED)+-24.951(G/R+G+B)
CORNEAL STAINING EXTENT	CCLRU	Y = 1.210 + 4.090(AREA SELECTED/TOTAL)
	EFRON	Y = 0.856 + 6.015(AREA SELECTED/TOTAL)
CORNEAL STAINING DEPTH	CCLRU	Y = 3.426 + 1.264(AREA SELECTED/TOTAL)

After the combination of the ED and RCE values into formulae for an objective grade the correlations that were first demonstrated in Figures 5.6 to 5.13 are re-composed in Figures 5.14 to 5.18. They show the results of the strength of the subjective grade verses the combination of the objective assessments.

FIGURE 5.14: Demonstration of the agreement between the subjective grades and the calculated objective grades of bulbar hyperemia. n = 10

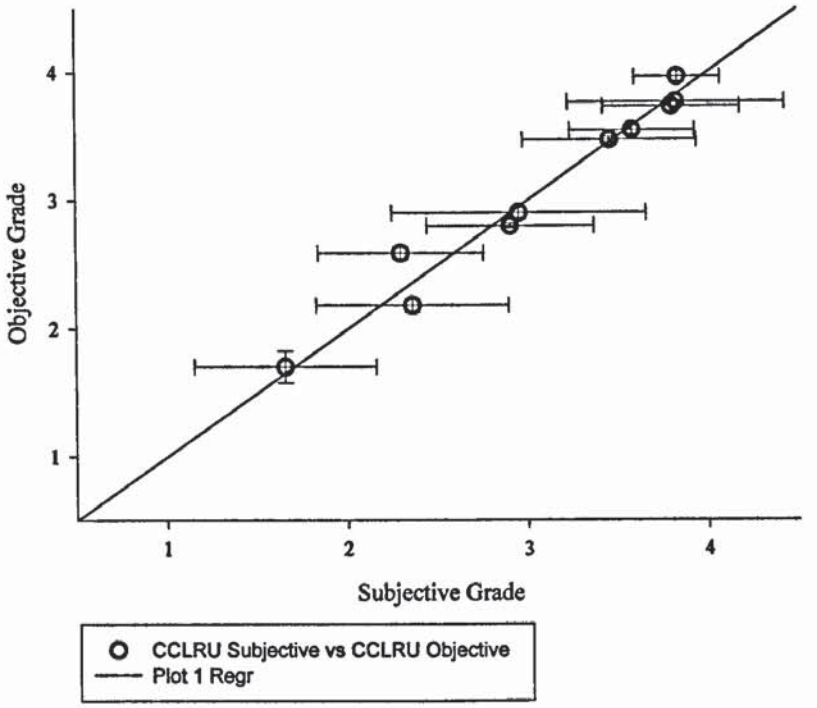

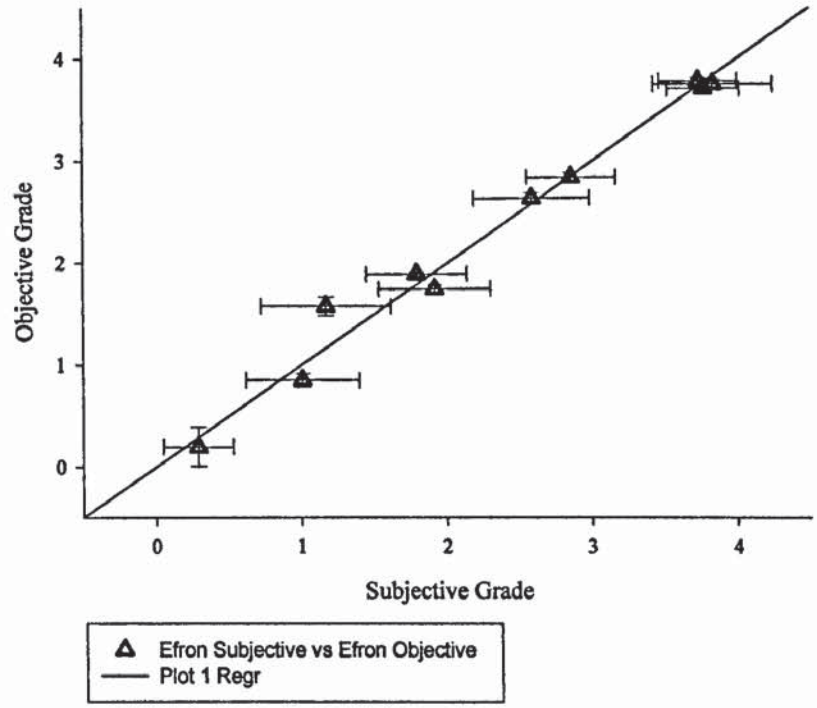

FIGURE 5.15: Demonstration of the agreement between the subjective grades and the calculated objective grades of palpebral redness. n = 10

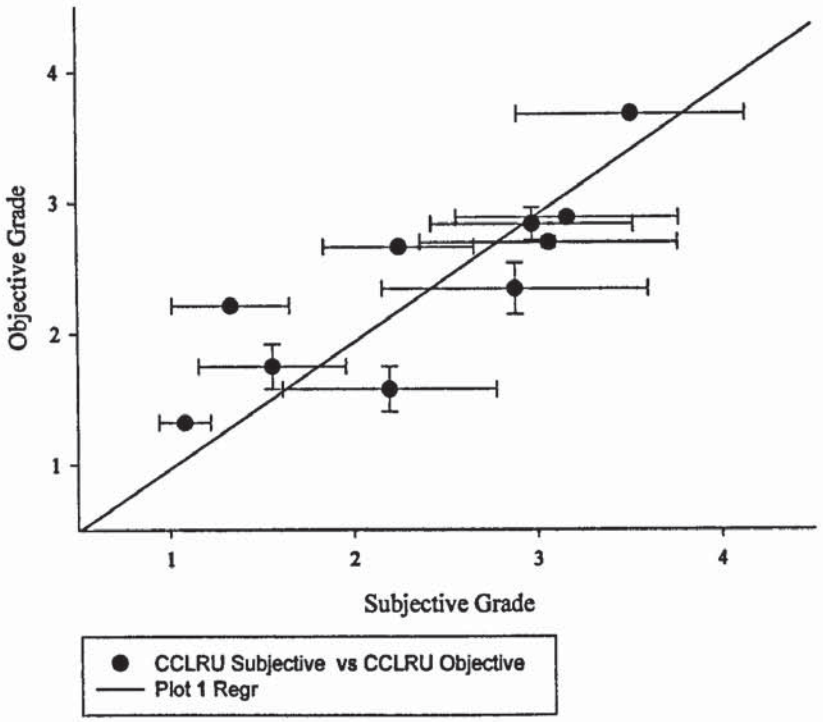

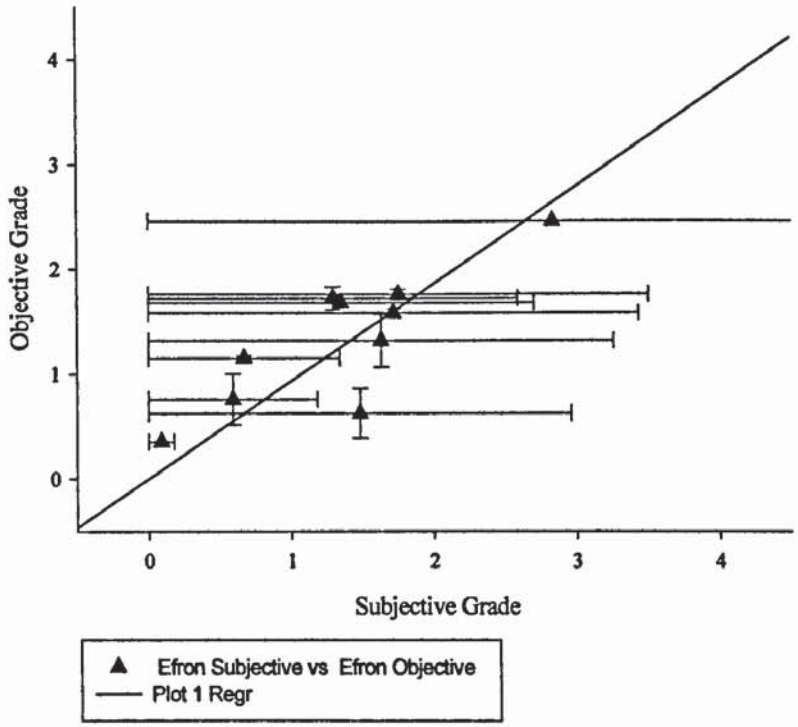

FIGURE 5.16: Demonstration of the agreement between the subjective grades and the calculated objective grades of palpebral roughness. n = 10

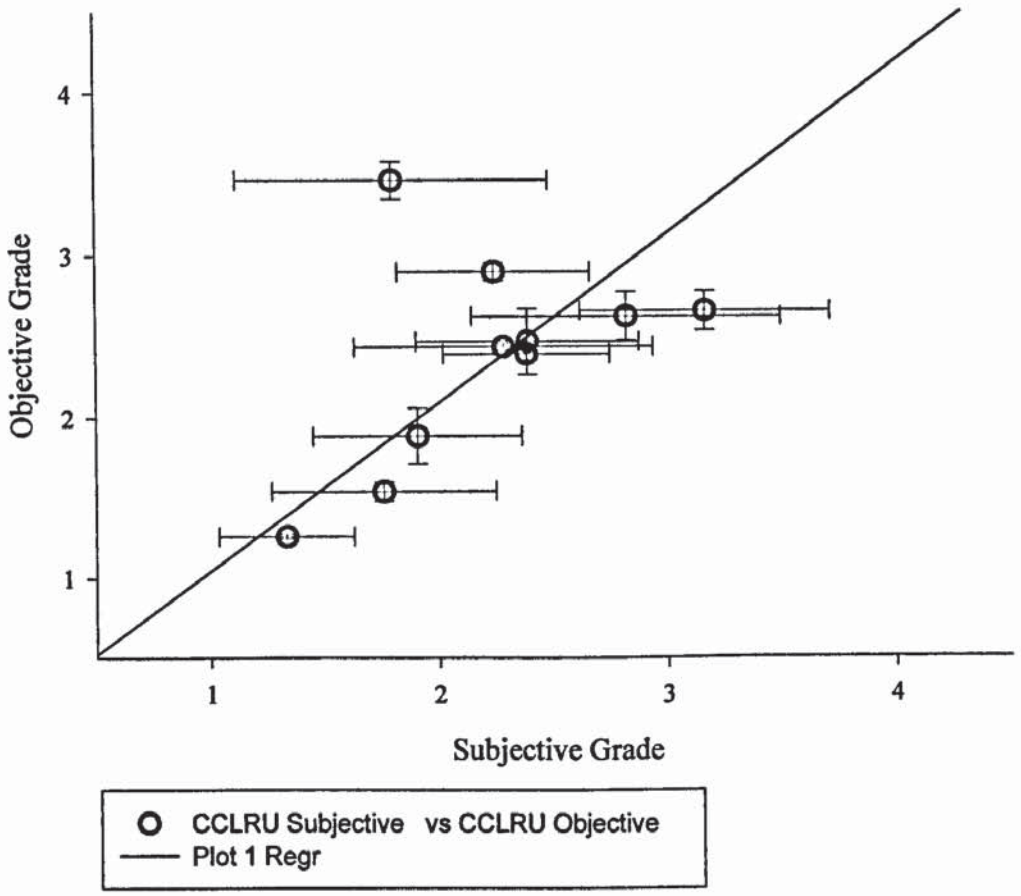

FIGURE 5.17: Demonstration of the agreement between the subjective grades and the calculated objective grades of the extent of corneal staining. n = 10

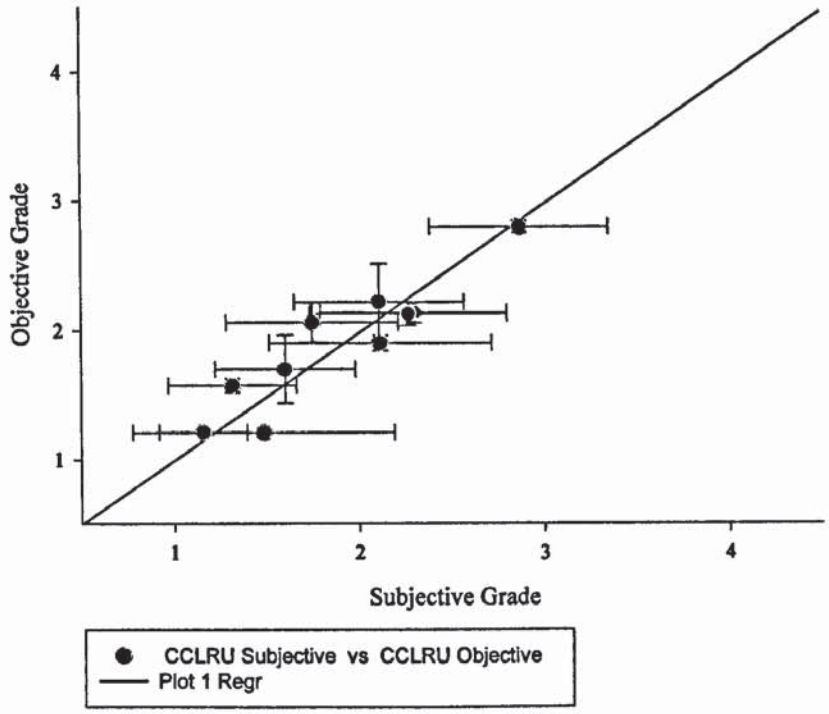

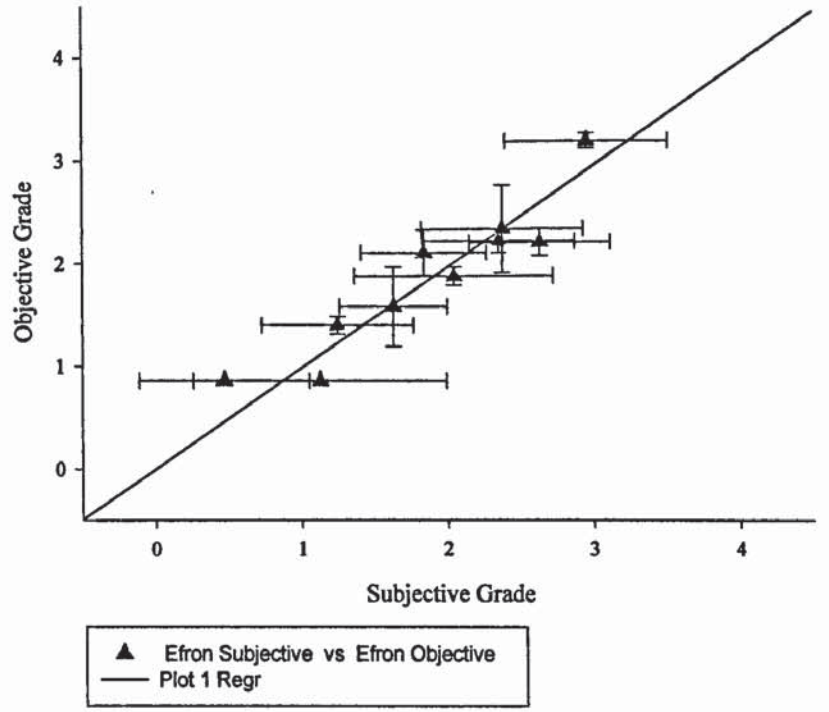

FIGURE 5.18: Demonstration of the agreement between the subjective grades and the calculated objective grades of the depth of corneal staining. n = 10

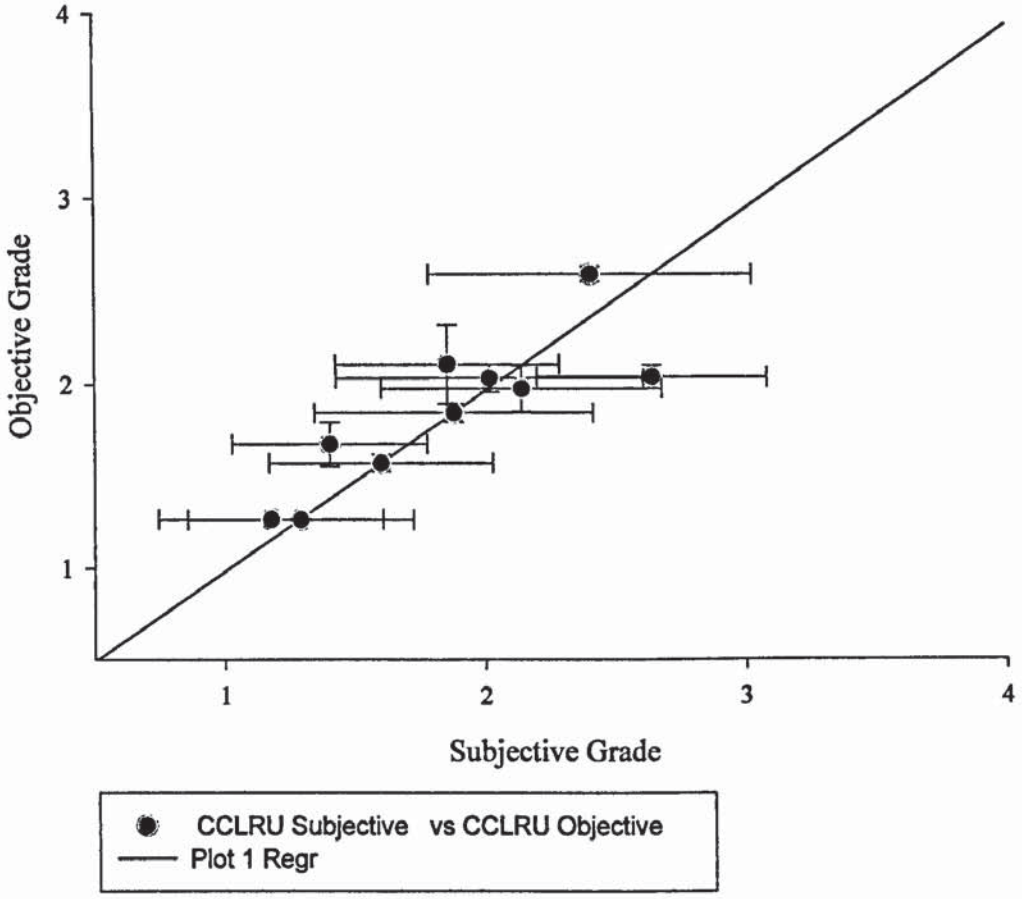

5.5 DISCUSSION

This study aimed to determine the ratio of ED and RCE objective analysis values that correspond to CCLRU and Efron subjective grades of surfaces of the anterior eye. The results were used to form equations for the purpose of adapting an objective measure into a value which is reliable and sensitive, yet can be easily recognised and interpreted by clinicians. The lowest significant adjusted r^2 found was for palpebral redness (in comparison to the Efron scale), where the objective grade still accounted for 60% of the variance. The highest adjusted r^2 were found for bulbar hyperaemia with values of 0.96 and 0.98 for CCLRU and Efron grades respectively. Therefore the formulae in Table 5.4 are appropriate for development into the image analysis computer programming to convert image characteristics to clinically recognisable scale grades.

For objective image analysis to be useful in detecting abnormality and monitoring disease progression, a comparison baseline must be known. Ideally this would come from the patient themselves (before they develop an eye disease) but in reality this isn't often available. Hence, data from a healthy population can provide a substitute. It is also important to account for diurnal variations as patients cannot be limited to attending for an examination at a fixed time of day. Therefore the formulae developed in this chapter are used to investigate diurnal variation and age-related changes (in bulbar hyperaemia, palpebral redness, palpebral roughness and corneal staining) in the next 2 chapters, with a view to introducing compensatory factors if necessary to reduce clinical measurement variability.

CHAPTER 6

AGE-RELATED CHANGES

6.1 INTRODUCTION

The principal reason for assessing anterior eye features such as bulbar and palpebral hyperaemia is to detect disease and to monitor that disease to its resolution. To achieve these aims, knowledge of the baseline 'normal' anterior ocular surface appearance is required. However, it is often the case that this information is not available, and a wide variety of factors can cause changes in these surfaces, leading to altered grades of severity of their condition. Population data on the average healthy eye baseline measures, together with its variability can be used instead to determine whether a patient falls outside the range of 'normal' for their age.

There appears to be very little literature published that examines age related changes of the bulbar hyperaemia, palpebral redness, palpebral roughness or corneal staining. Out of these four measures of ocular condition, bulbar hyperaemia has been the most examined, partly due to its importance as a predictor or measure of pathology, and partly due to its accessibility. One study, by Mikhailishchuk demonstrated that changes in bulbar hyperaemia do occur with age, and are due to a change in the form of the microvasculature and capillaries of the conjunctiva. These changes were enhanced in arterial hypertensive subjects of all age groups, [93] possibly due to the decrease with age in oxygen provision of the conjunctival tissue. [94] They could also be linked to cellular changes, such as in the Goblet or Langerhans cells, although opinion is divided as to whether there are any changes in these structures at all with age. [95-97] Other studies have determined that there are no changes with age in conjunctival surface features such as folds [77] and a study performed on a total of 479 subjects (252 females and 227 males, ages ranging from 1 to 89) by McMonnies and Ho found that although they noted a general increase in their subjective grades of hyperaemia with age, the variability of the study led to no significance for age or gender.[38]

To our knowledge, MacKinven et al are the only group to have reported a trend between age and palpebral surface appearance. Their study set out to determine the 'normal' grade of the redness and roughness of the palpebral conjunctiva (n = 96, ages ranging from 18 to 75). Their results showed a significant trend (Spearmans rank; rho= -0.36, $p<0.001$) for a decrease in palpebral roughness with age, but no significant change in redness. They determined that a CCLRU grade of 2 or below could be considered normal. [16]

The effects of various factors on corneal staining have been documented, for example; topical drug insertion, pathological conditions, contact lenses and solutions, dryness etc. [22, 70, 98-100] The prevalence of corneal staining in healthy non-contact lens wearers has been examined by several studies and is summarised by Dundas et al who state that the variety of staining reported is from 4 to 79% - including their study results. [30] However, the methods of grading vary between these studies, and some are more specific than others in their grading or estimation of staining extent and depth. [99, 101-103] Dundas et al did not include subjects aged over 50 in their study, as these were reported to be affected by factors which may influence staining. [30, 84, 104, 105] Schwallie et al attempted to establish a baseline for 'normal' levels of corneal staining in non-contact lens wear. [103] They evaluated 16 subjects (34.0 ± 4.0 years) by subjective grading (Efron scale) and reported a mean staining grade of 0.5 to 0.6 units.

Although previous work examining baseline measures for the healthy anterior ocular surfaces has been undertaken, none has conclusively established average measures for different age groups of the normal population. Previous studies have utilised subjective grading which is possibly the cause of such a wide variety of reported values (for example between 4 to 79% of the population apparently having corneal staining). In order to achieve a consistent and sensitive baseline objective image analysis should be utilised. [30]

6.2 PURPOSE

The aim of this study was to determine baseline levels of bulbar hyperaemia, palpebral redness, palpebral roughness and corneal staining, and their variability in healthy eyes over a range of ages, using objective image analysis grading. This will permit a comparison in a clinical or research environment, where an individual patient's findings will be assessed to suggest whether their anterior eye appearance is within normal limits.

6.3 METHODS

Four age groups spanning approximately 20 years each were chosen in order to obtain an even spread of subjects per group with the population available. The grouped age ranges were 0-20 years, 21-40 years, 41-60 years and greater than 61 years old. One hundred and twenty subjects were recruited, 30 subjects for each age group. The average ages of the groups were; 16 ± 3.44 years, 28 ± 5.29 years, 46 ± 6.08 years and 73 ± 5.36 years. Patients with any form of vasculature related ocular or systemic pathology or any acute ocular condition were excluded from the study. Ethical approval for the measures was previously given by the institutional ethical committee. The subjects gave written consent to the study after a full explanation of the methods to be used

Images of the palpebral conjunctiva (for redness and roughness) and corneal surface staining were captured for the right eyes only bulbar conjunctival images were taken of the right and left temporal conjunctivae to determine if any difference occurs. All images were captured with previously described standardised methods set out in Table 5.1. 10x magnification was used with a JAI camera (CV-53200, Yokohama, Japan), with a resolution of 767x569 pixels, through a Takagi SM-70 slit-lamp biomicroscope (Nagano-Ken, Japan). The images were captured by the same optometrist as throughout this thesis. The images were stored as TIFF files and were not compressed into JPEG due to the initial resolution of the camera. Images were taken between the hours of 9.00 to 13.00, to try to ensure minimal variability of anterior ocular appearance (see Chapter 7).

Masked analysis of the images was conducted with purpose designed and previously validated software [35] (LabView™, National Instruments, Austin, Texas, USA). A rectangular area of the same size (per ocular surface) was selected on each image, this process was repeated twice further to determine the variation of the objective measures. The size of the area selected was dependant on the physiological deviation of the specific anterior feature over the study population. The different area sizes selected per ocular surface are displayed in the previous chapter, in Table 5.1. ED and RCE values were determined for each of the anterior ocular surfaces.

Statistical analysis took the form of a repeated measures ANOVA as the objective data is parametric, and the measures were all repeated 3 times leading to the decision to use this form of evaluation.

The age-grouped data was then combined and a Pearsons r and p value was determined to examine the correlation with the objective measures and the age of the subjects T-tests were then used to evaluate the right and left bulbar hyperemia objective values to see if there were any differences between these.

6.4 RESULTS

The repeated measures ANOVA showed differences for bulbar hyperaemia over the age groups by Red RCE measures ($F= 31.51$ $p< 0.001$), and also for palpebral redness and roughness by ED measures only ($F=6.98$ $p<0.001$, $F=10.70$ $p< 0.001$ respectively). Tukey analysis was used to determine the extent of the significant differences. Results for all of the objective measures, repeats and analyses are displayed numerically in Table 6.1, and graphically in Figures 6.1 to 6.8.

Scatter plots representing the correlation of the changes in ocular surfaces with age are displayed in Figures 6.9 to 6.16. The Pearsons r and p values for these correlations are displayed with the graphs.

No difference was found between the measures of the right and left temporal bulbar conjunctivae with T-tests $p> 0.05$ (ranging from 0.66 to 0.96).

TABLE 6.1: Average ± Standard Deviation, Variance and ANOVA of redness, roughness and staining detected by objective image analysis

	Objective measures	**BULBAR HYPEREMIA**		**PALPEBRAL REDNESS**		**PALPEBRAL ROUGHNESS**		**CORNEAL STAINING**	
AGE		ED	RCE	ED	RCE	ED	RCE	ED	RCE
0-20 years	Average ± S.D	10.77±3.11	0.41±0.01	9.47±5.24	0.50±0.04	53.70±18.73	0.61±0.02	1.61±2.12	0.64±0.07
	Variance	0.10±0.11	0.00±0.00	0.11±0.08	0.00±0.00	0.26±0.09	0.00±0.00	0.19±0.15	0.00±0.00
21-40 years	Average ± S.D	12.70±4.96	0.42±0.01	11.65±4.10	0.49±0.03	40.42±24.24	0.60±0.04	0.74±0.64	0.63±0.05
	Variance	10.13±0.06	0.00±0.00	0.05±0.03	0.00±0.00	0.34±0.37	0.00±0.00	0.09±0.07	0.00±0.00
41-60 years	Average ± S.D	12.60±5.96	0.41±0.02	7.47±4.50	0.50±0.04	53.88±26.03	0.59±0.04	0.73±0.46	0.67±0.02
	Variance	0.10±0.09	0.00±0.00	0.16±0.17	0.00±0.00	0.78±0.31	0.00±0.00	0.14±0.70	0.00±0.00
61+ years	Average ± S.D	12.16±6.14	0.44±0.03	6.73±3.98	0.49±0.04	28.68±26.66	0.60±0.05	1.91±2.11	0.64±0.05
	Variance	0.01± 0.13	0.00±0.00	0.05± 0.15	0.00±0.00	0.78± 0.35	0.00± 0.00	0.11±0.14	0.00 ±0.00
ANOVA:	F Value	0.85	**31.51**	**6.99**	1.06	**10.70**	1.04	0.61	2.23
	p Value	0.47	**0.00**	**0.00**	0.37	**0.00**	0.39	0.61	0.09

FIGURE 6.1: Changes in bulbar hyperaemia with age measured by Edge Detection.
Error bars = 1 S.D. n = 120

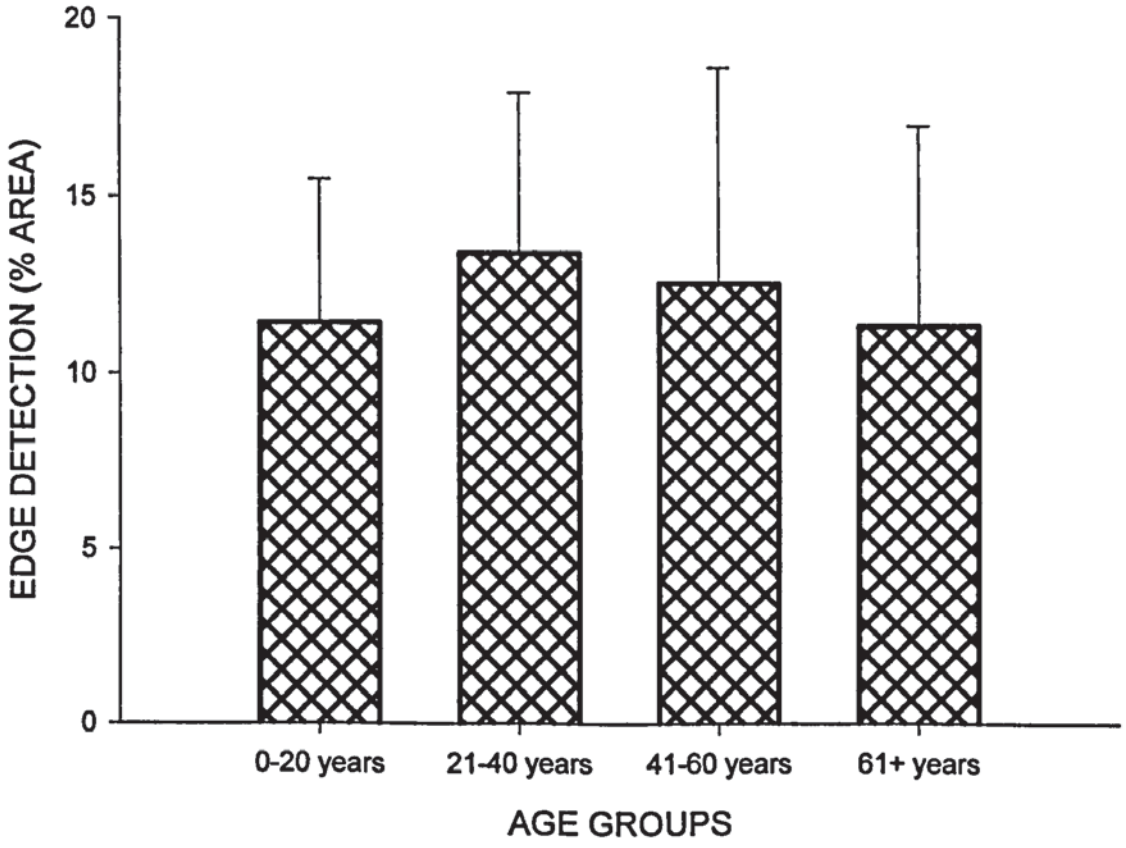

FIGURE 6.2: Changes in palpebral redness with age measured by Edge Detection. Significant differences determined by Tukey analysis are bracketed under the groups with corresponding p values. Error bars = 1 S.D. n = 120

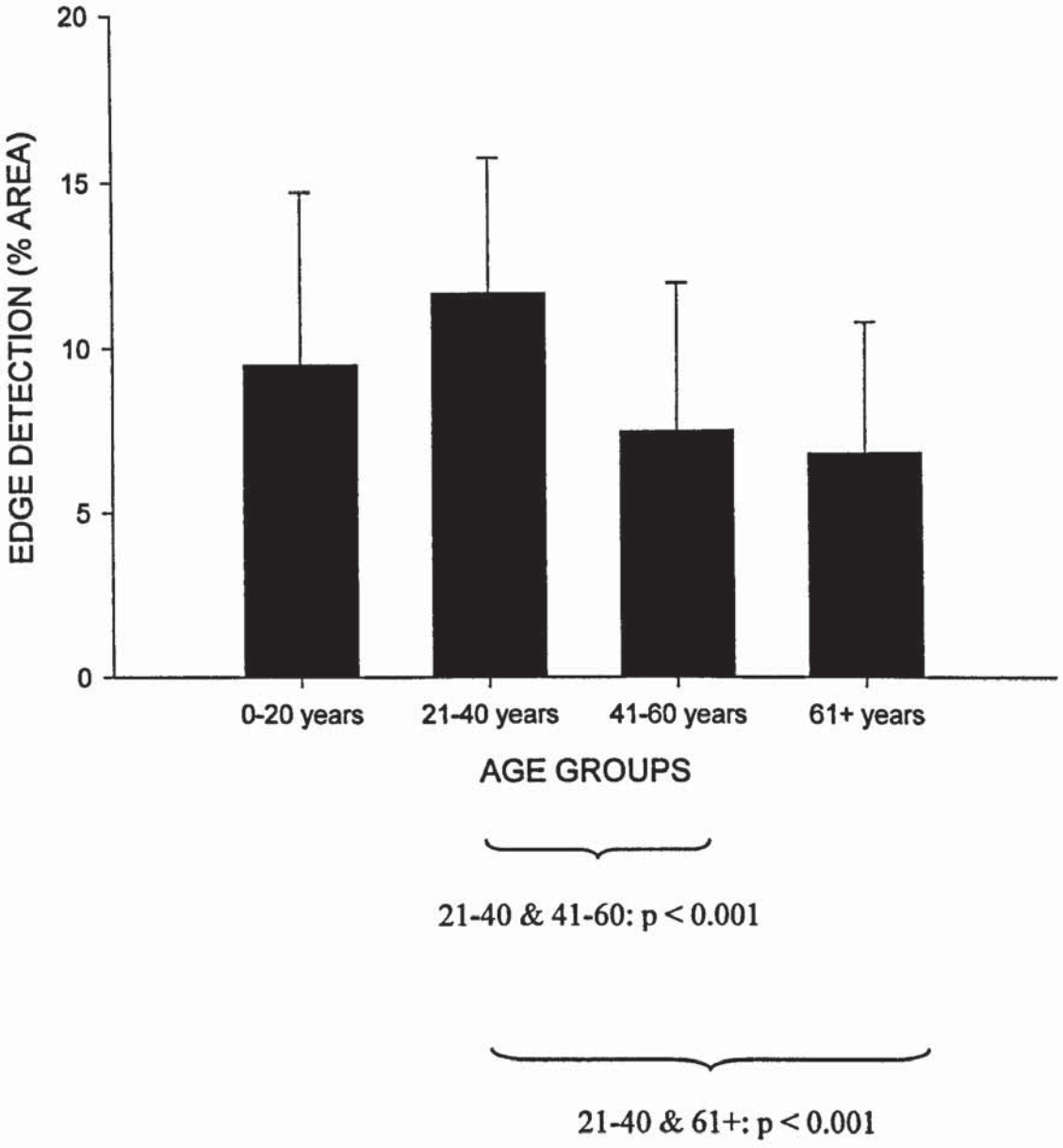

FIGURE 6.3: Changes in palpebral roughness with age measured by Edge Detection. Significant differences determined by Tukey analysis are bracketed under the groups with corresponding p values. Error bars = 1 S.D. n = 120

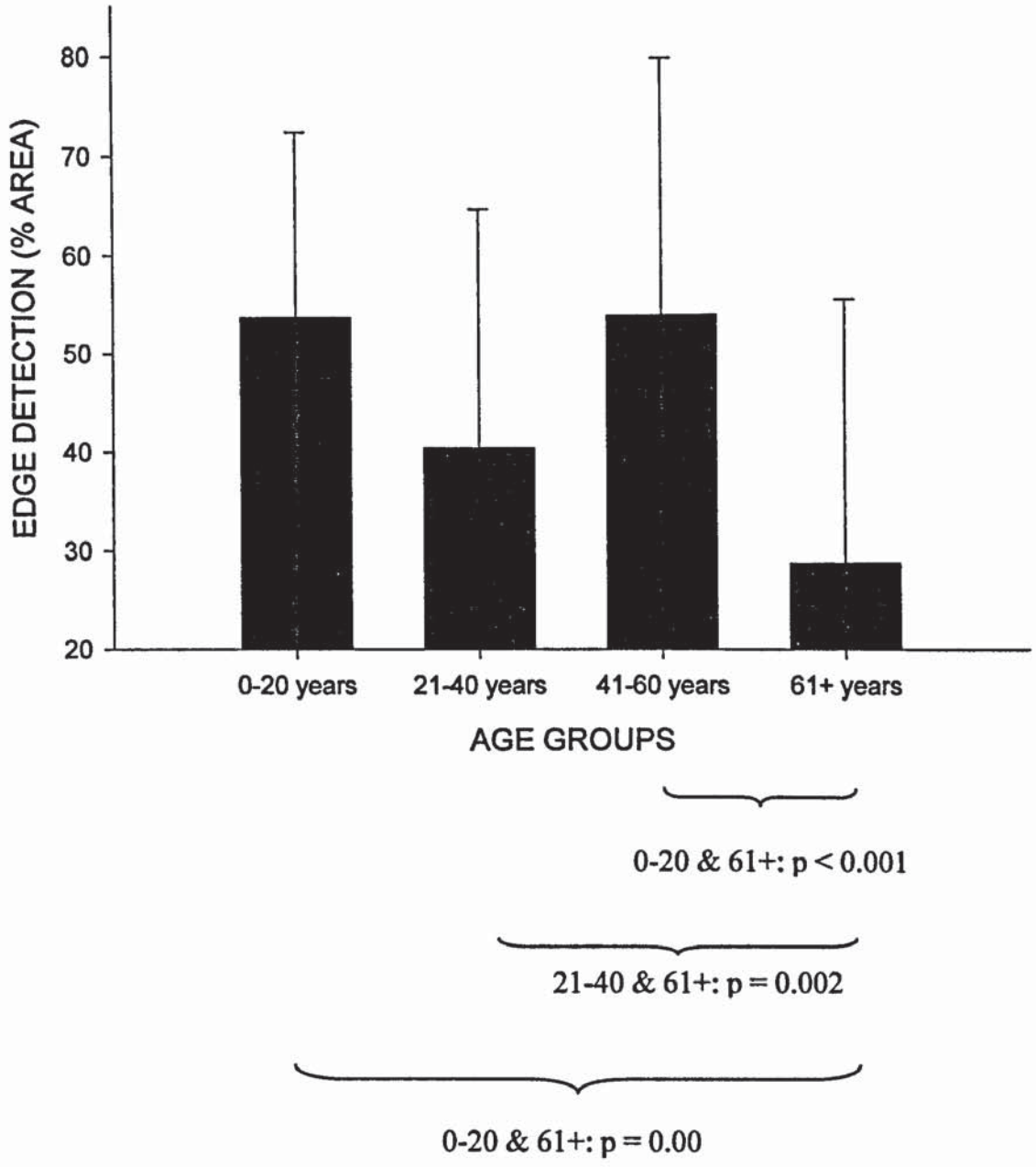

FIGURE 6.4: Changes in corneal staining with age measured by Edge Detection. Error bars = 1 S.D. n = 120

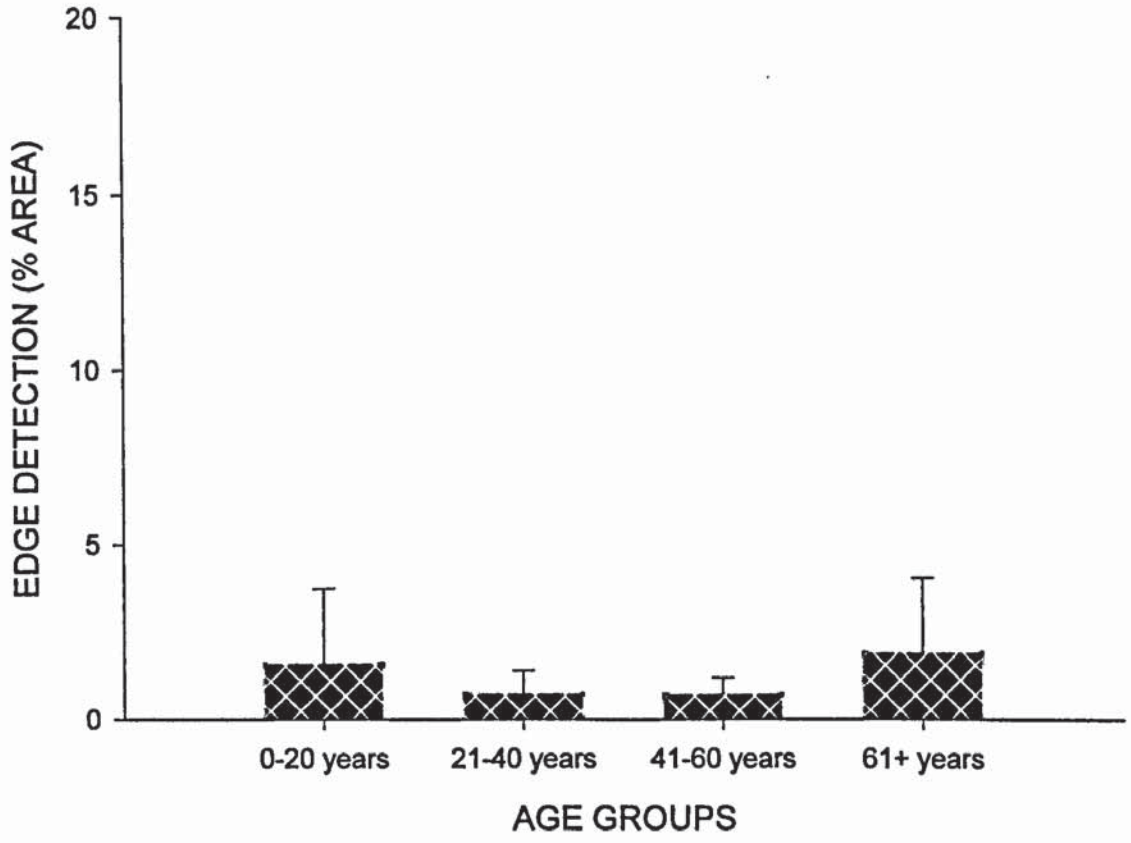

FIGURE 6.5: Changes in bulbar hyperaemia with age measured by Red Relative Colour Extraction. Significant differences determined by Tukey analysis are bracketed under the groups with corresponding p values. Error bars=1 S.D. n=120

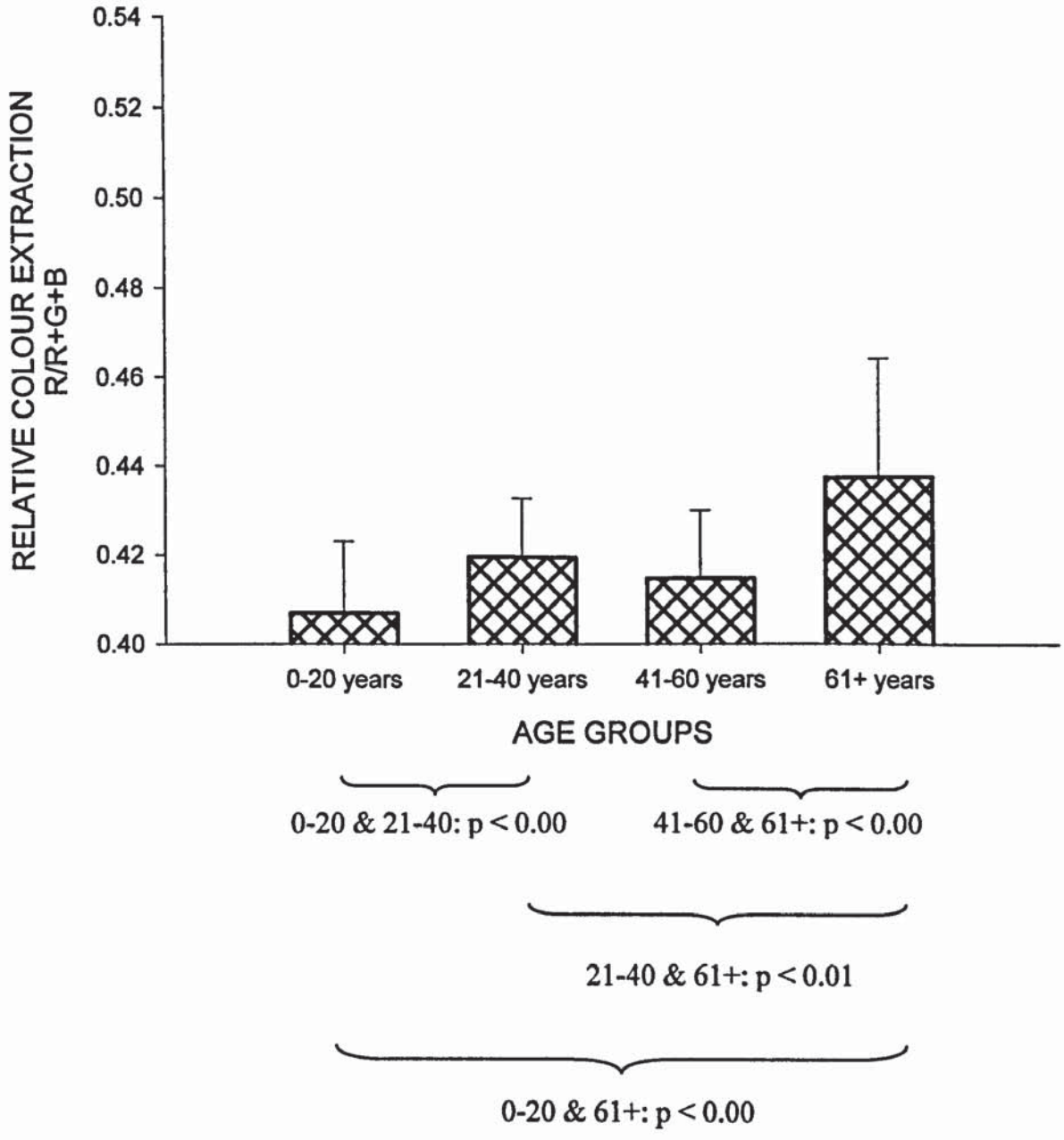

FIGURE 6.6: Changes in palpebral redness with age measured by Red Relative Colour Extraction. Error bars=1 S.D. n=120

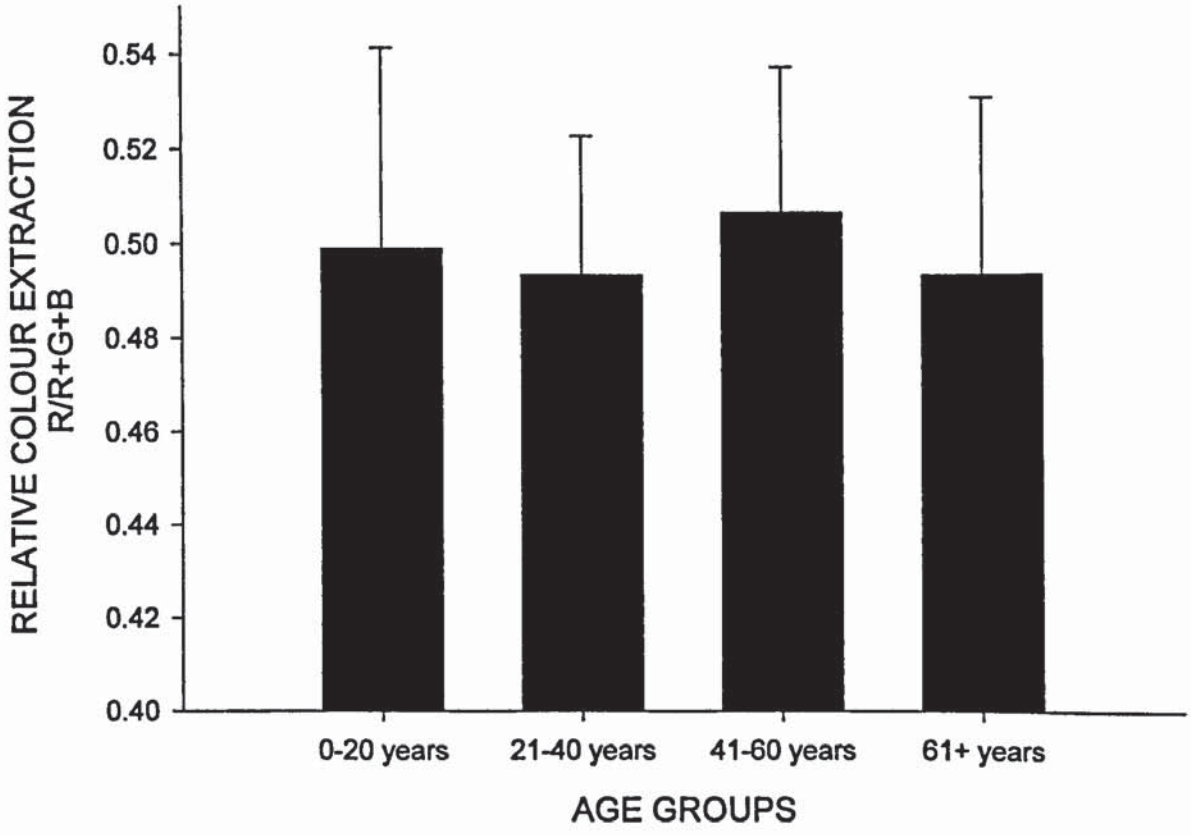

FIGURE 6.7: Changes in palpebral roughness with age measured by Green Relative Colour Extraction. Error bars=1 S.D. n=120

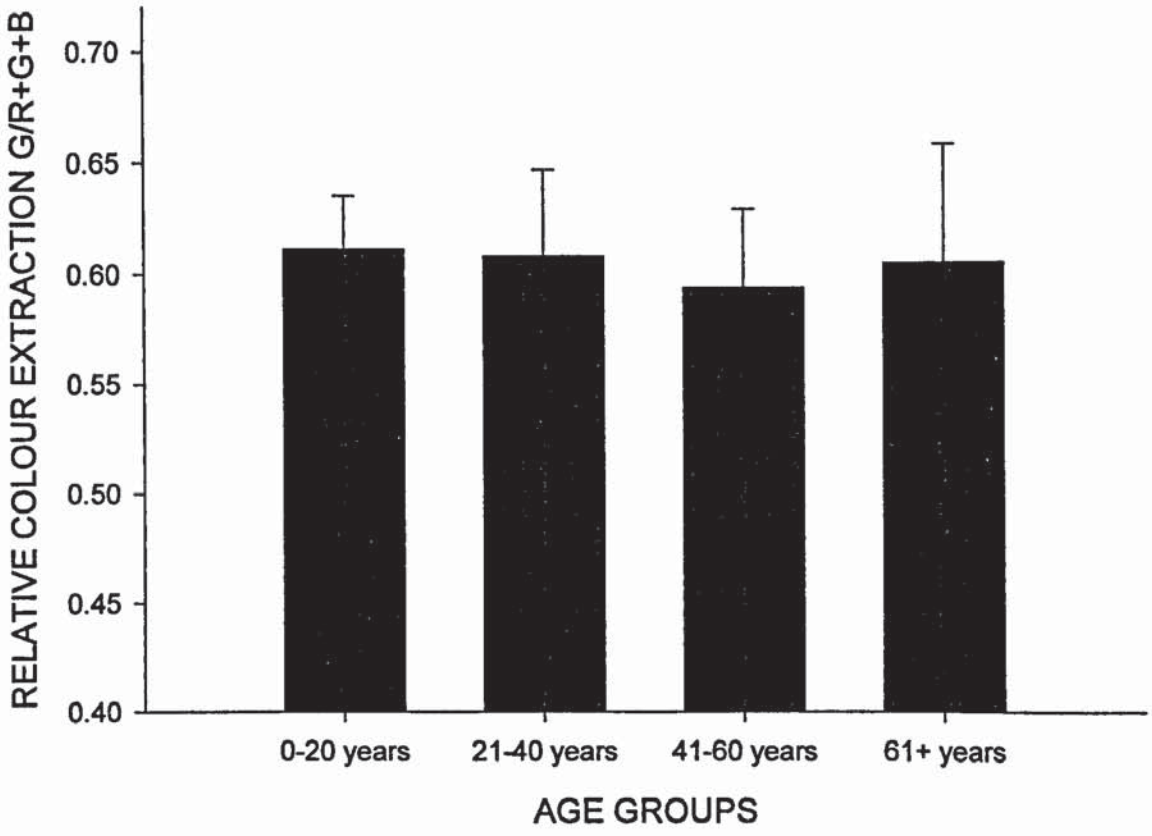

FIGURE 6.8: Changes in corneal staining with age measured by Green Relative Colour Extraction. Error bars=1 S.D. n=120

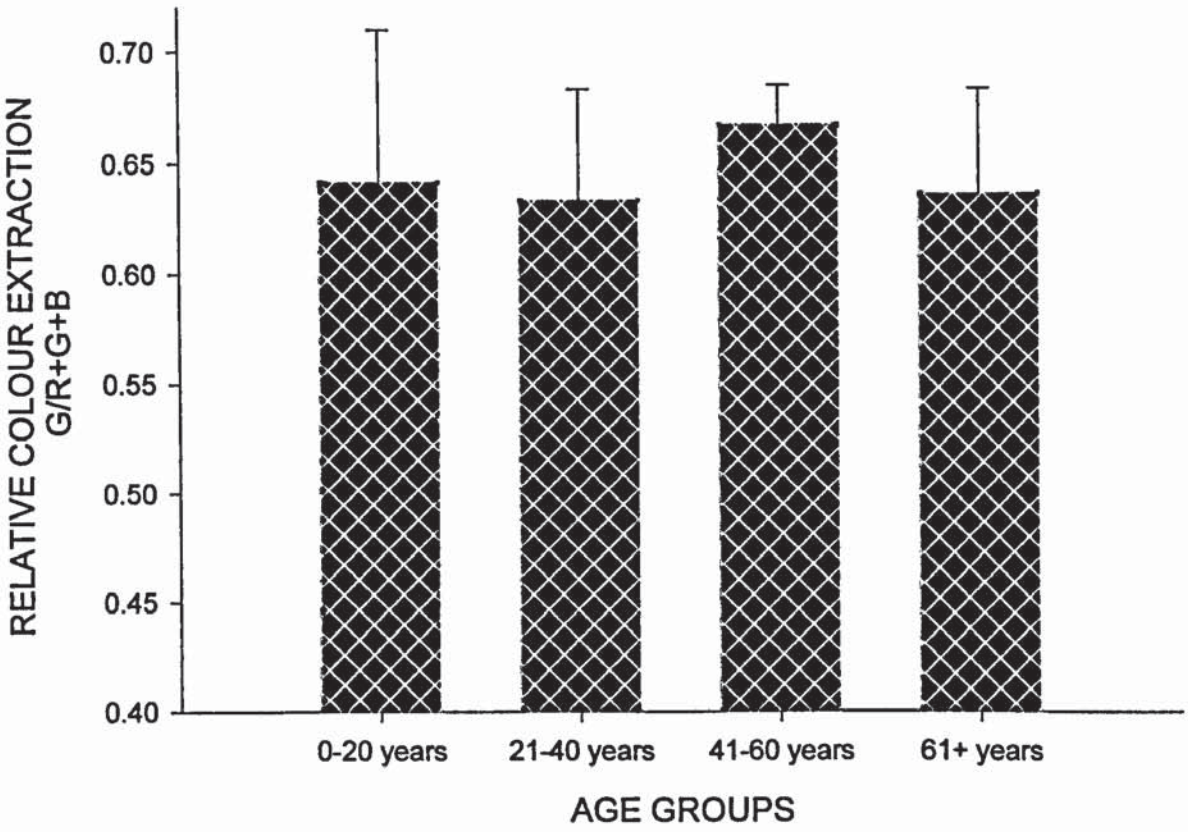

FIGURE 6.9: Correlation and scatter plot to display changes in the measures of ED for bulbar hyperaemia with age. n = 120 Correlation coefficient r = 0.22 p = 0.017

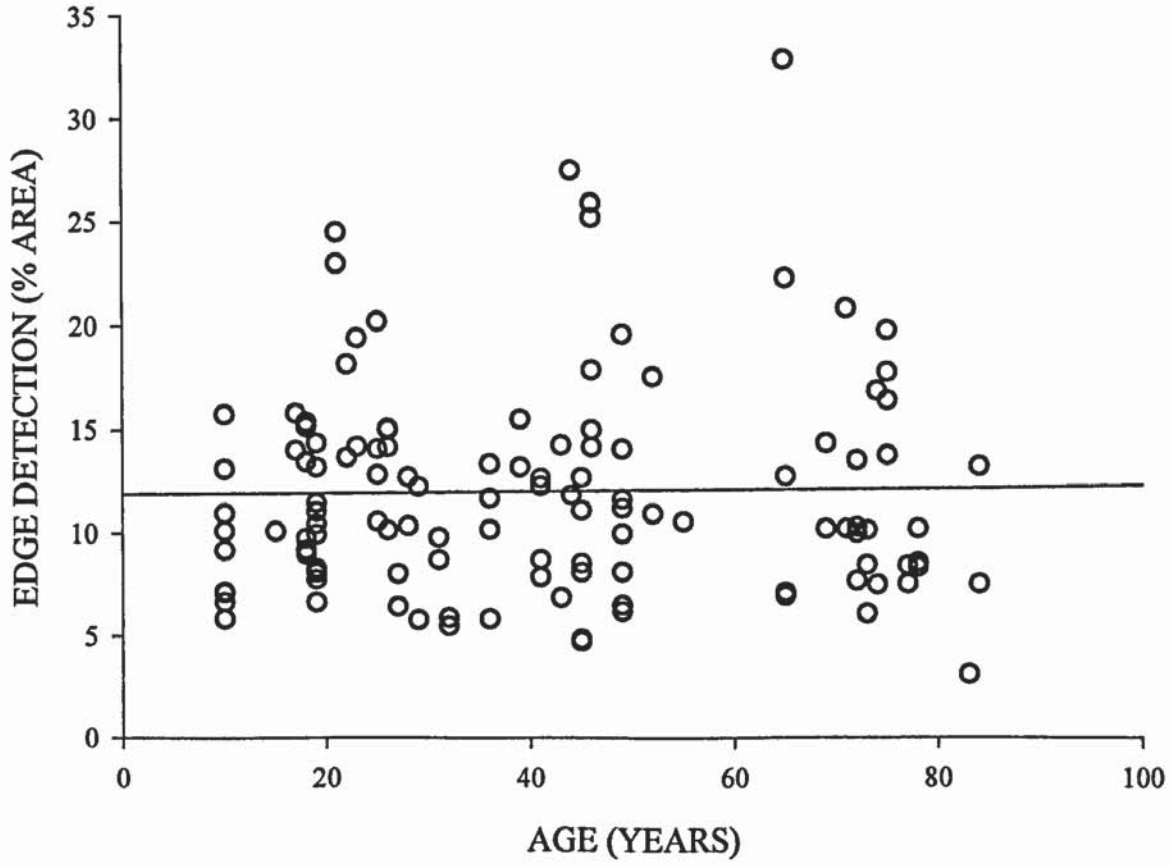

FIGURE 6.10: Correlation and scatter plot to display changes in the measures of ED for palpebral redness with age. n =120 Correlation coefficient r = -0.31 p = 0.001

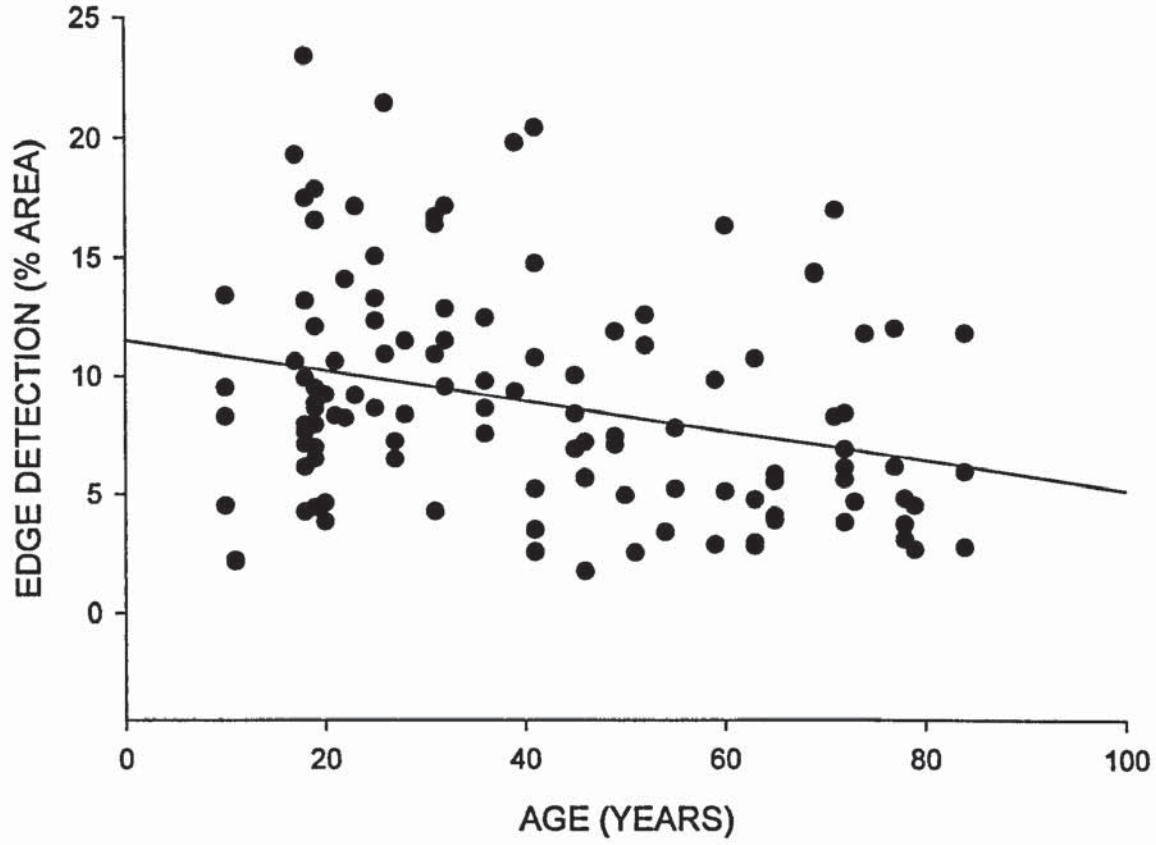

FIGURE 6.11: Correlation and scatter plot to display changes in the measures of ED for palpebral roughness with age. n = 120 Correlation coefficient r = -0.24 p = 0.009

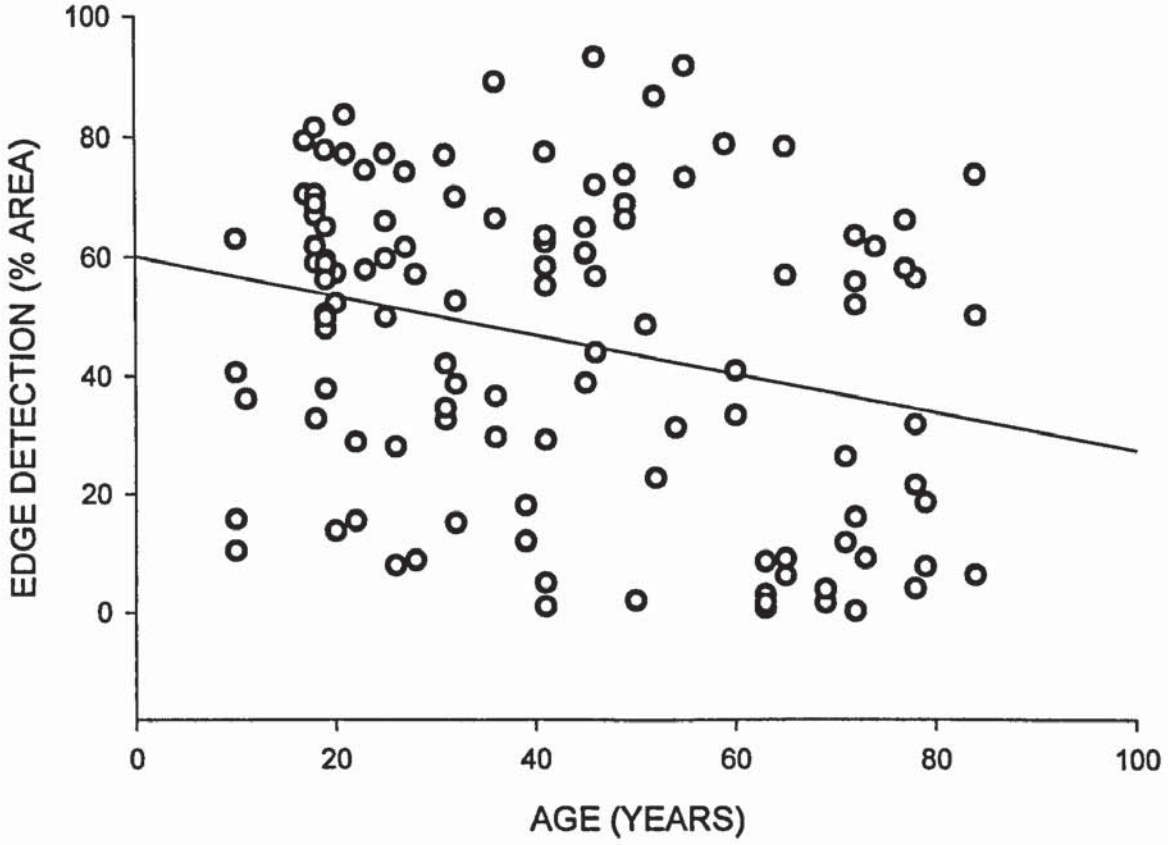

FIGURE 6.12: Correlation and scatter plot to display changes in the measures of ED for corneal staining with age. n = 120 Correlation coefficient r = 0.05 p = 0.58

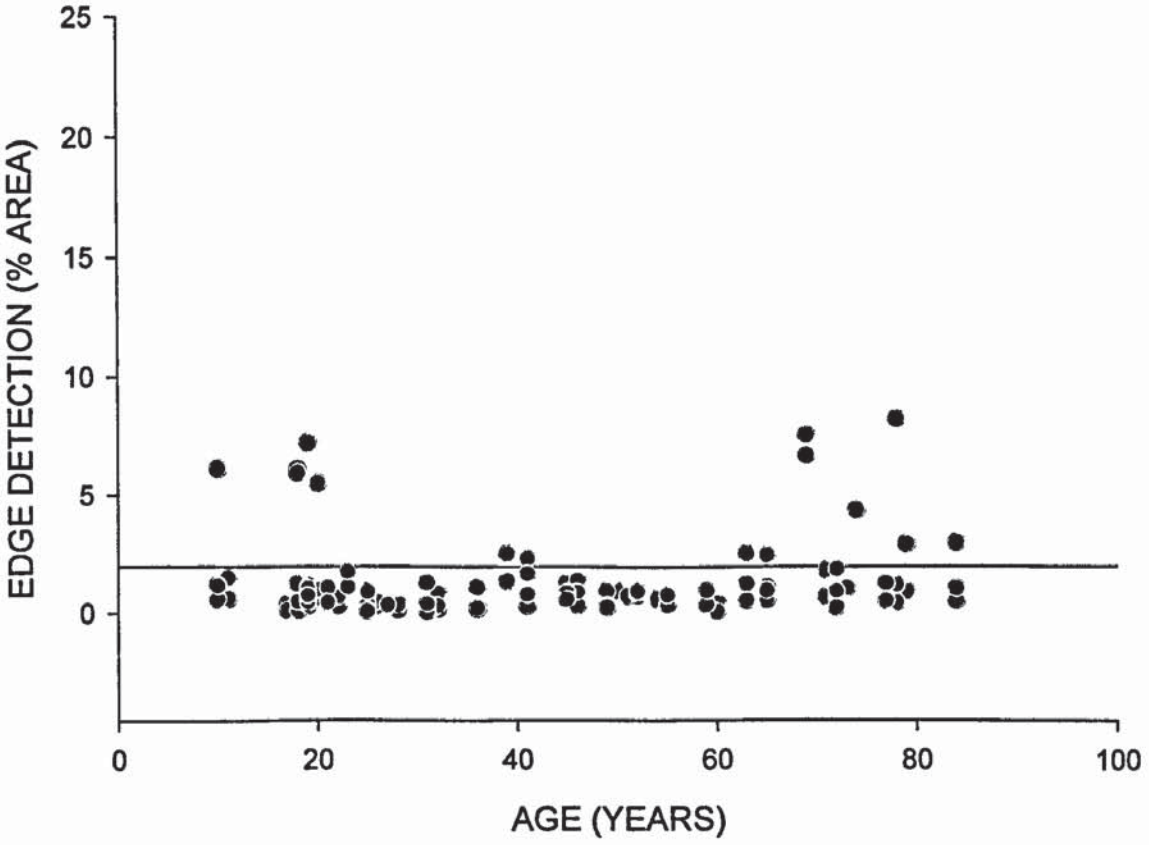

FIGURE 6.13: Correlation and scatter plot to display changes in the measures of Red RCE for bulbar hyperaemia with age. n = 120 Correlation coefficient r = 0.23 p = 0.006

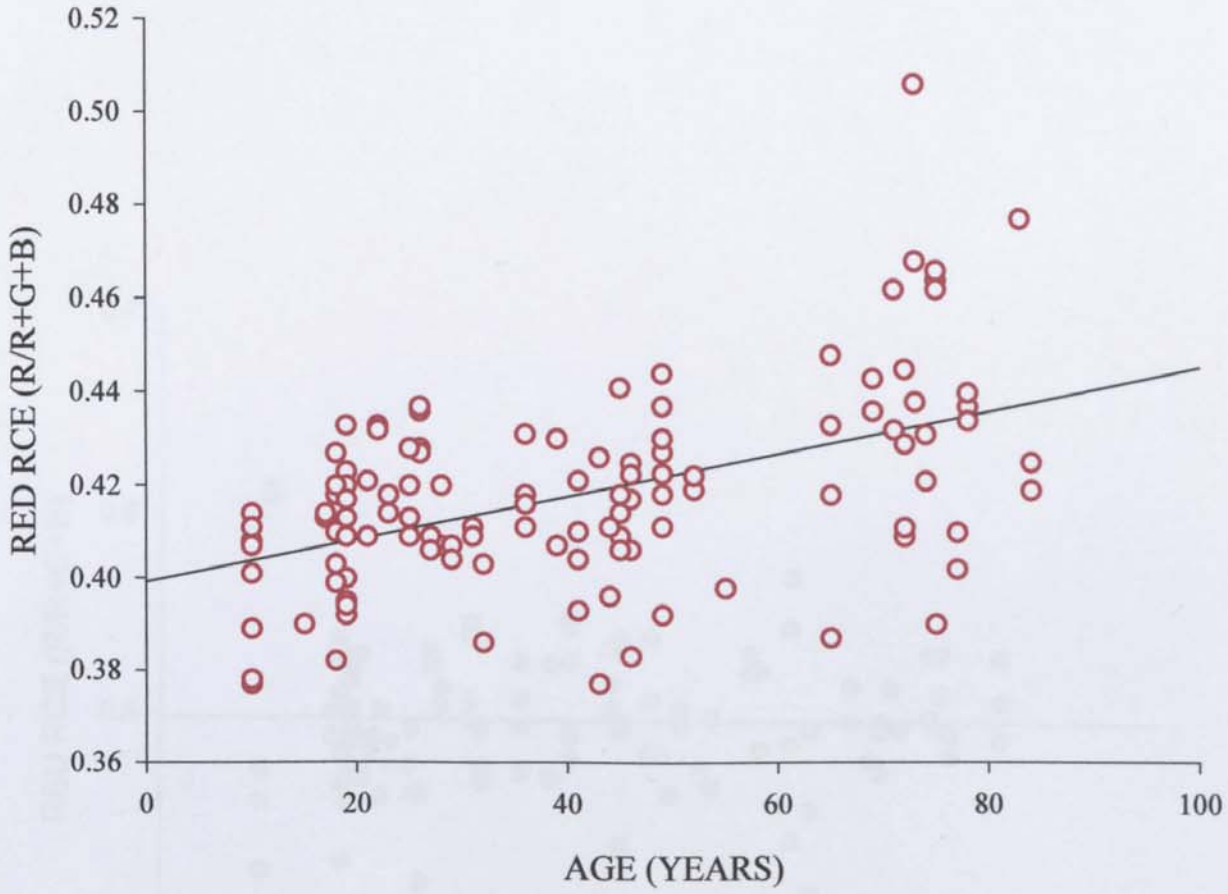

FIGURE 6.14: Correlation and scatter plot to display changes in the measures of Red RCE for palpebral redness with age. n = 120 Correlation coefficient r = -0.05 p = 0.62

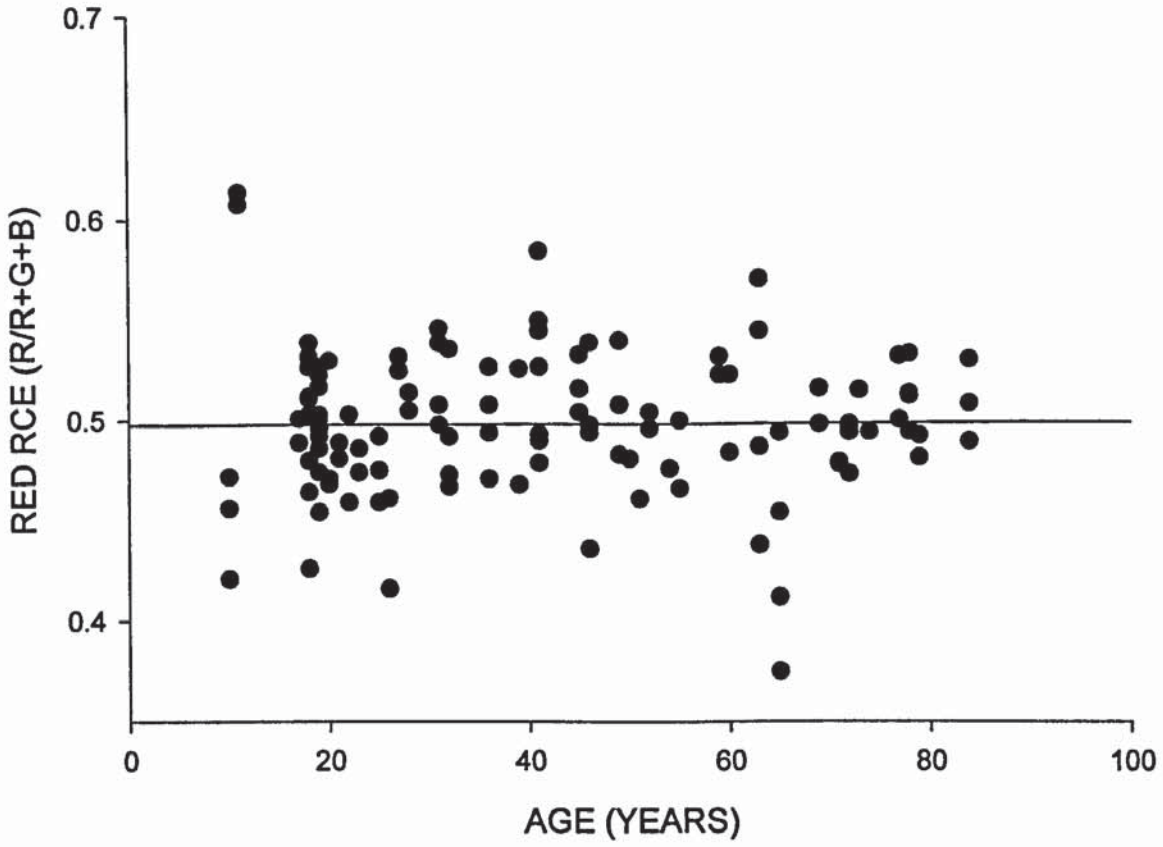

FIGURE 6.15 Correlation and scatter plot to display changes in the measures of Green RCE for palpebral roughness with age. n = 120 Correlation coefficient r = -0.004 p = 0.97

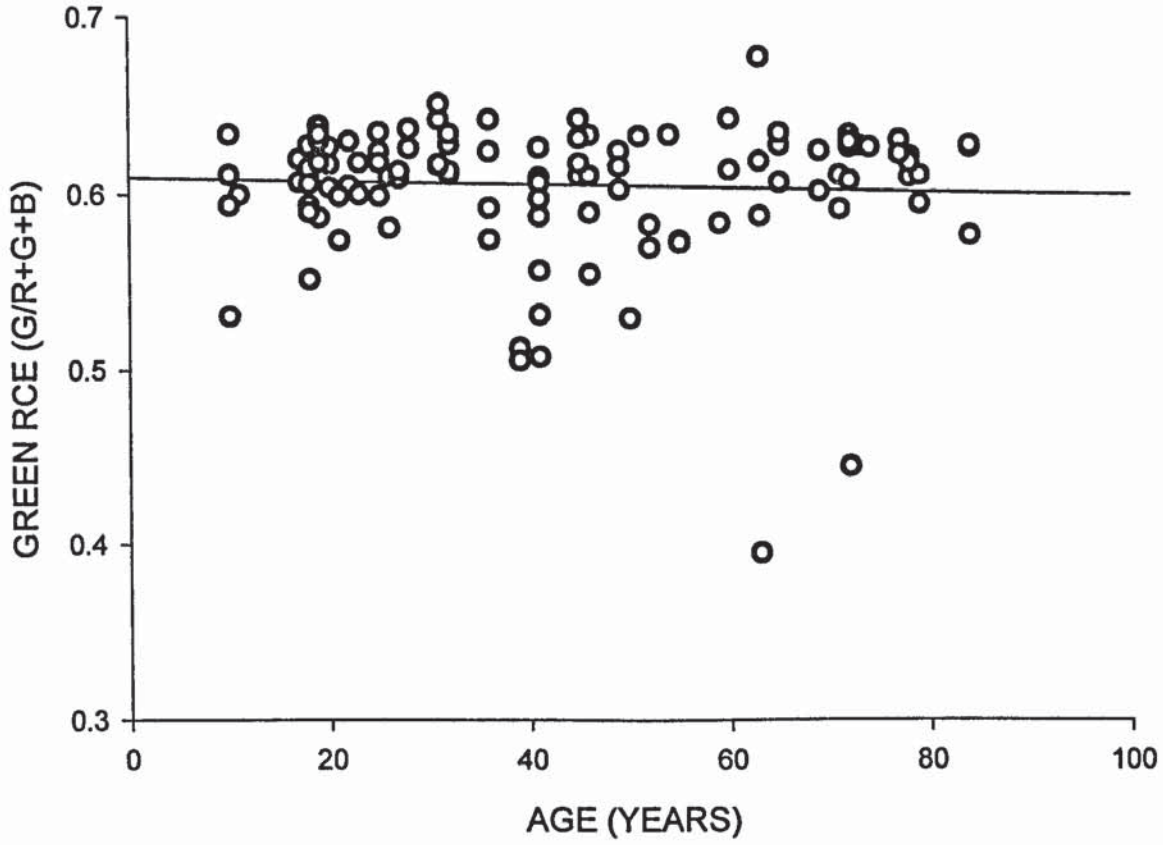

FIGURE 6.16: Correlation and scatter plot to display changes in the measures of Green RCE for corneal staining with age. n = 120 Correlation coefficient r = 0.02 p = 0.85

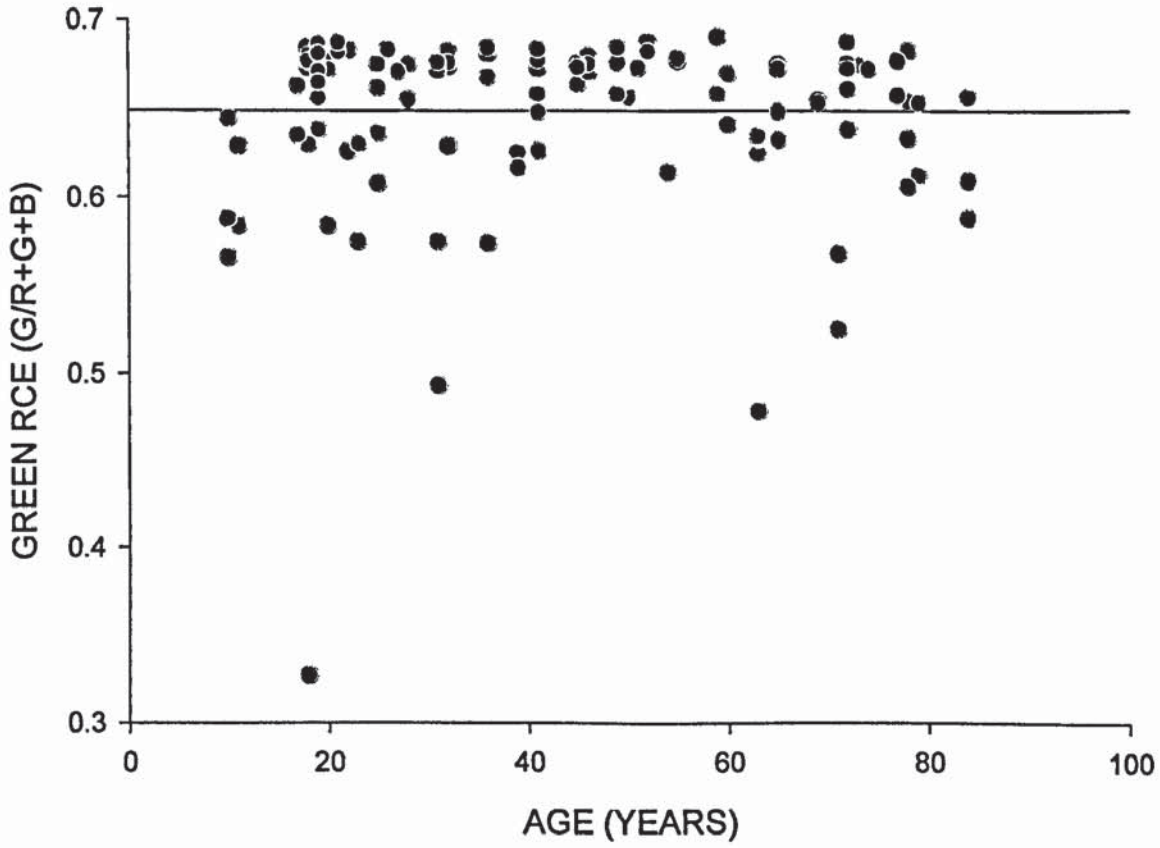

6.5 DISCUSSION

Red RCE measures of bulbar hyperaemia were found to change significantly with age ($p=0.49$). These results perhaps indicate that the effect of age is of an increase in the background vasculature, which effects the 'redness' of the area analysed; a conclusion which can also be drawn from the analysis of the bulbar hyperaemia in Chapter 4, and the work by Mikhailishchuk which suggested that only microvasculature and capillaries changed with age. [93] Reductions in palpebral redness and roughness were apparent, but only using the ED measures, indicating that the visible vasculature measured changes significantly with age, rather than perhaps the background chroma. An example of the average difference in palpebral conjunctival redness with age is given in Figure 6.17

FIGURE 6.17: Images of the palpebral conjunctiva of two subjects (ages 0-20 and 61+), which display **average** RCE values for their age.

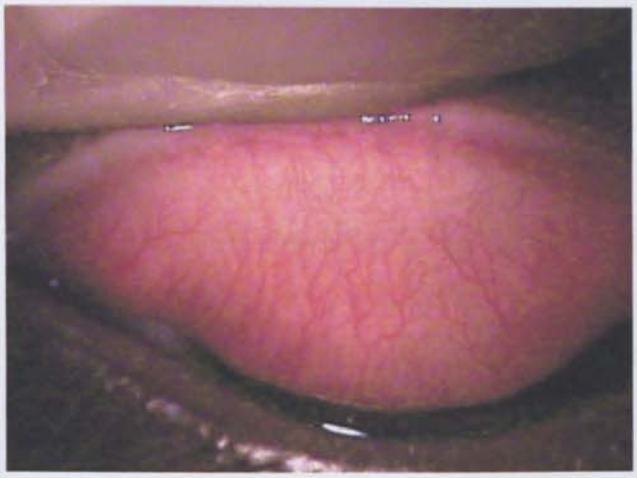

Age 0-20 years. RCE = 0.50, ED = 19.36

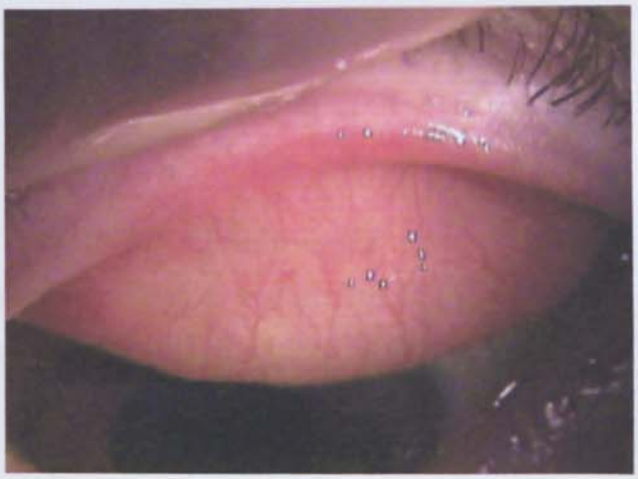

Age 61+ years. RCE = 0.49, ED = 2.62

The decrease in palpebral roughness measured by ED suggests that the number of papillae highlighted by the 'moats' of fluorescein on the palpebral conjunctiva are also found to be reduced with subjects in the over 61 years group. This effect is displayed in Figure 6.18.

FIGURE 6.18: Images of the palpebral conjunctiva (with fluorescein inserted under blue illumination with a Wratten-type filter), of two subjects (ages 0-20 and 61+), which display **average** ED values for their age.

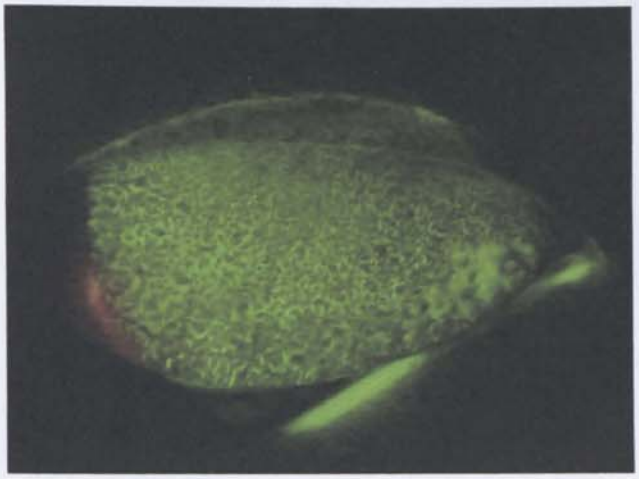

Age 0-20 years. ED = 52.31, RCE = 0.63

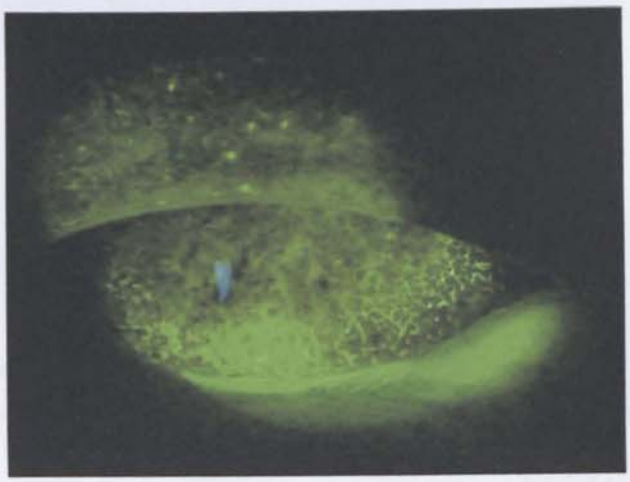

Age 61+ years ED = 26.21, RCE = 0.59

In accordance with the findings in Chapter 5, the *area* of corneal staining was also measured objectively, and the difference approached significance within the age groups ($F = 2.59$, $p = 0.058$). However, there was poor correlation between the area of staining observed and the age of the subject, $r = 0.00$.

The results of Chapter 5 enabled the formation of grading formulae. In order to now examine the clinical effects of age on anterior ocular surfaces, the findings from this chapter should be converted into equivalent subjective grades. These are displayed in Table 6.2

TABLE 6.2: Average equivalent grades for ocular surfaces over the four age groups

SURFACE ANALYSED	SCALE UTILISED	AVERAGE ± S.D EQUIVALENT GRADES				
		0-20	**21-40**	**41-60**	**61+**	**ANOVA**
BULBAR HYPEREMIA	CCLRU	2.56±0.30	2.88±0.26	2.61±0.23	2.69±0.31	F=8.67 **p<0.001**
	EFRON	1.50±0.44	1.98±0.34	1.61±0.32	1.79±0.45	F=10.31 **p<0.001**
PALPEBRAL REDNESS	CCLRU	1.96±1.11	1.63±0.90	2.31±0.69	2.11±0.87	F=3.20 **p<0.05**
	EFRON	0.94±0.98	0.66±0.79	1.25±0.61	1.06±0.78	F=3.04 **p<0.05**
PALPEBRAL ROUGHNESS	CCLRU	2.44±0.62	2.44±0.90	3.31±2.74	2.21±1.31	F=2.52 p=0.06
CORNEAL STAINING	CCLRU	1.24±1.24	1.26±1.26	1.25±1.25	1.29±1.29	F=2.40 P=0.07
EXTENT	EFRON	0.90±0.15	0.93±0.08	0.92±0.03	0.97±0.12	F=3.20 **p<0.05**
DEPTH	CCLRU	1.29±0.08	1.31±0.05	1.30±0.02	1.33±0.07	F=3.04 **p<0.05**

In Chapter 4 subjective grading of the bulbar hyperaemia was found to be able to differentiate up to a maximum of 0.3 of an Efron scale unit. Objective grading was 20 times more sensitive and up to 82% more reliable than the subjective graders.

The results of the 3 repeated objective measures for each subject (Table 6.1) indicate low variability similar to that determined in Chapter 4, particularly with the Red and Green RCE measures. This finding ensures that patients can act as their own 'baseline' for normal, and that any change in their ocular surfaces outside the normal limits is likely to be detected.

ED and RCE ocular surface measures were used to calculate the range of CCLRU or Efron grades that predict a 'normal' baseline for the 4 age groups. Despite the sensitivity and reliability of the objective analysis and the high correlation values found for the formulae constructed in Chapter 5, the baseline values seem high, particularly for bulbar hyperaemia assessments (Table 6.2). This result gives some cause for concern, as the grade which may be calculated for an ocular surface, may lead to a clinician accepting a high grade as 'within normal limits' and therefore cause only the most severe changes in surface health to be described as abnormal for that age group. However, on further examination of the images that were collected and analysed, the bulbar conjunctiva does indeed correspond well overall to a grade above 2 for the CCLRU and above 1 for the Efron scale. A recent article re-examined the actual grade of the bulbar hyperemia with two observers subjectively grading 121 eyes with a median age of 28. With the CCLRU scale an average grade of 1.93±0.32 was determined. [106] These results correspond closely to our own findings and may indicate that although as clinicians we do not expect grades to be around 2 on average, this is indeed representative of the population.

Other factors which may have produced this result are firstly that the subjective scales are not linear in nature, and have a sensitivity weighed towards the lower end of the scale. This would mean that a small increase in hyperaemia above a certain level would transpose into a larger difference in an objective grade. Secondly, most of the 0-20 year olds in the sample were recruited from a university student population which may not be representative of the normal population.

Previous studies have reported changes in bulbar hyperaemia, but none have gone so far as to attempt to quantify the differences between changes in age. The measures above will improve

the accuracy of the interpretation of grades, and allow for a baseline prediction of normal which can be utilised in a clinical or research environment.

The palpebral conjunctiva is a surface which has generally been neglected regarding clinical research, as it is a relatively more complicated area to observe and measure than the others. The fact that this surface appears to be susceptible to changes in age indicates that it may be useful in measuring other changes (such as dryness or allergens), and this finding may provide the impetus for a new direction in ocular surface monitoring. MacKinven et al examined the palpebral redness and roughness of a group of 96 subjects (age 18 to 75) and determined that a CCLRU grade over 2 units is abnormal. [16] The average equivalent CCLRU grade determined by objective analysis over the 4 groups is 2.12 ± 0.18 for palpebral redness (which is over their estimation of 'normal'), and 0.94 ± 0.00 for palpebral roughness, which would appear to concur reasonably with their findings.

This study found no age-related changes in corneal staining, and determined that the average corneal staining extent is 1.30 ± 0.00 (CCLRU), 0.98 ± 0.00 (Efron), and 1.32 ± 0.02 (CCLRU) for depth. This result would allow researchers a broader net with which to recruit subjects for corneal surface studies, as the Dundas et al study was limited to an age range of less than 50 years. [30]

One limitation with this study could possibly be that the images were all taken in the morning, and that this could increase the grades of redness as shown by McMonnies and Ho. [38]] This method was used due to the constraints of the hospital department where most of the clinics occurred in the morning, and also as long as the images were taken at a consistent time there should not be too detrimental effect on the results of the comparison. The issue of diurnal variation is important and the baseline measures that are being established are incomplete without them. In order to compensate fully for any diurnal as well as age-related changes, a similar study is undertaken in Chapter 7 to determine the effects of time of day on the ocular surfaces.

CHAPTER 7

DIURNAL CHANGES IN OCULAR SURFACES

7.1 INTRODUCTION

The conversion of objective measures into the Efron or CCLRU equivalents in Chapter 5 was completed so that eye-care practitioners (ECPs) may recognise and utilise the objective grades with relative ease. The measures of the ocular surface changes with age reported in Chapter 6 gave a baseline of 'normal' for the ocular surfaces evaluated. The other factor which could affect the objective boundary of 'within normal limits' and therefore should be controlled or compensated for is the possible change in grade with time.

Compared even with the literature on ocular surface changes with age, there are few published reports which confirm or deny changes in time *over one day* with normal non-contact lens wearing subjects. One study which does investigate this matter is that of Guillon and Shah who examined changes in bulbar hyperaemia. [55] 10 non-contact lens wearers (no age given) were found to show an overall difference over the course of a day for percentage blood vessel coverage. They report that in the evening the conjunctival blood vessels were significantly more dilated, and covered a greater percentage of the conjunctival surface area than at 2 hours after waking ($p<0.05$). The method of examination was an objective analysis programme designed to measure vessel coverage at distinct 'sampling lines' positioned (by the programme) at 1, 2 and 3mm from the edge of 4 quadrants of the limbus. [55]

The investigation by Josephson and Caffery into diurnal changes in corneal staining is to our knowledge the only report of its kind with human subjects (n=21, aged 27±12.72years). [99] The study used a grading system based on that of Korb and Herman where a note of the presence of staining is made over 5 regions of the cornea. [102] Josephson and Caffery determined that there are variations in the amount and location of fluorescein staining throughout the day, with a trend towards higher grades in the morning (8.00am). Their study involved extracting half of their sample (10 out of 21 subjects) who were classified as 'stainers' and the daily variation was determined for 6 subjects in this group only, therefore it may not be representative of the 'normal' population. [99] However, the work of Dundas et al and others suggests that up to 79% of the population have corneal staining at any one time, and so the study may be more representative than on first inspection. [30, 103]

Reasons for diurnal variations in corneal staining were examined by Fullard and Wilson who suggested that epithelial 'sloughing' (physiological squamous cell turnover) was the cause due

to interrupted epithelial continuity [107, 108]. This and other factors such as changes in tear secretion could affect all of the anterior ocular surfaces over time. [109]

MacKinven et al state that "the appearance of the normal, healthy, adult [palpebral] conjunctiva seems to have received scant attention" and this statement appears to still be correct even five years later. [16] The investigations that have examined the palpebral redness and roughness describe a range of prevalence of papillae. Allensmith et al reports that 24% of contact lens wearers have a 'satin-smooth' palpebral appearance. [110] This figure is reduced in the study by Saini et al to 0% in a group of 20 non-contact lens wearers. [111] Until the MacKinven study, none had set out to examine the grade of palpebral redness and roughness of the 'normal' non-contact lens wearing population. Their study, however, took measures irrespective of time of day, was subjective and the repeatability was not measured. [16]

7.2 PURPOSE

Previous work on the determination or dismissal of anterior ocular surface changes throughout the day is minimal, and although the evaluation of the bulbar conjunctiva by Guillon and Shah used objective analysis, the work was limited by the method and positioning of the sampling lines that they took. [55] Therefore this chapter examines the effect of time of day on the anterior ocular surfaces, so that any diurnal variation can be compensated for when objective grades and estimations of normality are given.

7.3 METHODS

In order to obtain the most relevant data, the times over which the images were to be taken had to have maximum possible separation during the normal working day. 35 optometry students were recruited and surveyed for any abnormal ocular condition and level of dry eye using the McMonnies dry-eye questionnaire. [112] 30 subjects were found to be suitable with no ocular pathology or significant dry eye, their average age was 21 ± 1.46 years. The subjects were instructed not to wear any contact lenses or to swim a day before or during the data collection. Images of the right bulbar conjunctiva, palpebral conjunctiva (for redness and roughness) and corneal surface staining were taken on 3 occasions over one day, with 5 hours between each sitting. Ethical approval for these measures was previously given by the institutional ethical committee. The subjects gave written consent to the study after a full explanation of the methods to be used. The imaging sessions took place at 8.30am, 1.30pm, and 6.30pm. These times were chosen to examine the change in the ocular surfaces over the course of a *working day* i.e. the period of time over which a subject may be examined by a clinician.

The images of the anterior ocular surfaces were captured using the methods indicated in Table 5.1 in order to maintain standardisation across the data collection. All images were captured by the same optometrist as consistent throughout this thesis at 10x magnification with a JAI camera (CV-53200, Yokohama, Japan, with a resolution of 767x569 pixels) through a Takagi SM-70 slit-lamp biomicroscope (Nagano-Ken, Japan). The images were stored as TIFF files and were not compressed into JPEG due to the initial resolution of the camera. Masked analysis of the images was conducted with purpose designed and previously validated software (LabView, National Instruments, Austin, Texas, USA) which was achieved by each of the images and folders labelled in a code that was non-specific to the age or time of day that the image was captured at. [35]

3 rectangular areas of the same size (per ocular surface) were selected on each image in order to obtain average values and to cover the majority of the surface area of interest. The size of the area selected was dependant on the physiological deviation of the specific anterior feature over the study population. The different areas selected per ocular surface are displayed in a previous chapter, in Table 5.1. ED and RCE imaging techniques were used to assess the baseline appearance of bulbar hyperaemia, palpebral redness, palpebral roughness and corneal staining in the study population.

7.4 RESULTS

A repeated measures ANOVA was used to determine if there were any significant changes in the ocular features over time. Differences found were for bulbar and palpebral redness only by increases in Red RCE ($F=6.47$ $p=0.002$, $F=4.31$ $p=0.02$ respectively) between the morning (8.30am) and the evening (6.30pm) for both ocular surfaces (Tukey analysis $p=0.002$, $p=0.02$). Results for all of the objective measures, repeats and analyses are displayed numerically in Table 7.1, and graphically in Figures 7.1 and 7.8.

TABLE 7.1: Average ± Standard Deviation, Variance and ANOVA of redness, roughness and staining detected by objective image analysis

	Objective measures	BULBAR HYPEREMIA		PALPEBRAL REDNESS		PALPEBRAL ROUGHNESS		CORNEAL STAINING	
TIME		ED	RCE	ED	RCE	ED	RCE	ED	RCE
Morning	Average ±S.D	9.61±4.05	0.40±0.012	11.92±4.55	0.49±0.03	52.91±21.62	0.490±0.030	1.71±1.84	0.66±0.027
	Variance	0.07±0.01	0.00±0.00	0.05±0.02	0.00±0.00	0.42±0.19	0.00±0.00	0.02±0.00	0.00±0.00
Afternoon	Average ± S.D	10.08±4.35	0.41±0.013	9.78±5.35	0.50±0.03	49.74±20.23	0.501±0.034	1.45±1.09	0.66±0.030
	Variance	0.12±0.04	0.00±0.00	0.60±0.08	0.00±0.00	0.93±0.84	0.00±0.00	0.06±0.08	0.00±0.00
Evening	Average ± S.D	10.11±4.53	0.41±0.012	9.85±3.80	0.51±0.02	51.43±18.64	0.51±0.024	1.15±0.96	0.66±0.020
	Variance	0.07±0.04	0.00±0.00	0.49±0.18	0.00±0.00	0.95±0.61	0.00±0.00	0.08±0.05	0.00±0.00
ANOVA:	F Value	0.50	**6.47**	2.57	**4.31**	0.17	0.37	1.84	0.04
	p Value	0.61	**0.002**	0.09	**0.02**	0.85	0.70	0.17	0.96

FIGURE 7.1: Changes in bulbar hyperaemia with time measured by Edge Detection. Error bars=1 S.D. n=30

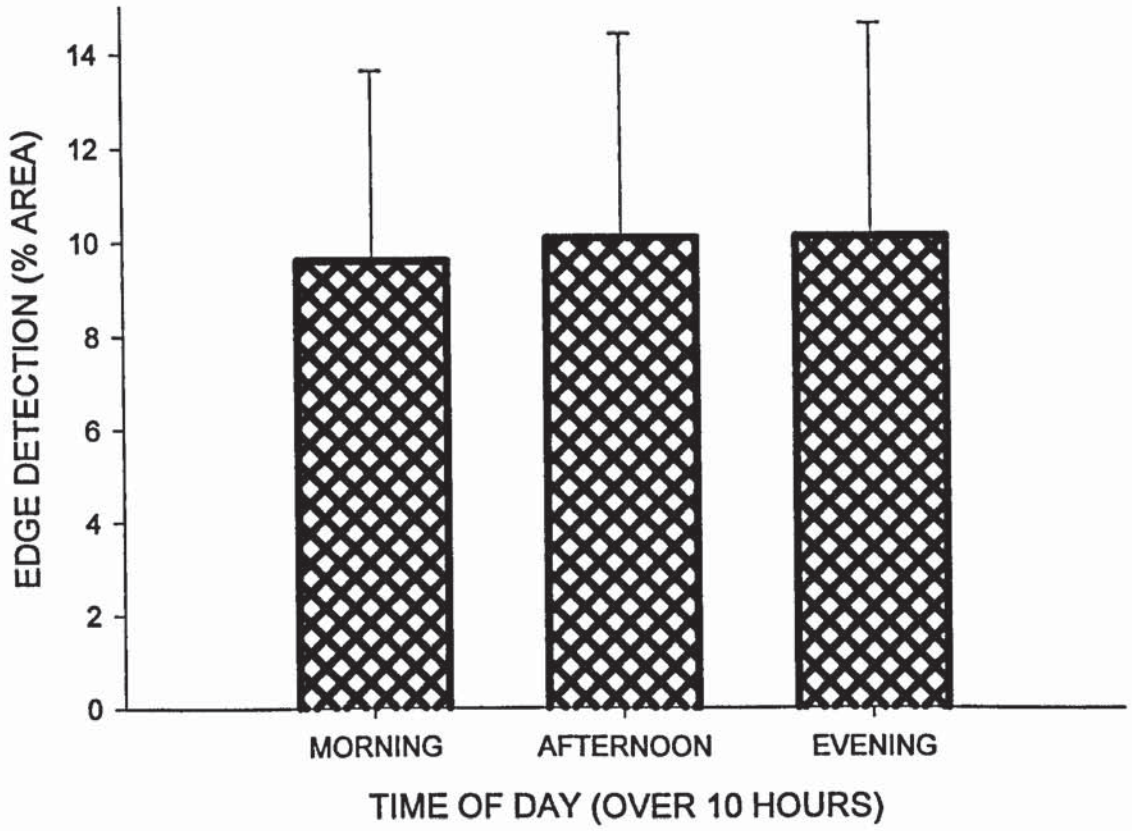

FIGURE 7.2: Changes in palpebral redness with time measured by Edge Detection. Error bars=1 S.D. n=30

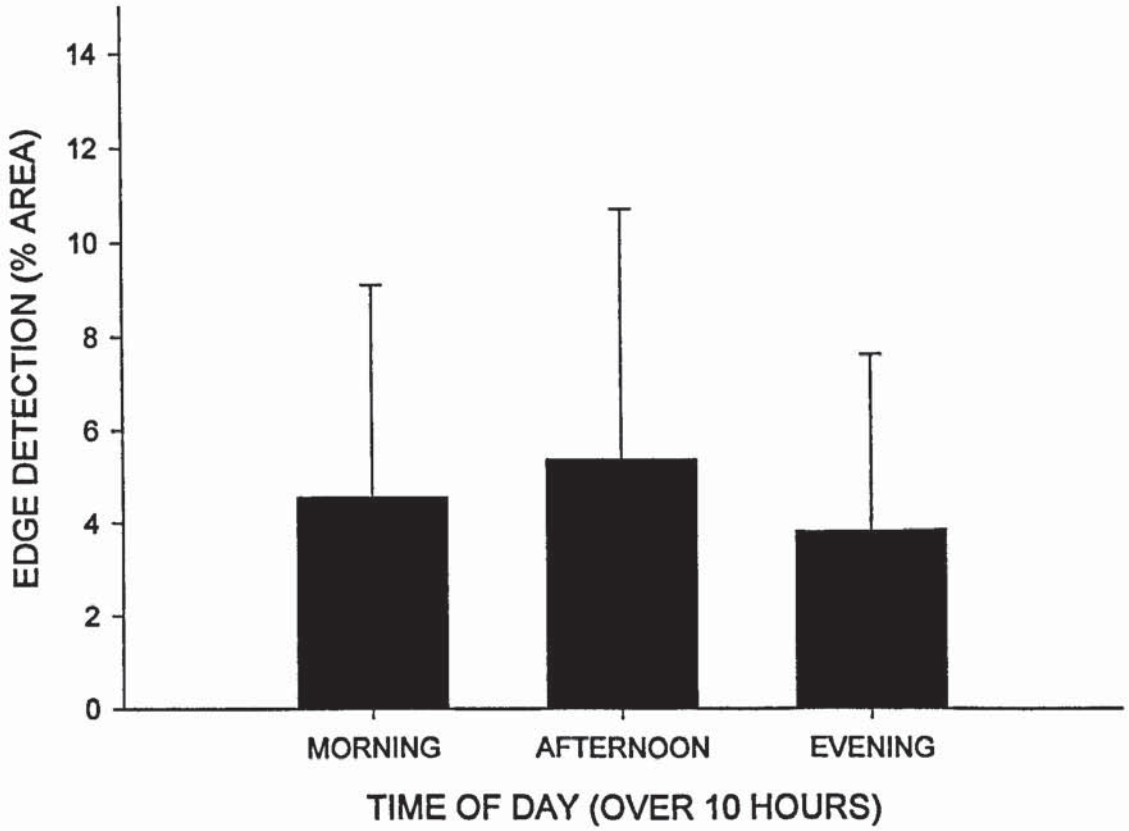

FIGURE 7.3: Changes in palpebral roughness with time measured by Edge Detection. Significant differences determined by Tukey analysis are bracketed under the groups with corresponding p values. Error bars=1 S.D. n=30

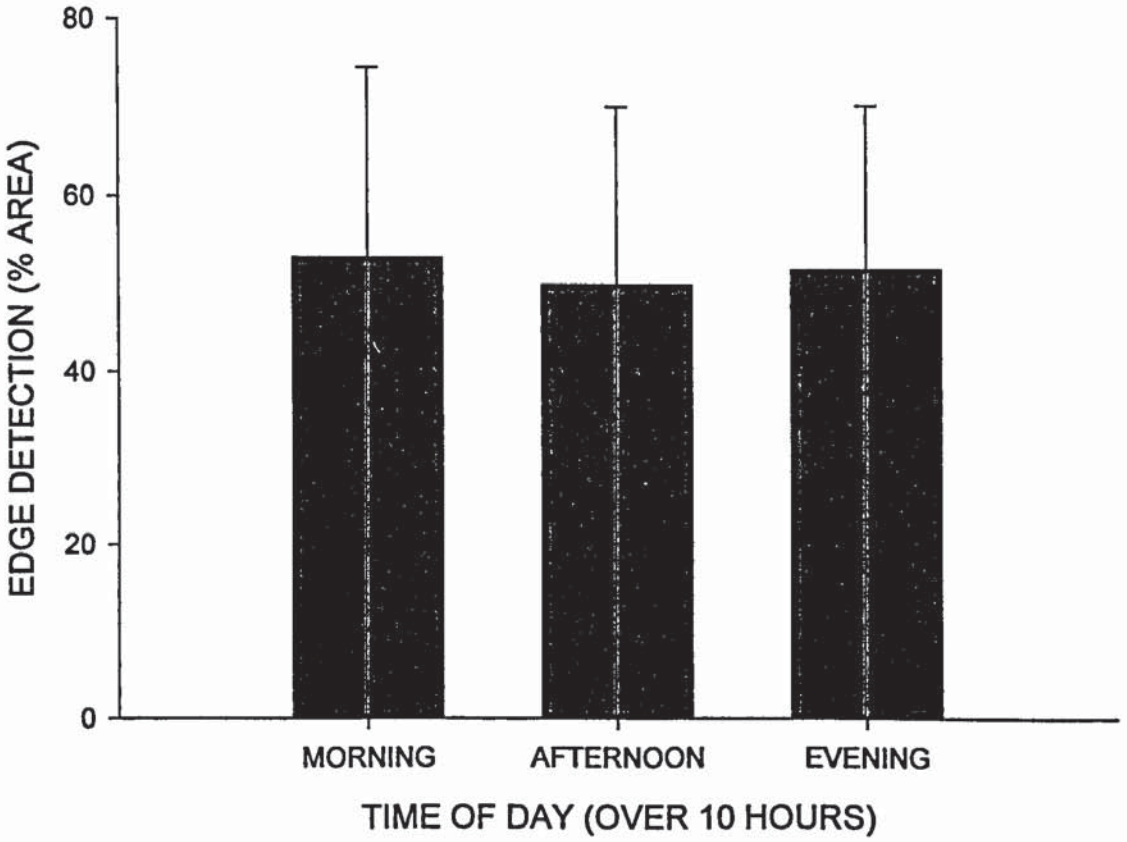

FIGURE 7.4: Changes in corneal staining with time measured by Edge Detection. Error bars=1 S.D. n=30

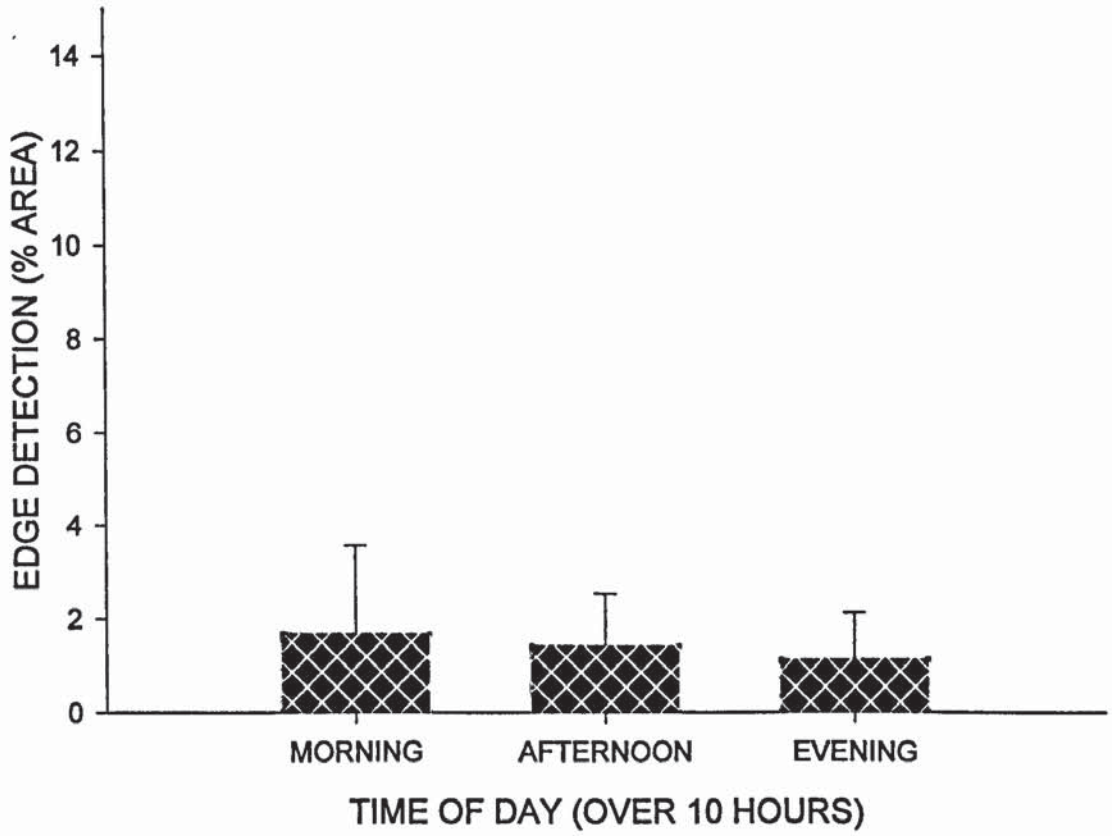

FIGURE 7.5: Changes in bulbar hyperaemia with time measured by Relative Colour Extraction. Significant differences determined by Tukey analysis are bracketed under the groups with corresponding p values. Error bars=1 S.D. n=30

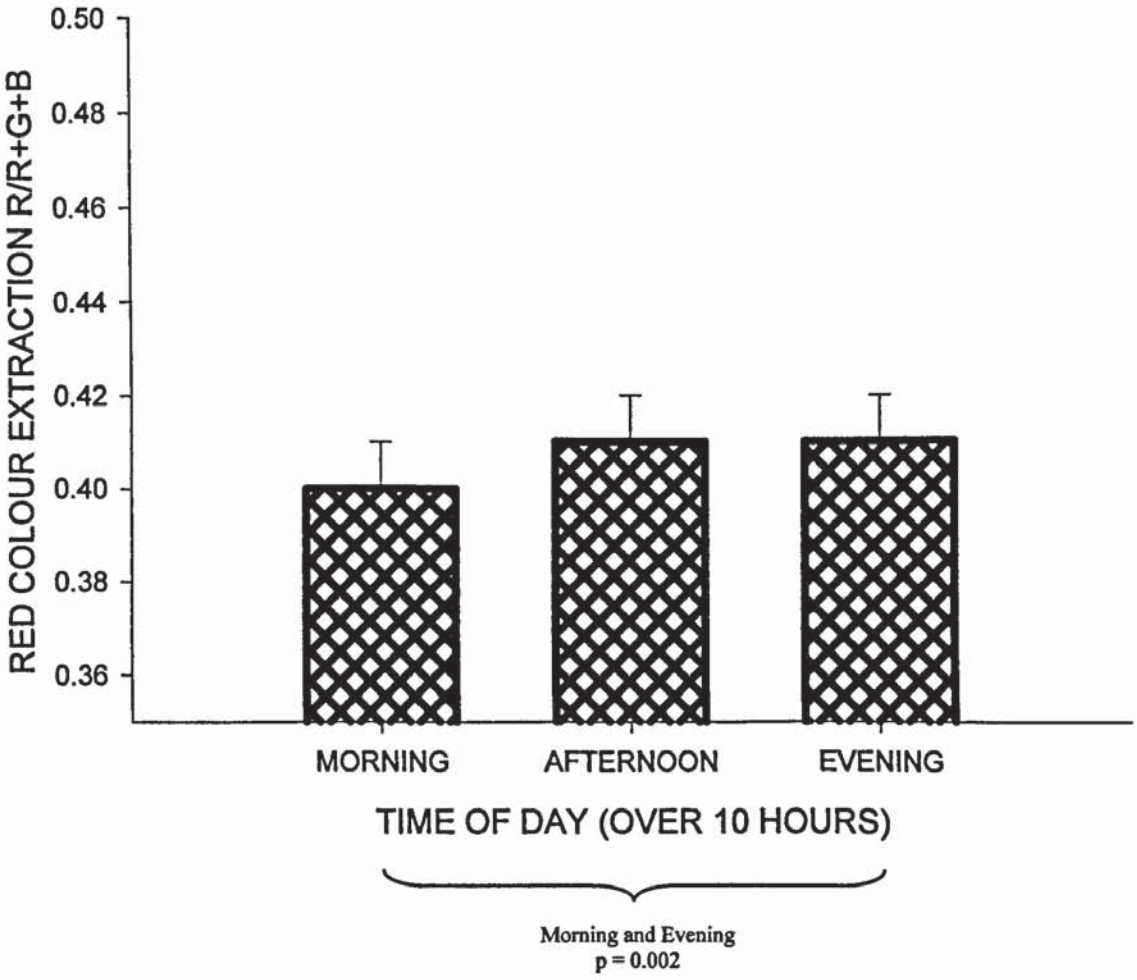

FIGURE 7.6: Changes in palpebral redness with time measured by Relative Colour Extraction. Significant differences determined by Tukey analysis are bracketed under the groups with corresponding p values. Error bars=1 S.D. n=30

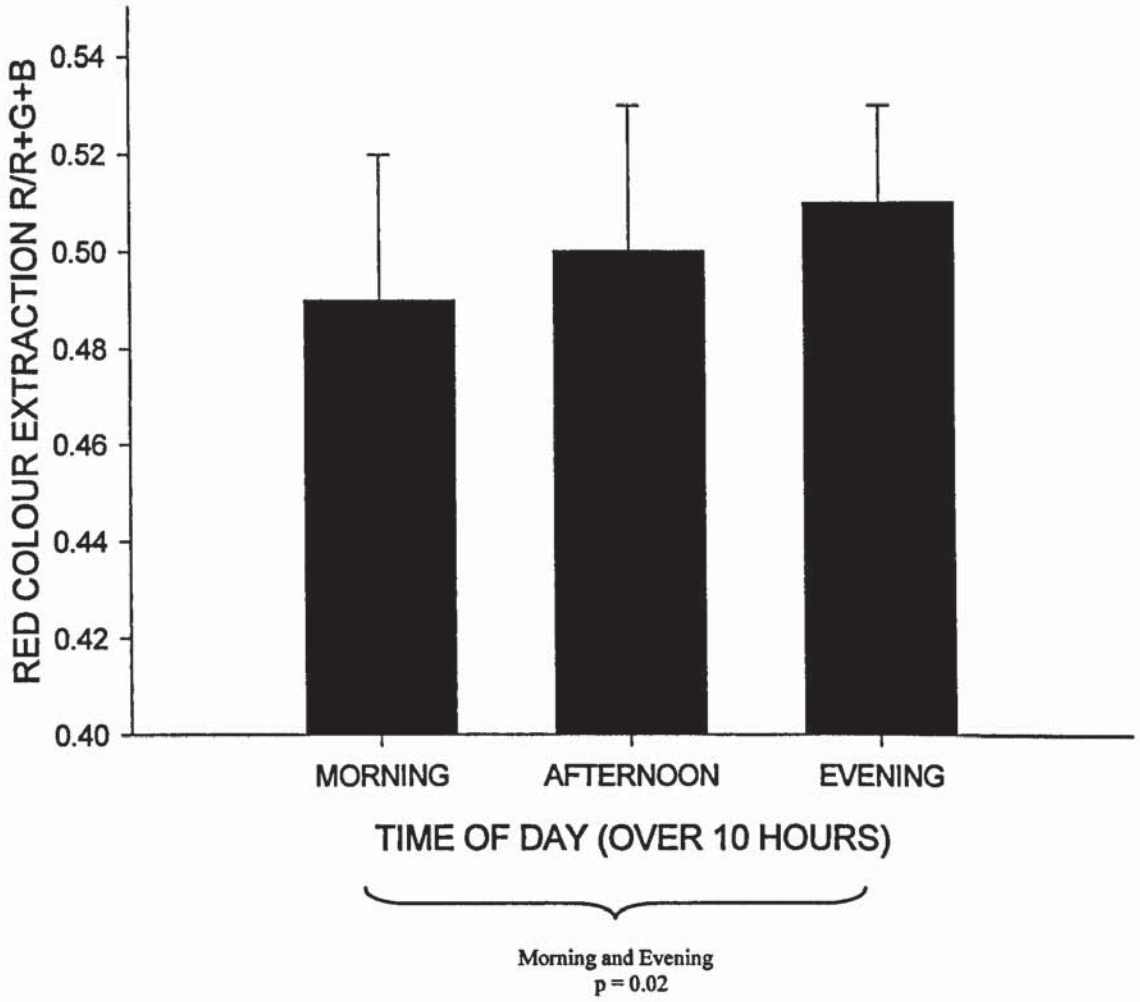

FIGURE 7.7: Changes in palpebral roughness with time measured by Relative Colour Extraction. Error bars=1 S.D. n=30

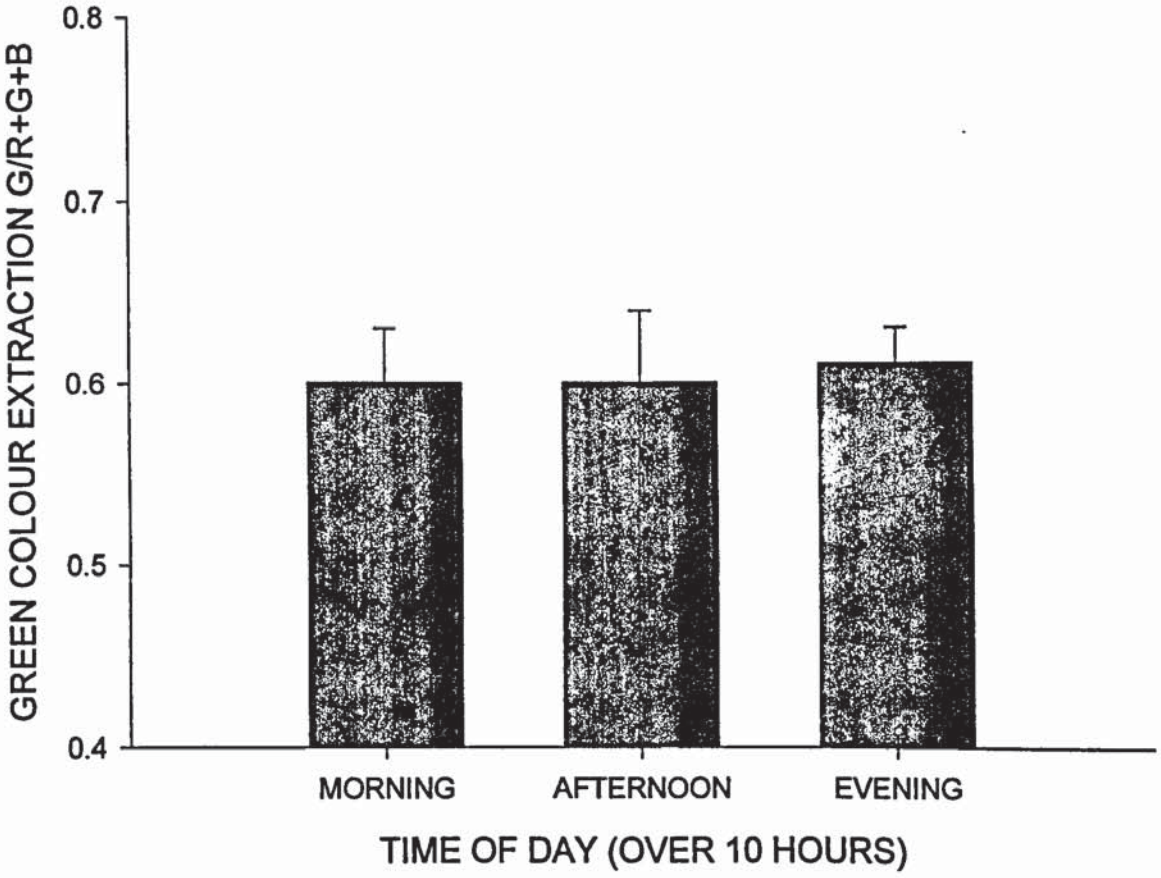

FIGURE 7.8: Changes in corneal staining with time measured by Relative Colour Extraction. Error bars=1 S.D. n=30

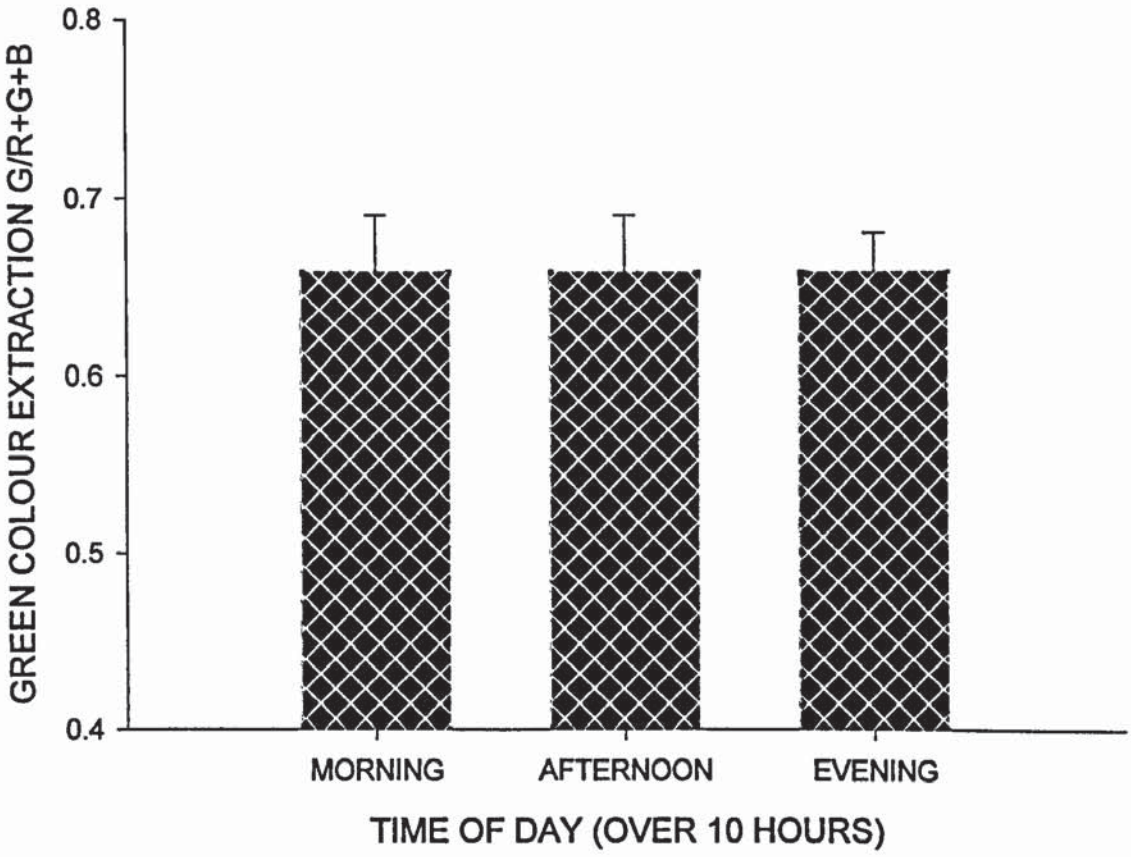

7.5 DISCUSSION

Significant changes were found only in the measures of bulbar and palpebral redness, implying that factors which could cause corneal staining and increased palpebral roughness are not sufficient over the course of one day to be a cause of significant change. The results of the 3 repeated objective measures for each subject (Table 7.1) indicate low variability for bulbar hyperaemia, (similar to that determined in Chapter 4) particularly with the Red RCE measures. Variability remains low for corneal staining analysis, but increases for palpebral redness, and again for palpebral roughness.

The changes in bulbar and palpebral redness were detected by Red RCE only. This perhaps demonstrates a more 'background' change in the tissue and deeper vasculature structures than would be identified by surface vessel changes in ED analysis. An example of the average change in RCE of the bulbar and palpebral redness is displayed in Figure 7.3.

If there was to be a hypothesis regarding the possible changes over the course of one working day, the RCE measures would be a more plausible prediction than ED, as there were no pathological episodes during the study that could have caused major surface effects. The ED changes found in Chapter 4 were induced by significant ocular irritation, and so if pathology was implicated, changes in the ED values might be the first indicator. More work needs to be done to support this theory, and a comparison between pathological cases to the baseline measures determined during Chapter 6 and 7 would be valuable.

FIGURE 7.9: Images of the bulbar and palpebral conjunctiva which demonstrate the **average** changes in Red RCE over the course of one working day. The corresponding images are taken from the same subject.

MORNING Red RCE = 0.40
ED = 6.32

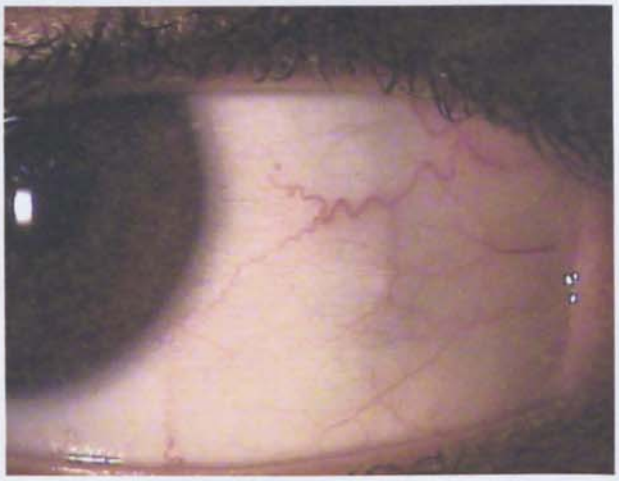

EVENING Red RCE = 0.41
ED = 3.63

MORNING Red RCE = 0.49
ED = 14.29

EVENING Red RCE = 0.51
ED = 5.20

In accordance with the alternate method related in Chapter 5, the *area* of corneal staining was also measured objectively, and although close to significance, was found to have no change with time over the course of the working day, ($F = 3.26$, $p = 0.062$).

The objective measures found should be converted into CCLRU and Efron form in order to facilitate a comparison between the sensitivity and relevance of the changes detected. The formulae constructed in Chapter 6 were utilised accordingly, and the results are displayed in Table 7.2

TABLE 7.2: Average equivalent grades for ocular surface changes over the course of a working day.

SURFACE ANALYSED	SCALE UTILISED	AVERAGE ± S.D EQUIVALENT GRADE				
		0-20	**21-40**	**41-60**	**61+**	**ANOVA**
BULBAR HYPEREMIA	CCLRU	2.56±0.30	2.88±0.26	2.61±0.23	2.69±0.31	F= 8.67 **p<0.000**
	EFRON	1.50±0.44	1.98±0.34	1.61±0.32	1.79±0.45	F= 10.31 **p<0.000**
PALPEBRAL REDNESS	CCLRU	1.96±1.11	1.63±0.90	2.31±0.69	2.11±0.87	F= 3.20 **p<0.05**
	EFRON	0.94±0.98	0.66±0.79	1.25±0.61	1.06±0.78	F= 3.04 **p<0.05**
PALPEBRAL ROUGHNESS	CCLRU	2.44±0.62	2.44±0.90	3.31±2.74	2.21±1.31	F= 2.52 p=0.06
CORNEAL STAINING EXTENT	CCLRU	1.24±1.24	1.26±1.26	1.25±1.25	1.29±1.29	F= 2.40 p=0.07
	EFRON	0.90±0.15	0.93±0.08	0.92±0.03	0.97±0.12	F= 3.04 **p<0.05**
DEPTH	CCLRU	1.29±0.08	1.31±0.05	1.30±0.02	1.33±0.07	F= 3.04 **p<0.05**

Results displayed in Table 7.2 show a clear increase in bulbar hyperaemia, and also palpebral redness with time. Fascinatingly, the depth of corneal staining also appears to decrease with time, although this difference was not found to be significant. The variability in the measures of this surface (Table 7.1) is low, and therefore it is feasible that this measure is demonstrating the effect of corneal healing. This adds weight to the argument that objective analysis could be an invaluable tool in the monitoring of progression of ocular pathology, such as corneal abrasions or ulcers.

The difference found in the RCE averages was 0.005 for bulbar redness and 0.02 for palpebral redness. This equates to 0.08 CCLRU or 0.13 Efron scale units for bulbar hyperaemia, and 0.57 CCLRU or 0.88 Efron scale units for palpebral redness over the 10 hour period. Chapter 4 determined that ECPs could distinguish between 0.3 units of an Efron scale hence the changes detected for the bulbar conjunctiva are too small to be reported by clinicians. However, if it is presumed that the ECP sensitivity measured for bulbar hyperaemia may be used in comparison with other surfaces of the anterior eye, then the changes in palpebral redness are certainly within these limits. A change of 0.88 Efron scale units is close to 1 grading scale unit, and in accordance with clinical practice is therefore approaching a significant clinical change between a patient examined in the morning verses one in the evening. [18] It is therefore vital that a correction be made to the grade derived from the formula if the estimation of 'normality' it to be accurate.

If images had been captured hourly for the 30 subjects, a regression plot would have offered a calculation for the changes in time. Since the data offers 3 values only, an estimation of the change per hour is the appropriate course: The correction factors required are displayed in Table 7.3

TABLE 7.3: Hourly correction factors to be added to the formulated grades determined by objective analysis.

	BULBAR HYPEREMIA		PALPEBRAL REDNESS	
TIME	CCLRU	EFRON	CCLRU	EFRON
8.30	8.30	-0.05	-0.18	-0.45
9.30	9.30	-0.04	-0.15	-0.36
10.30	10.30	-0.03	-0.11	-0.27
11.30	11.30	-0.02	-0.07	-0.18
12.30	12.30	-0.01	-0.04	-0.09
13.30	13.30	0.00	0.00	0.00
14.30	14.30	0.03	0.02	0.05
15.30	15.30	0.05	0.04	0.10
16.30	16.30	0.08	0.07	0.15
17.30	17.30	0.11	0.09	0.20
18.30	18.30	0.14	0.11	0.25

Worked example:

A 29 year old female attended for a routine contact-lens after-care at 4.30pm. She had no complaints regarding her comfort or acuity.

The clinician captured images of her anterior ocular surfaces, with a 1.3 mega-pixel camera of resolution 1280x1024 pixels, and compresses the resulting images into 100% JPEG format. Images of the palpebral conjunctiva and cornea were taken after the instillation of the minimum quantity of fluorescein (via fluoret) into the lower conjunctival sac. 'Fluoro-enhance' blue' illumination was applied from the Takagi SM-70 slit-lamp and the latest barrier filter held over the observation system back.

The Clinician preferred the Efron scale; hence interpretation was related to the Efron objective grading equivalent formulae. A correction factor was added to the objective grades of the bulbar hyperaemia (+0.066) and palpebral redness (+0.141).

Objective grading with correction determined values of 2.41 for bulbar hyperaemia, 2.45 for palpebral redness, and 0.86 corneal staining.

These measures were consistent with the baseline normal values for her age group. $p>0.05$.

CHAPTER 8

CONTRALATERAL CONTACT LENS TRIAL USING OBJECTIVE IMAGE ANALYSIS

8.1 INTRODUCTION

Dryness is acknowledged as the most common complaint of the contact lens wearer and is a significant problem within that population. [113] Over 70% of wearers report dryness symptoms late in the day, [114] and up to 35% of these suffer enough discomfort to cause permanent cessation of wear. [115]

Contact lens associated dryness is a difficult complaint to quantify, partly due to the patient specific nature of the reported symptoms, and due to the lack of correlation between severity of patient symptoms and ophthalmic signs. [116] There are a variety of factors that are involved in the creation and propagation of 'dry eye' symptoms in the contact lens wearing population, including lens materials, thickness, water content, coatings and care solutions. [117-119] These variables can be controlled to some extent by the clinician, who may try alternatives to improve patient comfort and compliance. Other factors which are not so easily altered are those which affect the tear-film – such as environment and physiological variety. [120]

The tear film consists of a delicate balance between aqueous, mucin and lipid constituents. It is widely acknowledged that the presence of a contact lens causes instability in the tear film which can lead to discomfort and reduction in wear time. [113, 116, 121, 122] It has been suggested that this is due to the lens causing lipid and mucin abnormalities, increasing evaporation which subsequently causes symptoms of dryness. [123-125]

The symptoms reported include itchy, grittiness and sore, often hot, eyes. [126] These can be relieved by the use of artificial tears, which cool the eye on contact and lubricate the contact lens, reducing the friction between the lid interactions and washing out any foreign bodies. [127] A common constituent of these drops is polyvinyl alcohol (PVA) which is found in comfort drops such as Blink, Hypotears, Refresh, SnoTears and Liquifilm tears. These drops are considered to be appropriate for use for mild to moderate dry eye. The PVA component is approximately 1% of the solution. Other ingredients may include polyethylene glycol 400 (1%), lipiden (a vehicle), dextrose, edetate disodium, purified water and also benzalkonium chloride (0.1 Mg/ml) as preservative. PVA is credited with having a stabilising effect on the tear film, increasing its persistence and reducing evaporation. [128] The use of artificial tears can improve contact lens wear time and reduce ocular signs of dryness such as staining and redness. [127] PVA has been used in contact lens materials for some time and has been shown to increase

properties such as tensile strength and elongation at break in comparison to other materials such as hydroxyethyl methacrylate (HEMA), it also reduces protein absorption. [129, 130]

The contact lens material nelfilcon A is created by polymerising partially acetalized PVA with N-formylmethyl acrylamide. This polymer forms 31% of the finished contact lens and is referred to as 'functionalised' as the PVA is bound in the matrix as a functional part of the lens (8.9% water content). The nelfilcon A manufacturing process utilises patented 'LightStream™ Technology' to activate this polymerisation. During the 'LightStream™' process, there can be a deliberate incorporation of non-functionalised PVA (extra, non-bound carefully selected molecular weight PVA), which will remain free in the lens matrix after lens formation. Some PVA, approximately 2%, is therefore unattached to the lens and uniformly distributed through its matrix. This wetting agent is then released slowly into the tear film (assisted by the mechanical effect of blinking and could assist in maintaining tear stability and patient comfort. [131] This deliberate release, and subsequent moisturising effect that occurs as a result, has been termed 'AquaRelease™'.

The average duration of wear has been reported to be around 13-14 hours a day, with a standard deviation of about 4 hours a day. [114, 132] The wide variation is probably due to 'social' wears for perhaps 4 hours twice a week compared to 'dependant' wear from perhaps 7am on waking, until 11pm (16 hours). Patients report finding their lenses comfortable for about 1 hour less than the wearing time, and this seems to be a factor influencing wearing time proportionately. [132] Interestingly, a recent paper reported that previous contact lens wearers who wore lenses on a daily basis had more symptoms of dryness than those who previously wore lenses on an extended wear basis, suggesting that many of these would have been unsuitable for extended wear and require lenses that enhance comfort over long wearing times. [133] In 1993 the CCLRU published standards for successful soft contact lens wear which contained a recommended wear time of 12 hours for 6 days a week (non-overnight wear). [129] There have been many advances in materials since that publication, but no further standards appear to have been suggested in the literature. Recently there have been two studies published which examine contact lens wearers who have an average wear time of 12-18 hours, [113, 116] but to our knowledge, no previous studies have performed a systematic assessment of lens performance after wearing times greater than 12 hours.

8.1 PURPOSE

To test the hypothesis that AquaRelease contact lenses offer wearers improved end-of-day comfort, and to monitor the effect of contact lenses over 16 hours wear time. This study gives the opportunity to include objective image analysis in addition to subjective grading in order to evaluate the effect of potential sustained PVA release from a contact lens.

8.3 METHODS

Both the pilot and full studies described here were carried out by the same optometrist who performed the data collection and analysis throughout this thesis.

8.3.1 Pilot study

An initial pilot study examined the effect of adding non-functionalized PVA to nelfilcon A (AquaRelease). 5 subjects were recruited for this initial study (31.2 ± 4.5 years; 3 male). Exclusion criteria included any ocular medication, ocular injury or surgery within the last twelve weeks, no pre-existing ocular irritation or displayed evidence of systemic or ocular abnormality, infection or disease likely to affect successful wear of contact lenses. The subjects were all regular contact lens wearers. Informed consent to take part in the study was received from all subjects. The study was approved by the Human Sciences Ethical Committee and conformed to the Declaration of Helsinki.

One eye, randomly selected, from each of the 5 subjects was fitted with a conventional nelfilcon A contact lens, and the other eye was fitted with the AquaRelease lenses, for a total of 16 hours daily wear. Both lenses were CE marked. The investigators were masked throughout the study, but due to the loss of sterility that would result in re-packaging, the study was open label. Measures were taken of the subjective comfort on a scale of 0 (extreme discomfort) to 100 (unaware of lens presence), and Non-Invasive Tear Break-Up Time (NITBUT) using a Tearscope Plus (Keeler Ltd, Windsor UK). These questions and measurements were taken at 6 time points throughout the day, after 6, 8, 10, 12, 14 and 16 hours of wear.

8.3.2 Nelfilcon A with AquaRelease versus ocufilcon B study

Using the same exclusion criteria from the pilot study 34 subjects were enrolled on a subsequent contralateral, investigator masked, open label, prospective 1 week evaluation. The sample size calculation was based on paired t-test (normal approximation), 2-sided, at α=0.05. Using the variances calculated from the pilot data, the study was powered to detect a 1.5 s difference in tear film stability (NIBUT) with 28 completing subjects. To allow for drop-outs and potential non-fitting lenses, 34 subjects were enrolled. One eye, randomly selected, of 34 subjects (average age 21.3 ± 2.6 years; 10 male) was fitted with AquaRelease contact lenses and the other with the ocufilcon B lenses worn on a daily disposable basis for 16 hours wear. Lens parameters are displayed in Table 1. Informed consent to take part in the study was received from all subjects.

TABLE 8.1: Details of the contact lenses trialled.

Commercial name	OSI Biomedics 1-Day	CIBA Vision Focus Dailies
Material	ocufilcon B	nelfilcon A with additional 2% nonfunctionalized PVA.
Water content	55 %	67 %
FDA material group	IV	II
Base curve	8.7	8.6
Diameter	14.2 mm	13.8 mm
Storage solution	Sterile buffered saline	Sterile buffered saline

Initial assessment consisted of a baseline visit at which the following measures were taken:

- Autorefraction and autokeratometry (Topcon KR.7500 Autokerato refractometer, Tokyo, Japan)
- Distance visual acuity was measured (Bailey-Lovie logMAR chart, NVRI, Melbourne, Australia)
- Full slit-lamp examination was conducted with the CCLRU grading scale (CCLRU, Sydney, Australia) [129] utilised to grade the bulbar redness, limbal redness, palpebral redness and epithelial staining;
- NIBUT (average of three readings of first grid distortion from blink) was assessed using the Tearscope Plus with inserted grid.

The lenses were then inserted and allowed to settle for 15 minutes. The fit was evaluated

- Centration on a 4 point scale (between 1 (optimal) and 4 (corneal exposure)) and the
- Movement on a 5 point scale (between -2 (very loose) and +2 (very flat) with 0 = optimum fit).
- Comfort of each lens was then rated by the subject on a 10 point scale. (0 = must remove, 10 = no awareness of lens).

Half way through the week of 16 hour daily wear, three assessments were made at 8, 12 and 16 hours with the lens in situ. On each of these three visits, measurements were taken in strict order to reduce the effect of extra illumination on aspects such as the tear film.

- Visual acuity was measured with a LogMar chart at 3m.
- Slit lamp image capture with a JAI C-S2300 digital slit lamp camera (resolution of 767x569 pixels) was conducted firstly of the tear meniscus (3x images), then the limbal and bulbar areas. The limbal and bulbar redness were graded using the CCLRU scale as previously.
- Average NIBUT was recorded from three readings
- Subjective rating the comfort of each lens at each visit (again on the 0-10 scale).

Objective image analysis grading was carried out on an area of 6.82x5.68mm on the nasal and temporal bulbar conjunctiva using purpose-written LabView software. The method used was consistent with the previous chapters and is outlined in Table 5.1. ED and RCE techniques were utilised. [35]

The three images of the tear-meniscus height were captured at 40x magnification. LabView programming was used to measure average tear meniscus heights (with 1 pixel relating to 0.006 mm) from the line of reflection along the top of the tear prism, to the very first visible edge of the eyelid.

The final visit occurred one week after the initial dispense. At this time, a repeat of all of the baseline measures was undertaken, with the addition of an extensive subjective questionnaire into the comfort, clarity of vision and overall preference between the lenses that were worn in each eye.

Analysis of variance was used to assess differences between the lenses with time. T-tests were used to assess differences in parametric variables such as NIBUT and sign tests used to assess differences in non-parametric variables such as subjective ratings of comfort. All subjects in the pilot and main study successfully completed the wearing schedule of 16 hours each day for the entire trial period.

8.4 RESULTS

8.4.1 Pilot Study

Data from the subjective ratings of lens comfort over the 16 hours period were consistently higher for the eye wearing AquaRelease than the conventional nelfilcon A lenses (92.67 ± 5.32 vs 69.33 ± 4.50; $F = 39.83$, $p<0.01$; Figure 8.1A). NIBUT was greater with AquaRelease than the conventional nelfilcon A lenses (16.0 ± 5.81 s vs 10.25 ± 3.0 s; $F = 7.38$, $p<0.05$; Figure 8.1B).

FIGURE 8.1: Pilot study A) comfort rating and B) Non-invasive tear break-up time nelfilcon A with AquaRelease compared to conventional nelfilcon A contact lenses. n=5. Error bars = ±1S.D.

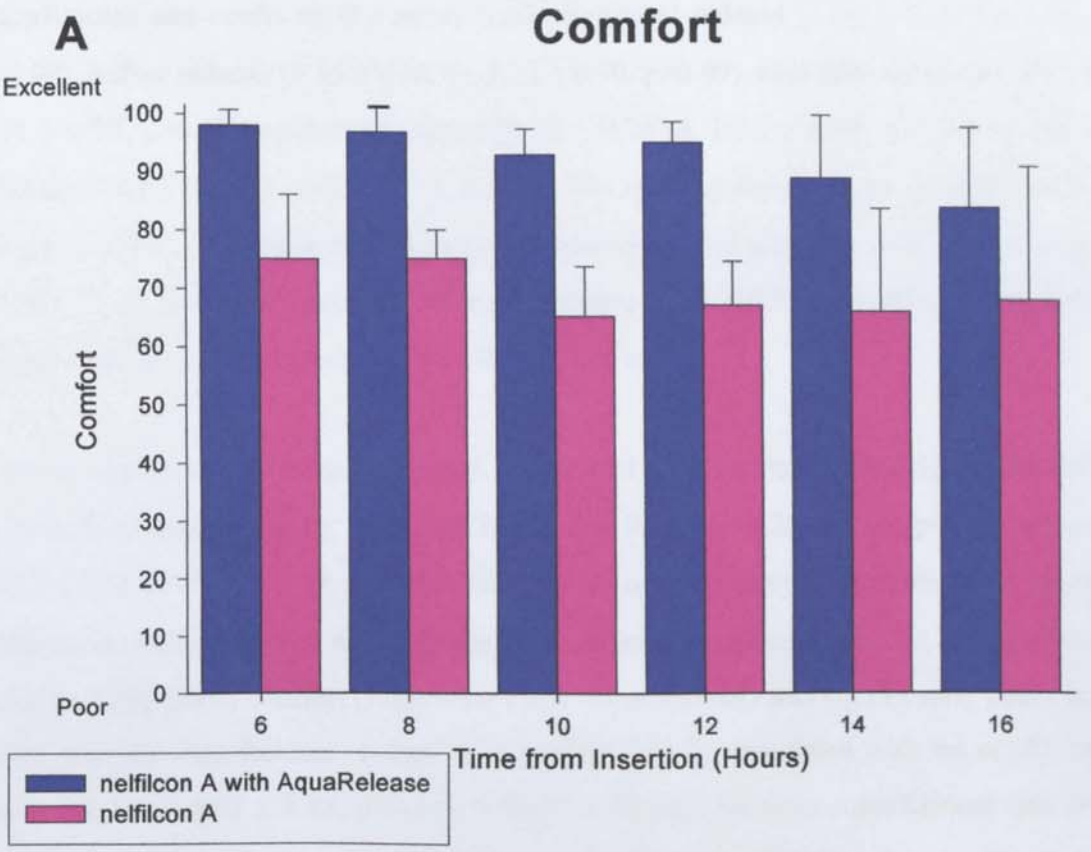

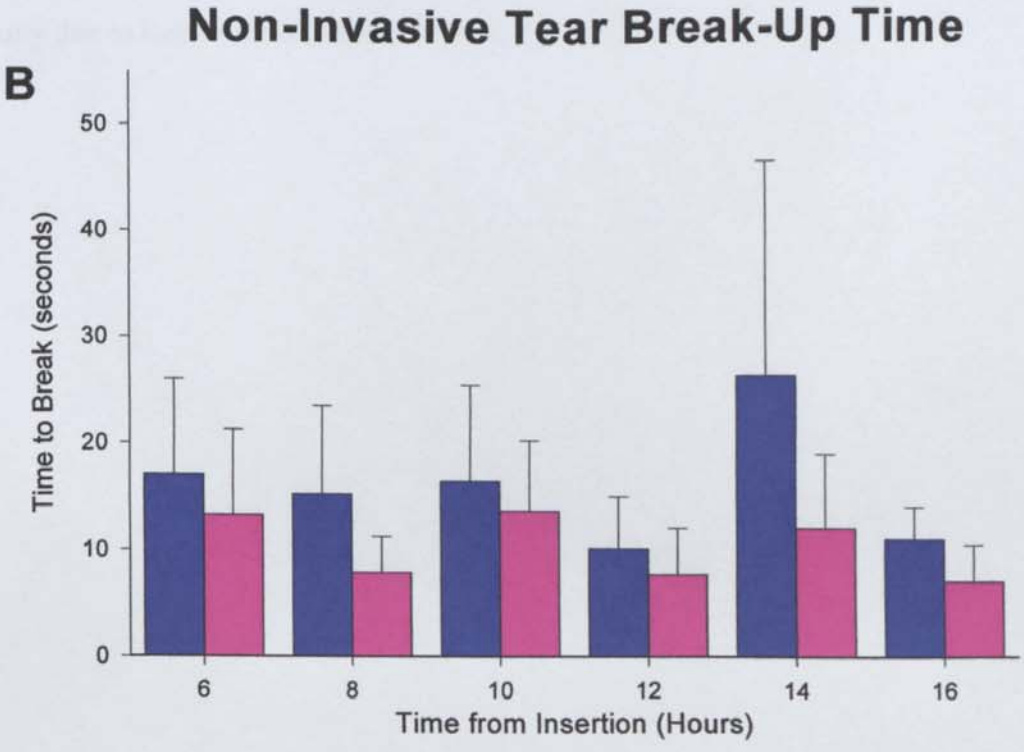

8.4.2 Nelfilcon A with AquaRelease versus ocufilcon B study

8.4.2.1 Initial Visit

Prior to lens wear there was no significant difference between the eyes subsequently fitted with AquaRelease and ocufilcon B contact lenses in limbal redness (1.03 ± 0.63 vs. 1.06 ± 0.66, p>0.99), bulbar redness (1.15 ± 0.66 vs. 1.15 ± 0.70, p>0.99), palpebral redness (0.88 ± 0.73 vs. 0.91 ± 0.75, p=0.57), epithelial staining (0.38 ± 0.74 vs. 0.38 ± 0.70, p>0.99) or conjunctival staining (0.68 ± 0.73 vs. 0.65 ± 0.73, p>0.99). No eye had any evidence of infiltrates. One eye (fitted with the ocufilcon lens) had an old peripheral corneal scar. The average prescription was –3.00 ± 1.56 D and the average corneal curvature 7.72 ± 0.25 mm. The average difference between the two corneal meridians was 0.16 ± 0.10 mm.

Once the lenses had been inserted, there were found to be no statistically significant differences in lens fit (AquaRelease vs. ocufilcon B; -0.18 ± 0.67 vs. -0.24 ± 0.65, p=0.78) or centration (0.12 ± 0.33 vs -0.09 ± 0.29, p>0.99) with no cases of an unacceptable fit observed. Initial visual acuity was similar between AquaRelease and ocufilcon B contact lenses (-0.12 ± 0.17 vs -0.12 ± 0.12, p=0.75). Initial comfort (scale 0-10 where 10 is the best) was significantly better in the eye fitted with the AquaRelease contact lens compared to the eye fitted with the ocufilcon B lens (8.94 ± 1.18 vs 8.03 ± 1.88, p=0.01). NIBUT difference between AquaRelease lens fitted eye (11.65 ± 15.64s) and the ocufilcon B fitted eye (8.35 ± 6.79s) was not significant (p=0.26), essentially due to large inter and between-subject variability.

8.4.2.2 Assessment over 16 Hours of Lens Wear

A within-subject multivariate ANOVA (time [8 hrs, 12 hrs, and 16 hrs] and contact lens [AquaRelease and ocufilcon B]) was performed on the variable assessed mid-wear period. Subjective comfort decreased with time ($F=17.28$, $p<0.001$), but there was no significant difference between the AquaRelease and ocufilcon B lens ($F=2.09$, $p=0.16$; Figure 8.2). NIBUT was not significantly affected by time ($F=0.58$, $p=0.56$) or between the eye wearing the AquaRelease and ocufilcon B lens ($F=0.99$, $p=0.33$; Figure 8.3). Subjectively graded limbal redness was not significantly affected by time ($F=2.62$, $p=0.09$) or between the eye wearing the AquaRelease and ocufilcon B lens ($F=0.81$, $p=0.37$; Figure 8.4A). Bulbar redness approached a significant increase with time ($F=3.01$, $p=0.06$), but there was no significant difference on subjective grading between the AquaRelease and ocufilcon B lens ($F=0.02$, $p=0.90$; Figure 8.4B).

FIGURE 8.4: Subjective CCLRU Scale grade of A) limbal and B) bulbar hyperaemia with time for the nelfilcon A with AquaRelease compared to ocufilcon B contact lenses. n=34. Error bars = ±1S.D.

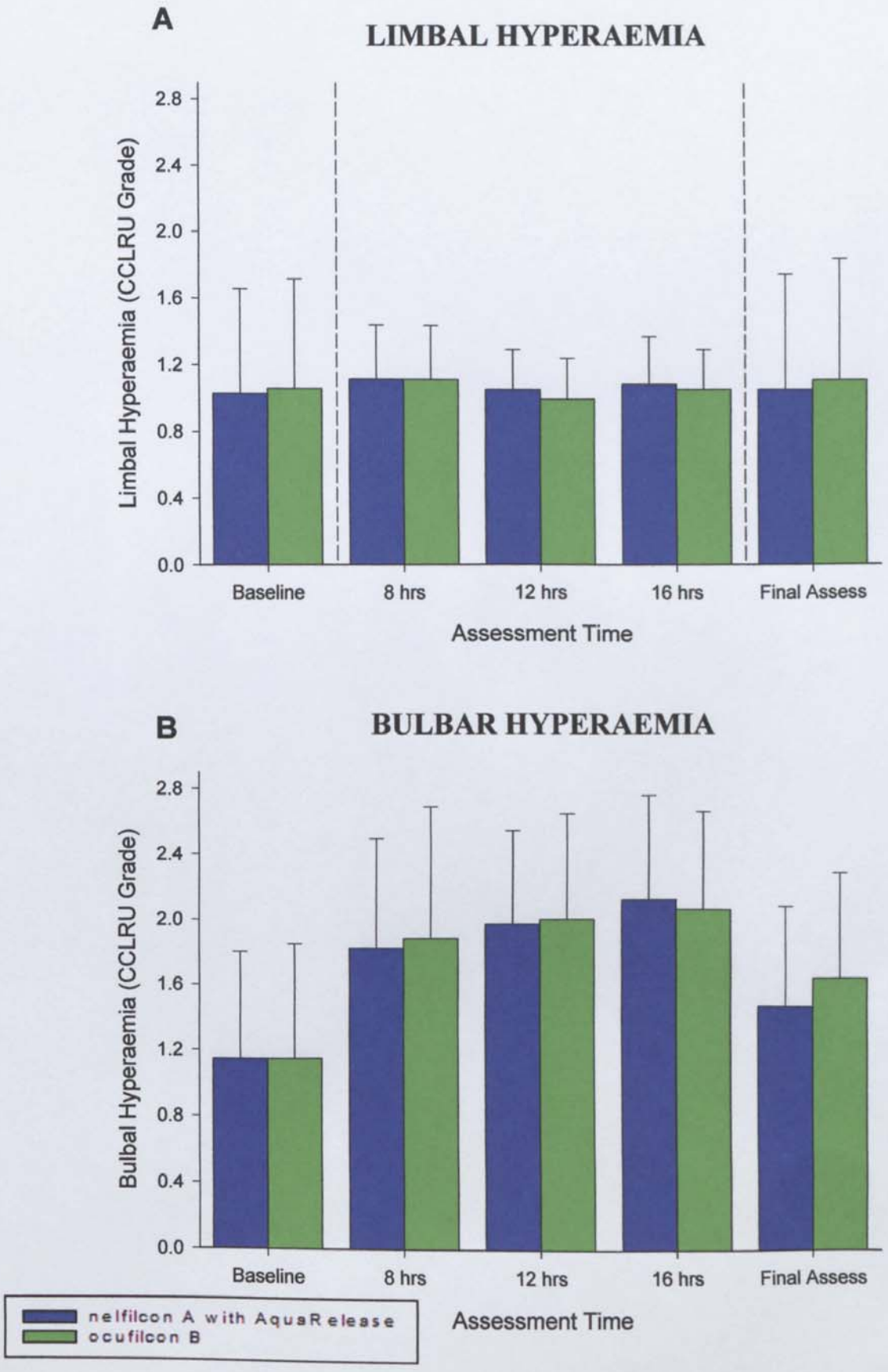

FIGURE 8.3: Comfort rating with time for the nelfilcon A with AquaRelease compared to ocufilcon B contact lenses. n=34. Error bars = ±1S.D.

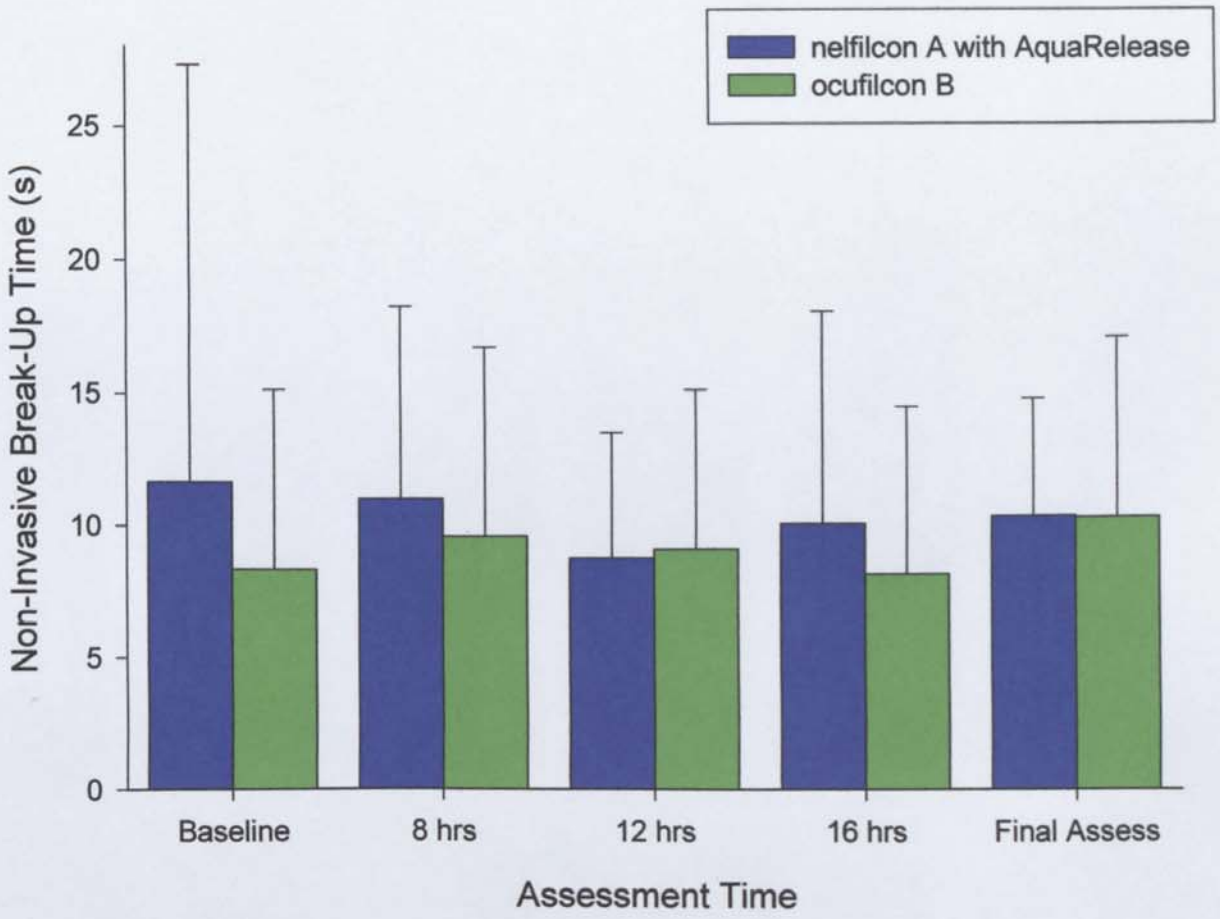

FIGURE 8.2: Comfort rating with time for the nelfilcon A with AquaRelease compared to ocufilcon B contact lenses. n=34. Error bars = ±1S.D.

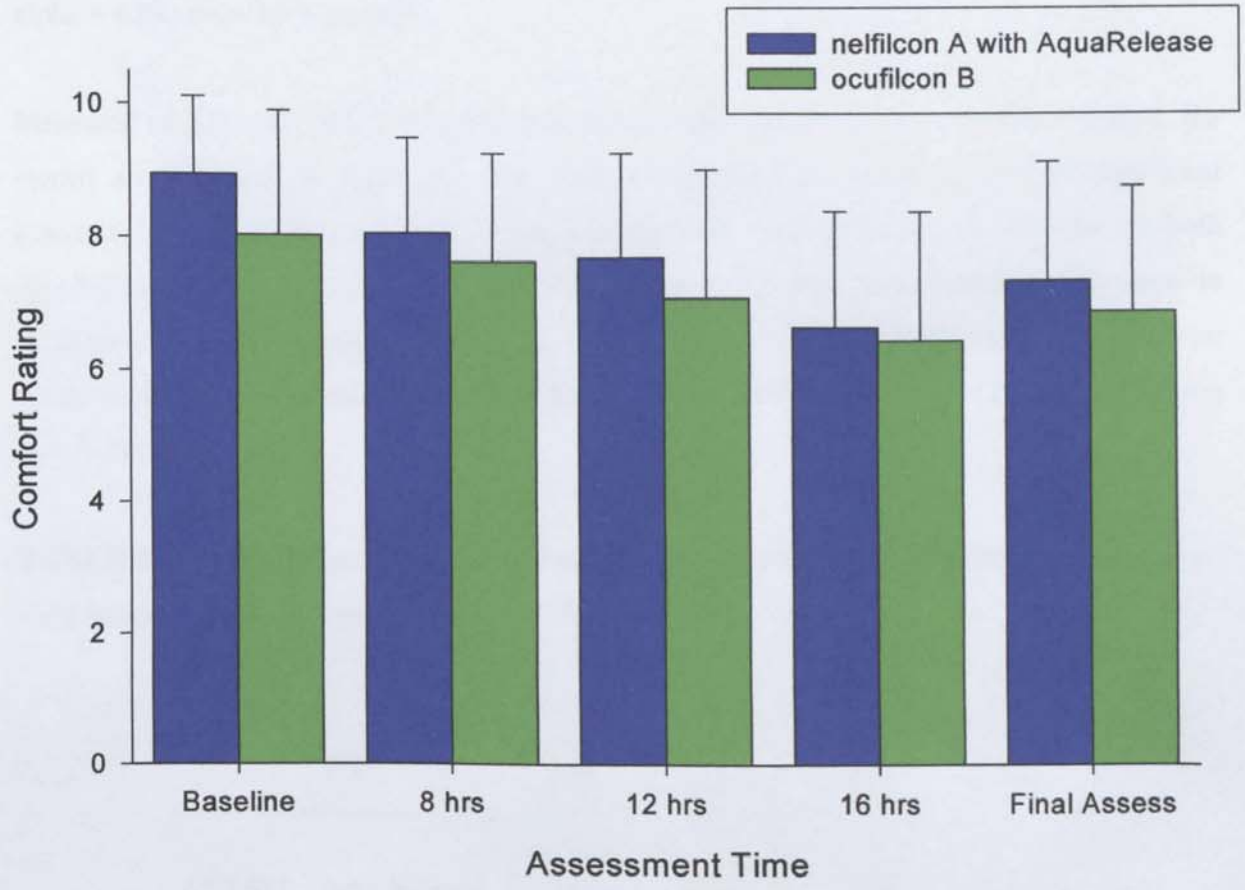

Objective grading of bulbar hyperaemia showed no difference in edge detection with time ($F=1.80$, $p=0.17$) or between the lenses ($F=0.44$, $p=0.55$; Figure 8.5A). Objective relative redness of the conjunctiva, however, showed an increase with time for both lens types ($F = 9.87$, $p < 0.005$), but there was no difference between the lenses themselves ($F = 1.76$, $p = 0.19$; Figure 8.5B). Tear meniscus height did not significantly change with time ($F=1.4$, $p=0.27$) or between the lenses ($F = 3.29$, $p = 0.08$; Figure 8.5C). Repeatability was found to be high (Cronbach's alpha = 0.94) over the 3 measures.

Measures of ED and RCE for bulbar hyperaemia were converted into objective grades, the results are displayed in Table 8.2. The objective grades were found to indicate significant differences between the measures of hyperaemia with the two lenses ($p = 0.006$ for both CCLRU and Efron equivalents). Repeated measures ANOVA determined a difference in hyperaemia over the duration of the study. ($F = 52.34$, $p = 0.007$). Significant differences were found between all time points (Tukey: $p<0.001$) except between the 8 and 12 hour comparison ($p = 0.23$).

TABLE 8.2: Objective grades of bulbar hyperaemia for eyes which wore the Nelfilcon A lens with AquaRelease™ in comparison to the Ocufilcon B.

Scale	Lens	OBJECTIVE GRADE			
		8 hrs	12 hrs	16hrs	1 week
CCLRU	AquaRelease	2.54	2.52	2.58	2.47
CCLRU	Ocufilcon B	2.56	2.54	2.62	2.49
Efron	AquaRelease	1.48	1.45	1.55	1.38
Efron	Ocufilcon B	1.52	1.50	1.60	1.40

FIGURE 8.5: Objective grading of A) conjunctival blood vessel edges, B) relative redness and C) tear meniscus height with time for the nelfilcon A with AquaRelease compared to ocufilcon B contact lenses. n=34. Error bars = ±1S.D

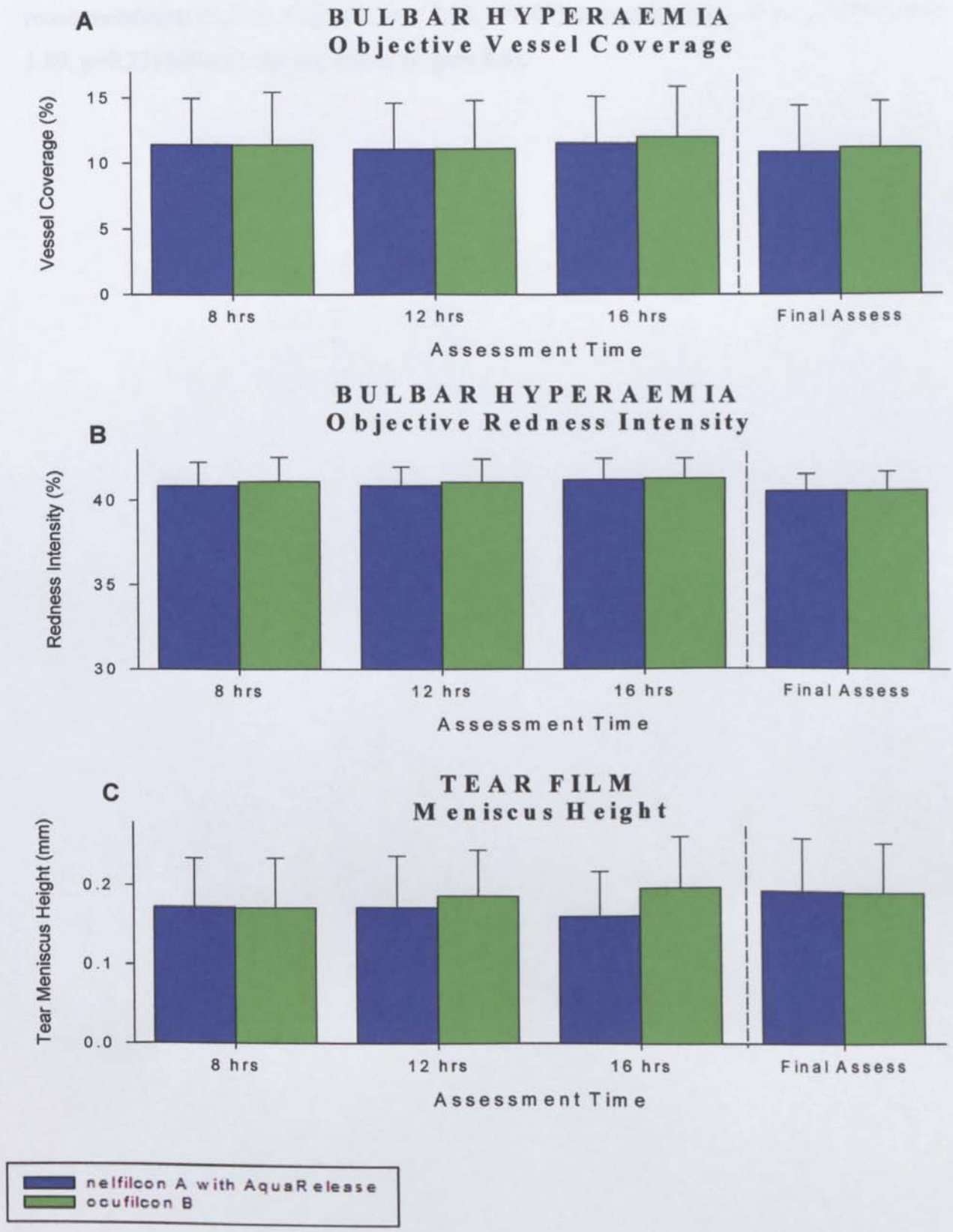

8.4.2.3 Final Assessment

Lenses had been worn for between 0.50 and 3.00 hours at the final assessment. The initial comfort of the AquaRelease contact lens was rated as significantly higher than the ocufilcon B lens (7.76 ± 1.78 vs 6.82 ± 2.05, p=0.03), but there were no statistically significant difference in rated end of day comfort (6.68 ± 2.18 vs 6.53 ± 2.08, p=0.76), strength of recommendation (7.35 ± 2.23 vs 6.44 ± 2.12, p=0.09) or overall rating (7.32 ± 1.79 vs 6.85 ± 1.89, p=0.27) between the two lenses (Figure 8.6).

FIGURE 8.6: Subjective rating of the nelfilcon A with AquaRelease compared to the ocufilcon B contact lenses after 1 week of wear. n=34.

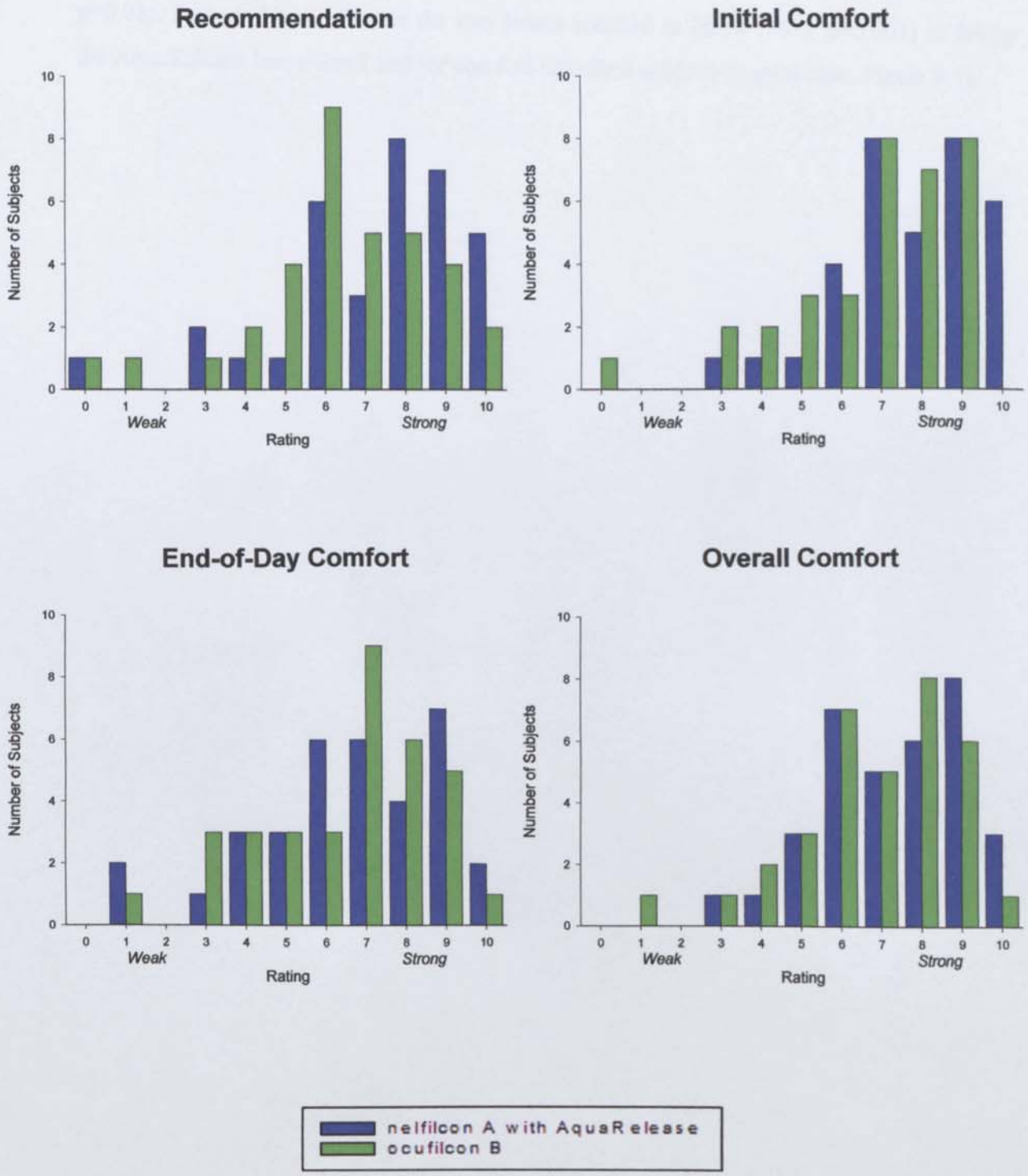

However, in a direct comparison of preference between the two lenses, initial comfort (0.76 ± 1.13, $p<0.001$ where 0 indicated no preference between the lenses, +2 an extreme preference to the AquaRelease lens and -2 an extreme preference to the ocufilcon B lens), end-of-day comfort (0.68 ± 1.09, $p=0.001$), visual acuity (0.32 ± 0.68, $p<0.01$) and overall comfort (0.65 ± 1.20, $p<0.01$) were rated as significantly better with the AquaRelease compared to the ocufilcon B lens. There was no significant difference in lens handling between the two lenses (0.32 ± 1.04, $p=0.08$). Forced choice between the two lenses resulted in 26/34 (76%; $p=0.001$) in favour of the AquaRelease lens overall and for comfort (identical subjects in each case; Figure 8.7).

FIGURE 8.7: Subjective preference for the nelfilcon A with AquaRelease compared to ocufilcon B contact lenses after 1 week of wear. n=34.

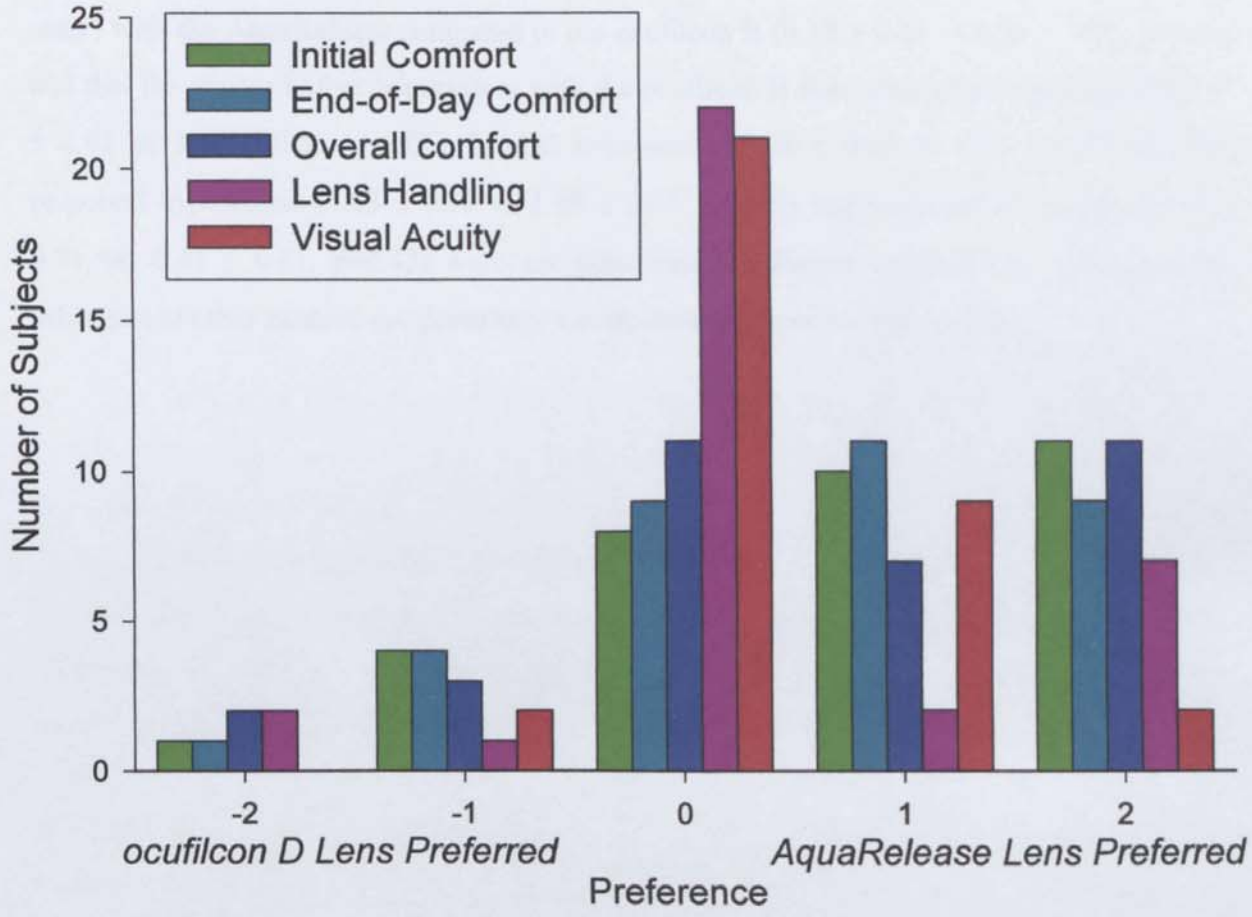

The lens fit was significantly looser with the AquaRelease compared to the ocufilcon B contact lens (-0.21 ± 0.41 vs 0.00 ± 0.00, p=0.02), but in no cases was the lens unacceptably loose. Centration was optimal in all subjects with both lenses. Visual acuity was similar in the AquaRelease and ocufilcon B lenses following a week of lens wear (-0.08 ± 0.14 vs -0.10 ± 0.12, p=0.34). The NIBUT between the AquaRelease contact lens fitted eye (10.32 ± 4.44s) and the ocufilcon B fitted eye (10.25 ± 6.80s) was not significantly different (p=0.95). Slit-lamp biomicroscopy subjective grading identified that there was less epithelial staining (CCLRU scale) with the AquaRelease compared to the ocufilcon B (0.12 ± 0.41 vs 0.29 ± 0.58, p=0.03) and that the greater bulbar hyperaemia with the ocufilcon B lens approached significance (1.47 ± 0.61 vs 1.65 ± 0.65, p=0.06). Limbal hyperaemia (1.06 ± 0.69 vs 1.12 ± 0.73, p=0.50), palpebral hyperaemia (1.03 ± 0.58 vs 1.09 ± 0.62, p=0.50) and conjunctival staining (0.53 ± 0.71 vs -0.47 ± 0.61, p=0.42) were not significantly different between the two lenses. No infiltrates or other anterior eye pathology was observed with either type of lens.

8.5 DISCUSSION

Adding non-functionalised PVA to nelfilcon A enhanced tear stability and subjective comfort over a 16 hour a day wearing period. Hence, AquaRelease lenses have the potential to alleviate end of day dryness symptoms. Although few studies present the average wearing time of contact lenses in a general population, data is consistent in suggesting this to be 13-14 hours, with a reasonable proportion of subjects limited in their wearing time due to end of day discomfort. [114, 132] Therefore a contact lens that could be worn throughout the day with no increase in discomfort is an attractive option. The subjects investigated completed 16 hours wear on each day with relative comfort (approximately 6.5 to 8.5 out of 10). The subjects were young adults and therefore the end of day comfort may be expected to be worse in an older population, [134] but none of the subjects was to remove the lenses due to discomfort at any time.

The use of a contralateral lens trial allowed the subjects other eye to act as a control and resulted in equivalent baseline conditions. However, the contralateral design may have minimised the perceived comfort differences between the two lenses and one lens may alter the blink pattern adversely affecting the other. The open-label nature of the pilot study is unlikely to have affected the subjects rating as both lenses were in currently marketed blister packaging and they were not aware of the lens which had been modified. Initial comfort was better in the eye fitted with the AquaRelease contact lens compared to the eye fitted with the ocufilcon B lens and this was reflected clinically in the tear stability, although the latter did not reach statistical significance.

As usually experienced with contact lens wear, subjective comfort decreased with time, but there was no difference between the AquaRelease and ocufilcon B lens in comfort, tear film stability (NIBUT or tear meniscus height) or subjective indicators of ocular physiology (limbal or bulbar redness) between 12 and 16 hours of wear. These results were strengthened by the objective findings, which showed that although there was a change in bulbar hyperaemia with time, there was no difference between the lenses.

NIBUT and objective tear meniscus height showed no significant changes with time or between the lenses. These measures were consistent with those reported in the literature. [121, 135, 136] Not surprisingly therefore, there was not much difference in the rating of AquaRelease contact lens compared to ocufilcon B lens except in initial comfort on lens insertion. Despite this, in a direct comparison of preference between the two lenses, end-of-day comfort, visual acuity and

overall comfort as well as initial comfort were rated as significantly better with the AquaRelease compared to the ocufilcon B lens, with 76% of subjects favouring the AquaRelease lens material overall and for comfort.

The enhanced comfort of the AquaRelease over the ocufilcon B contact lens suggests that the release of non-functionalised PVA is sustained over at least a 16 hour period. Although there is an obvious peak at 14 hours of lens wear which might possibly suggest a second burst of PVA release in the pilot study (consistent with ex-vivo material analysis), this was not evident in the main study, perhaps due to the greater separation between measurements.

In conclusion, subjects preferred the nelfilcon A with AquaRelease™, especially for initial comfort. Objective image analysis showed a significant increase in bulbar redness later in the day ($p < 0.005$), which only approached significance with subjective grading ($p = 0.06$). It also identified this to be due to a change in background redness rather than an expansion / extension in bulbar vasculature.

A follow-up study of longer duration and including tear sampling at regular internals throughout a 16 hour wearing day is warranted to further examine the in-vivo release of PVA into the tears and coating of the lens, together with its effects on comfortable, healthy eye, contact lens wear. It would also be essential to complete the full study on the lenses used in the pilot and other market leaders before absolute conclusions regarding the nature and benefits of this lens are confirmed.

CHAPTER 9

OBJECTIVE COMPARISON OF PATHOLOGICAL CONDITIONS TO BASELINE NORMAL EYES

9.1 INTRODUCTION

In the previous chapters the sensitivity and reliability of the LabView technique was established. It was then utilised to ascertain the healthy/normal population baseline measures that would form the basis for comparison, against general or suspicious ocular surface changes. The previous chapter proved that the technology can be used as part of a clinical study as a valuable research tool. At this point it is now fitting to verify the ability of the programme to identify pathological conditions.

There are two areas in which the objective measures could be utilised in clinical or research environments. The first is in the early detection and diagnosis of an anterior ocular pathology, or the monitoring of the progression/ resolution of a condition.

The second is in the evaluation/re-evaluation of the direct or indirect effects of pathology on the ocular surfaces. It has been established that subjective measures which have been utilised in the past for ocular examination do not have a high level of accuracy or reliability that can be achieved by objective image analysis grading. Therefore more subtle changes in the ocular surfaces with pathology could be detected, assisting in a greater understanding of the disease process than has previously been possible.

Situation 1 involves detection, diagnosis and monitoring of an anterior ocular condition. Anterior uveitis, or iritis is one of the most common serious anterior ocular conditions, the reported prevalence varies from between 38 to 714 cases per 100,000 of the population [137] and it accounts for up to 92% of all uveitis cases. [138] Iritis can become a recurrent problem for many patients of whom up to 35% will suffer from significant visual impairment. [139]
Its clinical features include symptoms of ocular pain, periorbital ache and photophobia often with reduced visual acuity. Signs include bulbar and perilimbal hyperaemia, keratic precipitates, cells in the anterior chamber and watery discharge. Hypopyon and posterior synechiae can occur with severe inflammation. [140]

There have been many investigations into ocular changes in iritis, such as laser flare-cell photometry, intra ocular pressure, ultrasound biomicroscopy, grading of heterochromia and other features such as cells in the anterior chamber. [141-143] However no detailed grading or evaluation of the bulbar hyperaemia or any measures of palpebral changes can be found in the literature. Benezra et al examined 821 patients with ocular inflammation and although they

performed slit-lamp examination on each subject, the findings are not recorded. They did, however, report that in 15.9% the patient's 'red-eye' was the initial cause for referral. [144] Fluorescein evaluations in iritis have been limited to such investigations as fundus angiography, fluorescein clearance from the anterior chamber, and for investigation of blood-ocular barriers. [145-147] No corneal staining or palpebral roughness evaluations have been discovered in the literature.

Situation 2 involves the evaluation or re-evaluation of the eye with pathological conditions that may have a direct or indirect effect on the ocular surfaces. keratoconus is one such condition that may affect the anterior ocular surfaces other than the corneal layers, but has not been investigated by objective analysis in this manner previously. The term keratoconus was first coined in 1869 by Johann Horner, 14 years after its first description by Nottingham who distinguished it from other corneal ectasias. [148, 149] Keratoconus is a non-inflammatory corneal condition [150, 151] that is acquired usually in adolescence and is characterised by progressive, changeable and often binocular, myopic astigmatism. [152] Measurements of Keratoconic eyes have previously concentrated on the corneal scarring which occurs in 43-53 % of sufferers, [153, 154] stromal thinning, curvature of the posterior and anterior corneal surfaces. Even the articles on 'baseline' measures relate changes in corneal scarring, visual acuity, keratometry, and quality of life without reporting any other effect on the ocular surfaces. [152, 153, 155-158].

No literature that investigates differences from the normal healthy population and palpebral redness or roughness in keratoconus was found. One study by Dogru et al remarked on the difference in corneal and conjunctival staining with 38 Keratoconic subjects verses healthy normals. [151] They used a scale from 0-9 where >3 was an abnormal amount of staining. Bulbar hyperaemia has not been explored in the literature with respect to keratoconus, but a study by Yue et al (1995) did report that the "conjunctival epithelium may be involved in keratoconus" due to the increased conjunctival histochemical staining (for lysosomal enzymes) that they observed in comparison to normal subjects. [159]

9.2 PURPOSE

To examine the ocular surface characteristics of patients diagnosed with iritis and keratoconus, to determine if objective image analysis grading can differentiate between pathological and normal eyes, and determine if there are any changes in ocular surfaces with pathology that have not been previously investigated. For the subjects with iritis, it is expected that objective bulbar hyperaemia measures will be significantly different as this is a major sign of the condition. Other effects however are less well known, and therefore it will be interesting to determine if any other differences are detected. For the subjects with keratoconus the predicted findings are less clear as there has been little evaluation in the literature. Corneal staining may be affected in accordance with the report by Dogru et al [151]

9.3 METHODS

20 Patients suffering from their first onset acute anterior iritis (ages 37 ± 13.20 years, 9 male 11 female) and 14 who had been previously diagnosed with keratoconus (ages 31 ± 7.46 years, 9 male 5 female) were recruited from a Hospital based Eye-department/Eye-casualty (Queen's Medical Centre, University Hospital, Nottingham). The diagnosis of acute anterior iritis had been delivered by an ophthalmologist that day after a full examination. The severity of the condition of the subjects ranged from mild to severe. The keratoconic subjects had all been diagnosed with the condition a minimum of 1 year prior to this examination; the group recruited for this study fell into the mild-moderate range of severity. The keratoconic group were all regular RGP wearers, but had removed the lenses at least 1 hour prior to investigation.

Images were taken of the bulbar hyperaemia, palpebral redness, roughness, and corneal staining between the hours of 09.00 and 13.00 (to reduce the effects of any diurnal variation (see Chapter 7). LabView objective image analysis was then performed. Both image capture and analysis were performed by one individual only, as has been the case throughout all of the investigations in this thesis. The methods used in the image capture and analysis were consistent with previous chapters and outlined in Table 5.1.

The subjects with pathology were age-matched to normal subjects from those assessed in Chapter 6 for the purposes of statistical comparison. A two-tailed T-test comparison was conducted for each of ocular surface measures of irits and Keratoconus verses age-matched normal eyes.

Due to the number of T-tests conducted in this investigation a Bonferroni comparison could be seen to be appropriate and therefore the level that must be reached for significance would be p=0.006 for iritis and keratoconus. However, each of the ocular surface measures could be considered as individual, not part of a group and in a normal study not all these image analysis characteristics would be assessed, in which case this correction would not be required.

9.4 RESULTS

The results of the analysis are found in Table 9.1 and Figures 9.1 to 9.4. Table 9.2 displays the objective CCLRU and Efron grades calculated from the formulae in Chapter 5.

9.4.1: Iritis

Subjects with iritis were found to have a significant increase in both ED ($p = 0.014$) and RCE ($p < 0.001$) measures of bulbar hyperaemia in comparison with age-matched normals (Table 9.1). Conversion to an objective CCLRU or Efron grade showed a significant increase in bulbar hyperaemia in patients with iritis (objective CCLRU grade 3.64 ± 0.28 vs. 2.63 ± 0.34; $p <0.001$, objective Efron grade 3.21 ± 0.49 vs. 1.61 ± 0.48; $p <0.001$). See Table 9.2.

The measures of palpebral redness and roughness indicated that there was no difference between the pathological and normal groups. Differences in objective CCLRU and Efron grades also indicated no significant differences ($p>0.05$).

No significance was found between the ED or RCE measures of corneal staining of those with iritis, and normal, healthy eyes. Conversion to an objective CCLRU and Efron grades also showed no differences in corneal staining in patients with iritis ($p >0.05$).

9.4.2: Keratoconus

Differences in bulbar hyperaemia between the keratoconic and normal groups approached, but did not reach significance with original ED and RCE measures, (Table 9.1) but conversion into objective grades did show a difference between the hyperaemia of keratoconic and healthy eyes ($p<0.05$, See Table 9.2). Palpebral redness was found to be slightly higher for the normal group but again this was not significantly different with the original, or the graded values. The differences in palpebral roughness by both ED and Green RCE were found to be significant and indicate a much greater roughness in the normal group than those with the pathology ($p=0.021$ and $p=0.028$ respectively). However with conversion into an objective CCLRU grade (there being no Efron scale), the differences between these groups narrowly missed significance ($p=0.052$). See Table 9.2.

Significant differences in corneal staining were found between the pathological and normal groups, with lower RCE values, and higher total area of staining in the keratoconic group. Conversion into objective grades showed a significant increase in corneal staining in patients with keratoconus for all measures of extent and depth of staining ($p <0.05$), see Table 9.2.

TABLE 9.1: Average ± Standard Deviation and T-tests between objective measurements of the ocular surfaces of subjects with Keratoconus, Iritis, and corresponding age-matched normals.

	Objective measures	**BULBAR HYPEREMIA**		**PALPEBRAL REDNESS**		**PALPEBRAL ROUGHNESS**		**CORNEAL STAINING**		
		ED	RCE	ED	RCE	ED	RCE	ED	RCE	AREA
Iritis	Average±S.D	18.91±9.02	0.47±0.05	9.42±4.08	0.49±0.042	35.02±23.99	0.59±0.04	1.41±1.13	0.62±0.04	0.01±0.01
Age-matched normals	Average±S.D	12.45±4.96	0.41±0.01	8.78±5.16	0.50±0.04	47.04±19.77	0.60±0.03	1.37±1.74	0.65±0.03	0.01±0..02
	T-Test: p =	**0.014**	**0.000**	0.654	0.579	0.154	0.055	0.930	0.093	0.973
Keratoconic	Average±S.D	16.96±10.58	0.42±0.02	9.58±3.69	0.47±0.04	29.54±15.86	0.56±0.07	2.33±3.50	0.52±0.08	0.085±0.12
Age-matched normals	Average±S.D	10.55±3.92	0.41±0.01	10.97±3.80	0.50±0.02	48.05±18.71	0.61±0.04	1.58±1.97	0.65±0.03	0.01±0.01
	T-Test: p =	0.061	0.051	0.434	0.071	**0.021**	**0.028**	0.516	**0.000**	**0.046**

TABLE 9.2: Average ± S.D and T-test comparison between objective grades for ocular surfaces of subjects with pathological, or age-matched normal eyes.

SURFACE ANALYSED	SCALE USED	AVERAGE ± S.D EQUIVALENT GRADE					
		Iritis	**Normal**	**p**	**Keratoconus**	**Normal**	**p**
BULBAR HYPEREMIA	CCLRU	3.64±0.28	2.63±0.34	**0.00**	3.00±0.64	2.52±0.28	**0.035**
	EFRON	3.21±0.49	1.61±0.48	**0.00**	2.14±0.86	1.47±0.41	**0.031**
PALPEBRAL REDNESS	CCLRU	1.85±1.02	2.01±0.89	1.615	1.47±0.95	1.77±0.59	0.37
	EFRON	0.84±0.91	0.98±±0.79	0.496	0.50±0.85	0.78±0.52	0.34
PALPEBRAL ROUGHNESS	CCLRU	2.81±0.79	2.52±0.82	3.369	3.37±1.46	2.37±0.90	0.052
CORNEAL STAINING EXTENT	CCLRU	1.26±0.05	1.26±0.07	1.557	1.56±0.50	1.25±0.04	**0.047**
	EFRON	0.93±0.08	0.93±0.10	1.367	1.37±0.74	0.92±0.06	**0.047**
DEPTH	CCLRU	1.31±0.04	1.31±0.06	1.555	1.56±0.42	1.30±0.03	**0.047**

FIGURE 9.1: A representation of the difference between the ED objective measures of the ocular surfaces of subjects with iritis verses age-matched normals. Error bars = 1 S.D, n = 20. Significance is marked by a star.

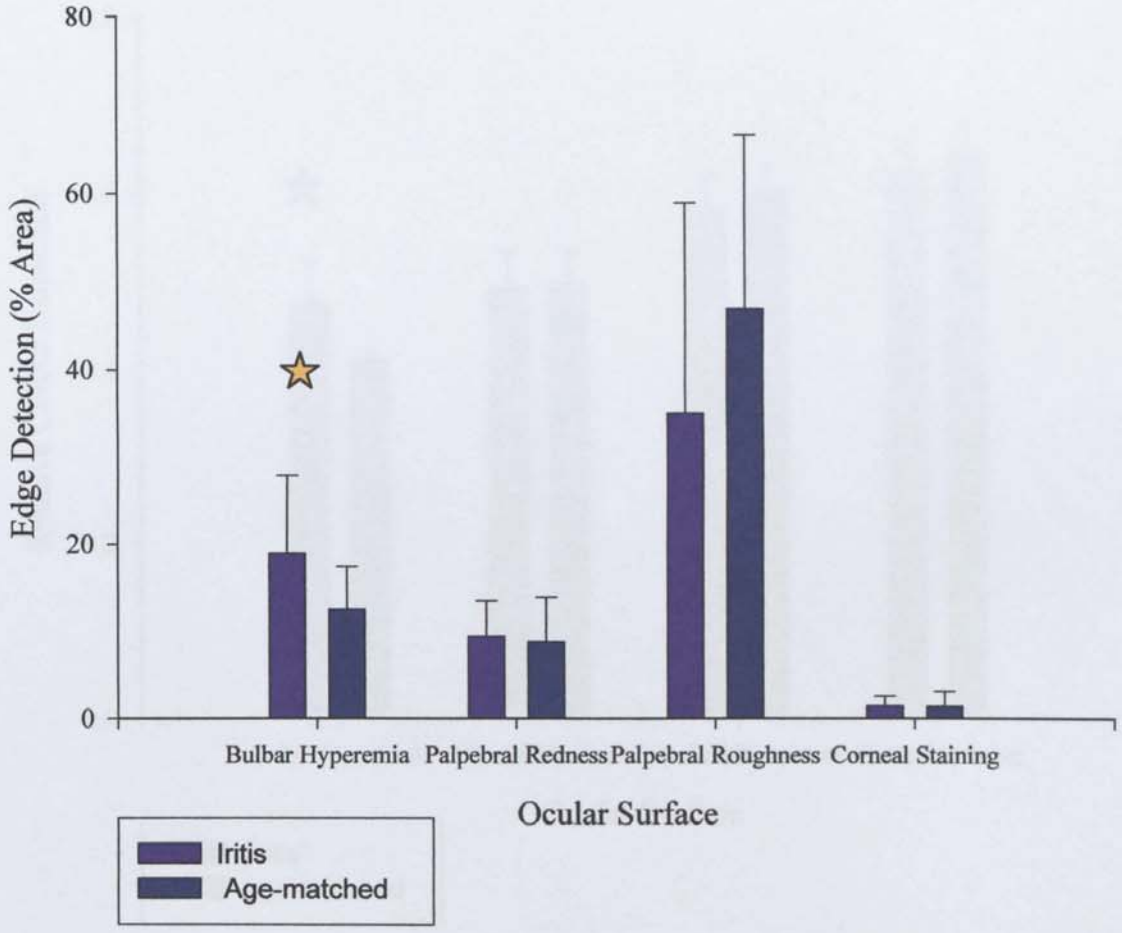

FIGURE 9.2: A representation of the difference between the RCE objective measures of the ocular surfaces of subjects with iritis verses age-matched normals. Error bars = 1 S.D, n = 20. Significance is marked by a star.

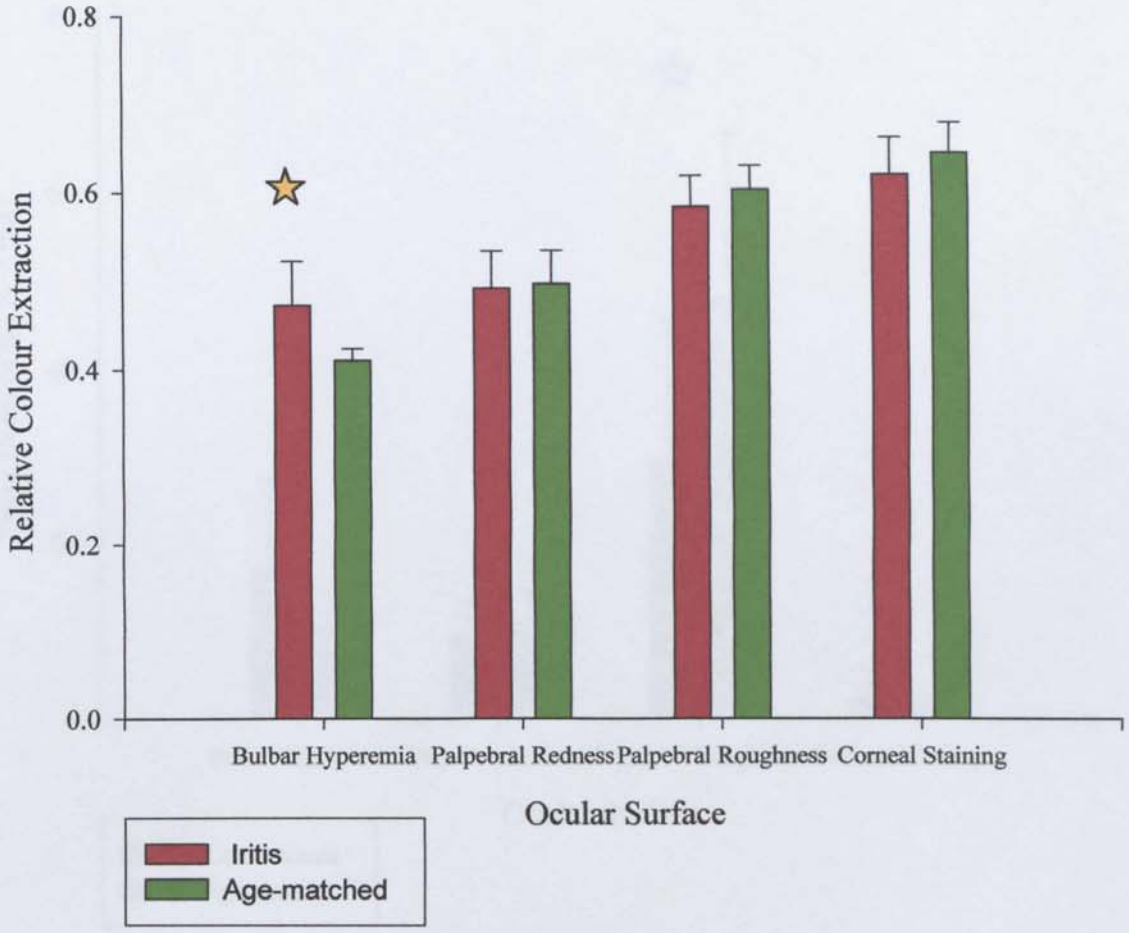

FIGURE 9.3: A representation of the difference between the ED objective measures of the ocular surfaces of Keratoconic verses age-matched normal subjects. Error bars = 1 S.D, n = 14. Significance is marked by a star.

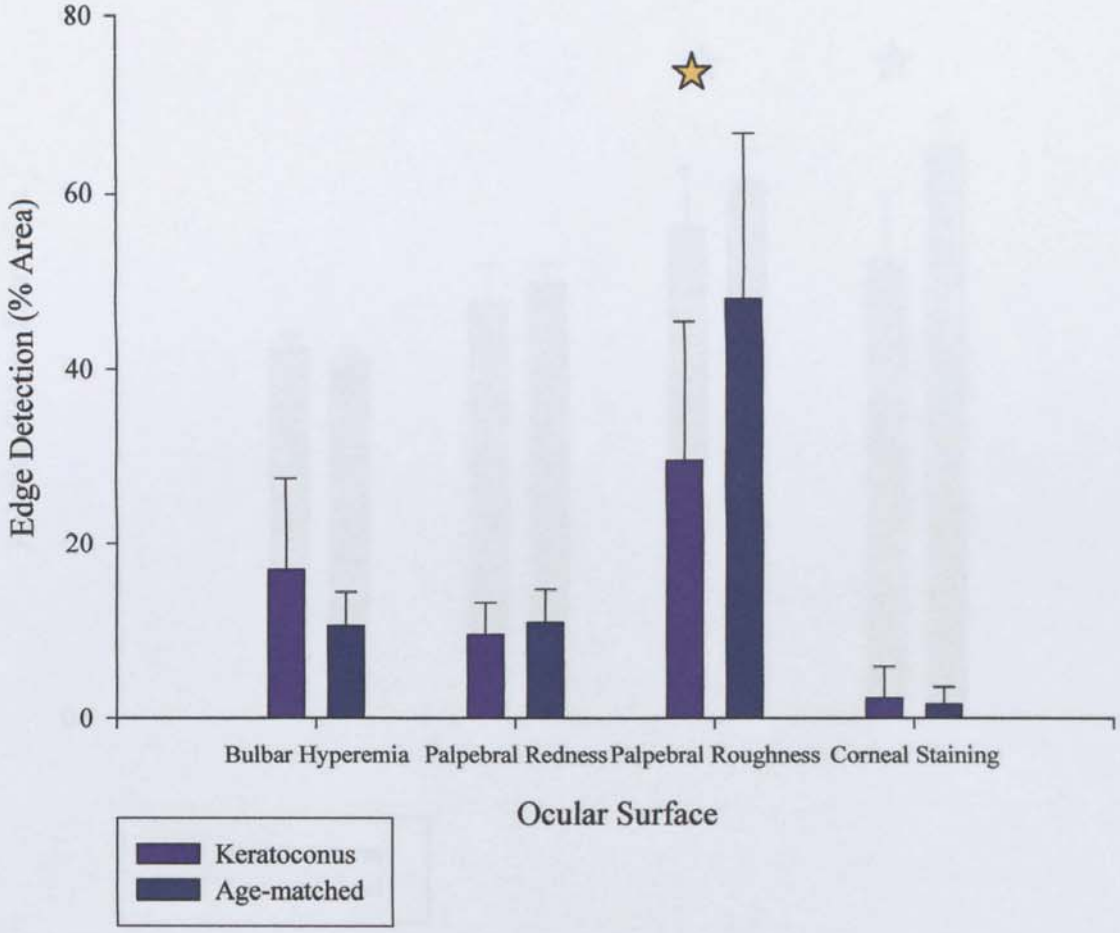

FIGURE 9.4: A representation of the difference between the RCE objective measures of the ocular surfaces of Keratoconic verses age-matched normal subjects. Error bars = 1 S.D, n = 14. Significance is marked by a star.

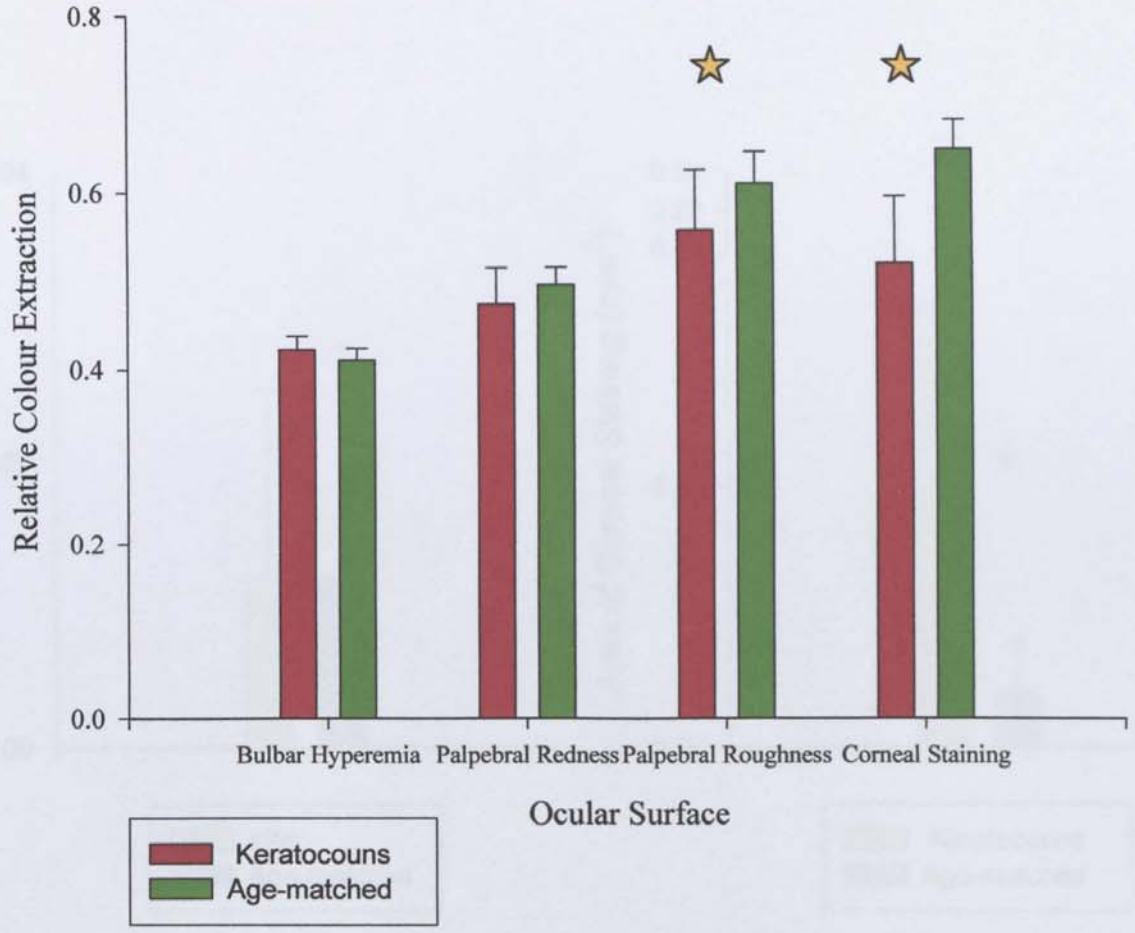

FIGURE 9.5: A representation of the difference between the Area of corneal staining for pathological verses age-matched normal corneas. Error bars = 1 S.D. Significance is marked by a star.

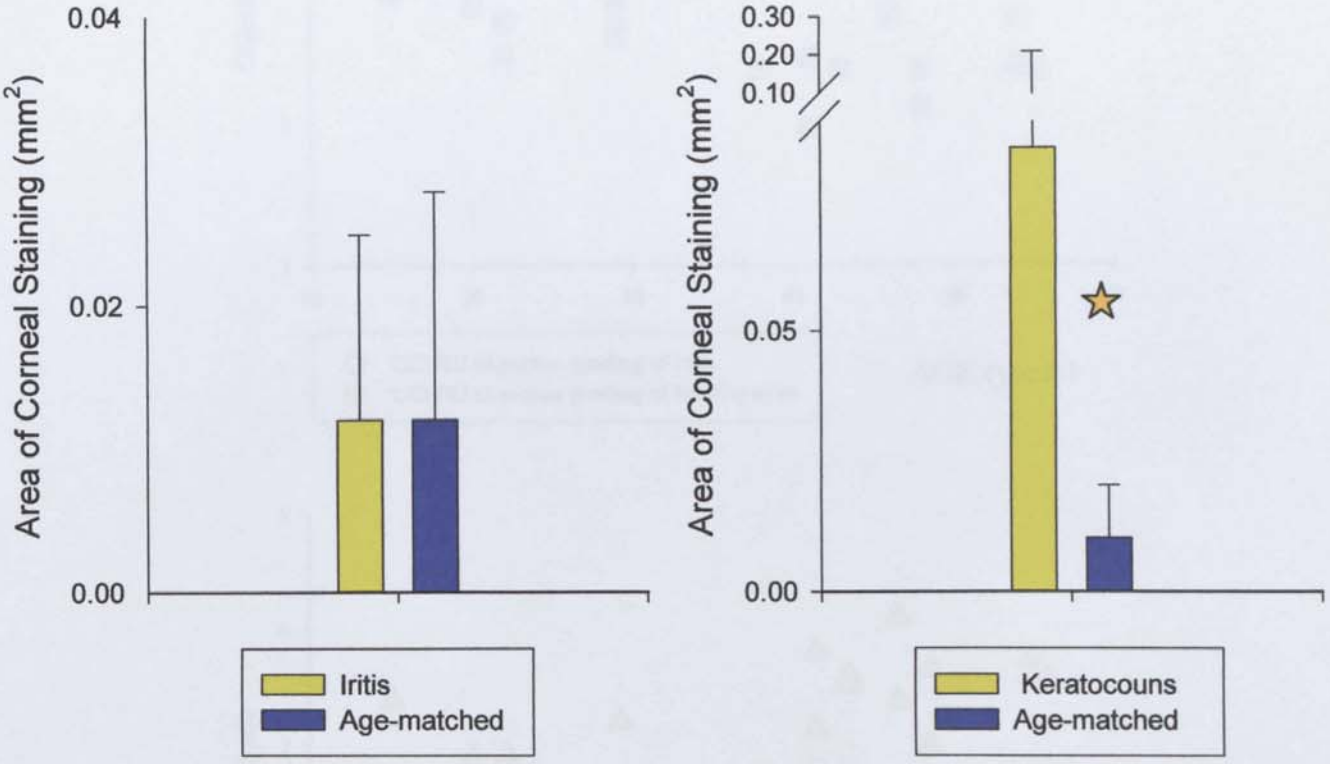

FIGURE 9.6: Scatter plot to display the differences in objective CCLRU and Efron grades of bulbar hyperaemia in subjects with iritis verses age-matched normal eyes. n = 20

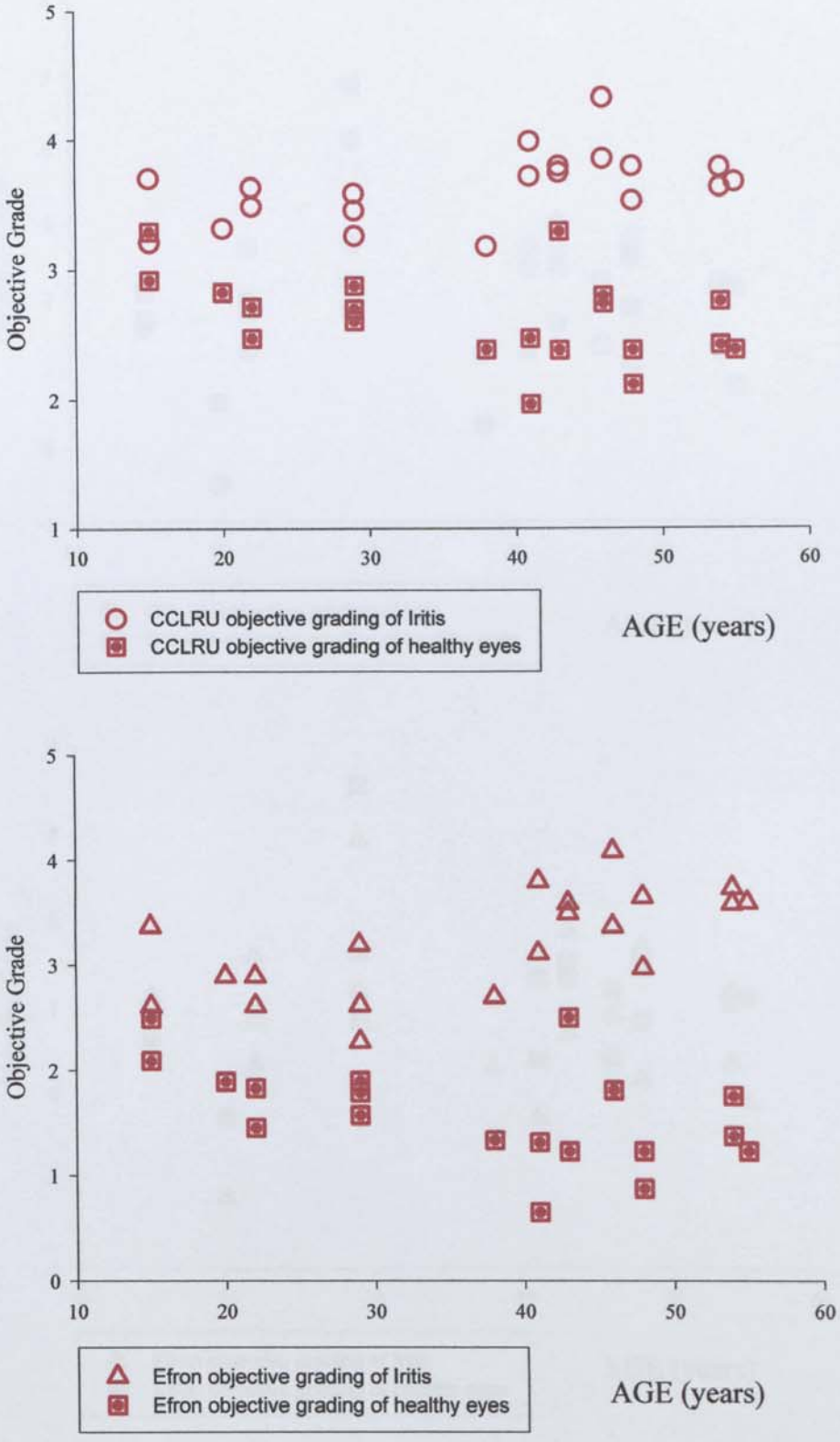

FIGURE 9.7: Scatter plot to display the differences in objective CCLRU and Efron grades of palpebral redness in subjects with iritis verses age-matched normal eyes. n = 20

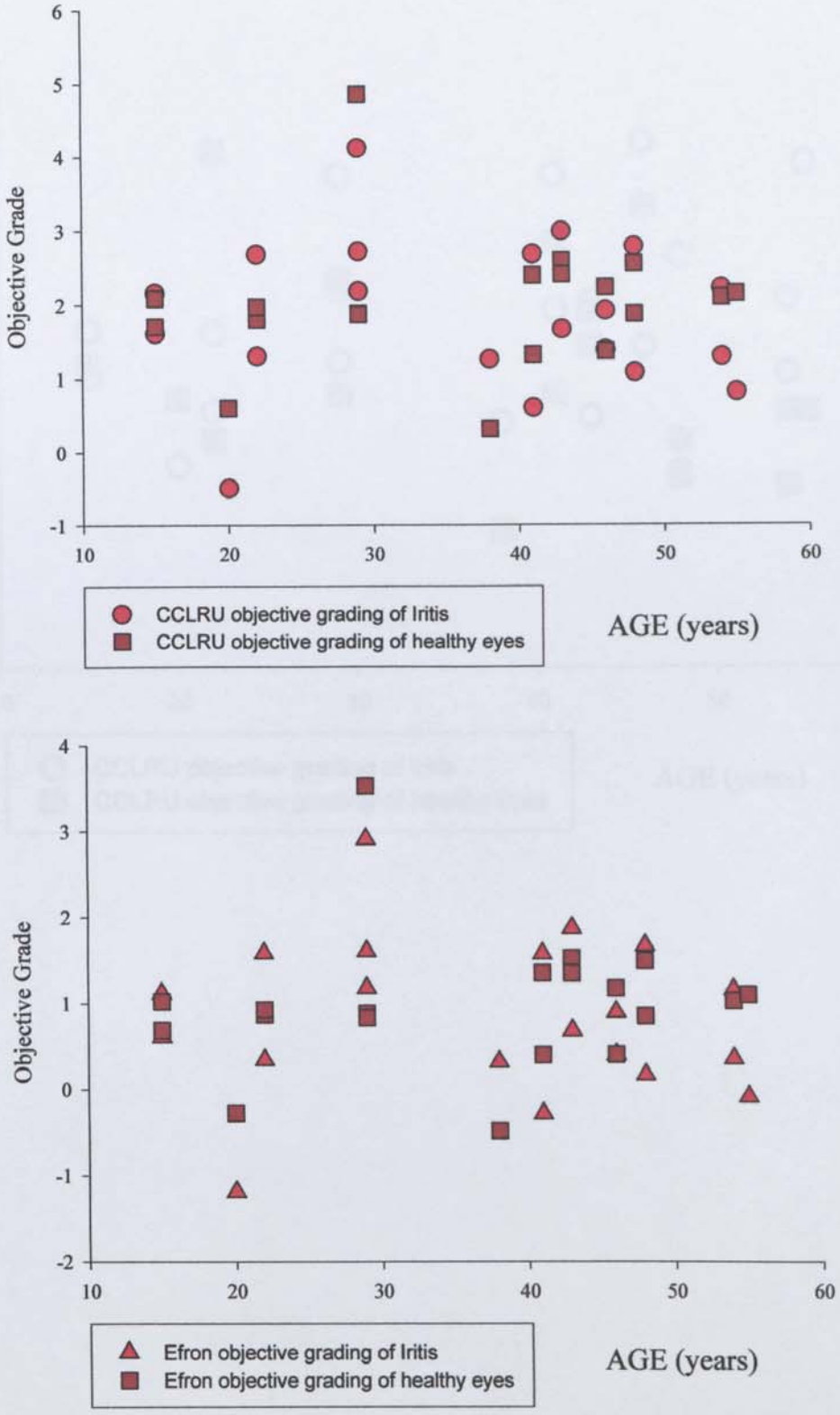

FIGURE 9.8: Scatter plot to display the differences in objective CCLRU and Efron grades of palpebral roughness in subjects with iritis verses age-matched normal eyes. n = 20

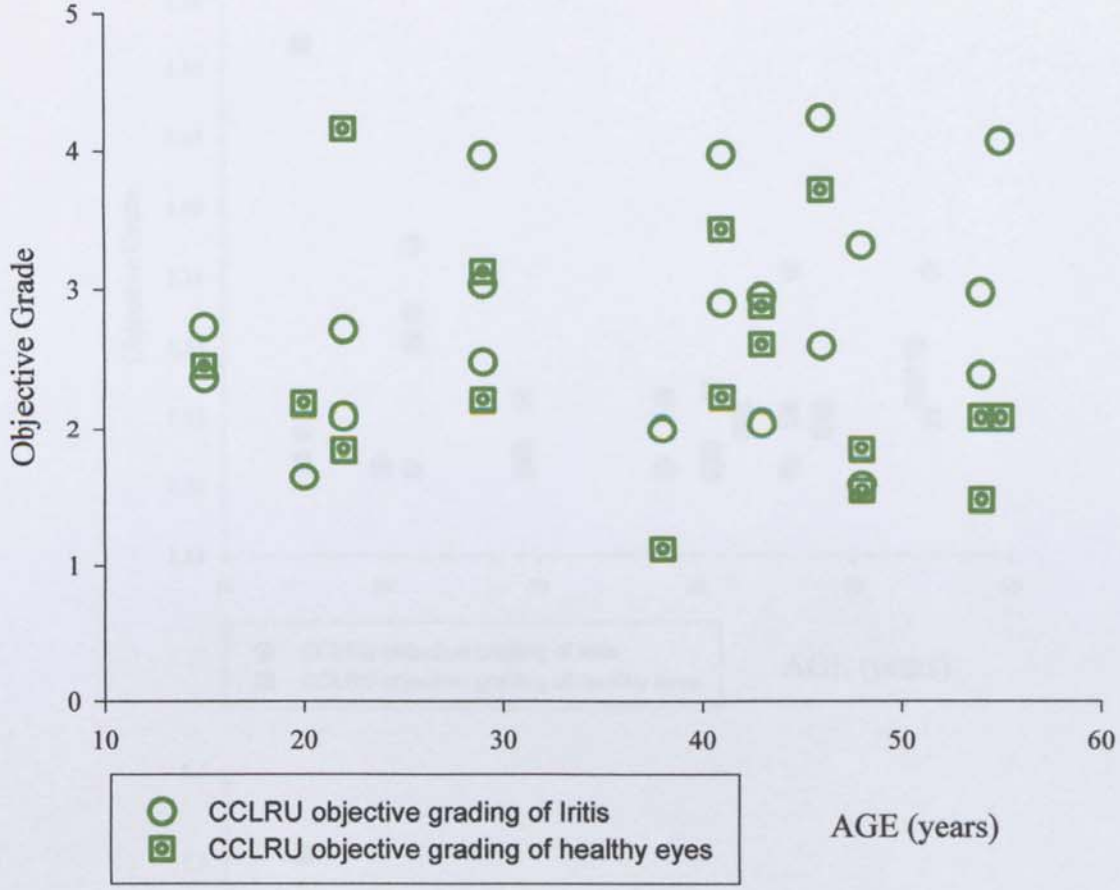

FIGURE 9.9: Scatter plot to display the differences in objective CCLRU and Efron grades of corneal staining (extent) in subjects with iritis verses age-matched normal eyes. n = 20

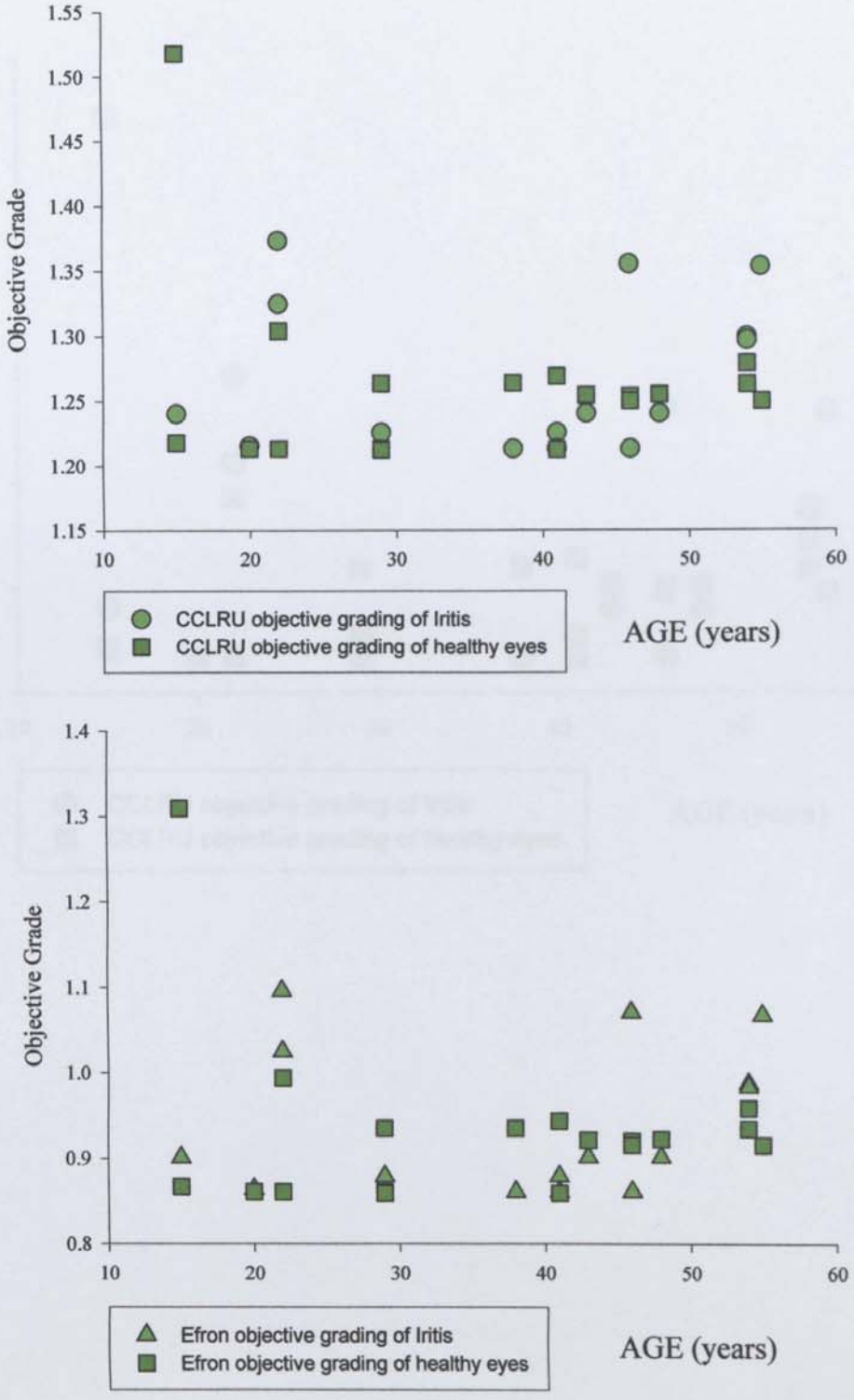

FIGURE 9.10: Scatter plot to display the differences in objective CCLRU and Efron grades of corneal staining (depth) in subjects with iritis verses age-matched normal eyes. n = 20

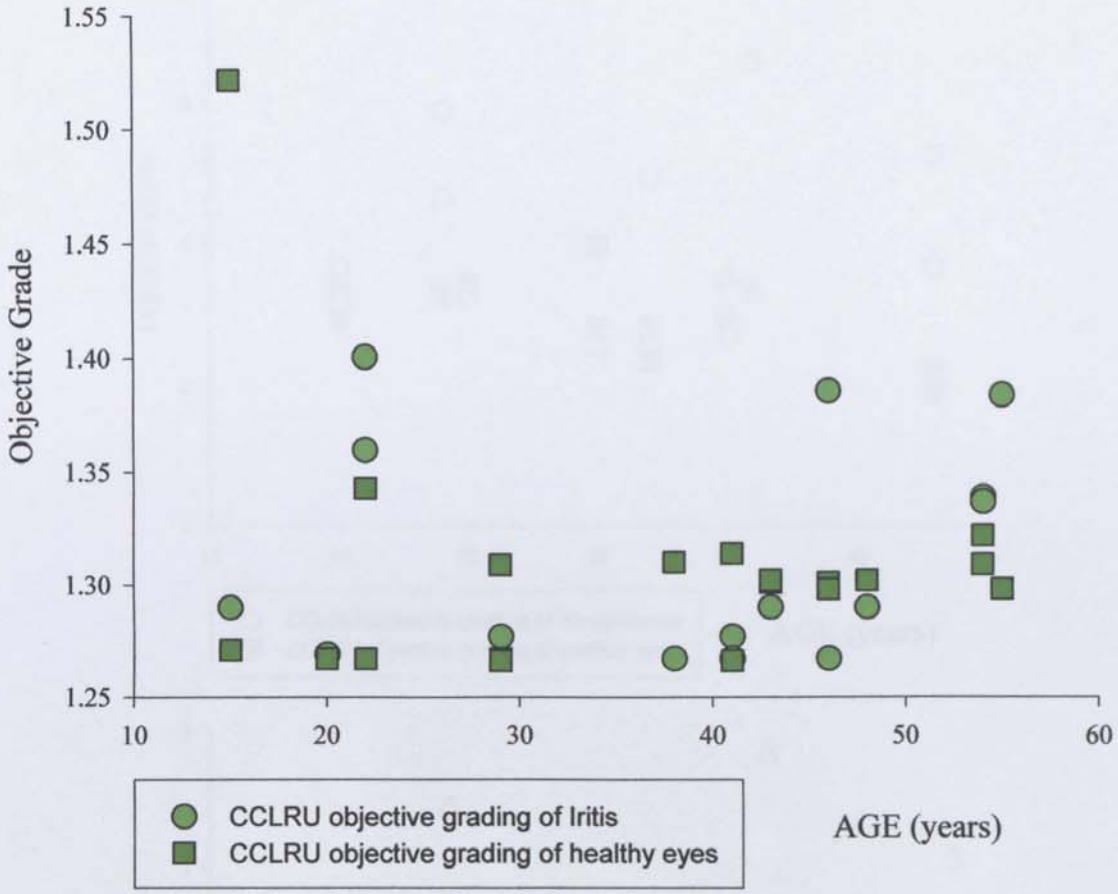

FIGURE 9.11: Scatter plot to display the differences in objective CCLRU and Efron grades of bulbar hyperaemia in subjects with keratoconus verses age-matched normal eyes. n = 14

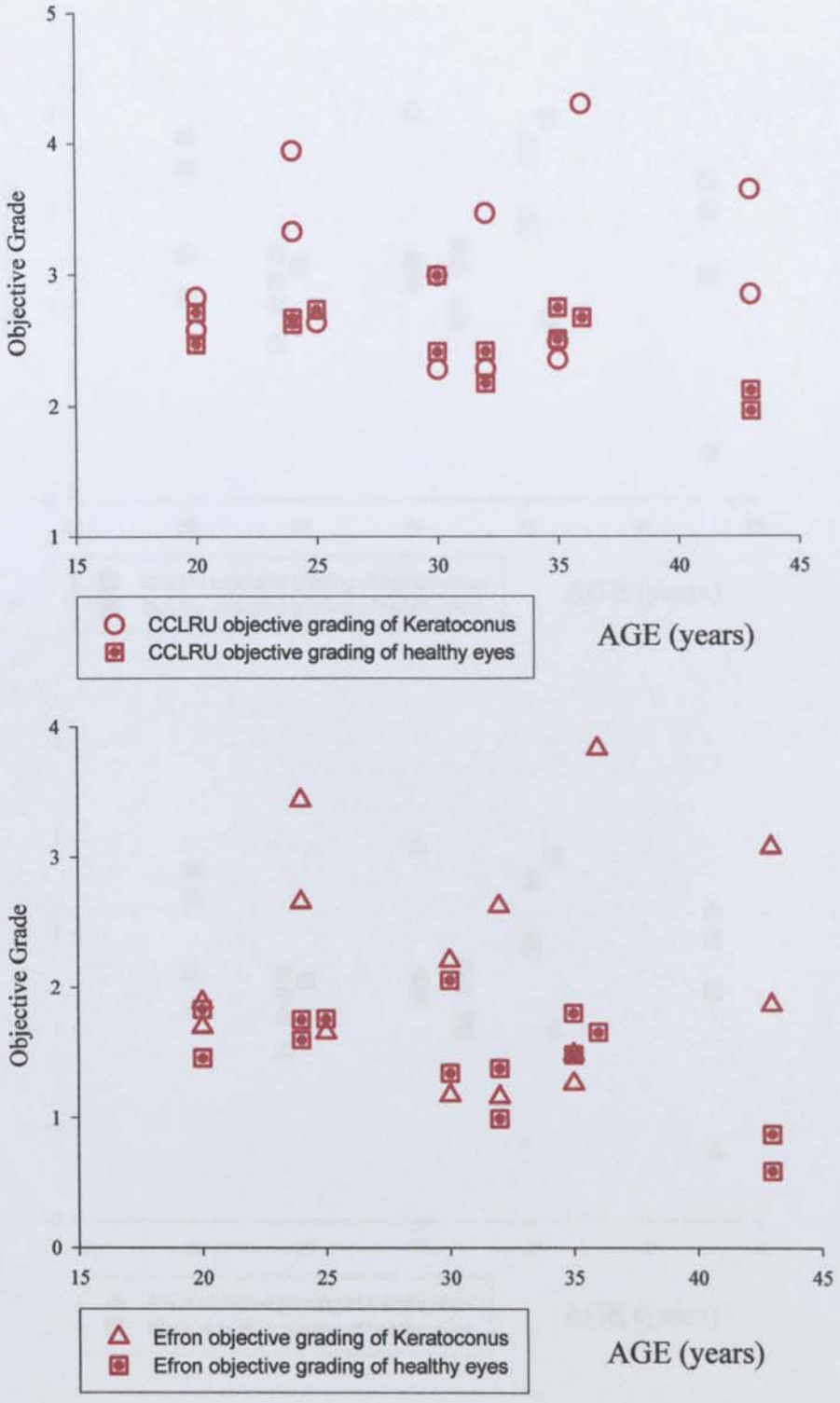

FIGURE 9.12: Scatter plot to display the differences in objective CCLRU and Efron grades of palpebral redness in subjects with keratoconus verses age-matched normal eyes. n = 14

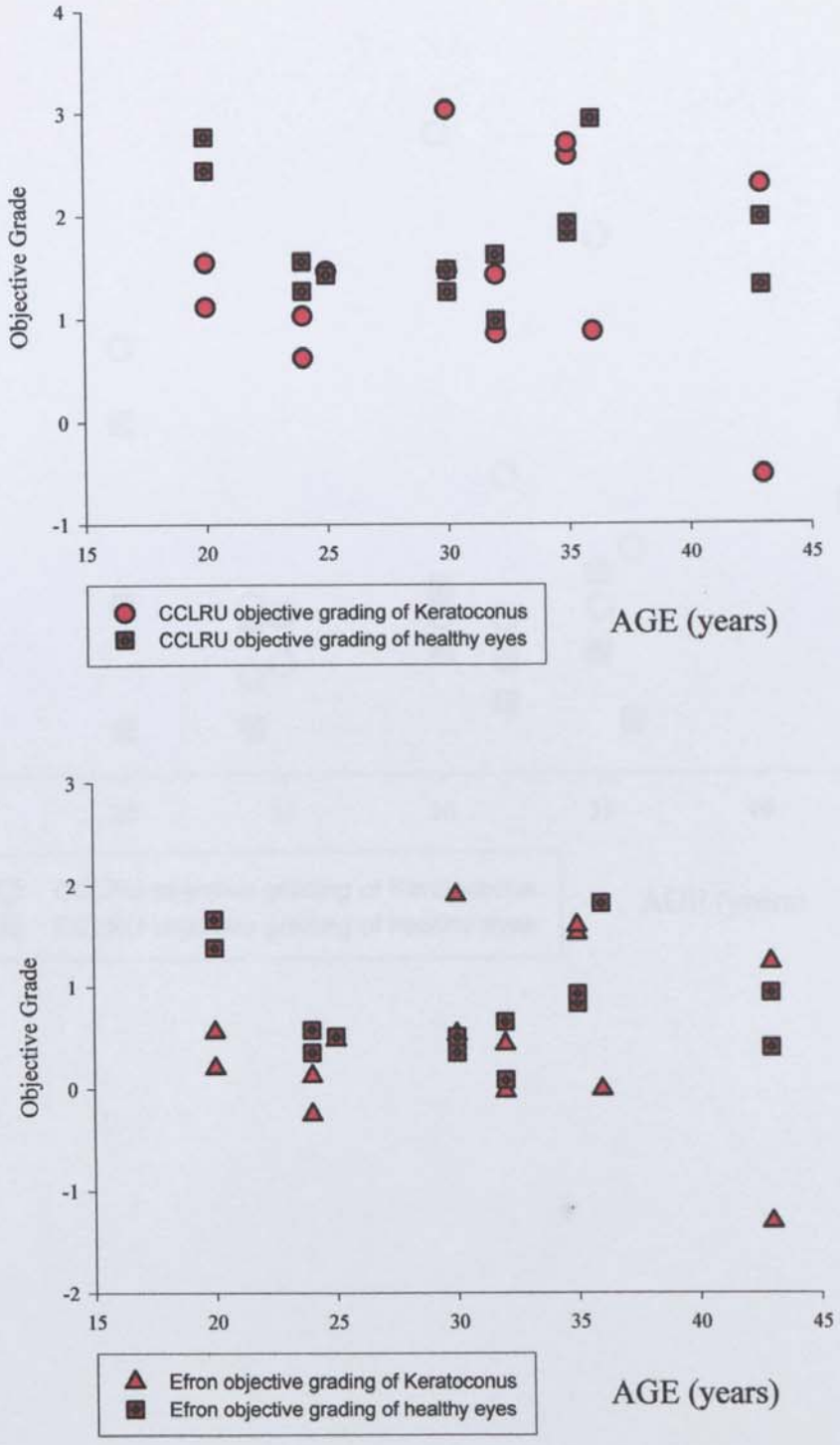

FIGURE 9.13: Scatter plot to display the differences in objective CCLRU and Efron grades of palpebral roughness in subjects with keratoconus verses age-matched normal eyes. n = 14

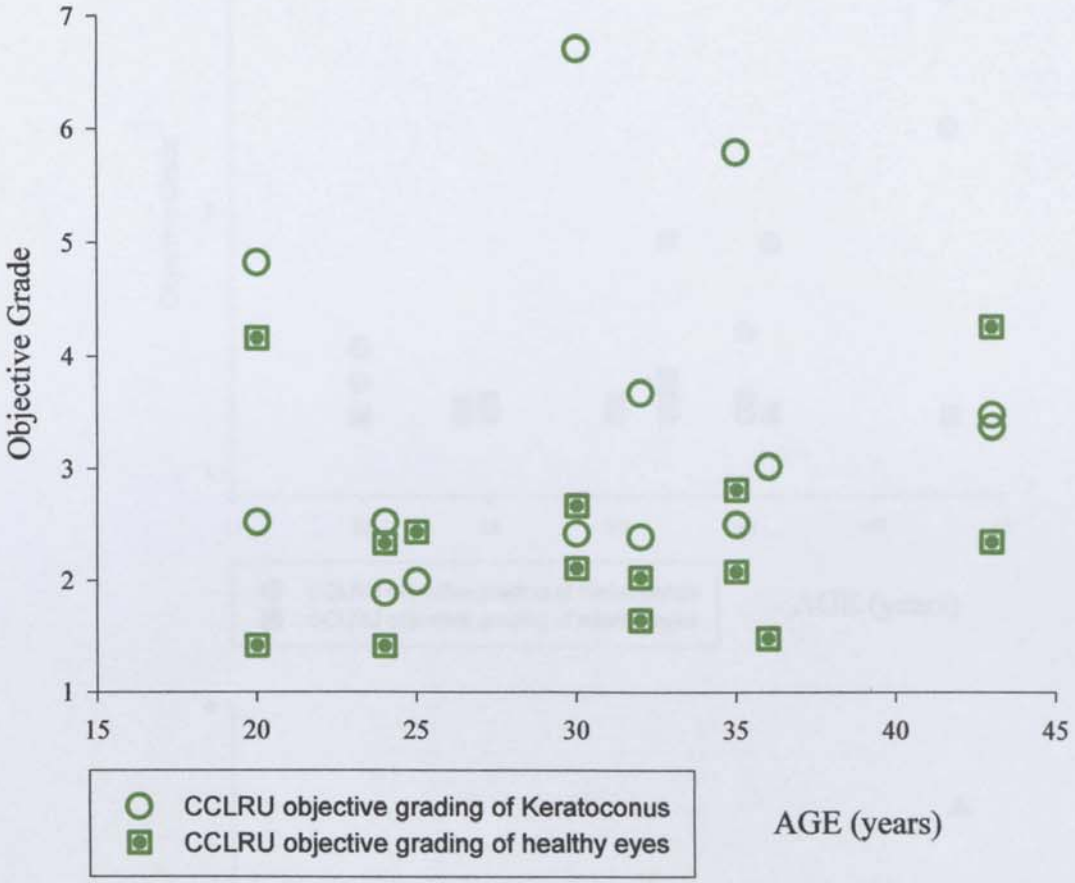

FIGURE 9.14: Scatter plot to display the differences in objective CCLRU and Efron grades of corneal staining (extent) in subjects with keratoconus verses age-matched normal eyes. n = 14

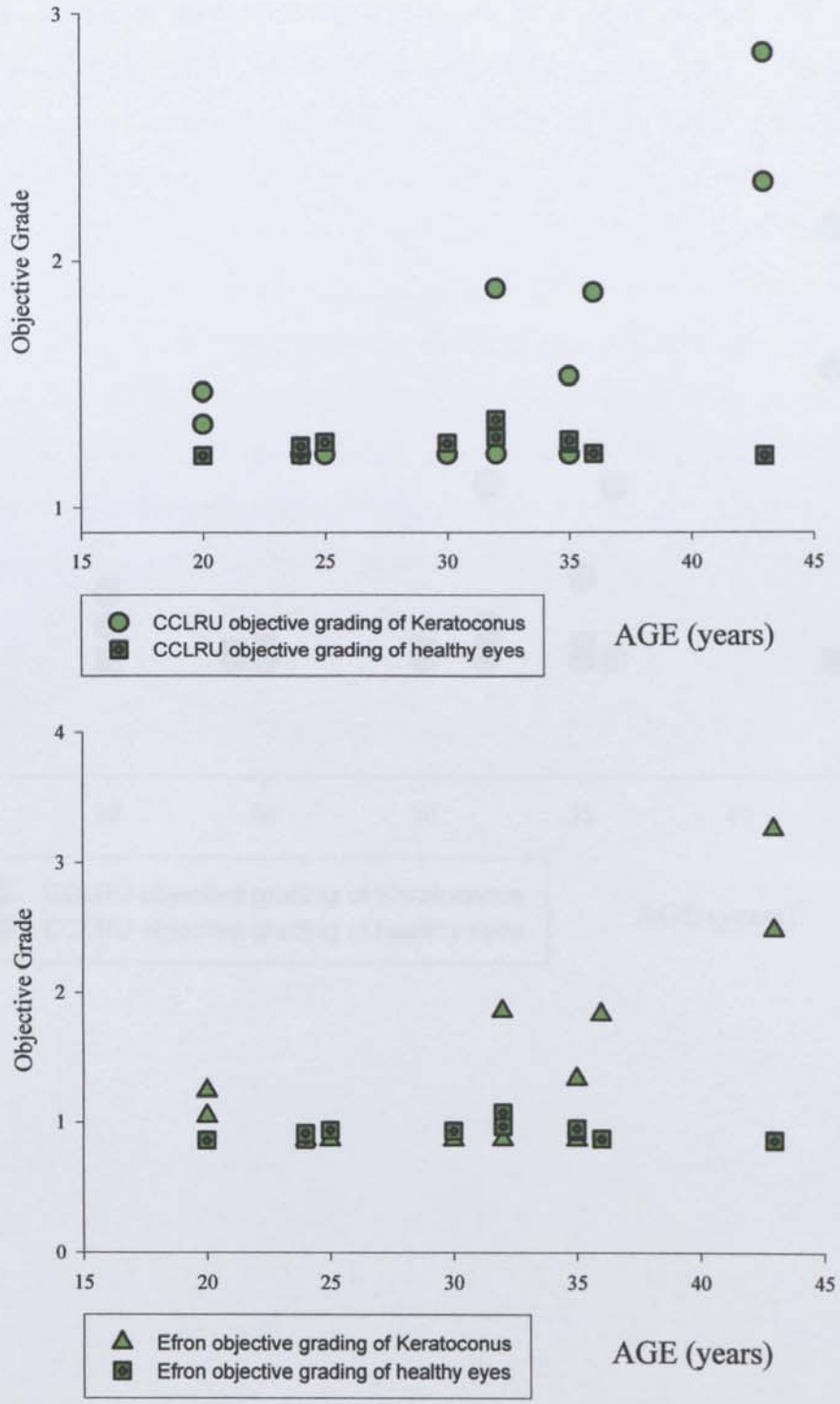

FIGURE 9.15: Scatter plot to display the differences in objective CCLRU and Efron grades of corneal staining (depth) in subjects with keratoconus verses age-matched normal eyes. n = 14

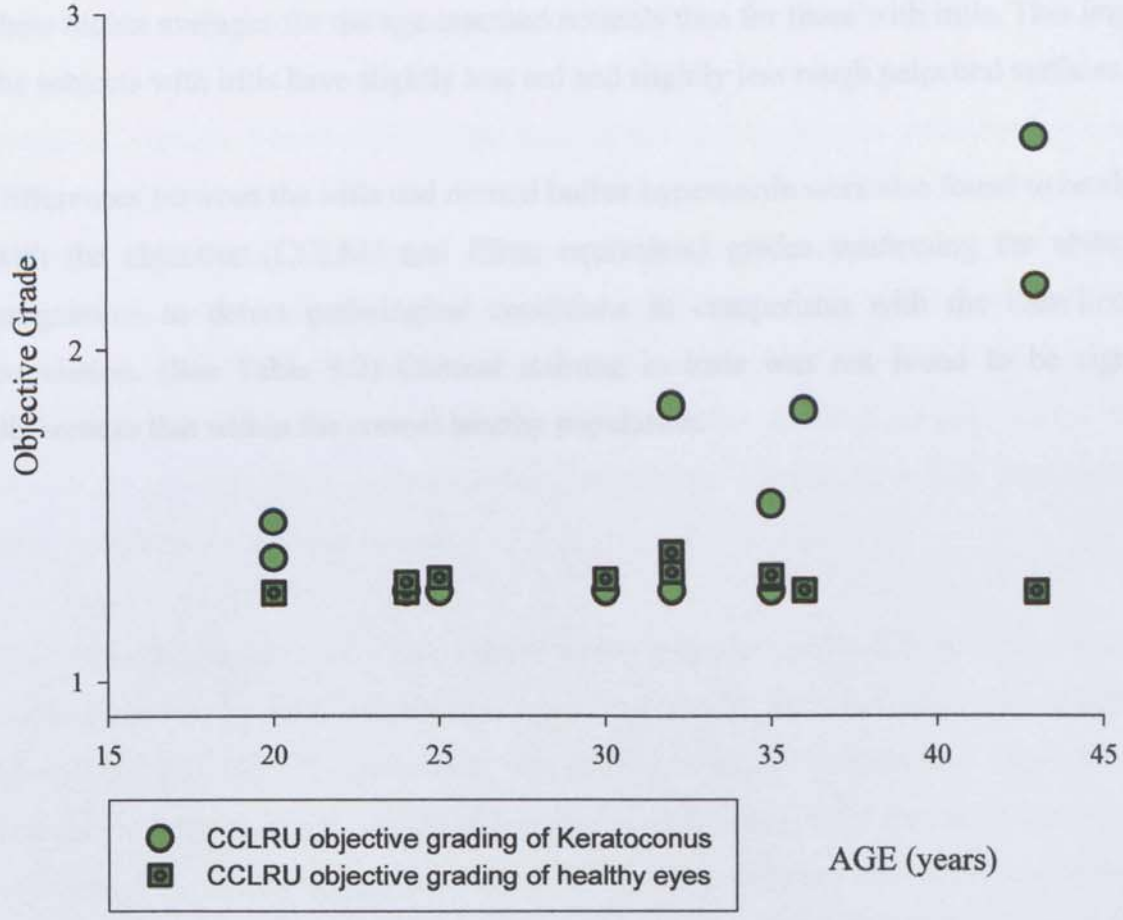

9.5 DISCUSSION

9.5.1: Iritis

Significant increases were found in hyperaemia between the subjects with iritis and the age-matched normals with both ED and RCE measures. This results was expected.

Due to the large change in bulbar vasculature, a difference in all of the anterior ocular vessels may have been expected, but this does not appear to be the case and the palpebral conjunctiva is evidently unaffected. In-fact, the red and green RCE values for the 2 palpebral surfaces show higher averages for the age-matched normals than for those with iritis. This implies that the subjects with iritis have slightly less red and slightly less rough palpebral surfaces.

Differences between the iritis and normal bulbar hyperaemia were also found to be significant with the objective (CCLRU and Efron equivalent) grades confirming the ability of the programme to detect pathological conditions in comparison with the base-line normal population. (See Table 9.2) Corneal staining in iritis was not found to be significantly different to that within the normal healthy population.

9.5.2: Keratoconus

No previous study has examined the relationship between bulbar hyperaemia and keratoconus, but it seems to be an appropriate investigation of a condition so closely associated with atopic disease and eye-rubbing. [160-165] The findings of this study indicated a trend towards higher levels of hyperaemia with keratoconus. The results do not reach significance when measured by ED and RCE alone, but show a significant increase in hyperaemia when combined in the form of the objective grades. (See Table 9.2). This result demonstrates the value of combining the two objective (ED and RCE) measures and again indicates the ability of the programme to detect abnormal ocular changes.

Palpebral redness measures for the keratoconic group do not indicate any significant difference, but was generally less than that of the normal eyes. This is surprising as all of the Keratoconic subjects are regular RGP lens wearers and investigations into the ocular surfaces with RGP wear have determined changes in redness of the palpebral conjunctiva along with squamous and goblet cell metaplasia (of the palpebral conjunctiva). [111, 166, 167] This said, other studies have actually used RGP lenses to treat giant papillary conjunctivitis [168] which would correspond with our findings that keratoconic patients have less papillae/roughness than within the normal population.

This study determined that corneal staining was prominent in the Keratoconic subjects verses the healthy eyes by RCE and area measures, and also by the three objective combined grades (See Table 9.2). [151] Previous work into corneal staining in Keratoconic subjects has shown that this is a characteristic feature of the condition. It is suggested that this is due partly to the nature of the corneal changes at a cellular level, [169, 170] and also partly due to the reduced tear film stability widely noted in Keratoconic patients. [151, 171, 172] Moon and colleagues showed that although corneal staining is a frequent finding in Keratoconic patients, this is possibly due to the RGP wear and the rubbing of the pronounced corneal cone on the lens surface, which would concur with our findings, and other similar reports in the literature. [56, 171, 173-176] The decreased green RCE value for corneal staining in keratoconic subjects is likely to be due to the poorer tear film providing less background fluorescence.

9.4.3: Conclusion

In the Introduction it was proposed that this investigation should endeavour to determine if the recognition of a pathological condition was possible with the objective image analysis, and also if the programme could be used to evaluate aspects of conditions which have previously been neglected due to insensitive/unreliable observation techniques. The results strongly indicate that both of these aims were met by the objective grading.

This study has demonstrated that objective image analysis is capable of determining a significant difference form the base-line by detecting changes in bulbar hyperaemia in iritis, and recognising changes in the anterior ocular surfaces with keratoconus that have been previously undetermined. The sensitivity of the programme to detect small changes (as determined in Chapter 4) and differences from the 'normal' population baseline (evidence provided in this investigation) gives support to the hypothesis that the objective grading could indicate a change in ocular surface features before any difference is evident to human observers. This unique and valuable system could greatly improve the early detection and even diagnosis of anterior ocular abnormalities, and facilitate reliable monitoring of disease progression or treatment regimes in clinical practice or research.

DISCUSSION
AND CONCLUSIONS

DISCUSSION

This thesis set out to develop an objective analysis program that correlates with subjective grades but has improved sensitivity and reliability in its measures, so that the possibility of early detection and reliable monitoring of changes in anterior ocular surfaces could be increased.

The literature review highlighted the importance of resolution and compression in capture and storage of images. Knowing that many images would be needed during the studies performed in this thesis it was first necessary to determine which resolutions and compressions would results in no loss of image quality subjectively or objectively. As minimum values only were recommended, the results of this work will remain applicable in the future, as improvements in technology will only increase the number of pixels available. A future change will almost certainly be an increase in the monitor resolution available and hopefully this will reduce the current detrimental effect of interpolation when displaying higher resolution images than the screen is capable of showing.

Fluorescein application and viewing was evaluated in Chapter 3 to obtain best practice methods for standardised instillation for the purposes of image capture. It was recommended that minimal fluorescein from a fluoret or one drop from a 1% fluorescein minim should be used for fluorescein instillation to reduce the quenching effect. Fluorescence viewing / image capture should use a blue light of a wavelength that provides optimal excitation of the fluorescein (approximately 485-495nm) and a barrier filter that cuts off the excess blue illumination at approximately 495-500nm. It is not difficult to instil a minimal amount of fluorescein from a fluoret given practice. However, a more standardised approach might be easier for the practitioner if large amounts of fluorescein were not available in the first place. This point is taken up by Abdul-Fattah et al who have examined florets with reduced surface areas and found that this method is successful in reducing the quenching effect. [177] It would be interesting to monitor the results of this work objectively. The quenching study itself might have benefited from more patients however the point is successfully proven that the different concentrations and instillation methods cause a significant change in the time that is required before the fluorescence is useful.

Chapter 4 investigates the relationship between subjective grading and the objective measures obtained by the analysis programme. The purpose of this was to indicate whether objective

image analysis would enhance the clinical quantification and monitoring of anterior eye disease in terms of sensitivity and reliability, in comparison with that of subjective grading by trained clinicians. Sensitivity of the programme was found to be up to 0.01 of an Efron grade unit which was up to 20x greater than subjective grading. The reliability of the programme was found to be optimal and subjective grading was up to 144 times more variable. Benefit may have been gained from including more optometric subjective graders as might an increase in the number of repeats. A larger number of images taken over a longer duration might have improved differentiation between the images recognised as significantly different by the objective and subjective groups, but due to the large number of images (135) and the three repeats the fatiguing effect was judged to be too great. It is not clear that 3 subjects were needed for the instillation of thymoxamine. Perhaps one subject recorded for a longer duration would have been adequate to examine the effect of the vasodilator, and then the number of images would have been less, reducing the fatigue effect also. However, at the time the level of vasodilation after 2 drops of thymoxamine could not be fully predicted therefore 3 subjects were used to ensure that the best reaction was observed. The evidence from this study which suggests that an optometrist can differentiate between grades with a sensitivity of up to 0.3 of an Efron scale is a little surprising, and more work is required into this result. The Efron scale was chosen for use in this study as it has the most linear progression of grades that would therefore complement the objective grade more than perhaps the CCLRU, however it would have been interesting to compare the results of the objective grading against subjective against the CCLRU also.

Chapter 5 continued the evolution of the objective analysis programme by endeavouring to develop the programme further into a user-friendly grading system that would produce results which could be universally recognised by eye-care practitioners. Formulae were devised to combine the objective measures of the ocular surfaces to produce a 'grade', equivalent to those displayed by the CCLRU or Efron subjective scales. The correlation between new-objective and subjective grades of the same series of images was high, with a maximum adjusted r^2 of 0.96 indicating that the new grading system could be comparable with the old and hence objective results would be easily recognised by clinicians.

The results for the relationship between objective formulated grades and subjective grading of the bulbar hyperemia, palpebral redness and roughness are conclusive. However, there is some cause for concern regarding the method of measuring corneal staining objectively.

Neither ED nor Green RCE values were able to predict the extent or depth of corneal staining in comparison to optometrists. There were also complications involved in selecting the whole area of the cornea using rectangular sections. Significant results were found however for the second method of corneal analysis which involved manually selecting areas on the image of patches or dots of staining. This was both labour intensive and of course – relatively subjective but reduced the limbal-overlapping and other inaccuracies caused by attempting to select the corneal area with rectangular sections. The total areas of staining selected correlated with the extent of staining (as would be predicted, $p<0.001$) but also the depth of staining ($p<0.001$), which was not strictly measured by the program. This is the main weakness in anterior evaluation with the LabView program as utilising a method that is not entirely subjective will reduce the sensitivity and reliability of the results. Further investigation is required to improve evaluation of corneal staining. One solution could be to use the program to measure the intensity of a specific wavelength of light (e.g.510-520nm for fluorescein fluorescence). If applied to the selected areas of staining, the depth would be measured more appropriately if compared to background tear-film fluorescence, and if applied to the total area, this objective measure may offer significant correlation with subjective grading.

The regression equations used to derive the images are based on the results of subjective assessment of only 10 images per ocular surface. Initially there were 50 images selected per ocular surface, but this led to a total of 200 images to be graded by both the Efron and CCLRU scales. The time taken to achieve this was over an hour and it was judged that the fatigue was detrimental to the results and that as long as the images covered a full range of severity less than 50 could be used. Figures 5.14 to 5.18 generally show good agreement between the subjective and objectively calculated grades. However Chapters 6 and 7 which go on to investigate the baseline grades of the ocular surfaces with factors of age and diurnal variation show much higher objective-grade values than had been expected. There are several possible reasons for this; the objective grade could be affected by the non-linear nature of subjective grades used to derive the formulae, it could possibly be due to the subjects recruited not being indicative of the normal population, or not enough subjects. It could also be that the values are an accurate representation of the actual ocular surface grades. The images were all taken in the morning and there could be an effect due to this or other external factors, or they are higher than would be *expected* as eye-care-practitioners are trained to regard grades of below 2 as normal but indeed this may not be the case. Is it possible that practitioners do not wish to grade within these higher boundaries when they consider an eye

to be normal as this would mean that they put themselves at risk of being accused of not acting/referring when they could have? An investigation into whether a practitioner grades differently when they have responsibility for the patient is warranted.

Chapter 7 uses the formulae developed in Chapter 5 and applies it to the investigation of diurnal variation in ocular surfaces, in order to account for any change that may affect the baseline. Increases in bulbar hyperaemia and palpebral redness were found between examinations in the morning, and the evening. Correction factors were recommended. Diurnal changes in baseline measures have been evaluated in this thesis, but daily changes should also be considered as there are naturally changes to ocular surfaces according to environment and other factors that a subject is exposed to but should not constitute a deviation from the subjects 'normal' limits. This investigation is ongoing.

The third and final segment of the thesis utilised the developed programme in two chapters which evaluate changes in the anterior ocular surfaces. Chapter 8 describes a contralateral contact lens trial that includes analysis of changes in bulbar hyperaemia by objective grading. Chapter 9 aimed to verify the ability of the programme to identify pathological conditions in a comparison with iritis and keratoconus with age-matched normal/healthy eyes. Objective image analysis was found to be capable of determining a significant difference from the base-line by detecting changes in bulbar hyperaemia in iritis, and recognising changes in the anterior ocular surfaces with keratoconus that have been previously undetermined.

FUTURE DEVELOPMENTS

The objective grading program was made possible by improvements in technology regarding both the potential of digital processes and accessibility. It is certain that as technology advances further new ground will be broken in the design and application of objective image analysis of the anterior ocular surfaces. Certain adjustments to the program that has been proven in this thesis may therefore be possible in the future. For example: The analysis of an image is achieved by the selection of a constant area which is currently in rectangular form which cannot cover a specific ocular surface without overlapping onto another. It may by possible in the future to achieve intelligent surface recognition which will be able to automatically define the whole bulbar conjunctiva for example. If this was the case, the limbal area may also be able to be assessed and objective grading applied which would be an added benefit particularly in the examination of contact lens related changes in clinical or research environments.

Other similar improvements could be written into the program if area definitions were possible, such as splitting a surface like the tarsal-plate into a number of different areas to facilitate more specific analysis (which was demonstrated in the article by MacKinven and colleagues [16]

Assessment of the cornea by objective grading is the next step in the completion of an anterior ocular grading tool. An objective image analysis programme has been developed for evaluation of corneal transparency by intensity variation across the width of a corneal section. [21] The programme has not yet been fully evaluated but the indications form the article by O'Donnell and Wolffsohn are promising. A difficulty may arise (in the experience of the author) when attempting to capture consistent images of the corneal section at high magnifications. A magnification of (maximum) 25x may be more effective than 40x, as more of the cornea could be evaluated, and the minute movements or focusing differences caused by the beam-splitter in the slit-lamp would not have such a large impact on the image quality.

Further investigation using the LabView program is needed to obtain measures of those patients with vasculature disease. There is evidence to suggest that hypertension can be observed in the vessels of the conjunctiva, [178-180] in which case an objective evaluation may provide a another tool for the early diagnosis and monitoring of the condition.

A profile of the proportionate effects on edge detection (ED) and relative colour extraction (RCE) of any ocular pathology on each of the anterior surfaces could help to make a differential diagnosis and lead to more effective, and earlier treatment regime whilst monitoring the progression.

CONCLUSIONS

The culmination of the investigations in this thesis may lead to the use of the LabView program in both clinical and research practice:

- In clinical practice the objective grading offers a 20x more sensitive and optimally reliable source of information on the condition of the ocular surfaces. In comparison with the baseline measures from the patient themselves or with those established in Chapter 6, the objective grade can determine whether a change is 'outside of the normal limits'. In this manner the program is capable of detecting pathology prior to subjective recognition, and monitoring progression or treatment effects with more accuracy than is possible by trained practitioners

- In research practice the objective grade removes observer bias and the variability of subjective measures. The high levels of repeatability will allow studies to have powered significance with smaller numbers of subjects, which would save time and money whist obtaining an accurate result.

Therefore, objective analysis may offer a new gold-standard in anterior ocular examination, and should be developed as a clinical tool for use in research and to enhance the monitoring and detection of anterior ocular pathology.

REFERENCES

1. Justice J. *Ophthalmic photography.* 1982, Boston: Little Brown and Company.
2. Jackman W T and Webster J D. *On photographing the retina of the living human eye.* Philadelphia photographer 1886. **23**(275).
3. Charman W N. *Imaging in the 21st century.* Ophthalmic and Physiological Optics, 1998. **18**(2): p. 210-223.
4. Yannuzzi L A, Ober M D, Slakter J S, *et al. Ophthalmic fundus imaging: today and beyond.* American Journal of Ophthalmology, 2004. **137**(3): p. 511-524.
5. Rosenfeld A. *From Image Analysis to Computer Vision: An Annotated Bibliography, 1955-1979.* Computer Vision and Image Understanding, 2001. **84**(2): p. 298-324.
6. Hellstedt T, Vesti E, and Immonen I. *Identification of individual microaneurysms: a comparison between fluorescein angiograms and red-free and colour photographs.* Graefes Archive for Clinical & Experimental Ophthalmology, 1996. **234** Suppl 1: p. S13-7.
7. Gilchrist J. *Analysis of early diabetic retinopathy by computer processing of fundus images--a preliminary study.* Ophthalmic & Physiological Optics, 1987. **7**(4): p. 393-9.
8. Basu A, Kamal A D, Illahi W, *et al. Is digital image compression acceptable within diabetic retinopathy screening?* Diabetic Medicine, 2003. **20**(9): p. 766-71.
9. Taylor D J, Jacob J S, and Tooke J E. *The integration of digital camera derived images with a computer based diabetes register for use in retinal screening.* Computer Methods & Programs in Biomedicine, 2000. **62**(3): p. 157-63.
10. Cox I. *Digital imaging in the contact lens practice.* International Contact Lens Clinic, 1995. **22**(3-4): p. 62-66.
11. Handy B, *The CCD Nitty Gritty Ditty.* 2000, Quoting J Janesick at Pixelvision, Inc.
12. Zadnik K, Steger-May K, Fink B A, *et al. Between-eye asymmetry in keratoconus.* Cornea, 2002. **21**(7): p. 671-9.
13. Technical Advisory Service for Images (TASi) h w t a u. *Advise paper on digital cameras.* [cited 2004 June]; Available from: http://www.tasi.ac.uk.
14. Foveon. *Foveon chip diagram.* [cited May 2006]. Available from: www.foveon.com
15. Fraser B. *Colour management explained.* Photo Electronic Imaging 1998. **471**(5): p. 30-35.

16. MacKinven J, McGuinness C L, Pascal E, *et al. Clinical grading of the upper palpebral conjunctiva of non-contact lens wearers.* Optometry & Vision Science, 2001. **78**(1): p. 13-8.
17. Miyata K, Amano S, Sawa M, *et al. A novel grading method for superficial punctate keratopathy magnitude and its correlation with corneal epithelial permeability.* Archives of Ophthalmology, 2003. **121**(11): p. 1537-9.
18. Efron N. *Grading scales for contact lens complications.* Opthalmic and Physiological Optics, 1998. **18**(2): p. 182-186.
19. Fieguth P and Simpson T. *Automated measurement of bulbar redness.* Investigative Ophthalmology & Visual Science, 2002. **43**(2): p. 340-7.
20. Doughty M J, Potvin R, Pritchard N, *et al. Evaluation of the range of areas of the fluorescein staining patterns of the tarsal conjunctiva in man.* Documenta Ophthalmologica, 1995. **89**(4): p. 355-71.
21. O'Donnell C and Wolffsohn J S. *Grading of corneal transparency.* Contact Lens and Anterior Eye, 2004. **27**(4): p. 161-170.
22. Pritchard N, Young G, Coleman S, *et al. Subjective and objective measures of corneal staining related to multipurpose care systems.* Contact Lens and Anterior Eye, 2003. **26**(1): p. 3-9.
23. Mandell R B. *Slit lamp classification system.* Journal of the American Optometric Association, 1987. **58**(3): p. 198-201.
24. Woods R. *Quantitative slit lamp observations in contact lens practice.* Journal of The British Contact Lens Association, 1989. **12**(2): p. 42-45.
25. Annunziato T, Davidson R G, Christensen M T, *et al. Atlas of Slit Lamp Findings and Contact-Lens Related Anomalies*. Southwest Independent Institutional Review Board. 1992, Fort Worth, TX, USA: Southwest Independent Institutional Review Board.
26. Andersen J S, Davies I P, Kruse A, *et al. Handbook of Contact Lens Management.* 1996, Jacksonville: Vistakon.
27. Phillips A J and Speedwell L. *CCLRU Grading Scale. Contact Lenses. Appendix D.* 1997, Oxford: Butterworth-Heinemann.
28. Efron N. *Grading Scales for Contact Lens Complications*. Millennium Edition ed. 2000, Farnborough: Hydron.
29. Chong E, Simpson T, and Fonn D. *The repeatability of discrete and continuous anterior segment grading scales.* Optometry & Vision Science, 2000. **77**(5): p. 244-51.

30. Dundas M, Walker A, and Woods R L. *Clinical grading of corneal staining of non-contact lens wearers.* Ophthalmic and Physiological Optics, 2001. **21**(1): p. 30-35.
31. Papas E B. *Key factors in the subjective and objective assessment of conjunctival erythema.* Investigative Ophthalmology & Visual Science, 2000. **41**(3): p. 687-91.
32. Twelker J D and Bailey I L. *Grading conjunctival hyperaemia using a photography-based method.* Investigative Ophthalmology & Visual Science, 2000. **41**: p. s927.
33. Efron N, Morgan P B, and Katsara S S. *Validation of grading scales for contact lens complications.* Ophthalmic and Physiological Optics, 2001. **21**(1): p. 17-29.
34. Efron N, Morgan P B, and Jagpal R. *Validation of computer morphs for grading contact lens complications.* Ophthalmic & Physiological Optics, 2002. **22**(4): p. 341-9.
35. Wolffsohn J S and Purslow C. *Clinical monitoring of ocular physiology using digital image analysis.* Contact Lens and Anterior Eye, 2003. **26**(1): p. 27-35.
36. Wolffsohn J S. *Incremental nature of anterior eye grading scales determined by objective image analysis.* British Journal of Ophthalmology, 2004. **88**(11): p. 1434-8.
37. Efron N, Morgan P B, and Jagpal R. *The combined influence of knowledge, training and experience when grading contact lens complications.* Ophthalmic & Physiological Optics, 2003. **23**(1): p. 79-85.
38. McMonnies C W and Ho A. *Conjunctival hyperaemia in non-contact lens wearers.* Acta Ophthalmologica, 1991. **69**(6): p. 799-801.
39. Lofstrom T, Anderson J S, and Kruse A. *Tarsal abnormalities: a new grading system.* CLAO Journal, 1998. **24**(4): p. 210-5.
40. Efron N, Morgan P B, Farmer C, *et al. Experience and training as determinants of grading reliability when assessing the severity of contact lens complications.* Ophthalmic & Physiological Optics, 2003. **23**(2): p. 119-24.
41. Bailey I L, Bullimore M A, Raasch T W, *et al. Clinical grading and the effects of scaling.* Investigative Ophthalmology & Visual Science, 1991. **32**(2): p. 422-32.
42. Hellstedt T, Palsi V P, and Immonen I. *A computerized system for localization of diabetic lesions from fundus images.* Acta Ophthalmologica, 1994. **72**(3): p.352-6.
43. Hurcomb P G, Wolffsohn J S, and Napper G A. *Ocular signs of systemic hypertension: A review.* Ophthalmic and Physiological Optics, 2001. **21**(6): p. 430-440.
44. Goatman K A, Cree M J, Olson J A, *et al. Automated measurement of microaneurysm turnover.* Investigative Ophthalmology & Visual Science, 2003. **44**(12): p. 5335-41.

45. Usher D, Dumskyj M, Himaga M, *et al. Automated detection of diabetic retinopathy in digital retinal images: a tool for diabetic retinopathy screening.* Diabetic Medicine, 2004. **21**(1): p. 84-90.

46. Wu D C, Schwartz B, Schwoerer J, *et al. Retinal blood vessel width measured on color fundus photographs by image analysis.* Acta Ophthalmologica Scandinavica Supplement, 1995(215): p. 33-40.

47. Gang L, Chutatape O, and Krishnan S M. *Detection and measurement of retinal vessels in fundus images using amplitude modified second-order Gaussian filter.* IEEE Transactions on Biomedical Engineering, 2002. **49**(2): p. 168-72.

48. Larsen M, Godt J, Larsen N, *et al. Automated detection of fundus photographic red lesions in diabetic retinopathy.* Investigative Ophthalmology & Visual Science, 2003. **44**(2): p. 761-6.

49. Sinthanayothin C, Boyce J F, Cook H L, *et al. Automated localisation of the optic disc, fovea, and retinal blood vessels from digital colour fundus images.* British Journal of Ophthalmology, 1999. **83**(8): p. 902-10.

50. Hipwell J H, Strachan F, Olson J A, *et al. Automated detection of microaneurysms in digital red-free photographs: a diabetic retinopathy screening tool.* Diabetic Medicine, 2000. **17**(8): p. 588-94.

51. Chen P C, Kovalcheck S W, and Zweifach B W. *Analysis of microvascular network in bulbar conjunctiva by image processing.* International Journal of Microcirculation: Clinical & Experimental, 1987. **6**(3): p. 245-55.

52. Villumsen J, Ringquist J, and Alm A. *Image analysis of conjunctival hyperemia. A personal computer based system.* Acta Ophthalmologica, 1991. **69**(4): p. 536-9.

53. Willingham F F, Cohen K L, Coggins J M, *et al. Automatic quantitative measurement of ocular hyperaemia.* Current Eye Research, 1995. **14**: p. 1101-8.

54. Horak F, Berger U, Menapace R, *et al. Quantification of conjunctival vascular reaction by digital imaging.* Journal of Allergy & Clinical Immunology, 1996. **98**(3): p. 495-500.

55. Guillon M and Shah D. *Objective measurement of contact lens-induced conjunctival redness.* Optometry & Vision Science, 1996. **73**(9): p. 595-605.

56. Owen C G, Fitzke F W, and Woodward E G. *A new computer assisted objective method for quantifying vascular changes of the bulbar conjunctivae.* Ophthalmic & Physiological Optics, 1996. **16**(5): p. 430-7.

57. Maldonado M J, Arnau V, Martinez-Costa R, *et al. Reproducibility of digital image analysis for measuring corneal haze after myopic photorefractive keratectomy.* American Journal of Ophthalmology, 1997. **123**(1): p. 31-41.

58. Simpson T L, Chan A, and Fonn D. *Measuring ocular redness: first order (luminance and chromaticity) measurements provide more information than second order (spatial structure) measurements.* Optometry & Vision Science, 1998. **75**: p. 279-283.

59. Chan J W W, Edwards M H, Woo G C, *et al. Objective method to measure corneal clarity before and after laser in situ keratomileusis.* Journal of Cataract & Refractive Surgery, 2003. **29**(1): p. 118-24.

60. Owen C G, Ellis T J, and Woodward E G. *A comparison of manual and automated methods of measuring conjunctival vessel widths from photographic and digital images.* Ophthalmic & Physiological Optics, 2004. **24**(2): p. 74-81.

61. Jensen P K and Scherfig E. *Resolution of retinal digital colour images.* Acta Ophthalmologica Scandinavica, 1999. **77**(5): p. 526-9.

62. George L D, Leverton C, Young S, *et al. Can digitised colour 35 mm transparencies be used to diagnose diabetic retinopathy?* Diabetic Medicine, 1997. **14**(11): p. 970-3.

63. Lim J I, LaBree L, Nichols T, *et al. A comparison of digital nonmydriatic fundus imaging with standard 35-millimeter slides for diabetic retinopathy.* Ophthalmology, 2000. **107**(5): p. 866-870.

64. Prasad S, Bannon P, Clearkin L G, *et al. Digital fundus imaging: a quality and cost comparison with 35-mm film.* Acta Ophthalmologica Scandinavica, 1999. **77**(1): p. 79-82.

65. Olson J A, Strachan F M, Hipwell J H, *et al. A comparative evaluation of digital imaging, retinal photography and optometrist examination in screening for diabetic retinopathy.* Diabetic Medicine, 2003. **20**(7): p. 528-34.

66. British Diabetic Association, *Guidelines on screening for diabetic retinopathy.* 1999, BDA: London.

67. Fdez-Valdivia J A, Fdez-Vidal X R, and Rodriguez-Sanchez R. *On the concept of best achievable compression ratio for lossy image coding.* Pattern Recognition, 2003. **36**: p. 2377-94.

68. Newsom R S, Clover A, Costen M T, *et al. Effect of digital image compression on screening for diabetic retinopathy.* British Journal of Ophthalmology, 2001. **85**(7): p. 799-802.

69. Kocsis O, Costaridou L, Mandellos G, *et al. Compression assessment based on medical image quality concepts using computer-generated test images.* Computer Methods & Programs in Biomedicine, 2003. **71**(2): p. 105-15.

70. Tabery H M. *Corneal surface changes in keratoconjunctivitis sicca. Part I: The surface proper. A non-contact photomicrographic in vivo study in the human cornea.* Eye, 2003. **17**(4): p. 482-7.

71. Zantos S G. *Cystic formations in the corneal epithelium during extended wear of contact lenses.* Int. Contact Lens Clin, 1983. **10**: p. 128-68.

72. Keay L, Jalbert I, Sweeney D F, *et al. Microcysts: clinical significance and differential diagnosis.* Optometry (St Louis, Mo), 2001. **72**(7): p. 452-60.

73. Alpert B and Vasconez L. *The Intraoperative Use of Fluorescein as an Indicator of Tissue Viability.* West J Med 1980. **133**(1): p. 58-59.

74. Bron A J, Evans V E, and Smith J A. *Grading of corneal and conjunctival staining in the context of other dry eye tests.* Cornea, 2003. **22**(7): p. 640-50.

75. Jennings B J and Mathews D E. *Adverse reactions during retinal fluorescein angiography.* Journal of the American Optometric Association, 1994. **65**(7): p. 465-71.

76. Maurice D M. *The use of fluorescein in ophthalmological research.* Investigative Ophthalmology, 1967. **6**(5): p. 464-77.

77. Miller W L, Narayanan S, Jackson J, *et al. The association of bulbar conjunctival folds with other clinical findings in normal and moderate dry eye subjects.* Optometry (St Louis, Mo), 2003. **74**(9): p. 576-82.

78. Macri A, Rolando M, and Pflugfelder S. *A standardized visual scale for evaluation of tear fluorescein clearance.* Ophthalmology, 2000. **107**(7): p.1338-43.

79. Romanchuk K G. *Fluorescein. Physiochemical factors affecting its fluorescence.* Survey of Ophthalmology, 1982. **26**(5): p. 269-83.

80. McLaren J W and Brubaker R F. *Light sources for fluorescein fluorophotometry.* Applied Optics, 1983. **22**: p. 2897-2905.

81. Margrain T H, Boulton M, Marshall J, *et al. Do blue light filters confer protection against age-related macular degeneration?* Progress in Retinal & Eye Research, 2004. **23**(5): p. 523-31.

82. Calkins J L, Hochheimer B F, and D'Anna S A. *Potential hazards from specific ophthalmic devices.* Vision Research, 1980. **20**(12): p. 1039-53.

83. Wang L and Gaigalas A K. *Quantitating fluorescence intensity from fluorophores: practical use of MESF values.* Journal of the National Institute of Standards and Technology, 2002. **1.7**: p. 339-353.

84. Norn M S. *Tear fluid pH in normals, contact lens wearers, and pathological cases.* Acta Ophthalmologica, 1988. **66**(5): p. 485-9.

85. Kinura S J. *A simple means of insuring the use of sterile fluorescein.* American Journal of Ophthalmology, 1951. **34**(3): p. 446-7.

86. Cheung A T, Ramanujam S, Greer D A, *et al. Microvascular abnormalities in the bulbar conjunctiva of patients with type 2 diabetes mellitus.* Endocrine Practice, 2001. **7**(5): p. 358-63.

87. Klaassen-Broekema N and van Bijsterveld O P. *Diffuse and focal hyperaemia of the outer eye in patients with chronic renal failure.* International Ophthalmology, 1993. **17**(5): p. 249-54.

88. Wikipedia. On-line encyclopaedia. *Reliability.* [cited may 2006]. Available from: www.wikipedia.com,

89. Bland J M and Altman D G. *Measurement error and correlation coefficients.* BMJ, 1996. **313**(7048): p. 41-2.

90. Mercsourse. Online dictionary. *Sensitivity.* [Cited may 2006]. Available from: www.mercksource.com,

91. Altman D G and Bland J M. *Diagnostic tests. 1: Sensitivity and specificity.[see comment].* BMJ, 1994. **308**(6943): p. 1552.

92. Peterson R C and Wolffsohn J S. *The effect of digital image resolution and compression on anterior eye imaging.* British Journal of Ophthalmology, 2005. **89**(7): p. 828-830.

93. Mikhailishchuk V S. *Age-related characteristics of the conjunctival microcirculation in healthy persons and hypertensives.* Kardiologiia, 1982. **22**(3): p. 62-6.

94. Korkushko O V, Lishnevs'ka V I, Chyzhova V P, *et al. [Characteristics of hypoxia development in aged people].* Fiziologicheskii Zhurnal, 2003. **49**(3): p. 50-7.

95. Connor C G, Flockencier L L, and Hall C W. *The influence of gender on the ocular surface.* Journal of the American Optometric Association, 1999. **70**(3): p. 182-6.

96. Steuhl K P, Sitz U, Knorr M, *et al. [Age-dependent distribution of Langerhans cells within human conjunctival epithelium].* Ophthalmologe, 1995. **92**(1): p.21-5.

97. Vujkovic V, Mikac G, and Kozomara R. *Distribution and density of conjunctival goblet cells.* Medicinski Pregled, 2002. **55**(5-6): p. 195-200.

98. Josephson J E and Caffery B E. *Corneal staining after instillation of topical anesthetic (SSII).* Investigative Ophthalmology & Visual Science, 1988. **29**(7): p. 1096-9.

99. Josephson J E and Caffery B E. *Corneal staining characteristics after sequential instillations of fluorescein.[erratum appears in Optom Vis Sci 1992 Sep;69(9):727].* Optometry & Vision Science, 1992. **69**(7): p. 570-3.

100. Korb D R. *Survey of preferred tests for diagnosis of the tear film and dry eye.* Cornea, 2000. **19**(4): p. 483-6.

101. Caffery B E and Josephson J E. *Corneal staining after sequential instillations of fluorescein over 30 days.* Optometry & Vision Science, 1991. **68**(6): p. 467-9.

102. Korb D R and Herman J P. *Corneal staining subsequent to sequential fluorescein instillations.* Journal of the American Optometric Association, 1979. **50**(3): p. 361-7.

103. Schwallie J D, McKenney C D, Long W D, Jr., *et al. Corneal staining patterns in normal non-contact lens wearers.* Optometry & Vision Science, 1997. **74**(2): p. 92-8.

104. Millodot M. *The influence of age on the sensitivity of the cornea.* Investigative Ophthalmology & Visual Science, 1977. **16**: p. 240-242.

105. Millodot M and Owens H. *The influence of age on the fragility of the cornea.* Acta Ophthalmologica 1984. **62**: p. 819-824.

106. Murphy P J, Lau J S C, Sim M M, *et al. How red is a white eye? Clinical grading of normal conjunctival hyperaemia.* Eye, 2006. E-publication ahead of print.

107. Fullard R J and Wilson G S. *Investigation of sloughed corneal epithelial cells collected by non-invasive irrigation of the corneal surface.* Current Eye Research, 1986. **5**(11): p. 847-56.

108. Schwallie J D, Long W D, Jr., and McKenney C D. *Day to day variations in ocular surface staining of the bulbar conjunctiva.* Optometry & Vision Science, 1998. **75**(1): p. 55-61.

109. Carney L. *Human tear pH. Diurnal variations.* Archives of Ophthalmology, 1976. **94**(5): p. 821-4.

110. Korb D R, Allansmith M R, Greiner J V, *et al. Biomicroscopy of papillae associated with hard contact lens wearing.* Ophthalmology 1981. **88**(11):p.1132-6

111. Saini J S, Rajwanshi A, and Dhar S. *Clinicopathological correlation of hard contact lens related changes in tarsal conjunctiva by impression cytology.* Acta Ophthalmologica, 1990. **68**(1): p. 65-70.

112. McMonnies C W. *Key questions in a dry eye history.* Journal of the American Optometric Association, 1986. **57**(7): p. 512-7.

113. Maruyama K, Yokoi N, Takamata A, *et al. Effect of environmental conditions on tear dynamics in soft contact lens wearers.* Investigative Ophthalmology & Visual Science, 2004. **45**(8): p. 2563-8.

114. Begley C G, Chalmers R L, Mitchell G L, *et al. Characterization of ocular surface symptoms from optometric practices in North America.* Cornea, 2001. **20**(6): p. 610-8.

115. Pritchard N, Fonn D, and Brazeau D. *Discontinuation of contact lens wear: a survey.* Int. Contact Lens Clin, 1999. **26**(6): p. 157-162.

116. Riley C, Chalmers R L, and Pence N. *The impact of lens choice in the relief of contact lens related symptoms and ocular surface findings.* Contact Lens & Anterior Eye, 2005. **28**(1): p. 13-9.

117. Foulks G N. *What is dry eye and what does it mean to the contact lens wearer?* Eye & Contact Lens: Science & Clinical Practice. 2003 **29**(1 Suppl): p. S96-100; discussion S115-8.

118. Fonn D, Situ P, and Simpson T. *Hydrogel lens dehydration and subjective comfort and dryness ratings in symptomatic and asymptomatic contact lens wearers.* Optometry & Vision Science, 1999. **76**(10): p. 700-4.

119. Garofalo R J, Dassanayake N, Carey C, *et al. Corneal staining and subjective symptoms with multipurpose solutions as a function of time.* Eye & Contact Lens: Science & Clinical Practice, 2005. **31**(4): p. 166-74.

120. Jones L, May C, Nazar L, *et al. In vitro evaluation of the dehydration characteristics of silicone hydrogel and conventional hydrogel contact lens materials.* Contact Lens & Anterior Eye, 2002. **25**(3): p. 147-56.

121. Guillon M, Styles E, Guillon J P, *et al. Preocular tear film characteristics of nonwearers and soft contact lens wearers.* Optometry & Vision Science, 1997. **74**(5): p. 273-9.

122. Ketelson H A, Meadows D L, and Stone R P. *Dynamic wettability properties of a soft contact lens hydrogel.* Colloids & Surfaces: Biointerfaces, 2005. **40**(1): p.1-9

123. Cedarstaff T H and Tomlinson A. *A comparative study of tear evaporation rates and water content of soft contact lenses.* American Journal of Optometry & Physiological Optics, 1983. **60**(3): p. 167-74.

124. Lemp M A. *Is the dry eye contact lens wearer at risk? Yes.* Cornea, 1990. **9** Suppl 1: p. S48-50; discussion S54.

125. Perry H D and Donnenfeld E D. *Dry eye diagnosis and management in 2004.* Current Opinion in Ophthalmology, 2004. **15**(4): p. 299-304.

126. Sorbara L, Simpson T, Vaccari S, *et al. Tear turnover rate is reduced in patients with symptomatic dry eye.* Contact Lens and Anterior Eye, 2004. **27**(1): p. 15-20.

127. Doughty M J. *Re-wetting, comfort, lubricant and moisturizing solutions for the contact lens wearer.* Contact Lens & Anterior Eye, 1999. **22**(4): p. 116-26.

128. Kita M, Ogura Y, Honda Y, *et al. Evaluation of polyvinyl alcohol hydrogel as a soft contact lens material.* Graefes Archive for Clinical & Experimental Ophthalmology, 1990. **228**(6): p. 533-7.

129. Terry R L, Schnider C M, Holden B A, *et al. CCLRU standards for success of daily and extended wear contact lenses.* Optometry & Vision Science, 1993. **70**(3): p. 234-43.

130. Lloyd A W, Faragher R G, and Denyer S P. *Ocular biomaterials and implants.* Biomaterials, 2001. **22**(8): p. 769-85.

131. Gulsen D and Chauhan A. *Ophthalmic drug delivery through contact lenses.* Investigative Ophthalmology & Visual Science, 2004. **45**(7): p. 2342-7.

132. Long B and McNally J. *The clinical performance of a silicone hydrogel lens for daily wear in an asian population.* Eye & Contact Lens, 2006. **32**(2): p. 65-71.

133. Chalmers R L, Dillehay S, Long B, *et al. Impact of previous extended and daily wear schedules on signs and symptoms with high Dk lotrafilcon A lenses.* Optometry & Vision Science, 2005. **82**(6): p. 549-54.

134. Hom M and De Land P. *Prevalence and severity of symptomatic dry eyes in Hispanics.* Optometry & Vision Science, 2005. **82**(3): p. 206-8.

135. Glasson M J, Stapleton F, Keay L, *et al. Differences in clinical parameters and tear film of tolerant and intolerant contact lens wearers.* Investigative Ophthalmology & Visual Science, 2003. **44**(12): p. 5116-24.

136. Johnson M E and Murphy P J. *The agreement and repeatability of tear meniscus height measurement methods.* Optometry & Vision Science, 2005. **82**(12): p. 1030-7.

137. Wakefield D and Chang J H. *Epidemiology of uveitis.* International Ophthalmology Clinics, 2005. **45**(2): p. 1-13.

138. Chang J H, McCluskey P J, and Wakefield D. *Acute anterior uveitis and HLA-B27.* Survey of Ophthalmology, 2005. **50**(4): p. 364-88.

139. Rothova A, Suttorp-van Schulten M S, Frits Treffers W, *et al. Causes and frequency of blindness in patients with intraocular inflammatory disease.* British Journal of Ophthalmology, 1996. **80**(4): p. 332-6.

140. Wirbelauer C. *Management of the red eye for the primary care physician.* American Journal of Medicine, 2006. **119**: p. 302-306.

141. Yang P, Fang W, Jin H, *et al. Clinical features of Chinese patients with Fuchs' syndrome.* Ophthalmology, 2006. **113**(3): p. 473-80.

142. Suarez E, Torres F, Vieira J C, *et al. Anterior uveitis after laser in situ keratomileusis.* Journal of Cataract & Refractive Surgery, 2002. **28**(10): p.1793-8.

143. Hogan M J, Kimura S J, and Thygeson P. *Signs and symptoms of uveitis. I. Anterior uveitis.* 1959. **47**(5 part 2): p. 155-170.

144. BenEzra D, Cohen E, and Maftzir G. *Uveitis in children and adolescents.* British Journal of Ophthalmology, 2005. **89**(4): p. 444-8.

145. Herman D C, Palestine A G, and Nussenblatt R B. *Ocular fluorescein clearance in patients with hypotony secondary to chronic uveitis.* Journal of Ocular Pharmacology, 1988. **4**(4): p. 327-33.

146. Blanksma L J, Kooijman A C, Roze J H, *et al. Clinical applications of fluorometry.* Documenta Ophthalmologica, 1983. **55**(1-2): p. 37-40.

147. Saari K M. *Anterior segment fluorescein angiography in inflammatory diseases of the cornea.* Acta Ophthalmologica, 1979. **57**(5): p. 781-93.

148. Sherwin T and Brookes N H. *Morphological changes in keratoconus: pathology or pathogenesis.* Clinical & Experimental Ophthalmology, 2004. **32**(2): p. 211-7.

149. Wikipedia. Online encyclopaedia. *Keratoconus.* [cited may 2006] Available from: www.wikipedia.com

150. Assiri A A, Yousuf B I, Quantock A J, *et al. Incidence and severity of keratoconus in Asir province, Saudi Arabia.* British Journal of Ophthalmology, 2005. **89**(11): p. 1403-6.

151. Dogru M, Karakaya H, Ozcetin H, *et al. Tear function and ocular surface changes in keratoconus.* Ophthalmology, 2003. **110**(6): p. 1110-8.

152. Zadnik K, Barr J T, Edrington T B, *et al. Corneal scarring and vision in keratoconus: a baseline report from the Collaborative Longitudinal Evaluation of Keratoconus (CLEK) Study.* Cornea, 2000. **19**(6): p. 804-12.

153. Zadnik K, Barr J T, Edrington T B, *et al. Baseline findings in the Collaborative Longitudinal Evaluation of Keratoconus (CLEK) Study.* Investigative Ophthalmology & Visual Science, 1998. **39**(13): p. 2537-46.

154. Edwards M, McGhee C N, and Dean S. *The genetics of keratoconus.[see comment].* Clinical & Experimental Ophthalmology, 2001. **29**(6): p. 345-51.

155. Barr J T and Yackels T. *Corneal scarring in keratoconus-measurements and influence on visual acuity.* Int Contact Lens Clin, 1991. **22**: p. 173-175.

156. Barr J T, Gordon M O, Zadnik K, *et al. A corneal scarring photodocumentation and reading method.* J Refract Surg 1996. **12**: p. 492-500.

157. Barr J T, Schechtman K B, Fink B A, *et al. Corneal scarring in the Collaborative Longitudinal Evaluation of Keratoconus (CLEK) Study: baseline prevalence and repeatability of detection.* Cornea, 2000. **18**: p. 34-46.

158. Tomidokoro A, Oshika T, Amano S, *et al. Changes in anterior and posterior corneal curvatures in keratoconus.* Ophthalmology, 2000. **107**(7): p. 1328-1332.

159. Yue B, Zhou L, Fukuchi T, *et al. 2313 Lysosomal enzyme activities in conjunctivae and skin biopsy specimens of patients with keratoconus.* Vision Research, 1995. **35**(Supplement 1): p. S103-S103.

160. McMonnies C W and Boneham G C. *Keratoconus, allergy, itch, eye-rubbing and hand-dominance.* Clinical & Experimental Optometry, 2003. **86**(6): p. 376-84.

161. McMonnies C W. *The biomechanics of keratoconus and rigid contact lenses.* Eye & Contact Lens: Science & Clinical Practice, 2005. **31**(2): p. 80-92.

162. Ioannidis A S, Speedwell L, and Nischal K K. *Unilateral keratoconus in a child with chronic and persistent eye rubbing.* American Journal of Ophthalmology, 2005. **139**(2): p. 356-357.

163. Cristina Kenney M and Brown D J. *The Cascade Hypothesis of Keratoconus.* Contact Lens and Anterior Eye, 2003. **26**(3): p. 139-146.

164. Krachmer J H, Feder R S, and Belin M W. *Keratoconus and related noninflammatory corneal thinning disorders.* Survey of Ophthalmology, 1984. **28**(4): p. 293-322.

165. Coyle J T. *Keratoconus and eye rubbing.* American Journal of Ophthalmology, 1984. **97**(4): p. 527-8.

166. Stein H A, Demers J P, Searle R R, *et al. Multicentre comparative clinical evaluation of daily care solutions for rigid gas-permeable contact lenses.* Canadian Journal of Ophthalmology, 1984. **19**(4): p. 169-72.

167. Jupiter D and Karesh J. *Ptosis associated with PMMA/rigid gas permeable contact lens wear.* CLAO Journal, 1999. **25**(3): p. 159-62.

168. Dunn J P, Jr., Weissman B A, Mondino B J, *et al. Giant papillary conjunctivitis associated with elevated corneal deposits.* Cornea, 1990. **9**(4): p. 357-8.

169. Wilson S E and Kim W J. *Keratocyte apoptosis: implications on corneal wound healing, tissue organization, and disease.* Investigative Ophthalmology & Visual Science, 1998. **39**(2): p. 220-6.

170. Kaldawy R M, Wagner J, Ching S, *et al. Evidence of apoptotic cell death in keratoconus.* Cornea, 2002. **21**(2): p. 206-9.

171. Moon J W, Shin K C, Lee H-J, *et al. The effect of contact lens wear on the ocular surface changes in keratoconus.* Eye & Contact Lens: Science & Clinical Practice, 2006. **32**(2): p. 96-101.

172. Itoh R, Yokoi N, and Kinoshita S. *Tear film instability induced by rigid contact lenses.* Cornea, 1999. **18**(4): p. 440-3.

173. Fonn D, Gauthier C A, and Pritchard N. *Patient preferences and comparative ocular responses to rigid and soft contact lenses.* Optometry & Vision Science, 1995. **72**(12): p. 857-63.

174. Begley C G, Weirich B, Benak J, *et al. Effects of rigid gas permeable contact lens solutions on the human corneal epithelium.* Optometry & Vision Science, 1992. **69**(5): p. 347-53.

175. Dangel M E, Kracher G P, and Stark W J. *Anterior corneal mosaic in eyes with keratoconus wearing hard contact lenses.* Archives of Ophthalmology, 1984. **102**(6): p. 888-90.

176. Caldwell D R, Kastl P R, Dabezies O H, *et al. The effect of long-term hard lens wear on corneal endothelium.* Contact & Intraocular Lens Medical Journal, 1982. **8**(2): p. 87-91.

177. Abdul-Fattah A M, Bhargava H N, Korb D R, *et al. Quantitative in vitro comparison of fluorescein delivery to the eye via impregnated paper strip and volumetric techniques.* Optometry & Vision Science, 2002. **79**(7): p. 435-8.

178. Harper R N, Moore M A, Marr M C, *et al. Arteriolar rarefaction in the conjunctiva of human essential hypertensives.* Microvascular Research, 1978. **16**(3): p. 369-372.

179. Owen C G, Newsom R S B, Rudnicka A R, *et al. Vascular Response of the Bulbar Conjunctiva to Diabetes and Elevated Blood Pressure.* Ophthalmology, 2005. **112**(10): p. 1801-1808.

180. Fenton B M, Zweifach B W, and Worthen D M. *Quantitative morphometry of conjunctival microcirculation in diabetes mellitus.* Microvascular Research, 1979. **18**(2): p. 153-166.

APPENDICIES

APPENDIX A:

PUBLISHED WORK

1. Wolffsohn JS, Peterson RC. Anterior Ophthalmic Imaging. Clin Exp Optom. 2006; 89 (4) 205-214. *Refer to Chapter 1*

2. Peterson RC, Wolffsohn JS. The Effect of Digital Image Resolution and Compression on Anterior Eye Imaging. BrJ Ophthalmol 2005; 89:828-830. *Refer to Chapter 2.*

3. Peterson RC, Wolffsohn JS, Fowler CF. Optimization of Anterior eye Fluorescein Viewing. *In Press. Refer to Chapter 3*

4. Peterson RC, Wolffsohn JS. Nick J. Winterton L, Lally J.Clinical Performance of Daily Disposable Soft Contact Lenses Using Sustained Release Technology. *Refer to Chapter 8.*

APPENDIX B:

SAMPLE DATA.

The nature of the data collected is complex and the full extent is considered too large (mainly due to the many different superfluous objective measures and the repeats) to include in this thesis. A sample of raw and filtered data has therefore been extracted from each chapter, and is displayed over the following pages.

CHAPTER 2: Example of raw data from objective analysis of images taken from the CoolPix camera.
Highlighted measures were utilised to compare the changes in objective assessement

Image Quality Comp or Res	Area of Vessel cover % Area of Vessels	Overall Severity	Max Severity	Area Selected 1000 Square Pixels	No.of particles	Red Intensity	Blue Intensity	Green Intensity	R/R+G+B	G/R+G+B
						Luminance Intensity			Proportion of Total Luminance	
BULBAR										
JPEG12	0.588	18.379	180	574.464	884	204.31	173.106	117.397	0.413	0.35
JPEG9	0.587	18.466	180	574.464	899	204.36	173.045	117.591	0.413	0.35
JPEG6	1.257	21.738	200	574.464	2253	204.322	173.094	117.427	0.413	0.35
JPEG3	0.479	12.873	200	574.464	582	204.61	172.936	117.707	0.413	0.349
JPEG0	0.596	14.049	220	574.464	765	204.722	173.177	117.999	0.413	0.349
BMP	0.884	21.341	180	574.464	1616	204.213	173.141	117.215	0.413	0.35
2048	0.884	21.341	180	574.464	1616	204.213	173.141	117.215	0.413	0.35
1600	1.189	20.736	200	351.816	951	204.018	173.003	117.056	0.413	0.35
1280	1.778	21.126	200	223.232	737	204.059	173.067	117.122	0.413	0.35
1024	2.87	22.565	220	143.5	644	204.123	173.008	117.078	0.413	0.35
767	4.683	25.238	240	79.56	514	204.19	173.25	117.285	0.413	0.35
640	6.81	28.212	240	55.372	405	204.375	173.339	117.431	0.413	0.35
320	12.958	36.929	255	13.86	195	204.274	173.351	117.4	0.413	0.35
160	11.529	39.026	255	3.348	75	204.698	173.568	117.657	0.413	0.35
PALPEBRAL										
JPEG12	0.219	19.708	140	965.568	1397	237.823	85.569	2.852	0.729	0.262
JPEG9	0.231	20.156	140	965.568	1515	237.694	85.521	3.191	0.728	0.262
JPEG6	0.25	18.591	140	965.568	1527	237.972	85.267	3.323	0.729	0.261
JPEG3	0.033	12.263	100	965.568	196	237.96	85.127	3.476	0.729	0.261
JPEG0	0.011	10.743	100	965.568	57	237.803	85.085	3.37	0.729	0.261
BMP	0.143	19.102	120	965.568	979	238.022	85.543	2.201	0.731	0.263
2048	0.143	19.102	120	965.568	979	238.022	85.543	2.201	0.731	0.263
1600	0.043	17.415	120	596	182	237.128	84.909	2.103	0.732	0.262
1280	0.008	15.464	100	296.8	18	238.924	87.726	2.298	0.726	0.267
1024	0.002	14.766	80	234.98	5	238.803	86.125	2.308	0.73	0.263
767	0.016	14.835	80	135.184	17	237.895	85.46	2.358	0.73	0.262
640	0.043	15.731	100	91.008	26	238.604	86.005	2.404	0.73	0.263
320	0.846	21.235	100	22.932	83	238.273	85.83	2.401	0.73	0.263
160	1.525	24.61	100	4.72	32	239.522	86.126	2.382	0.73	0.263
STAINING										
JPEG12	0.168	12.703	255	906.752	755	2.852	13.631	3.117	0.146	0.695
JPEG9	0.19	13.783	255	906.752	927	3.103	13.647	3.295	0.155	0.681
JPEG6	0.22	11.854	255	906.752	1052	3.084	13.447	3.231	0.156	0.68
JPEG3	0.076	5.908	255	906.752	281	3.004	13.197	3.237	0.155	0.679
JPEG0	0.024	4.4	255	906.752	41	2.913	13.142	3.327	0.15	0.678
BMP	0.162	12.407	255	906.752	737	2.664	13.672	2.972	0.138	0.708
2048	0.155	12.255	255	904.728	706	2.631	13.223	2.936	0.14	0.704
1600	0.048	10.435	255	555.408	94	2.655	13.418	2.956	0.14	0.705
1280	0.035	8.66	255	352.656	14	2.662	13.353	2.962	0.14	0.704
1024	0.045	7.34	255	224	4	2.676	13.355	2.977	0.141	0.703
767	0.037	6.224	255	129.888	4	2.649	13.446	2.946	0.139	0.706
640	0.037	6.466	140	85.488	1	2.654	12.478	2.952	0.147	0.69
320	0.111	7.44	100	22.436	14	2.755	14.079	3.049	0.139	0.708
160	0.49	10.426	100	5.304	10	2.661	11.834	2.957	0.152	0.678

CHAPTER 2: Example of collated data from subjective results ranking of images taken with the CoolPix camera.
Subjective results were re-ordered and ranked.

Separated ranks of resolution

	Image order	A	B	C	D	E	F	G
bulbar	Quality	1600	1280	1024	767	640	320	160
CPX	Px 1	1	3	4	2	5	6	7
	Px 2	3	1	4	2	5	6	7
	Px 3	3	2	4	1	5	6	7
	Px 4	3	2	4	1	5	6	7
	Px 5	2	5	1	3	4	6	7
	Px 6	2	4	3	1	5	6	7
	Px 7	1	3	4	2	5	6	7
	Px 8	4	3	2	1	5	6	7
	Px 9	1	3	2	5	4	6	7
	Px 10	3	2	1	4	5	6	7
	Px 11	4	1	3	2	5	6	7
	Px 12	4	6	1	3	2	5	7
	Px 13	4	5	2	1	3	6	7
	Px 14	4	1	3	6	2	5	7
	Px 15	3	6	1	4	2	5	7
	Px 16	4	1	3	2	5	6	7
	Px 17	4	1	6	3	2	5	7
	Px 18	4	1	3	2	5	6	7
	Px 19	3	2	4	5	1	6	7
	Px 20	4	1	3	2	5	6	7
	MEAN	3.05	2.65	2.9	2.6	4	5.8	7

Separated ranks of compression

	Image or	Ac	Bc	Cc	Dc	Ec	Fc
bulbar	Quality	JPEG12	JPEG9	JPEG6	JPEG3	JPEG0	BMP
CPX	Px 1	4	1	2	5	6	3
	Px 2	2	1	4	5	6	3
	Px 3	5	1	4	2	6	3
	Px 4	3	1	4	2	6	5
	Px 5	3	1	4	2	6	5
	Px 6	3	1	4	2	6	5
	Px 7	4	1	2	5	6	3
	Px 8	3	1	4	2	6	5
	Px 9	1	3	2	4	6	5
	Px 10	5	1	3	4	2	6
	Px 11	1	3	2	4	6	5
	Px 12	3	5	2	1	4	6
	Px 13	4	3	5	1	2	6
	Px 14	3	5	2	4	6	1
	Px 15	2	3	5	4	6	1
	Px 16	3	5	2	6	1	4
	Px 17	3	5	2	4	6	1
	Px 18	3	4	1	6	2	5
	Px 19	3	5	2	6	4	1
	Px 20	3	5	2	4	6	1
		3.05	2.75	2.9	3.65	4.95	3.7

CHAPTER 3: Examples of raw data obtained from objective analysis of video images of fluorescein fluorescence.

Data up to 4 seconds is displayed. The measures continued over 8 minutes. Objective analysis was in the form of luminous intensity measures.

TIME		FLUORET MOISTENED , IMAGE SUBJECT												
SECONDS	MINUTES	ANALYSED	1								10	Av	SD	
1	0.0166667	1	0.40	0 00	0.20	0 00	0.00	0.00	0.00	21.00	24.80	2.60	4.90	9.56
		2	0.40	0 00	0.20	0.00	0.00	0.00	0.00	22.00	26.00	2.80	5.14	10.02
		3	0.40	0.00	0.20	0.00	0.00	0.00	0.00	23.40	27.00	2.60	5.36	10.52
		4	0.40	0.00	0.20	0.00	0.00	0 00	0.00	23 80	27.20	2.60	5.42	10 64
		5	0 20	0.00	0.20	0 00	0.00	0.00	12.40	24 00	25.00	2.60	6.44	10 26
		6	0.20	0.00	0.20	0 00	0.00	0.00	20.00	24.00	23.60	2 60	7.06	10.76
		7	0.00	0.00	0.20	0.00	0.00	0.00	19 60	23.80	21 80	2.80	6.82	10 37
		8	0 00	0.00	0.20	0.00	0.00	0.00	24.60	23 60	21.40	2.60	7.24	11.07
		9	0.00	0.00	0.20	0.00	0.00	0.00	26 00	23.60	21.60	2.60	7.40	11.35
		10	0.00	0.00	0.20	0.00	0.00	0.00	25 60	23.40	22.00	2.60	7.38	11.30
		11	0 00	0.00	0.20	0.00	0.00	0 00	22.40	21.80	19 40	2.60	6 64	10 11
		12	0 00	0.00	0.20	0 00	0.00	0.00	13.80	19 40	5.60	2.60	4 16	6 93
		13	0.00	0.00	0.20	0.00	0.00	0.00	10.60	19.20	0.00	2.20	3.22	6.52
		14	0.00	0.00	0.20	0.00	0.00	0.00	10 40	19.20	13.20	2.40	4.54	7.08
		15	0.00	0.00	0.20	0 00	0.00	0 00	10.20	19.80	25.80	2.40	5.84	9 58
		16	0.00	0.00	0.20	0.00	0.00	0.00	10.20	20.00	24 80	2.40	5.76	9.39
		17	0 00	0.00	0.20	0.00	0 00	0 00	9.80	20.40	24.20	2.00	5.66	9 32
		18	0.00	0.00	0.20	0.00	0.00	0.00	3.80	20.60	23.60	0.00	4.82	9.21
		19	0 00	0.00	0.20	0.00	0.00	0.00	2.80	20.60	23.00	0.00	4 66	9.09
		20	0 00	0.00	0.20	0 00	0.00	0.00	2.60	20.80	22.60	0 80	4 70	9 01
		21	0.20	0 00	0.20	0.00	0.00	0.00	2.60	21.00	22.00	7.20	5.32	8 82
		22	0 20	0.00	0.20	0.00	0 00	0.00	2.60	21 00	21 60	10 40	5 60	8 88
		23	0.40	0.00	0.20	0.00	0.00	0.00	2.60	21.00	21.60	11.40	5.72	8 93
		24	0.40	0.00	0 20	0.00	0 00	0.00	2.60	21.00	21 60	11.60	5.74	8 94
2	0.0333333	25	0.20	0.00	0.20	0.00	0.00	0.00	2.80	21.20	21.60	12.00	5.80	9.02
		26	0 40	0.00	0.20	0.00	0.00	0.20	2.80	21.00	21.60	12.20	5 84	8.97
		27	0.40	0.00	0.20	0.20	0.00	0.20	3.20	21.00	21.40	12.20	5 88	8 90
		28	0.60	0.00	0.20	0.20	0 00	0.20	3.20	21.00	21.00	12.40	5.88	8.82
		29	0.40	0.00	0 20	0.20	0.00	0.20	2.80	22.00	20.80	12.40	5.90	9 01
		30	0 40	0.00	0.20	0.20	0 00	0 60	2 60	25.00	11.00	12.60	5.26	8.40
		31	0.40	0.00	0.20	0.20	0 00	0.60	3.00	18.80	0 00	12.80	3.60	6 64
		32	0.40	0.00	0.20	0.20	0.00	1.00	3 00	11.20	1.00	12.80	2.98	4 85
		33	0 40	0.00	0.20	0.20	0.00	1.00	2.60	9.80	17.40	13.00	4.46	6.47
		34	0.40	0.00	0.20	0.20	0 00	1.00	2.20	9.20	22.00	12.80	4 80	7.51
		35	0.40	0.00	0.20	0.20	0.00	0 80	2.40	9.20	20.00	13.20	4.64	7 07
		36	0.40	0.00	0.20	0.20	0.00	0 80	2.40	10.80	1.80	13.20	2.98	4.85
		37	0.40	0.00	0.20	0 20	0.00	0.80	2.40	10.60	1.80	13 00	2.94	4 77
		38	0.40	0.00	0.20	0.20	0.00	1.00	2.40	10 60	14.80	12.80	4.24	5 99
		39	0.40	0.00	0 20	0.20	0.00	1 00	2.40	10.40	19 60	13 00	4 72	7.04
		40	0.40	0.00	0 20	0.20	0.00	1.00	2.40	10.60	19.20	14.20	4.82	7.13
		41	0 40	0 00	0 20	0 20	0.00	1.00	2.60	11.20	17 00	15 80	4 84	6 97
		42	0 40	0.00	0.20	0.20	0.00	1.00	2.60	11.40	16.40	16.40	4.86	6.99
		43	0.40	0.00	0.20	0.20	0.00	1.00	2.60	12.20	14.80	16 80	4 82	6.88
		44	0.40	0.00	0.20	0.20	0.00	1.00	2.60	12.80	14 60	16.60	4 84	6 88
		45	0 40	0.00	0.20	0.20	0 00	1.00	1.40	13.00	15 40	16 80	4 84	7.13
		46	0 40	0.00	0.20	0.20	0.00	1.00	0 00	13.40	15.40	16 80	4 74	7.27
		47	0.40	0.00	0.20	0.20	0.00	1.00	0.00	11.60	14.00	16.60	4,40	6 78
		48	0.40	0.00	0.20	0 20	0.00	1.00	0.00	6.20	13.20	16.40	3.76	6.16
3	0.05	49	0.40	0.00	0.20	0.20	0.00	1.00	0.00	7 00	14.60	16.40	3.98	6.45
		50	0.40	0.00	0.20	0.20	0.00	1.00	0.00	8.40	17.20	16.00	4 34	6 95
		51	0.40	0.00	0.20	0.20	0.00	1.00	0.00	11.00	19 00	14.20	4.60	7.25
		52	0 40	0 00	0.20	0.20	0 00	1.00	0 00	12.20	20.00	10.20	4.42	7.14
		53	0.40	0 00	0.20	0.20	0.00	1 00	0.00	12.40	10.20	0.20	2.46	4 70
		54	0.40	0.00	0.20	0.20	0.00	1.00	0.00	16.00	0 00	1.20	1.90	4.97
		55	0.40	0.00	0.20	0.20	0.00	0 80	0.00	5.00	14 60	12.00	3.32	5.51
		56	0.40	0.00	0.20	0.20	0.00	0.80	0.00	0.20	29 60	16 80	4 82	10.15
		57	0.40	0.00	0.20	0.20	0.00	0 80	0.00	0.00	28.00	17 80	4.74	9 87
		58	0 40	0 00	0 20	0.20	0 00	0 80	4.20	0 00	26 80	18 00	5 06	9 46
		59	0.40	0.00	0.20	0.20	0.00	0.80	10 00	0.00	25.80	18.20	5 56	9 36
		60	0 40	0.00	0.20	0 20	0.00	0.60	12 80	0 00	25.00	18 20	5.74	9.38
		61	0 40	0.00	0.20	0.20	0.00	0 60	15.80	0 00	24 40	18.40	6.00	9.57
		62	0.40	0 00	0.20	0.20	0.00	0.60	18.60	0.00	23.00	18.60	6.16	9 67
		63	0.40	0.00	0.20	0.20	0.00	0.80	19.80	0 00	22.60	18.80	6.28	9.79
		64	0.40	0.00	0.20	0.20	0.00	0.60	20.40	0.00	22.20	19.00	6.30	9 85
		65	0 40	0.20	0 20	0.20	0.00	0 60	21.00	0 00	20 80	19.80	6.32	9.81
		66	0 40	0.20	0 20	0.20	0.00	0 60	21.40	0.00	20.20	19.80	6.30	9.79
		67	0.40	0.20	0.20	0 20	0.00	0.60	21.60	0.00	19.80	19.80	6.28	9.76
		68	0.40	0.00	0 20	0.00	0.00	0.60	22.00	0.00	19.80	20 20	6 32	9.92
		69	0.40	0.00	0.20	0.00	0.00	0.60	22.60	0.00	19 80	20 20	6.38	10.02
		70	0 40	0.20	0.20	0.00	0.00	0.80	23 40	0.00	19.60	19 80	6 44	10.05
		71	0 40	0.20	0.20	0.00	0.00	0 80	25.20	0.00	19.60	20 20	6.66	10.46
		72	0 40	0 40	0.20	0.00	0.00	0 80	25 80	0 00	19 20	20 20	6 70	10 51
4		73	0 40	0 40	0.20	0.00	0 00	0.80	26 60	0 00	19.20	20.00	6.76	10 65
		74	0 40	0.40	0.20	0.00	0.00	0.60	28 20	0 00	19.20	20.00	6.90	11.00
		75	0.40	0 60	0 20	0.00	0.00	0 60	29.20	0.00	18.80	19 80	6.96	11.13
		76	0 40	0 60	0.20	0.00	0.00	0.60	29.60	0.00	18.80	20.20	7.04	11.27
		77	0.40	0.60	0 20	0 00	0.00	0.60	30.20	0.00	3.60	20.40	5.60	10.69
		78	0.40	0.60	0.20	0.00	0.00	0.40	35.20	0.00	0.00	20.40	5.72	12.15
		79	0 40	0 40	0 20	0 20	0 00	0 20	35 00	0 00	9 20	20 00	6 56	11 92

TIME		FLUORET MAXIMUM IMAGE	SUBJECT										
SECONDS	MINUTES	ANALYSED	[redacted]									Av	SD
1	0.0166667	1	0.2	0 8	51 2	0	0	7	14	1.4	20 6	0.2	9.54 16.273236
		2	0.2	0.8	49.4	0	0	7	13 6	1.4	20.4	0.2	9.3 15.734816
		3	0 2	0.8	49	0	0	7	13.2	1 4	19 8	0.2	9.16 15.563147
		4	0.2	0 8	48.6	0	0	7.2	12.8	1.2	19.6	0.2	9 06 15.431296
		5	0.2	0 8	48 6	0	0	8 6	12.6	1 4	19.4	0.2	9.18 15 387571
		6	0.2	0.8	48.4	0	0	11.4	12.8	1.4	19.2	0.2	9.44 15.335304
		7	0.2	0 8	49	0	0	12.2	12 6	1.2	19.2	0 2	9.54 15.525191
		8	0.2	0.8	49.6	0	0	9	12.6	1.4	19.2	0.2	9.3 15.657231
		9	0.2	0 8	49 8	0	0	6 4	12.4	1.4	16.6	0.2	8 78 15 571041
		10	0.2	0 8	49.8	0	0	6.6	9	1.2	0	0.2	6.78 15.445517
		11	0.2	0 8	49.6	0	0	6.6	2.8	1.2	0	0.2	6 14 15.408237
		12	0.2	0.8	49 6	0	0	6 6	0.4	1.2	0.8	0.2	5 98 15.452709
		13	0.2	0 8	49 4	0	0	6.6	0.2	1.2	14.8	0.2	7.34 15.514882
		14	0.2	0.8	49.6	0	0	6 6	0.2	1.2	17.6	0 2	7 64 15.747959
		15	0.2	0.8	49 6	0	0	6.4	0.2	1.2	17.4	0.2	7 6 15.735593
		16	0 2	0.8	49 4	0	0	6.4	0.2	1.4	16.4	0.2	7.5 15.600926
		17	0.2	0.6	49 6	0	0	6 4	0.2	1.2	16.4	0.2	7.48 15 679059
		18	0.2	0.8	49 4	0	0	6.4	0.8	1.2	16	0 2	7.5 15.554992
		19	0.2	0.8	49 4	0	0	6.6	1	1.2	15.6	0.2	7.5 15.520381
		20	0.2	0 8	49.2	0	0	6 6	11 2	1.2	15.4	0.2	8 48 15.311056
		21	0.2	0.8	48 8	0	0	6.6	18.8	1.2	15	0.2	9.16 15.515383
		22	0.2	0 8	48 8	0	0	6.6	15 8	1.2	14 8	0.2	8 84 15.327477
		23	0.2	0.8	49.2	0	0	6 6	14	1.2	15	0.2	8.72 15.37305
		24	0.2	0 8	50 4	0	0	6 6	13	1.2	14.8	0 2	8.72 15 682744
2	0.0333333	25	0.2	0 8	51.8	0	0	6 8	12.8	1.2	14.8	0.2	8.86 16.088381
		26	0.2	0.8	51 6	0	0	7	12.2	1.2	14 6	0.2	8 78 16.002903
		27	0.2	0.8	52	0	0	6.6	13.2	1.2	14 6	0.2	8 88 16.154036
		28	0 2	0.8	51.6	0	0	6 6	12.6	1.2	14 6	0.2	8.78 16 018448
		29	0.2	0 8	51.4	0	0	6 6	11.8	1.2	14 6	0.2	8 68 15.939664
		30	0.2	0.8	51.6	0	0	6.6	12.2	1.2	10.2	0.2	8 3 15 889409
		31	0.2	0 8	51.2	0	0	6 6	11.6	1.2	0	0 2	7.18 15.938061
		32	0.2	0.8	51	0	0	6.6	11.8	1.2	0.2	0.2	7.2 15.873108
		33	0.2	0.8	50.6	0	0	6.6	13 8	1.2	15.4	0.2	8 88 15.794289
		34	0.2	0 8	50.2	0	0	6.6	14	1.2	21 6	0.2	9 48 16.088699
		35	0 2	0.8	50 2	0	0	6.6	14.2	1.2	22	0.2	9 54 16.128939
		36	0.2	0.8	50.4	0	0	6.4	14.8	1.2	21.4	0.2	9 54 16.159497
		37	0.2	0.8	50	0	0	6 4	15	1.2	21	0.2	9.48 16 022262
		38	0.2	0.8	49 8	0	0	6 4	15.2	1.2	20.8	0.2	9 46 15.958014
		39	0 2	1	49.6	0	0	6 6	15.2	1.2	20 2	0.2	9.42 15 839318
		40	0.2	1	49 6	0	0	6.6	14 8	1.2	20.2	0.2	9 38 15.823597
		41	0 2	1	49 8	0	0	6 4	13.6	1.2	20	0.2	9 24 15 827908
		42	0.2	1	49.6	0	0	6.6	13	1.2	19.6	0.2	9.14 15.719782
		43	0 2	1	49.4	0	0	6 6	13.4	1 2	19.4	0.2	9 14 15 659445
		44	0.2	1	49.2	0	0	6 8	12.2	1.2	19.4	0.2	9.02 15.567045
		45	0.2	1	49	0	0	6 8	10.4	1.2	19 2	0.2	8 8 15.463793
		46	0.2	1	49	0	0	6 8	23.6	1.2	19	0.2	10 1 16.150748
		47	0.2	1	48 8	0	0	6 8	26.4	1.2	18 8	0.2	10.34 16.368819
		48	0.2	1	48 4	0	0	6 8	25.6	1.2	19	0.2	10.24 16.190203
3	0 05	49	0.2	1	48.4	0	0	6.6	42.8	1.2	18.8	0	11 9 18.731376
		50	0.2	1	48.4	0	0	6 6	45.2	1.2	19.2	0	12.18 19.197095
		51	0.2	1	48.6	0	0	6.6	44	1.2	18.8	0	12.04 18.996561
		52	0.2	1	49	0	0	6.8	44.8	1.2	19	3.8	12.58 19.00186
		53	0.2	1	49	0	0	8 6	49	1.2	19	17.8	14.58 19 523536
		54	0 2	1	48 4	0	0	10 8	52	1.2	19	24	15 66 20.139304
		55	0 2	1	48	0	0	11	52.2	1	18 8	26 8	15.9 20 263432
		56	0.2	1	47 8	0	0	10	49 8	1.2	18 8	27 4	15.62 19 809414
		57	0.2	1	47.8	0	0	9.6	50.4	1.2	18 6	28	15.68 19 974918
		58	0 2	1	47.6	0	0	10 6	49	1	18 6	28	15 6 19.656834
		59	0.2	1	47.6	0	0	11.4	43.6	1	18 8	28 2	15.18 18 687714
		60	0 2	1	47 6	0	0	11 6	35.6	1.2	18 6	28	14.38 17.423726
		61	0.2	1	47.6	0	0	11 6	31.8	1	18 6	28.2	14 16.979726
		62	0.2	1	47.8	0	0	11 8	35.2	1.2	18 2	28.2	14.36 17.416416
		63	0 2	1	47 6	0	0	11.8	36 6	1.2	18	28 2	14.46 17.560575
		64	0.2	1	47.8	0	0	12.4	35.2	1	18	28	14.36 17.402375
		65	0.2	1	48	0	0	13.2	34 6	1	17.8	28	14.38 17.353949
		66	0.2	1	48	0	0	14	34.2	1	17 8	27 8	14 4 17.281204
		67	0.2	1	47.8	0	0	14.8	35	1	18	27.4	14 52 17.31209
		68	0.2	1	47.4	0	0	15.2	35.6	1	17.6	27.4	14 54 17.299981
		69	0.2	1	47 6	0	0	16.2	36	1	17.4	27 4	14 68 17.399668
		70	0.2	1	48.2	0	0	17	36.8	1	17.8	27.2	14 92 17.635621
		71	0.2	1	48.2	0	0	16 8	36.4	1	17.6	27.4	14 86 17.590414
		72	0.2	1	48	0	0	15 8	32	1	17.2	27 4	14 26 16.973195
4		73	0 2	1	48	0	0	14 8	29 8	1	9	27.4	13.12 16.744936
		74	0.2	1	48	0	0	14 8	30.8	1	0 4	27.2	12.34 17.291501
		75	0.2	1	48 2	0	0	15.4	32 6	1	0	27.2	12.56 17.598939
		76	0.2	1	47.8	0	0	15 8	34	1	18.2	27	14.5 17.160225
		77	0.2	1	47 6	0	0	15.6	35.6	1	24.8	26 8	15.26 17.585107
		78	0.2	1	47.6	0	0	15.2	35.8	1	24.2	26.8	15.18 17.575349
		79	0 2	1	47 8	0	0	15 2	34	1	22	26 6	14 78 17 259445

TIME		1% MINIM											
		IMAGE	SUBJECT										
SECONDS	MINUTES	ANALYSED	1									Av	SD
1	0.0166667	1	4.6	0.2	0	0	0	0	0	8	5.4	12	3.02	4.3096275
		2	12.2	0.2	0	0	0	0	0	8	5.4	12	3.78	5.1978201
		3	16	0	0	0	0	0	0	8	5 4	11.6	4.1	5.9218991
		4	16.8	0	0	0	0	0	0	7.6	5 6	9 8	3.98	5 8594274
		5	17.4	0	0	0	0	0	0	7.6	5.6	18.4	4.9	7.3812074
		6	17 6	0	0	0	0	0	0	7.8	5.2	20	5.06	7.7574624
		7	17.8	0	0	0	0	0	0	7.8	5 4	20	5.1	7.7941574
		8	17.8	0	0	0	0	0	0	7.8	5.4	19.2	5.02	7.6265326
		9	17.6	0	0	0	0	0	0	7.4	5 4	13 6	4 4	6 540812
		10	18	0	0	0	0	0	0	7.2	5.4	0	3.06	5.8818364
		11	17 8	0	0	0	0	0	0	6 8	5 4	4 4	3.44	5.7083175
		12	17.8	0	0	0	0	0	0	6.8	5.2	15.6	4.54	6 890928
		13	17.8	0	0	0	0	0	0	6.8	5	16.4	4.6	7.0351498
		14	18	0	0	0	0	0	0	6.8	4.8	16.4	4 6	7.0760943
		15	18	0	0	0	0	0	0	6.8	4 8	16 8	4 64	7.150944
		16	17.8	0	0	0	0	0	0 2	6.8	4 8	15.6	4 52	6.8735887
		17	17 6	0	0	0	0	0	0.2	6.8	4.8	14 4	4.38	6 6214802
		18	17.6	0	0	0	0	0	0	6.8	4 8	14.4	4.36	6.6357952
		19	18	0.2	0	0	0	0	0	6.8	4 8	14.2	4 4	6.6779904
		20	18	0.2	0	0	0	0	0	6 6	4.6	13.8	4.32	6.6045102
		21	18	0.2	0	0	0	0	0	6.4	4 6	13.6	4.28	6.5653637
		22	18	0.2	0	0	0	0	0	6.4	4 8	13 4	4.28	6.5355098
		23	17.8	0.2	0	0	0	0	0	6.4	4 6	12.8	4.18	6.3954498
		24	17.8	0	0	0	0	0	0	6.2	4 6	12.6	4 12	6.3723012
2	0 0333333	25	17.8	0.2	0	0	0	0	0	5.8	4.6	13	4 14	6.4055878
		26	17 8	0.2	0	0	0	0	0	5.8	4.6	13.8	4.22	6.5322788
		27	17.8	0.2	0	0	0	0	0	3	4 6	13.6	3.92	6.4836204
		28	17 8	0.2	0	0	0	0	0	0	4.6	13 8	3.64	6.6331156
		29	17.8	0.2	0	0	0	0	0	0.2	4.6	14.4	3 72	6.7252096
		30	17.6	0.2	0	0	0	0	0	2.4	4.4	14.6	3.92	6 6199698
		31	17.4	0.2	0	0	0	0	0	4.8	4 4	14 4	4.12	6.5218947
		32	17.4	0 2	0	0	0	0	0	5.6	4.2	14 8	4.22	6.6060242
		33	17.4	0.2	0	0	0	0	0	6	4.2	14 6	4.24	6.5813204
		34	17 4	0.2	0	0	0	0	0	6.2	4.2	13.6	4.16	6.4185841
		35	17.4	0 2	0	0	0	0	0	6.2	4.2	13.2	4.12	6.3541413
		36	17.2	0.4	0	0	0	0	0	6.4	4.2	13.2	4 14	6.3020632
		37	17.2	0 4	0	0	0	0	0	6 4	4.2	11 6	3 98	6.0622328
		38	17.2	0.4	0	0	0	0	0	6.4	4.2	11.2	3.94	6.0074398
		39	17.2	0.4	0	0	0	0	0	6 4	4 2	11.2	3.94	6 0074398
		40	17	0.4	0	0	0	0	0	6 4	4.2	11.2	3.92	5.9585233
		41	16 8	0.4	0	0	0	0	0	6.2	4 4	11	3.88	5.8751454
		42	16.8	0.4	0	0	0	0	0	6.2	4 6	11 2	3.92	5 9045745
		43	16 8	0.4	0	0	0	0	0	6.2	4.6	11	3.9	5.8774522
		44	16.4	0 4	0	0	0	0	0	6 2	4 8	11	3.88	5.7836551
		45	16 4	0.4	0	0	0	0	0	6	4 8	10 4	3 8	5 6952222
		46	16.8	0 4	0	0	0	0	0	6	4 8	10.2	3 82	5.7692287
		47	16.4	0.4	0	0	0	0	0	5.8	4.8	10.8	3 82	5.73988
		48	16.4	0.4	0	0	0	0	0	5 8	4.8	12.6	4	6 0051829
3	0.05	49	16 4	0.4	0	0	0	0	0	0 8	4 4	13.8	3.58	6.2485198
		50	16.2	0.4	0	0	0	0	0	0	4.4	14	3.5	6.284549
		51	16 2	0.4	0	0	0	0	0	2.6	4.4	14	3.76	6.1765147
		52	16.2	0.4	0	0	0	0	0	5	4 4	14	4	6.1730597
		53	16	0.4	0	0	0	0	0	5.4	4.4	14.2	4.04	6.1743556
		54	16	0.4	0	0	0	0	0	6.2	4 4	14.8	4 18	6.3093933
		55	15 6	0 4	0	0	0	0	0	6.6	4.4	15.2	4.22	6.3192475
		56	15 6	0.6	0	0	0	0	0	6.6	4 4	16	4.32	6 4637107
		57	15.4	0.4	0	0	0	0	0	6.8	4 4	17 6	4.46	6 7803966
		58	15.4	0.4	0	0	0	0	0	7	5	19.4	4.72	7.187149
		59	15.2	0.4	0	0	0	0	0	6.8	5.4	19 4	4.72	7.1505711
		60	15	0.4	0	0	0.2	0	0	6 8	5 4	19 8	4.76	7.1961718
		61	14.6	0.4	0	0	0.2	0	0	6.6	5.2	20.4	4.74	7.2682261
		62	14 4	0 4	0	0	0.2	0	0	6.4	5.4	21 2	4.8	7.429072
		63	14.4	0.4	0	0	0.2	0	0	6.4	5.4	22.2	4.9	7.6769496
		64	14.6	0.4	0	0	0.2	0	0	6.4	5.8	23	5.04	7.9088136
		65	14.4	0 4	0	0	0.2	0	0	6 6	6 6	23 6	5.18	8 0506452
		66	14.4	0.4	0	0	0 2	0	0	6.6	7.2	22.6	5.14	7.8139761
		67	14 4	0.4	0	0	0.2	0	0	6.6	6.4	23	5.1	7.8950055
		68	14 4	0.4	0	0	0 4	0	0	6.8	6 6	23.2	5.18	7.9400252
		69	14.4	0.4	0	0	0.6	0	0	6.8	7	22.8	5.2	7 8355316
		70	14.4	0.4	0	0	0.6	0	0	7	6 6	23.6	5.26	8.0327386
		71	14 4	0.4	0	0	0.6	0	0	7.2	7	23 6	5.32	8 0460895
		72	14.2	0.4	0	0	0 6	0	0	7.4	6.6	23.6	5.28	8 0184232
4		73	14.4	0 4	0	0	0.6	0	0	7 2	6.6	23.4	5 26	7.9872398
		74	14.4	0 4	0	0	0.6	0	0	7.2	6 8	23 8	5.32	8.0923558
		75	14.2	0 4	0	0	0 8	0	0	7.2	6.8	23.4	5.28	7.9533082
		76	14	0.4	0	0	0 8	0.2	0	7.2	6 8	23	5 24	7.8126962
		77	14	0.4	0	0	0 8	0 2	0	7.2	6.8	23.4	5.28	7 9140943
		78	14	0.4	0	0	0 6	0.2	0	7	6 6	23.6	5.24	7 9687166
		79	14	0 4	0	0	0 6	0 2	0	7	6 6	24	5 28	8 0714586

TIME		2% MINIM	SUBJECT										
SECONDS	MINUTES	IMAGE ANALYSED	[illegible]									Av	SD
1	0 0166667	1	0 4	0.2	0	0.4	0	0	1.4	2	11.6	2	1.8 3.5352196
		2	0.4	0.2	0	0.4	0	0	1.2	2	7.6	2	1.38 2.3217809
		3	0 4	0.2	0	0.4	0	0	0 8	2	7.4	2	1.32 2.2690184
		4	0.4	0.2	0	0.4	0	0	0.8	2	7.2	2	1.3 2.2095751
		5	0 4	0.2	0	0.4	0	0	0 8	2	7	2	1.28 2.1503488
		6	0 4	0.2	0	0.4	0	0	0.8	2	16.6	2	2.24 5.1032016
		7	0.4	0.2	0	0 4	0	0	0.8	2	72.2	2	7 8 22.64077
		8	0.2	0.2	0	0.4	0	0	0.8	1 8	95.4	1 8	10.06 29.993488
		9	0 4	0 2	0	0.2	0	0	0 8	1.8	94	1 8	9.92 29.55089
		10	0.4	0 2	0	0.2	0	0	0.8	1 8	64	1.8	6 92 20 067929
		11	0 4	0.2	0	0 4	0	0	0 8	2	14.2	2	2 4.3543082
		12	0 2	0.2	0	0.4	0	0	0.6	2	7.6	2	1.3 2.3442601
		13	0.2	0.4	0	0.2	0	0	0.8	2	6.6	2	1.22 2.042765
		14	0.2	0.4	0	0.4	0	0	0.6	2	6.8	2	1.24 2.0971939
		15	0.4	0.2	0	0.4	0	0	0.6	1.2	6.6	1.2	1.06 1.9978878
		16	0.2	0.2	0	0.4	0	0	0 6	0 8	6.4	0 8	0 94 1.943765
		17	0.2	0.4	0	0 4	0	0	0 6	0.6	6.6	0.6	0.94 2.0045504
		18	0.2	0.4	0	0.4	0	0	0.6	0.6	6.6	0.6	0.94 2.0045504
		19	0.2	0 4	0	0 4	0	0	0.6	0.6	6.4	0.6	0 92 1.9418205
		20	0.2	0.4	0	0.4	0	0	0.6	0.8	6 6	0 8	0.98 1.9987774
		21	0.2	0.4	0	0.4	0	0	0.6	0.8	6.6	0.8	0.98 1.9987774
		22	0 2	0.4	0	0.4	0	0	0 6	0 8	6.6	0.8	0.98 1.9987774
		23	0.4	0 4	0	0 4	0	0.2	0 6	0 8	6.6	0.8	1.02 1.9809089
		24	0 4	0 4	0	0 4	0	0 4	0.6	0 8	6 6	0 8	1.04 1.9727026
2	0.0333333	25	0.4	0.2	0	0.4	0	0.4	0.6	0.8	6.6	0.8	1.02 1.9809089
		26	0.4	0.4	0	0.4	0	0.4	0 6	0 8	6 8	0 8	1.06 2.0353542
		27	0.4	0.4	0	0.4	0	0.4	0 6	0.8	6.6	0.8	1.04 1.9727026
		28	0.4	0.4	0	0.4	0	0.2	0 6	0.8	6.6	0 8	1.02 1.9809089
		29	0.4	0.4	0	0 4	0	0.2	0.6	1	6.8	1	1.08 2.0400436
		30	0 2	0.4	0	0.4	0	0.2	0.6	0.2	6.6	0.2	0.88 2 01814
		31	0.2	0.4	0	0.4	0	0.2	0.6	0	6.6	0	0.84 2.0348082
		32	0.4	0 4	0	0 4	0	0 2	0.6	0	6.8	0	0.88 2.0916766
		33	0 4	0.4	0	0.4	0	0.2	0 6	1.6	6.8	1.6	1 2 2.0504742
		34	0.4	0 4	0	0.4	0	0.2	0 6	1.2	6.8	1.2	1.12 2.0400436
		35	0 4	0 4	0	0 4	0	0.2	0.6	0.8	6 6	0.8	1.02 1 9809089
		36	0.4	0 4	0	0 4	0	0.2	0.6	0.8	6 4	0.8	1 1.9183326
		37	0.4	0 4	0	0.4	0	0.2	0.6	0.8	6.4	0.8	1 1.9183326
		38	0 4	0.4	0	0.4	0	0.2	0 6	0.8	6.4	0.8	1 1.9183326
		39	0.4	0.4	0	0.4	0	0.2	0.6	1	6.4	1	1 04 1.9155504
		40	0.4	0 4	0	0.4	0	0.2	0.6	1	6.4	1	1.04 1.9155504
		41	0.4	0.2	0	0 4	0	0.2	0.6	1	6 6	1	1.04 1 9861744
		42	0.2	0.2	0	0.4	0	0.2	0 6	1	6 6	1	1.02 1.9943253
		43	0.2	0.2	0	0.4	0	0.2	0 4	0.8	6 4	0.8	0.94 1.9391865
		44	0.4	0.2	0	0.4	0	0 2	0 6	0 8	6 4	0.8	0.98 1.9263091
		45	0.4	0.2	0	0.4	0	0.2	0.6	0 8	6.4	0 8	0.98 1.9263091
		46	0 4	0	0	0.4	0	0	0 4	0 8	6 4	0.8	0 92 1.9509542
		47	0.4	0	0	0 4	0	0	0.6	0.8	6.4	0 8	0.94 1.9460501
		48	0.4	0	0	0.4	0	0	0.2	0 8	6.4	0 8	0.9 1.95789
3	0.05	49	0 4	0	0	0.4	0	0	0 6	1	6.2	1	0.96 1.8827875
		50	0.4	0	0	0.4	0	0	0.2	0 8	6.2	0.8	0.88 1.8954917
		51	0.4	0	0	0.4	0	0 4	0.2	0 8	6.4	0 8	0.94 1.9414771
		52	0.4	0	0	0 4	0	0.4	0.2	0.8	6	0.8	0.9 1 8165902
		53	0.4	0	0	0.4	0	0 6	0.2	0.8	6	0 8	0.92 1.8115678
		54	0 4	0	0	0.4	0	0 8	0.2	0 8	6	0 8	0.94 1.8087442
		55	0.4	0	0	0.4	0	1	0.2	0.8	6	0 8	0.96 1.8081298
		56	0.4	0	0	0.6	0	1	0.2	0 8	6	0.8	0.98 1.8023442
		57	0.2	0	0	0 8	0	1	0.2	0.8	6	0.8	0.98 1.8072693
		58	0.4	0	0	1	0	0.8	0.2	0.8	6	0 8	1 1.798765
		59	0.4	0	0	1	0	0 8	0.2	0 8	6	0.8	1 1.798765
		60	0.2	0	0	1	0	0.8	0 2	0 8	6	0 8	0.98 1 8072693
		61	0 2	0	0	1	0	0 8	0.2	0 8	6	0.8	0 98 1.8072693
		62	0.2	0	0	1 4	0	0 6	0.2	0 8	6	0.8	1 1 8159785
		63	0	0	0	1.8	0	0 6	0.2	0.8	6	0 8	1.02 1.8413763
		64	0	0	0	1.8	0	0.6	0.2	0.8	6	0 8	1.02 1.8413763
		65	0.2	0	0	2	0	0.6	0.2	0 8	6	0.8	1.06 1 8404106
		66	0 4	0	0	2	0	0.6	0.2	0.8	6	0.8	1.08 1.8310895
		67	0.4	0	0	2	0	0.6	0.2	0 8	6	0.8	1.08 1 8310895
		68	0 4	0	0	2	0	0.6	0.2	0.8	6	0 8	1.08 1 8310895
		69	0.4	0	0	2	0	0.6	0.2	0.8	6	0.8	1.08 1.8310895
		70	0.4	0	0	2.2	0	0.6	0.2	0.8	6	0 8	1.1 1 8433062
		71	0.4	0	0	2.6	0	0.6	0.2	0 8	6	0.8	1.14 1.8739145
		72	0.4	0	0	2.6	0	0 6	0.2	0.6	6	0 6	1.1 1.8838495
4		73	0 4	0	0	2.4	0	0 6	0 2	0 8	6	0.8	1.12 1.857597
		74	0.4	0	0	2.4	0	0.6	0.2	0.8	6	0.8	1.12 1.857597
		75	0.4	0.4	0	2.2	0	0 6	0.2	0 8	6.2	0 8	1.16 1.8804255
		76	0.4	0 8	0	2.2	0	0.4	0 2	0.8	6.2	0 8	1.18 1.874863
		77	0 4	0 8	0	2.2	0	0 6	0.2	0.8	6.2	0 8	1.2 1.8666667
		78	0.4	0.8	0	2.2	0	0 4	0.2	0.8	7	0 8	1.26 2.1146053
		79	0 2	0 8	0	2 2	0	0 4	0 2	0 6	8 2 2	0 6	8 72 25 826119

CHAPTER 4: Objective analysis of thymoxamine instillation for subject 1 (initials HB)
Each image is measured 6 times. Area of BV and R/RGB values are extracted form the many objective measures
A sample of the raw data which continues up to image 45 for each of the 3 subjects is hoswn below

HB		AREA BV,								R/R+G+B	
Repeats	Image no.	% AREA								luminance	
1	1	1.067	21.525	180	50.625	134	129.954	112.466	110.992	0.368	0.318
2	1	1.067	21.525	180	50.625	134	129.954	112.466	110.992	0.368	0.318
3	1	1.067	21.525	180	50.625	134	129.954	112.466	110.992	0.368	0.318
4	1	1.067	21.525	180	50.625	134	129.954	112.466	110.992	0.368	0.318
5	1	1.067	21.525	180	50.625	134	129.954	112.466	110.992	0.368	0.318
6	1	1.067	21.525	180	50.625	134	129.954	112.466	110.992	0.368	0.318
1	2	1.412	21.755	180	50.625	161	129.111	110.813	109.188	0.37	0.317
2	2	1.412	21.755	180	50.625	161	129.111	110.813	109.188	0.37	0.317
3	2	1.412	21.755	180	50.625	161	129.111	110.813	109.188	0.37	0.317
4	2	1.412	21.755	180	50.625	161	129.111	110.813	109.188	0.37	0.317
5	2	1.412	21.755	180	50.625	161	129.111	110.813	109.188	0.37	0.317
6	2	1.412	21.755	180	50.625	161	129.111	110.813	109.188	0.37	0.317
1	3	1.499	21.985	180	50.625	160	129.227	110.667	108.67	0.371	0.317
2	3	1.499	21.985	180	50.625	160	129.227	110.667	108.67	0.371	0.317
3	3	1.489	22.022	180	50.625	160	129.355	110.75	108.769	0.371	0.317
4	3	1.489	22.022	180	50.625	160	129.355	110.75	108.769	0.371	0.317
5	3	1.489	22.022	180	50.625	160	129.355	110.75	108.769	0.371	0.317
6	3	1.489	22.022	180	50.625	160	129.355	110.75	108.769	0.371	0.317
1	4	1.545	22.225	200	50.625	176	129.354	110.511	108.446	0.371	0.317
2	4	1.545	22.225	200	50.625	176	129.354	110.511	108.446	0.371	0.317
3	4	1.545	22.225	200	50.625	176	129.354	110.511	108.446	0.371	0.317
4	4	1.545	22.225	200	50.625	176	129.354	110.511	108.446	0.371	0.317
5	4	1.545	22.225	200	50.625	176	129.354	110.511	108.446	0.371	0.317
6	4	1.545	22.225	200	50.625	176	129.354	110.511	108.446	0.371	0.317
1	5	1.211	21.704	140	50.625	173	128.381	109.537	108.357	0.371	0.316
2	5	1.211	21.704	140	50.625	173	128.381	109.537	108.357	0.371	0.316
3	5	1.211	21.704	140	50.625	173	128.381	109.537	108.357	0.371	0.316
4	5	1.211	21.704	140	50.625	173	128.381	109.537	108.357	0.371	0.316
5	5	1.211	21.704	140	50.625	173	128.381	109.537	108.357	0.371	0.316
6	5	1.211	21.704	140	50.625	173	128.381	109.537	108.357	0.371	0.316
1	6	1.231	21.699	180	50.625	161	127.301	108.409	107.367	0.371	0.316
2	6	1.231	21.699	180	50.625	161	127.301	108.409	107.367	0.371	0.316
3	6	1.231	21.699	180	50.625	161	127.301	108.409	107.367	0.371	0.316
4	6	1.231	21.699	180	50.625	161	127.301	108.409	107.367	0.371	0.316
5	6	1.231	21.699	180	50.625	161	127.301	108.409	107.367	0.371	0.316
6	6	1.231	21.699	180	50.625	161	127.301	108.409	107.367	0.371	0.316
1	7	1.535	21.566	180	50.625	150	127.259	108.201	106.644	0.372	0.316
2	7	1.535	21.566	180	50.625	150	127.259	108.201	106.644	0.372	0.316
3	7	1.535	21.566	180	50.625	150	127.259	108.201	106.644	0.372	0.316
4	7	1.535	21.566	180	50.625	150	127.259	108.201	106.644	0.372	0.316
5	7	1.535	21.566	180	50.625	150	127.259	108.201	106.644	0.372	0.316
6	7	1.535	21.566	180	50.625	150	127.259	108.201	106.644	0.372	0.316
1	8	1.341	21.547	180	50.625	146	126.796	107.794	106.406	0.372	0.316
2	8	1.341	21.547	180	50.625	146	126.796	107.794	106.406	0.372	0.316
3	8	1.341	21.547	180	50.625	146	126.796	107.794	106.406	0.372	0.316
4	8	1.341	21.547	180	50.625	146	126.796	107.794	106.406	0.372	0.316
5	8	1.341	21.547	180	50.625	146	126.796	107.794	106.406	0.372	0.316
6	8	1.341	21.547	180	50.625	146	126.796	107.794	106.406	0.372	0.316
1	9	1.272	21.47	160	50.625	142	125.566	106.928	105.719	0.371	0.316
2	9	1.272	21.47	160	50.625	142	125.566	106.928	105.719	0.371	0.316
3	9	1.272	21.47	160	50.625	142	125.566	106.928	105.719	0.371	0.316
4	9	1.272	21.47	160	50.625	142	125.566	106.928	105.719	0.371	0.316
5	9	1.272	21.47	160	50.625	142	125.566	106.928	105.719	0.371	0.316
6	9	1.272	21.47	160	50.625	142	125.566	106.928	105.719	0.371	0.316
1	10	1.29	21.602	160	50.625	157	125.901	106.488	105.725	0.372	0.315
2	10	1.29	21.602	160	50.625	157	125.901	106.488	105.725	0.372	0.315
3	10	1.29	21.602	160	50.625	157	125.901	106.488	105.725	0.372	0.315
4	10	1.29	21.602	160	50.625	157	125.901	106.488	105.725	0.372	0.315
5	10	1.29	21.602	160	50.625	157	125.901	106.488	105.725	0.372	0.315
6	10	1.29	21.602	160	50.625	157	125.901	106.488	105.725	0.372	0.315
1	11	1.173	21.715	180	50.625	134	125.221	105.591	104.345	0.374	0.315
2	11	1.173	21.715	180	50.625	134	125.221	105.591	104.345	0.374	0.315
3	11	1.173	21.715	180	50.625	134	125.221	105.591	104.345	0.374	0.315
4	11	1.173	21.715	180	50.625	134	125.221	105.591	104.345	0.374	0.315
5	11	1.173	21.715	180	50.625	134	125.221	105.591	104.345	0.374	0.315
6	11	1.173	21.715	180	50.625	134	125.221	105.591	104.345	0.374	0.315
1	12	0.978	21.099	160	50.625	147	122.071	102.673	102.222	0.373	0.314
2	12	0.978	21.099	160	50.625	147	122.071	102.673	102.222	0.373	0.314
3	12	0.978	21.099	160	50.625	147	122.071	102.673	102.222	0.373	0.314
4	12	0.978	21.099	160	50.625	147	122.071	102.673	102.222	0.373	0.314
5	12	0.978	21.099	160	50.625	147	122.071	102.673	102.222	0.373	0.314
6	12	0.978	21.099	160	50.625	147	122.071	102.673	102.222	0.373	0.314

CHAPTER 4: Subjective grading results for 6 optometrists examining images from instillation of thymoxamine into subject 1 (HB)

A sample of the raw data which continues up to image 45 for each of the 3 subjects is shown below

Images (up to 11 from 45)		1	2	3	4	5	6	7	8	9	10	11
Optometrist	Repeated grades	Efron scale to 1 dp										
RP	DAY 1	1.2	1.3	1.2	1.1	1.2	1.1	1.3	1.1	1.3	1	1.2
JW	HB	1.2	1.7	1.6	1.7	1.5	1.3	1.7	1.7	1.7	1.9	1.9
MD		2.1	1.9	2.1	2.2	2.4	2.3	2.2	2	1.9	2.1	2.1
MC		1.6	1.5	1.5	1.4	1.3	1.4	1.8	1.4	1.6	1.4	1.3
FE		1.4	1.5	1.2	1.3	1.6	1.5	1.6	1.4	1.7	1.4	1.5
OH		0.8	1.1	1.2	1.7	1	1	1.1	1.8	2.6	1.6	0.9
RP	DAY 2	2.4	1.7	2	2	1.8	1.5	2.2	1.4	1.8	2	1.4
JW	HB	1.8	1.6	1.6	1.6	1.6	1.3	1.7	1.3	1.5	1.6	1.4
MD		2.1	2	2.1	2.1	2.1	2	2.1	2	2.1	2.2	2.1
MC		1.5	1.5	1.5	1.4	1.8	1.7	1.4	1.5	1.5	1.5	1.5
FE		1.5	1.36	1.4	1.6	1.7	1.6	1.5	1.5	1.5	1.6	1.6
OH		1.5	1.8	1.6	1.6	1	1.9	1.5	2	1.9	2	1.1
RP	DAY 3	2	1.5	1.9	1.9	2.1	1.7	2.3	1.4	1.8	1.8	1.4
JW	HB	1.8	1.4	1.6	1.6	1.6	1.4	1.7	1.3	1.5	1.5	1.3
MD		2.4	2.3	2.4	2.4	2.4	2	2.3	2.2	2.3	2.2	2.1
MC		1.5	1.6	1.5	1.5	1.4	1.4	1.5	1.8	1.5	1.5	1.5
FE		1.8	1.9	2	1.9	2.1	1.9	1.9	1.9	2	1.9	1.9
OH		1.5	1	2.1	1.8	2	1.8	2	2.1	2	1.7	1.8

CHAPTER 5: 10 images were selected to cover the range of surface severity. These images were placed in a random order and graded by 50 optometrists with the CCLRU and Efron scales.

The average and standard deviation of these results are displayed below for bulbar hyperaemia only

10 Bulbar Hyperaemia Slides

Slide no.	Subjective grading CCLRU Scale		Objective grading. Average of 3 repeated measures									
	AV	SD	AREA BV % AREA								R/R+G+B luminance	
1	1.66	0.37	5.342	28.959	255	87.399	898	250.181	227.194	200.512	0.369	0.335
2	2.36	0.43	10.966	37.384	255	87.399	1275	241.32	216.243	189.763	0.373	0.334
3	3.83	0.44	9.875	36.94	255	87.399	1709	151.437	69.812	61.528	0.536	0.247
4	2.91	0.52	13.041	40.41	255	87.399	1337	189.064	143.141	113.381	0.424	0.321
5	2.95	0.48	24.39	53.844	255	87.399	1231	235.973	201.241	198.179	0.371	0.317
6	3.59	0.44	27.338	57.141	255	87.399	1269	233.714	172.491	146.284	0.423	0.312
7	3.46	0.46	29.141	60.981	255	87.399	1385	227.575	172.456	162.475	0.405	0.307
8	3.84	0.26	18.227	46.397	255	87.399	1599	199.142	102.802	90.558	0.507	0.262
9	2.30	0.56	11.231	37.703	255	87.399	1393	214.377	165.904	132.017	0.418	0.324
10	3.80	0.32	6.181	32.59	255	87.399	1059	201.587	78.202	83.431	0.555	0.215

Slide no.	Subjective grading Efron Scale		Objective grading. Average of 3 repeated measures									
	AV	SD	AREA BV % AREA								R/R+G+B luminance	
1	0.29	0.24	4.056	27.207	240	60.3	593	254.083	239.384	213.5	0.359	0.339
2	1.01	0.39	12.519	39.095	255	60.3	962	242.085	217.16	191.354	0.372	0.334
3	3.77	0.25	8.224	35.172	255	60.3	1118	155.304	69.044	60.998	0.544	0.242
4	1.79	0.35	13.701	41.062	255	60.3	883	178.278	135.353	108.105	0.423	0.321
5	1.92	0.38	26.217	56.456	255	60.3	829	241.188	209.588	205.521	0.367	0.319
6	2.86	0.30	26.637	57.027	255	60.3	853	229.521	170.352	144.13	0.422	0.313
7	2.59	0.40	29.874	61.135	255	60.3	936	232.035	181.084	170.353	0.398	0.31
8	3.74	0.27	20.577	49.023	255	60.3	1191	208.14	110.901	96.948	0.5	0.267
9	1.17	0.45	11.449	38.29	255	60.3	1013	229.838	184.782	146.494	0.41	0.329
10	3.84	0.41	4.343	29.435	255	60.3	711	211.179	79.832	86.45	0.559	0.211

CHAPTER 5: The subjective and objective grade averages were re-ordered in accordance with the rank of image severity

The data below is a sample taken from the assessment of the bulbar hyperaemia

Slide no.	RANK SEVERITY	Subjective grading CCLRU Scale Ranked and re-ordered		Objective grading. Average of 3 repeated measures AREA BV		R/R+G+B	
		AV	SD	AV	SD	AV	SD
1	1	1.656	0.50303568	4.699	0.90933932	0.364	0.00707107
9	2	2.298	0.45859145	11.34	0.15414928	0.414	0.00565685
2	3	2.362	0.53316154	11.7425	1.09813683	0.3725	0.00070711
4	4	2.906	0.46433626	13.371	0.46669048	0.4235	0.00070711
5	5	2.954	0.70576634	25.3035	1.29188409	0.369	0.00282843
7	6	3.46	0.48168073	29.5075	0.51830927	0.4015	0.00494975
6	7	3.586	0.34662218	26.9875	0.49568185	0.4225	0.00070711
10	8	3.804	0.37876814	5.262	1.29966226	0.557	0.00282843
3	9	3.83	0.60114177	9.0495	1.1674333	0.54	0.00565685
8	10	3.838	0.23740949	19.402	1.66170094	0.5035	0.00494975

Slide no.	RANK SEVERITY	Subjective grading Efron Scale Ranked and re-ordered		Objective grading. Average of 3 repeated measures AREA BV		R/R+G+B	
		AV	SD	AV	SD	AV	SD
1	1	0.29	0.24011052	4.699	0.90933932	0.364	0.00707107
2	2	1.008	0.39062483	11.7425	1.09813683	0.3725	0.00070711
9	3	1.17	0.44778366	11.34	0.15414928	0.414	0.00565685
4	4	1.794	0.34723985	13.371	0.46669048	0.4235	0.00070711
5	5	1.918	0.38475542	25.3035	1.29188409	0.369	0.00282843
7	6	2.588	0.39981628	29.5075	0.51830927	0.4015	0.00494975
6	7	2.86	0.30438965	26.9875	0.49568185	0.4225	0.00070711
8	8	3.7376	0.2683172	19.402	1.66170094	0.5035	0.00494975
3	9	3.772	0.24829213	9.0495	1.1674333	0.54	0.00565685
10	10	3.838	0.40952436	5.262	1.29966226	0.557	0.00282843

CHAPTER 6: Results for objective image analysis of 30 right temporal bulbar conjunctival surfaces per age-group.

AGE GROUP	0-20		21-40		41-60		61+	
Objective measures	Area BV cover %	R/R+G+B	Area BV cover %	R/R+G+B	Area BV cover %	R/R+G+B	Area BV cover %	R/R+G+B
Subject								
1	11.51	0.42	13.75	0.43	19.69	0.43	10.28	0.43
2	15.21	0.42	18.25	0.43	14.12	0.43	20.97	0.46
3	8.11	0.42	15.15	0.43	12.35	0.41	10.27	0.44
4	7.78	0.43	14.24	0.43	12.73	0.42	14.45	0.44
5	13.26	0.39	12.89	0.41	10.96	0.42	8.38	0.44
6	9.99	0.40	20.30	0.42	17.63	0.42	10.29	0.44
7	9.22	0.38	14.27	0.42	8.13	0.41	7.15	0.42
8	9.02	0.41	19.50	0.41	8.55	0.44	6.97	0.43
9	8.23	0.39	10.40	0.42	17.98	0.41	7.71	0.41
10	14.43	0.40	12.78	0.41	15.07	0.42	10.35	0.43
11	15.86	0.41	14.15	0.41	4.83	0.41	7.57	0.40
12	14.05	0.41	10.62	0.43	11.14	0.41	8.47	0.41
13	15.45	0.40	23.08	0.41	6.50	0.42	13.33	0.42
14	9.78	0.40	24.59	0.42	6.20	0.41	7.57	0.43
15	6.66	0.41	8.07	0.41	11.90	0.40	13.62	0.45
16	8.32	0.41	6.45	0.41	27.62	0.41	10.06	0.41
17	13.52	0.43	10.19	0.44	10.00	0.44	7.53	0.42
18	15.25	0.42	15.09	0.44	11.67	0.44	16.97	0.43
19	10.48	0.42	12.31	0.41	12.74	0.42	22.40	0.42
20	11.09	0.42	5.80	0.40	4.74	0.42	12.84	0.45
21	10.13	0.39	5.89	0.40	6.89	0.38	8.63	0.43
22	6.66	0.39	5.50	0.39	14.34	0.43	8.49	0.44
23	10.97	0.40	15.60	0.41	8.74	0.40	19.90	0.46
24	7.10	0.41	13.26	0.43	7.90	0.39	17.88	0.46
25	13.13	0.41	8.75	0.41	14.24	0.38	32.96	0.39
26	10.12	0.41	9.83	0.41	25.32	0.42	3.13	0.48
27	9.19	0.41	13.42	0.42	26.02	0.42	6.11	0.51
28	7.16	0.41	10.22	0.41	8.13	0.42	10.22	0.47
29	15.76	0.38	11.75	0.43	11.25	0.39	13.87	0.47
30	5.84	0.38	5.83	0.42	10.59	0.40	16.53	0.39
AV	10.78	0.41	12.73	0.42	12.60	0.41	12.16	0.44
SD	3.11	0.01	4.96	0.01	5.96	0.02	6.14	0.03

CHAPTER 7: Results for diurnal observations of 30 subjects bulbar hyperemia (right temporal) with objective analysis. Raw data for bulbar hyperemia only

	MORNING	AFTERNOON	EVE		MORNING	AFTERNOON	EVE
	Area bv cover (%)				R/R+G+B (luminance)		
	3.76	6.58	5.57		0.41	0.40	0.40
	13.57	6.58	10.98		0.39	0.40	0.40
	5.79	7.33	10.47		0.41	0.41	0.41
	5.14	5.06	7.76		0.41	0.41	0.42
	10.13	8.10	6.93		0.39	0.40	0.39
	12.08	12.47	12.78		0.38	0.39	0.40
	6.66	7.42	4.01		0.39	0.40	0.40
	4.92	12.62	10.09		0.39	0.40	0.41
	10.97	11.52	11.98		0.40	0.41	0.40
	11.46	13.16	12.22		0.39	0.41	0.41
	7.10	8.81	7.34		0.41	0.40	0.40
	7.75	10.03	3.77		0.40	0.40	0.42
	13.13	17.88	15.26		0.41	0.42	0.42
	11.71	11.44	9.09		0.40	0.41	0.41
	10.12	8.77	10.13		0.41	0.42	0.41
	15.35	13.29	10.13		0.41	0.42	0.41
	9.19	14.94	11.76		0.41	0.42	0.41
	8.92	11.40	6.62		0.40	0.41	0.41
	7.16	5.83	7.36		0.41	0.41	0.41
	8.73	6.73	9.82		0.42	0.43	0.42
	15.76	10.88	19.16		0.38	0.41	0.42
	12.55	24.54	14.81		0.40	0.41	0.41
	5.84	22.79	29.29		0.38	0.41	0.42
	18.85	21.96	23.34		0.41	0.43	0.41
	12.62	9.82	8.91		0.42	0.44	0.44
	9.57	6.24	12.61		0.41	0.41	0.43
	3.24	7.85	12.03		0.41	0.44	0.44
	19.62	11.10	16.35		0.42	0.43	0.42
	7.89	13.46	10.17		0.40	0.42	0.42
	13.23	7.62	5.99		0.39	0.39	0.38
AV	9.61	10.08	10.11		0.404	0.407	0.409
SD	0.07	0 12	0.07		0.00	0.00	0 00

CHAPTER 8: Raw data from objective analysis of bulbar hyperemia of the eyes wearing the AquaRelease and Ocufilcon B l

Objective measures of proportionate redness (R/R+G+B (luminance)) over 16 hours

	Aqua R	Redness over time R / R + G + B				Ocufil	Redness over time R / R + G + B			
	Px	8 hrs	12 hrs	16hrs	1 week	Px	8 hrs	12 hrs	16hrs	1 week
NASAL	1	0.416	0.414	0.413	0.404	1	0.409	0.415	0.415	0.407
	2	0.425	0.416	0.424	0.421	2	0.422	0.422	0.423	0.424
	3	0.399	0.404	0.408	0.394	3	0.384	0.393	0.406	0.393
	4	0.408	0.409	0.409	0.412	4	0.412	0.416	0.423	0.424
	5	0.402	0.403	0.404	0.4	5	0.404	0.409	0.41	0.4
	6	0.407	0.391	0.407	0.405	6	0.392	0.393	0.399	0.397
	7	0.394	0.403	0.399	0.397	7	0.404	0.409	0.41	0.397
	8	0.401	0.401	0.407	0.394	8	0.402	0.404	0.415	0.392
	9	0.407	0.405	0.411	0.406	9	0.415	0.413	0.419	0.398
	10	0.391	0.386	0.396	0.387	10	0.396	0.389	0.396	0.388
	11	0.406	0.398	0.41	0.391	11	0.398	0.398	0.408	0.393
	12	0.42	0.414	0.42	0.411	12	0.412	0.41	0.424	0.414
	13	0.42	0.418	0.431	0.418	13	0.431	0.429	0.437	0.419
	14	0.42	0.417	0.425	0.415	14	0.426	0.423	0.426	0.422
	15	0.395	0.404	0.404	0.406	15	0.419	0.411	0.427	0.412
	16	0.428	0.42	0.411	0.411	16	0.425	0.431	0.422	0.41
	17	0.403	0.409	0.409	0.416	17	0.404	0.401	0.403	0.412
	18	0.438	0.437	0.438	0.411	18	0.423	0.425	0.423	0.409
	19	0.435	0.437	0.445	0.412	19	0.437	0.432	0.435	0.41
	20	0.406	0.402	0.416	0.401	20	0.428	0.418	0.408	0.428
	21	0.408	0.397	0.403	0.401	21	0.411	0.43	0.421	0.413
	22	0.409	0.409	0.416	0.399	22	0.408	0.399	0.409	0.399
	23	0.418	0.424	0.421	0.415	23	0.417	0.42	0.419	0.409
	24	0.414	0.423	0.405	0.427	24	0.427	0.436	0.421	0.424
	25	0.396	0.417	0.41	0.416	25	0.419	0.419	0.409	0.408
	26	0.418	0.416	0.425	0.412	26	0.404	0.404	0.421	0.41
	27	0.441	0.42	0.419	0.427	27	0.466	0.455	0.428	0.425
	28	0.415	0.402	0.43	0.401	28	0.417	0.413	0.427	0.4
	29	0.398	0.406	0.397	0.403	29	0.391	0.399	0.389	0.396
	30	0.407	0.405	0.407	0.403	30	0.396	0.393	0.39	0.389
	31	0.377	0.398	0.402	0.396	31	0.417	0.411	0.415	0.405
	32	0.422	0.433	0.441	0.408	32	0.425	0.419	0.419	0.415
	33	0.42	0.415	0.42	0.41	33	0.413	0.417	0.425	0.417
	34	0.402	0.409	0.413	0.407	34	0.417	0.416	0.421	0.412
TEMPORAL	1	0.396	0.395	0.404	0.395	1	0.404	0.403	0.402	0.396
	2	0.403	0.395	0.398	0.398	2	0.406	0.402	0.401	0.4
	3	0.389	0.404	0.399	0.396	3	0.392	0.406	0.405	0.396
	4	0.404	0.401	0.409	0.409	4	0.389	0.391	0.398	0.398
	5	0.39	0.392	0.396	0.382	5	0.4	0.401	0.402	0.397
	6	0.398	0.399	0.398	0.403	6	0.396	0.394	0.397	0.392
	7	0.404	0.404	0.406	0.405	7	0.409	0.409	0.413	0.395
	8	0.405	0.392	0.407	0.397	8	0.41	0.408	0.416	0.396
	9	0.418	0.41	0.418	0.41	9	0.421	0.421	0.421	0.402
	10	0.393	0.386	0.393	0.386	10	0.393	0.388	0.397	0.388
	11	0.405	0.403	0.403	0.395	11	0.4	0.395	0.402	0.389
	12	0.419	0.417	0.416	0.409	12	0.409	0.405	0.409	0.41
	13	0.42	0.425	0.428	0.411	13	0.413	0.409	0.422	0.382
	14	0.418	0.411	0.415	0.406	14	0.404	0.396	0.408	0.407
	15	0.406	0.397	0.407	0.407	15	0.411	0.405	0.41	0.407
	16	0.42	0.414	0.407	0.415	16	0.415	0.421	0.421	0.412
	17	0.393	0.393	0.397	0.399	17	0.403	0.396	0.4	0.4
	18	0.437	0.437	0.442	0.42	18	0.423	0.419	0.422	0.414
	19	0.431	0.415	0.433	0.406	19	0.438	0.438	0.433	0.413
	20	0.404	0.409	0.414	0.405	20	0.413	0.401	0.408	0.403
	21	0.421	0.412	0.409	0.41	21	0.406	0.401	0.395	0.406
	22	0.393	0.393	0.398	0.387	22	0.401	0.399	0.401	0.395
	23	0.402	0.419	0.418	0.416	23	0.416	0.433	0.429	0.417
	24	0.41	0.414	0.411	0.41	24	0.419	0.407	0.417	0.42
	25	0.388	0.388	0.398	0.397	25	0.409	0.411	0.409	0.399
	26	0.404	0.401	0.406	0.398	26	0.409	0.416	0.416	0.405
	27	0.428	0.415	0.418	0.415	27	0.438	0.437	0.433	0.422
	28	0.402	0.406	0.413	0.398	28	0.401	0.401	0.407	0.396
	29	0.388	0.394	0.387	0.392	29	0.388	0.393	0.388	0.39
	30	0.387	0.391	0.392	0.39	30	0.384	0.399	0.401	0.391
	31	0.381	0.403	0.402	0.393	31	0.401	0.396	0.398	0.391
	32	0.417	0.425	0.424	0.41	32	0.411	0.412	0.415	0.406
	33	0.415	0.419	0.417	0.423	33	0.417	0.418	0.42	0.416
	34	0.415	0.415	0.427	0.411	34	0 402	0.404	0.406	0.405
	MEAN	0.4083824	0.4081765	0.4118529	0.4050147	MEAN	0.4106176	0.4103971	0.4127206	0.4048088
	SD	0.0139851	0.0121887	0.0125487	0.0099123	SD	0.0142295	0.013781	0.0117497	0.0109956

CHAPTER 8: Raw data from objective analysis of bulbar hyperemia of the eyes wearing the AquaRelease and Ocufilcon B l

Objective measures of area of blood vessels (Area %) over 16 hours

	Aqua R	Area of BV coverage over time %				Ocufil	Area of BV coverage over time %			
	Px	N 8 HRS	N 12 HRS	N 16 HRS	N 1 WK	Px	Bio 8 HRS	BIO 12 HR	Bio 16 HR	Bio 1 WK
NASAL	1	6.889	9.217	9.033	9.675	1	9.694	11.864	16.358	9.467
	2	5.283	5.883	5.945	9.16	2	12.023	7.395	5.9	8.995
	3	11.966	9.798	17.177	11.04	3	7.943	9.903	11.527	9.07
	4	8.393	4.889	7.877	10.078	4	10.031	9.015	10.365	15.919
	5	8.206	7.077	8.288	10.741	5	6.877	8.442	10.001	8.464
	6	6.485	11.139	11.914	13.358	6	6.878	8.707	8.285	8.211
	7	7.247	7.533	8.025	5.332	7	8.07	7.428	6.219	8.837
	8	13.464	12.045	12.741	13.571	8	5.927	6.584	6.378	4.817
	9	10.288	10.936	11.98	13.316	9	7.628	7.551	10.599	13.643
	10	9.467	7.086	9.606	4.878	10	11.453	6.108	8.059	9.1
	11	11.826	11.029	5.608	11.867	11	9.541	7.115	9.558	8.809
	12	13.119	13.549	15.971	17.174	12	15.168	13.064	13.366	12.947
	13	15.013	17.728	12.585	6.082	13	18.75	15.813	19.775	11.054
	14	13.601	11.242	12.031	10.858	14	10.568	9.458	10.717	11.286
	15	6.524	7.4	8.782	9.785	15	9.34	9.129	12.221	9.478
	16	9.713	14.004	9.067	11.094	16	9.774	9.832	9.832	13.804
	17	4.603	7.377	9.401	6.511	17	7.192	8.938	9.042	9.751
	18	12.708	13.146	12.839	11.752	18	26.721	24.227	20.077	13.097
	19	17.312	18.076	17.567	19.281	19	13.44	18.319	17.611	19.974
	20	12.868	16.312	10.154	10.651	20	14.385	12.464	12.243	11.108
	21	16.342	14.764	19.615	12.012	21	10.651	14.679	13.349	13.525
	22	7.949	5.935	12.158	11.982	22	7.237	8.858	7.73	11.434
	23	16.618	16.884	16.344	12.881	23	12.615	11.878	12.791	15.851
	24	14.064	13.629	11.395	14.103	24	18.366	11.086	13.087	18.186
	25	16.032	9.792	10.943	14.612	25	5.234	6.885	4.08	9.04
	26	14.198	12.831	14.179	8.634	26	14.297	13.413	14.002	13.407
	27	17.106	15.33	10.34	20.515	27	16.106	14.939	10.67	17.626
	28	9.091	5.789	10.015	7.858	28	7.752	6.844	10.739	7.566
	29	5.231	8.713	10.758	8.684	29	10.094	12.309	9.327	8.795
	30	10.391	7.415	6.863	8.173	30	14.994	10.125	7.05	7.141
	31	24.387	17.663	22.425	18.183	31	12.394	16.027	22.143	9.785
	32	12.519	11.572	8.677	9.275	32	14.579	13.546	12.363	12.506
	33	12.593	13.039	16.232	5.592	33	17.515	11.61	13.859	12.002
	34	9.366	7.937	8.974	9.48	34	17.514	14.568	20.504	13.264
TEMPORAL	1	8.633	9.645	14.653	9.691	1	10.461	10.854	12.497	7.883
	2	8.73	9.388	10.095	11.654	2	8.974	5.763	7.973	9.792
	3	11.204	9.666	11.815	9.61	3	16.158	13.876	12.25	10.949
	4	17.629	10.796	9.557	8.601	4	14.182	4.634	18.282	10.562
	5	11.949	9.751	10.672	9.481	5	16.073	11.939	14.398	7.768
	6	8.615	8.566	7.403	9.87	6	9.374	8.445	10.232	5.885
	7	16.331	6.066	5.99	18.737	7	8.773	7.133	9.344	5.507
	8	10.048	15.278	12.536	11.905	8	9.34	10.281	13.996	11.357
	9	9.116	10.873	11.424	8.623	9	8.907	10.445	10.517	8.974
	10	10.552	6.844	10.054	9.144	10	9.045	8.285	7.666	8.001
	11	8.754	5.833	5.241	8.777	11	15.783	9.793	10.927	13.668
	12	8.571	13.341	11.617	11.251	12	6.526	6.735	7.672	15.486
	13	11.793	12.818	12.511	10.491	13	14.966	18.569	15.782	15.273
	14	14.577	11.817	13.015	5.959	14	10.398	12.903	13.706	14.558
	15	13.336	11.505	11.505	14.741	15	10.19	13.226	14.341	12.01
	16	12.848	13.084	10.82	6.935	16	8.614	9.135	11.165	8.881
	17	9.066	9.318	8.59	5.178	17	6.74	10.16	7.796	9.755
	18	11.469	14.089	12.916	9.01	18	12.672	13.04	13.998	8.93
	19	8.763	14.801	8.659	15.582	19	9.587	12.857	10.138	16.938
	20	10.162	9.069	7.274	8.165	20	13.272	9.576	6.98	12.451
	21	12.048	20.745	16.298	14.068	21	17.605	11.944	15.93	17.514
	22	10.58	7.93	14.725	13.873	22	6.255	11.628	14.475	8.333
	23	15.582	15.208	9.713	16.501	23	12.332	16.279	13.098	13.843
	24	10.894	13.42	13.604	14.295	24	17.479	13.232	11.278	18.301
	25	5.049	6.13	13.908	8.24	25	7.984	9.162	14.22	8.61
	26	10.538	10.174	12.102	7.94	26	5.181	8.376	9.629	8.653
	27	15.619	10.051	14.272	13.511	27	15.012	14.933	9.525	18.86
	28	11.267	9.916	10.569	7.015	28	11.1	8.993	7.308	8.133
	29	10.699	10.209	14.048	13.057	29	9.647	6.014	9.27	9.398
	30	12.358	9.924	6.866	6.337	30	11.297	11.44	18.147	6.187
	31	13.212	18.46	19.747	13.059	31	6.359	17.041	17.147	7.288
	32	12.536	9.028	7.732	6.9	32	8.907	6.184	13.615	7.855
	33	11.845	10.85	9.067	6.57	33	14.416	17.755	19.432	12.021
	34	12.941	11.069	17.278	14.476	34	11.905	15.533	12.949	16 925
	MEAN	11.44376	11.06501	11.49684	10.84463	MEAN	11.41566	11.09244	11.99279	11.24276
	Sdev	3.53654	3.563287	3.571984	3.597631	Sdev	4.053144	3.716854	3.911258	3.574366

CHAPTER 9: Results of objective analysis of the bulbar hyperaemia of subjects with irits or keratoconus in comparison with age-matched normals averaged over 3 repeats.

Bulbar Hyperaemia		Iritis		Age matched normal	
Subject	AGE	Area BV co'	R/R+G+B	Area BV co'	R/R+G+B
1	11	28.10	0.43	4.92	0.39
2	41	16.47	0.48	12.35	0.41
3	41	29.17	0.40	10.49	0.43
4	47	29.12	0.38	17.98	0.41
5	46	27.33	0.45	16.16	0.41
6	46	9.74	0.49	15.07	0.42
7	20	31.40	0.39	8.11	0.42
8	20	30.50	0.41	9.84	0.43
9	20	20.09	0.50	13.26	0.39
10	41	31.51	0.47	12.73	0.42
11	41	8.13	0.49	6.93	0.42
12	33	9.33	0.54	7.71	0.42
13	38	4.92	0.55	15.60	0.41
14	55	7.12	0.54	10.59	0.40
15	55	17.21	0.49	22.93	0.42
16	22	13.15	0.46	13.75	0.43
17	56	13.02	0.52	10.59	0.40
18	43	20.72	0.45	6.52	0.39
19	56	15.31	0.51	10.59	0.40
20	56	15.78	0.50	22.93	0.42
	AV	19.069789	0.4726316	11.900042	0.4108801
	SD	9.2335334	0.0506483	4.4236021	0.0138807

Bulbar Hyperaemia		Keratoconus		Age matched normal	
Subject	AGE	Area BV co'	R/R+G+B	Area BV co'	R/R+G+B
1	20	6.128	0.441	13.704	0.478
2	20	15.249	0.416	7.702	0.47
3	43	17.438	0.406	8.051	0.369
4	43	24.481	0.445	5.647	0.497
5	32	6.934	0.408	13.514	0.464
6	32	29.708	0.4	4.636	0.449
7	24	30.909	0.44	13.193	0.471
8	24	19.4	0.442	11.761	0.444
9	25	11.418	0.418	7.559	0.465
10	30	6.124	0.412	5.5	0.533
11	30	14.295	0.437	14.456	0.499
12	35	7.624	0.411	9.882	0.532
13	35	8.418	0.42	4.988	0.514
14	36	39.28	0.429	13.537	0.465
15	55	17.21	0.49	22.93	0.42
16	22	13.15	0.46	13.75	0.43
17	56	13.02	0.52	10.59	0.40
18	43	20.72	0.45	6.52	0.39
19	56	15.31	0.51	10.59	0.40
20	56	15.78	0.50	22.93	0.42
	AV	16.674053	0.4401579	10.447727	0.4574726
	SD	9.1273026	0.0346559	4.5343983	0.0471076